CONFORMATIONAL AND VIBRATIONAL ANALYSIS OF SOME CARBOXYLIC AND AMINO ACIDS: AN AB INITIO STUDY

A thesis Submitted

in Partial Fulfilment of the Requirements

for the Degree of

DOCTOR OF PHILOSOPHY

by

P. TARAKESHWAR

to the

DEPARTMENT OF CHEMISTRY

INDIAN INSTITUTE OF TECHNOLOGY KANPUR

JANUARY, 1994

1. Then was not non-existent nor existent: there was no realm of air, no sky beyond it.
What covered in, and where? and what gave shelter? Was water there, unfathomed depth of water?

2. Death was not then, nor was there aught immortal: no sign was there, the day's and night's divider.
The One Thing, breathless, breathed by its own nature: apart from it was nothing whatsoever.

3. Darkness there was: at first concealed in darkness this All was indiscriminated chaos.
All that existed then was void and formless: by the great power of Warmth was born that Unit.

4. Thereafter rose Desire in beginning, Desire, the primal seed and germ of Spirit.
Sages who searched with their heart's thought discovered the existent's kinship in the non-existent.

5. Transversely was their severing line extended: what was above it then, and what below it?
There were begetters, there were mighty forces, free action and energy up yonder.

6. Who verily knows and who can here declare it, whence it was born and whence it comes this creation?
The Gods are later than this world's production. Who knows then whence it first came into being?

7. He, the first origin of this creation, whether he formed it all or did not form it,
Whose eye controls this world in highest heaven, he verily knows it, or perhaps knows not.

(Hymn CXXIX, Book X, RIGVEDA)

Our life and our whole personality,
All our joys and all our pains,
Are bound up with one single thought,
And rapidly that moment passes.
And those skandhas which are stopped,
For one who's dying, or one remaining here,
They all alike have gone away,
And are no longer reproduced.
Nothing is born from what is unproduced;
One lives by that which is at present there,
When thoughts break up, then all the world is dead,
So't is when final truth the concept guides.

(Niddesa I, 42)

STATEMENT

I hereby declare that the matter embodied in this thesis is the result of investigations carried out by me in the Department of Chemistry, Indian Institute of Technology, Kanpur, India under the supervision of Dr. S. Manogaran.

In keeping with the general practice of reporting scientific observations, due acknowledgement has been made wherever the work described is based on the findings of other investigators.

P. Tarakeshwar

Kanpur

P. Tarakeshwar

DEPARTMENT OF CHEMISTRY
INDIAN INSTITUTE OF TECHNOLOGY KANPUR INDIA
CERTIFICATE I

This is to certify that Mr. P. Tarakeshwar has satisfactorily completed all the courses required for the Ph. D. degree program. These courses include:

CHM 505 Principles of Organic Chemistry

CHM 521 Chemical Binding

CHM 524 Modern Physical Methods in Chemistry

CHM 525 Principles of Physical Chemistry

CHM 545 Principles of Inorganic Chemistry

CHM 626 Solid State Chemistry

CHM 800 General Seminar

CHM 801 Special Seminar

CHM 900 Ph. D. Thesis

Mr. P. Tarakeshwar was admitted to the candidacy of the Ph. D. degree in September 1989, after he successfully completed the written and oral qualifying examinations.

P. K. Ghosh

(P. K. Ghosh)
Head,
Department of Chemistry
IIT Kanpur

Javed Iqbal

(J. Iqbal)
Convenor,
Departmental Post Graduate Committee
Department of Chemistry
IIT Kanpur

CERTIFICATE II

Certified that the work contained in this thesis entitled: "CONFORMATIONAL AND VIBRATIONAL ANALYSIS OF SOME CARBOXYLIC AND AMINO ACIDS: AN AB INITIO STUDY", has been carried out by Mr. P. Tarakeshwar under my supervision and that the same has not been submitted elsewhere for a degree.

(Dr. S. Manogaran)
Thesis Supervisor
Department of Chemistry
I. I. T, Kanpur - 208 016

ACKNOWLEDGEMENTS

I have great pleasure in thanking Dr. S. Manogaran for being a wonderful guide all through this years. The rare opportunity I got, to explore the vast frontiers of science was only possible under his astute guidance. I really admire his forbearance and humaneness in such a malevolent world.

Financial assistance of the Council of Scientific and Industrial Research, New Delhi is gratefully acknowledged.

I thank Professor N. Sathyamurthy for Gaussian 90 and for his interest in my work. I also thank Professor Javed Iqbal and Dr. R. N. Mukherjee for their interest in my work. The presence of Dr. P. K. Bharadwaj in the laboratory really made things more lively. I really thank him for all the care and advice he gave me during my stay in the lab.

This work would not have been feasible had it not been for the co-operation and support I received from the Computer Center. I thank Professor Gautam Barua, Dr. R. Tiwari, Dr. K. S. Singh, Mr. H. P. S. Parihar, Mr. Y. D. S. Arya, Mr. N. Roberts, Mr. A. Alam, Mr. B. J. Prabhucharan and all the operating staff for the patience with which they bore my byte crunching computations.

Dr. P. P. Thankachan needs special mention for getting me interested in this line.

Mrs. Geeta Manogaran, Divya and Kartik are fondly remembered for all the love and care they bestowed on me.

I thank all my labmates especially Debasish. Drs. N. Balakrishnan and Sanjay Kumar (Δ) were really friends in need and deed. Drs. P. K. Chaudhary, S. C. Sivasubramanian, B. R. Srinivasan, G. Ravi Kumar, S. S. Ray, A. K. Dubey, N. Subba Rao, Mr. U. Ilangovan and Mr. Sayan Kar were really a treasure trove of wisdom and wisecracks. Salim, Koshy, Jimmy, Ramesh, Prakash, Verma, Javed, Bhisma, Jayaraman, Kasi, Raghu, Abir, Alok, Nandy, Parmar, Sujoy, Damodar, Subrata (Mams), Samar, KMS, him, dmurthy and a host of others should really be thanked for making life more kaleidoscopic. The presence of my grandpa Dr. Sanjay Kumar and all my wing mates was really rejuvenating and revitalising.

Irfan, Kapil, Devesh and Neeti were always there when I needed them most.

My mother and sisters were the pillars on which I could really rest myself in times of need. Things would certainly have been different with the presence of my father but his advice "*Never roll stones like Sisyphus*" always kept me going and going.

P. Tarakeshwar

SYNOPSIS

There have been significant developments in ab initio calculations with the advent of new generation computers, improved programs and due to the wide accessibility to these programs. Most of the recent developments have focussed on the applicability of these calculations in predictions of a number of molecular properties like molecular structures, free energies and vibrational frequencies. The results of ab initio calculations can also be utilized in the development of force fields which find wide use in the prediction and modelling of biomolecular structures like proteins, nucleic acids, enzyme active sites and drugs. In the present study, the conformational and vibrational analysis of a number of carboxylic acids, carboxylate anions and amino acids using ab initio methods have been carried out.

In chapter 1 of the thesis, the use of ab initio calculations in the development of force fields has been reviewed. The use of force fields and the methods available in checking the accuracy of force fields have been discussed. An overview of the citric acid cycle and the relationship of all the carboxylic acids studied within the citric acid cycle has then been given. The importance of the amino acids included in the present study is then briefly discussed.

In chapter 2, the basis framework of ab initio calculations and normal coordinate analysis has been presented. A brief description of the basis sets employed, the Hartree Fock model, methods of inclusion of electron correlation, and the theory behind the evaluation of force constants is given. The concept of valence force fields, symmetry coordinates, potential energy distributions are briefly highlighted. A brief description of the methods available for the conversion of cartesian force constants (available from ab initio studies) to internal force constants and different scaling techniques is then given. Lastly the principles behind the calculation of Raman activities and IR intensities are briefly reviewed. All the ab initio calculations have been carried out with the Gaussian 90 suite of programs. The normal coordinate analysis had been done using the modified programs of Schachtschneider.

In chapter 3, the results of the calculations on pyruvic acid and the pyruvate anion are described in detail. The calculations on pyruvic acid have been carried out using the HF/4-21G and HF/6-31G** basis sets. The vibrational frequencies are evaluated

on the optimized structures and the effect of the methyl group rotation on the vibrational frequencies has been studied. The results have been compared with the earlier calculations on pyruvic acid done by Murto et al.. The pyruvate anion has then been studied using the 4-21G, 6-31G**, 6-31++G** basis sets at the Hartree Fock level and the 4-31G* and 6-31G** basis sets at the second order Moller Plesset level. The investigations are focussed on the orientation of the carboxylate group. The results at the MP2/6-31G** level indicate that the carboxylate group is in the same plane as the $CH_3C = O$ group. The barrier heights of the methyl group and carboxylate group rotation are evaluated at the MP2/6-31G** level. The vibrational frequencies of the pyruvate anion have been evaluated at all the levels except the MP2/6-31G** level. The calculated frequencies and intensities are used in assigning the solid state spectra of sodium pyruvate. The results indicate that the HF/4-21G basis describes the geometries and frequencies of anions quite satisfactorily.

In chapter 4, the calculations on dicarboxylic acids are described. Calculations on malonic, succinic, glutaric, adipic and hydroxymalonic acid have been carried out using the HF/4-21G basis set. Calculations using the HF/6-31G** basis set are also carried out on the smaller acids malonic, hydroxymalonic and succinic. The barrier heights of the carboxyl group rotation were evaluated at the HF/4-21G level on malonic, succinic and glutaric acids. The vibrational frequencies are evaluated on the optimized structures of all the acids and assigned to the corresponding solid state spectra of these acids. A strategy of assigning the calculated frequencies to the corresponding solid state frequencies has been developed. Since calculations at the MP2/4-31G* level have already been carried out on oxalic acid calculations were performed at the HF/4-21G and HF/6-31G** bases to evaluate the effect of the presence of the methylene groups in the higher dicarboxylic acids.

In chapter 5, calculations on a number of substituted citric acids and the citrate trianion have been carried out. The vibrational frequencies of citric acid and the citrate trianion have been evaluated on the HF/4-21G optimized structures. The frequencies evaluated are then used to assign the experimental vibrational spectra of citric acid and citrate trianion. The structures of monofluoro, difluoro and monohydroxy citric acids have been investigated at the AM1, STO-3G and HF/3-21G levels. Single point calculations at the HF/6-31G* level have also been carried out on the HF/3-21G optimized structures. Based on the results of the calculations on the various diastereomers an explanation on the inhibitory activity of only one set of the diastereomers is proposed.

In chapter 6, the vibrational frequencies of the gas phase and zwitterionic forms of cysteine and serine have been evaluated. Since the conformational analysis of cysteine and serine has already been carried out on gas phase structures using the HF/4-21G basis no further conformational analysis has been done. The vibrational frequencies of the lowest energy, second lowest energy and the highest energy conformers of the earlier conformational study of cysteine and serine are evaluated using the HF/4-31G* basis set. The calculated frequencies are then assigned to the experimental frequencies of the methyl ester, hydrochloride and the zwitterionic forms of cysteine and serine. Relationships between the geometry of the XH group and the $\nu(XH)$ frequencies (X = S or O) are then discussed. Based on the earlier study of zwitterionic L-alanine the neutron diffraction structures of L-cysteine and L-serine zwitterions are optimized at the HF/4-31G* level. The calculated vibrational frequencies are then assigned to the experimental frequencies of zwitterionic cysteine and serine. The similarities and differences in the structures and frequencies of cysteine and serine in the zwitterionic and gas phase forms are forwarded.

In chapter 7, calculations on proline and hydroxyproline gas phase forms have been performed. The optimizations have been carried out at the HF/4-21G level. Since the effect of pseudorotation and ring pucker has been studied extensively by other methods these aspects have not been studied. Calculations have been carried out on two conformations in which the orientation of the carboxyl hydrogens is cis or trans. The barrier heights of the carboxyl group rotation have been evaluated at the HF/4-21G level. The vibrational frequencies are then evaluated for both proline and hydroxyproline. A simple set of symmetry coordinates which take into consideration the ring pucker of proline and hydroxyproline are constructed for the first time. The calculated frequencies of proline and hydroxyproline are then assigned to the corresponding experimental vibrational spectra of the sodium salt, hydrochloride and zwiterionic forms.

In chapter 8, a summary of the findings of the present study and suggestions for future work have been forwarded.

Contents

List of Figures

List of Tables

Chapter 1

Introduction

Numerical simulations provide an invaluable complement to experiment in the study of structures and dynamics of molecules. The techniques rest on the hypothesis that the potential energy of a molecule or assembly of molecules can be reproduced by a low-order Taylor expansion in terms of internal coordinates. Several studies have been devoted to the refinement of parameters and the analysis of their transferability from small model systems [1–24]. As an outcome, the most recent force fields are perfectly adequate to the refinement of energy minima. However, the study of flexible molecules and of their conformational transitions requires a correct description of a much wider region of potential energy surfaces.

The refinement of parameters and the analysis of the transferability from model systems can be done by the calculation of molecular properties like dipole moments, force constants and vibrational frequencies. The calculated quantities can be compared with the corresponding experimental parameters to check the level of accuracy of these force fields. With the advent of faster computers and widely accessible programs, rapid strides have been made in the level of complexity at which these force fields are calculated [25–32]. Thus calculations at very high levels of sophistication (ab initio) can be done on relatively large molecules. Ab initio calculations due to their firm theoretical basis tend to be more systematic and reliable, than other methods available for the development of force fields.

Ab initio force fields can also be used in the prediction of vibrational spectra at different levels of accuracy [33–38]. At the harmonic level the prediction of good vibrational spectra greatly enhances its use as a structural tool in cases where other structural methods, such as NMR or diffraction methods, cannot be applied, e.g. transient species, polymers, low-temperature matrices, adsorbed layers or for structural phenomena which are fast in

the NMR time scale. Improved thermodynamic functions can be obtained from those experimental vibrational spectra whose fundamentals are correctly identified. The task of assignment of bands can be facilitated by a reliable prediction of the vibrational spectra [37]. Another important application of accurate force fields is the evaluation of vibrational averaging effects in observed molecular properties, e.g., geometries, dipole moments, etc. The main source of inaccuracy in, for example, microwave spectra stems from these effects. There is a great deal of interest in the field due to recent developments in spectroscopy [38–46].

The main distinction between the ab initio calculation and the normal coordinate calculation of vibrational spectra by spectroscopists is in the evaluation of force constants. In the ab initio method, the force constants are derived by the solution of the electronic Schrödinger equation of the molecule in the fixed nuclear approximation, (i.e. force constants are calculated by obtaining the second derivative of the potential surface by the force method [47,48]). In the other method, the force constants are simply guessed based on their values in related molecules. Thus the latter method is useful, if the molecule studied is similar to some other molecule with known force constants. Since there are usually more force constants than vibrational frequencies there are many ways to choose force constants in producing exact agreement with experimental frequencies [49]. However an unique set of force constants for a molecule can be evaluated by normal coordinate calculations with the help of the experimental spectra of its isotopomers. However the spectra of a large number of isotopomers is required to assign a reasonably large molecule with low symmetry. Ab initio calculations can aid in the choice of these force constants and more importantly it can help predict force constants for molecules, where comparisons with other molecules are difficult and the guessed force constants are doubtful.

Evaluation of force fields by ab initio methods is however not devoid of problems. It is computationally easier to evaluate force constants defined in terms of cartesian coordinates but these are not useful from the chemical point of view. Hence force constants defined in terms of cartesian coordinates have to be converted to force constants defined in terms of internal coordinates. Then they are transferable among similar molecules. This transferability can however break down due to any of the following factors: inductive effects, conjugation, hyperconjugation, steric effects (ring strain, steric hindrance, rotational isomerism etc.), tautomerism and external effects (phase, temperature, solvent). Within the harmonic approximation, calculations at the Hartree Fock level leads to a systematic overestimation of stretching, bending and coupling force constants due to neglect of elec-

tron correlation. Hence they have to be either scaled or electron correlation has to be explicitly included in the calculations. It has been observed that by the inclusion of electron correlation [50] or by scaling [51] force constants can be determined within reasonable limits to match with those determined from experimental data. The assignment of the experimental spectra using ab initio calculated frequencies is laborious in the absence of gas phase vibrational spectra. This is due to the presence of intermolecular forces in the solid and liquid phase which leads to shifts in the frequencies. Thus a number of factors have to be taken into account before the assignment of either solid state or liquid phase spectra.

The systems studied in this thesis were chosen for two reasons. First, all of them are biologically relevant and second, they are similar enough to correlate the calculated parameters to the observed properties. In the next two sections the biological importance of all the systems studied are discussed.

1.1 Carboxylic Acids

The citric acid (CA) cycle (tricarboxylate cycle or Kreb's cycle [52]) is the common final oxidation pathway for any metabolic fuel source that can be presented as an acetyl group or some C_4 dicarboxylic acid. Thus the metabolism of sugars, fatty acids and amino acids leads into the CA cycle [53–55]. A bare outline of the CA cycle is given in Figure 1.1. The operating mechanism of the CA cycle is to condense the acetyl unit of the entering acetyl-CoA (which is obtained from pyruvic acid) in a Claisen condensation with the C_4 electrophilic acceptor oxaloacetic acid to yield the C_6 CA by action of citrate synthase. The CA formed undergoes a series of transformations and in this process produces eight electrons which eventually yield twelve high energy ATP molecules. At biological pH all the acids exist in their anionic forms.

Most of the carboxylic acids and the corresponding anions studied in this thesis are related to the CA cycle. Thus pyruvic acid in its anionic form (pyruvate anion) is the key molecule which initiates the CA cycle. The enzyme pyruvate decarboxylase decarboxylases the pyruvate anion and gives the acetyl-CoA molecule. Citric acid in its trianionic form (citrate trianion) is one of the key substrates within the cycle. The enzymes citrate synthase, aconitase, citrate lyase and ATP citrate lyase need the citrate trinanion as their substrates. Succinic acid is also one of the substrates in the CA cycle. The enzyme succinic dehydrogenase uses succinate dianion as a substrate and eventualy produces fu-

marate. Hydroxymalonic acid though not a substrate is an inhibitor of one of the enzymes in the CA cycle. Its close similarity with L-malic acid makes it an inhibitor of the enzyme malate dehydrogenase. Glutaric acid has a close similarity to one of the substrates within the cycle (α-ketoglutarate). Malonic and adipic acids though not related to the CA cycle are interesting enough to warrant their study.

1.2 Amino Acids

Amino acids are of special interest in both biological chemistry and structural chemistry. The interest in biological chemistry stems from the fact that most biologically active compounds are built of α-amino acids. β-, γ- and higher amino acids are of minor biological signficance compared to α-amino acids. The interest in structural chemistry is due to the fact that amino acids form zwitterions, $H_3N^+ - CHR - COO^-$, in the solid state and in polar media (e. g. aqueous solution), whereas isolated molecules exhibit a neutral structure, $H_2N - CHR - COOH$. While the zwitterionic structure is accessible via X-ray methods, the structure determination of the neutral form poses severe experimental problems, since amino acids usually decompose before melting.

Cysteine owing to the presence of the thiol group (SH) is one of the most important amino acids. It is responsible for the stabilization of secondary structures of proteins through the formation of hydrogen bonds and more importantly disulfide bonds [56–59]. Its presence in the active site of some proteins [60–62] tend to prove its importance as an amino acid. The other amino acid serine, though very much similar to cysteine has a hydroxyl group (OH) instead of a thiol group. Thus serine owing to the presence of two hydroxyl groups readily forms hydrogen bonds and hence is found in turns of protein secondary structures [63]. The role of serine in serine proteases [64] only augments the importance of this amino acid.

Proline and hydroxyproline are two of the most important imino acids. They are present in structural proteins [65]. Until recently it has been thought that proline residues occurred as isolated residues, and sequences of two or more were absent in globular proteins. With the increasing size of the protein sequence database it became apparent that it is found at a much higher frequency than average in many proteins [66]. Evidences of the functional role of proline have emerged from the presence of proline in transmembrane proteins [67,68]. The spate of references on the presence of proline repeats in circumsporozite proteins [69], antibacterial peptides [70], only augment its importance as an amino acid.

In addition to their roles in proteins the above amino acids are important substrates [71]. In plants and bacteria, cysteine is required by the enzyme cystathiaone γ-synthetase for the biosynthesis of methionine. It activates peptidases (protein digesting enzymes), used in the biosynthesis of taurine (a synaptic mediator in the nervous system), coenzymes of pantothenic acid (vitamin-B5), 4-phosphopantathein, and CoA. Serine is a lipotropic factor (impedes the deposition of triglycerides in tissues) and also the substrate of serine hydroxymethylase, an enzyme which catalyzes the reversible conversion of L-serine to glycine. Proline and hydroxyproline are the substrates of the enzymes proline racemase and hydroxyproline epimerase respectively.

1.3 Outline of the Thesis

The thesis has been arranged in the following manner: In Chapter 2 the theory underlying ab initio calculations and normal coordinate analysis are discussed briefly. In chapter 3 the studies on pyruvic acid and the pyruvate anion are discussed in detail. In chapter 4 the conformational and vibrational analysis of the higher dicarboxylic acids are discussed. In chapter 5 the vibrational analysis of citric acid and citrate trianion are given. The results of the calculations on substituted citric acids are then presented. In chapter 6 the conformational effects on the vibrational frequencies of cysteine and serine in the gas phase are given. The vibrational analysis of cysteine and serine in the zwitterionic form is discussed. In chapter 7 the conformational and vibrational analysis of proline and hydroxyproline are discussed.

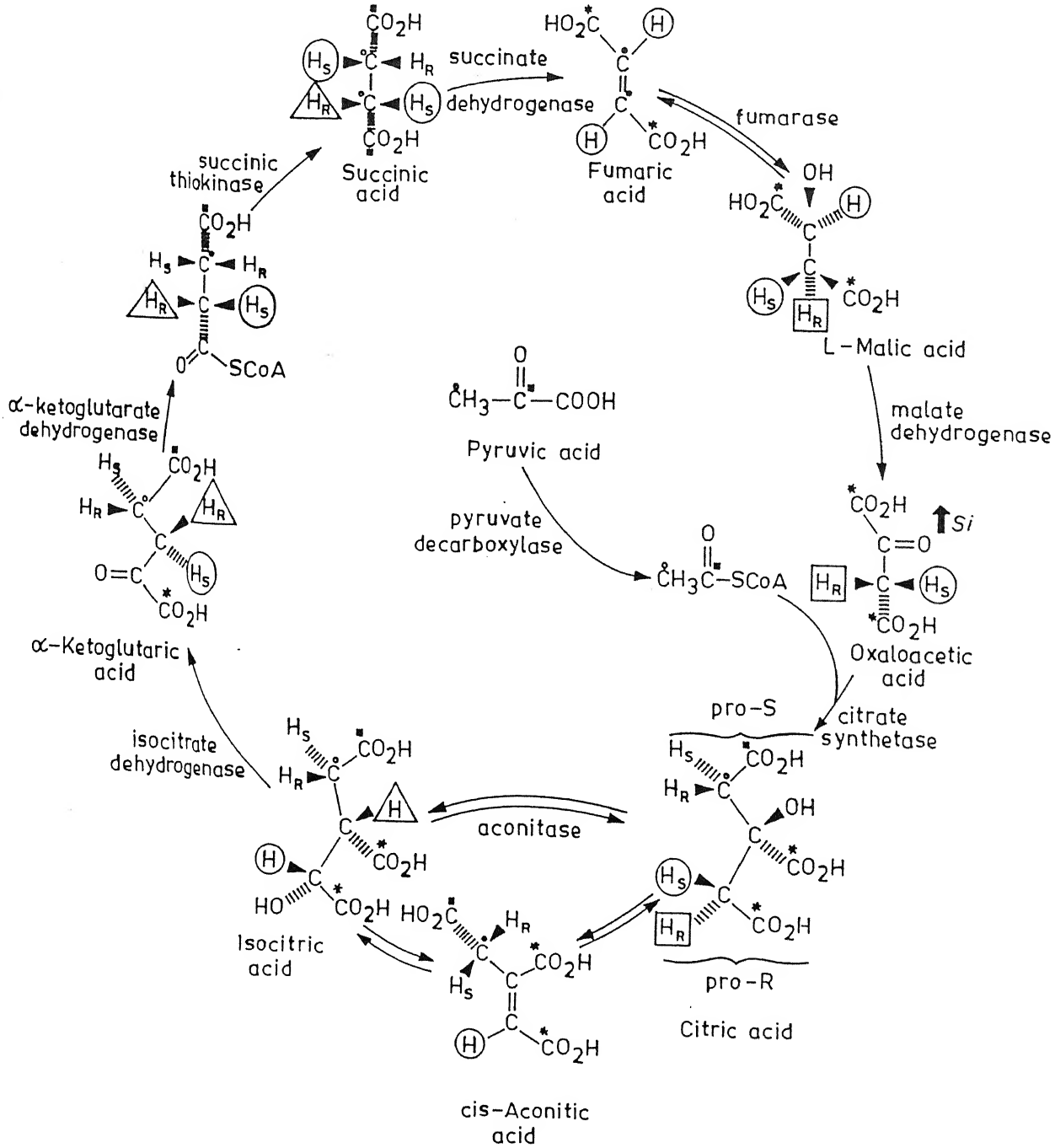

Figure 1.1: Outline of the Citric Acid Cycle

1.4 References

[1] F. A. Momany, R. F. McGuire, A. W. Burgess and H. A. Scheraga, J. Phys. Chem., 79 (1975) 2361.

[2] G. Nemethy, M. S. Pottle and H. A. Scheraga, J. Phys. Chem., 87 (1983) 1883.

[3] M. J. Sippl, G. Nemethy and H. A. Scheraga, J. Phys. Chem., 88 (1984) 6231.

[4] P. Weiner and P. Kollman, J. Comput. Chem., 2 (1981) 287.

[5] S. J. Weiner, P. A. Kollman, D. A. Case, U. C. Singh, C. Ghio, C. Alagona, S. Profeta and P. Weiner, J. Am. Chem. Soc., 106 (1984) 765.

[6] S. J. Weiner, P. A. Kollman, D. T. Nguyen and D. A. Case, J. Comput. Chem., 7 (1986) 230.

[7] B. R. Brooks, R. E. Bruccoleri, B. D. Olafson, D. J. States, S. Swaminathan and M. Karplus, J. Comput. Chem., 4 (1983) 187.

[8] F. A. Momany, V. J. Klimkowsky and L. Schafer, J. Comput. Chem., 11 (1990) 654.

[9] N. L. Allinger and U. Burkert, *Molecular Mechanics*, ACS Monograph 177, American Chemical Society, Washington DC, 1982.

[10] N. L. Allinger, J. Am. Chem. Soc., 99 (1977) 8127.

[11] (a) N. L. Allinger, Y. H. Yuh, H. J. Lii, J. Am. Chem. Soc., 111 (1989) 8551; (b) H. J. Lii and N. J. Allinger, J. Am. Chem. Soc., 111 (1989) 8566.

[12] H. J. Lii and N. J. Allinger, J. Comput. Chem., 12 (1991) 186.

[13] N. L. Allinger, J. Am. Chem. Soc., 114 (1992) 1.

[14] J. Hermans, H. J. C. Berendsen, W. F. van Gunsteren and J. P. M. Postma, Biopolymers, 33 (1984) 1513.

[15] W. L. Jorgensen and C. J. Swenson, J. Am. Chem. Soc., 107 (1985) 569.

[16] W. L. Jorgensen and C. J. Swenson, J. Am. Chem. Soc., 107 (1985) 1489.

[17] A. T. Hagler, S. Lifson and E. Huler, J. Am. Chem. Soc., 96 (1974) 5319.

[18] S. Lifson, A. T. Hagler and P. J. Dauber, J. Am. Chem. Soc., 101 (1979) 5111.

[19] A. T. Hagler, P. S. Stern, R. Sharon, J. M. Becker and F. Naider, J. Am. Chem. Soc., 101 (1979) 6842.

[20] S. Lifson and P. S. Stern, J. Chem. Phys., 77 (1982) 4542.

[21] P. Dauber-Osguthorpe, V. A. Roberts, D. J. Osguthorpe, J. Wolff, M. Genest and A. T. Hagler, Proteins: Struct. Funct. Genetics, 4 (1988) 31.

[22] S. L. Mayo, B. D. Olafson and W. A. Goddard III, J. Phys. Chem., 94 (1990) 8897.

[23] P. Amodeo and V. Barone, J. Am. Chem. Soc., 114 (1992) 9085.

[24] D. M. Seeger, C. Korzeniewski and W. Kowalchyk, J. Phys. Chem., 95 (1991) 6871-79.

[25] Gaussian 92, Revision I, M. J. Frisch, M. Head Gordon, G. W. Trucks, J. B. Foresman, H. B. Schlegel, K. Raghavachari, M. Robb, J. S. Binkley, C. Gonzalez, D. J. Defrees, D. J. Fox, R. A. Whiteside, R. Seeger, C. F. Melius, J. Backer, R. L. Martin, L. R. Kahn, J. J. P. Stewart, S. Topiol and J. A. Pople, Gaussian Inc., Pittsburgh PA, 1992.

[26] Texas: TX 90, P. Pulay, Fayetville, AR, 1990; P. Pulay, Theor. Chim. Acta, 50 (1979) 299.

[27] Gamess: M. W. Schmidt, K. K. Baldridge, J. A. Boatz, J. H. Jensen, S. Koseki, M. S. Gordon, L. A. Nguyen, T. L. Windus and S. T. Elbert, Quantum Chem. Program Exch. Bull., 10 (1990) 52.

[28] Hondo: M. Dupuis, J. Rys and H. F. King, Quantum Chem. Program Exch. Bull., 11 (1977) 336: 11 (1977) 338: 13 (1981) 401; J. Chem. Phys., 65 (1976) 111.

[29] Turbomole: R. Ahlrichs, M. Bär, M. Häser. H. Horn and C. Kölmel, Chem. Phys. Lett., 162 (1989) 165.

[30] Cadpac: R. D. Amos and J. E. Rice, CADPAC : The Cambridge Analytic Derivatives Package, Issue 4.0, Cambridge, 1987.

[31] Molecule-Sweden: J. Almlöf, C. W. Bauschlicher, M. R. A. Blomberg, D. P. Chong, A. Heiberg, S. R. Langhoff, P.-A. Malmqvist, A. P. Rendell, B. O. Roos, P. E. M. Siegbahn and P. R. Taylor.

[32] Monstergauss: M. R. Peterson and R. A. Poirier, Program MONSTERGAUSS, University of Toronto, Canada, 1981.

[33] C. J. H. Schutte, in *Structure and Bonding*, Vol. 9, p.213, Springer Verlag, Berlin, 1971.

[34] D. R. Fredkin, A. Komoronicki, S. R. White and K. R. Wilson, J. Chem. Phys., 78 (1983) 7077.

[35] B. Schrader, D. Bougeard and W. Niggeman, in *Computational methods in Chemistry*, (edited by J. Bargan), Plenum, New York, 1980.

[36] B. A. Hess, Jr., L. J. Schaad, P. Cársky and R. Zahradník, Chem. Rev., 86 (1986) 709.

[37] G. Fogarasi and P. Pulay, Annu. Rev. Phys. Chem., 35 (1984) 191; in *Vibrational Spectra and Structure*, Vol. 14, (edited by J. R. Durig), Elsevier, Amsterdam, 1985.

[38] J. R. Durig and A. Wang, J. Mol. Str., 294 (1993) 13.

[39] L. D. Barron, in *Vibrational Spectra and Structure*, Vol. 17B, p.343(edited by H. D. Bist, J. R. Durig and J. F. Sullivan). Elsevier, Amsterdam, 1989.

[40] L. A. Nafie and C. G. Zimba, in *Biological Applications of Raman Spectroscopy*, Vol. 1, p.307(edited by T. G. Spiro). Wiley, New York, 1987.

[41] P. K. Bose, L. D. Barron and P. L. Polavarapu, Chem. Phys., 155 (1989) 423.

[42] P. K. Bose, P. L. Polavarapu, L. D. Barron and L. Hecht, J. Phys. Chem., 94 (1990) 1734.

[43] T. M. Black, P. K. Bose, P. L. Polavarapu, L. D. Barron and L. Hecht, J. Am. Chem. Soc., 112 (1998) 1479.

[44] L. D. Barron, A. R. Gargaro and Z. Q. Wen, J. Chem. Soc., Chem. Comm., (1990) 1034.

[45] L. D. Barron, A. R. Gargaro, L. Hecht and P. L. Polavarapu, Spectrochim. Acta., 48A (1992) 261.

[46] L. D. Barron, Z. Q. Wen and L. Hecht, J. Am. Chem. Soc., 114 (1992) 784.

[47] P. Pulay, in *Modern Theoretical Chemistry*, Vol. 4, p.153, (edited by H. F. Schaefer III), Plenum, New York, 1977.

[48] M. C. Flanigan, A. Komornicki and J. W. McIver, in *Modern Theoretical Chemistry*, Vol. 8, p.1, (edited by G. A. Segal), Plenum, New York, 1977.

[49] I. M. Mills, Spec. Period. Rep., Theory. Chem., 1 (1974) 110.

[50] C. J. Marsden, J. C. S Chem. Commun., (1984) 401.

[51] P. Pulay, G. Fogarasi, G. Pongor, J. E. Boggs and A. Vargha, J. Am. Chem. Soc., 105 (1983) 7037.

[52] H. A. Krebs, Nature, 147 (1941) 560.

[53] L. Stryer, *Biochemistry*, W. H. Freeman and Co., San Francisco, 1975.

[54] P. Srere, in *Advances in Enzymology and Related areas of Molecular Biology*, Vol. 43, p.57(edited by A. Meister), Wiley, New York, 1975.

[55] C. A. Walsh, *Enzymatic Reaction Mechanisms*, p.899, W. H. Freeman and Co., San Francisco, 1979.

[56] P. A. Kollman, J. McKelvey, A. Johansson and S. Rothenberg, J. Am. Chem. Soc. 97 (1975) 955.

[57] J. A. Ippolito, R. S. Alexander and D. W. Christianson, J. Mol. Biol., 215 (1990) 457.

[58] S. K. Binley and G. A. Petsko, Adv. Protein Chem., 39 (1988) 125.

[59] M. E. McGarth, M. E. Wilke, J. N. Higaka, C. S. Kraik and R. S. Fletterick, Biochemistry, 20 (1989) 9264.

[60] B. Frei, R. Stocker and B. N. Ames, Proc. Natl. Acad. Sci., U. S. A , 85 (1988) 9748.

[61] A. Holmgren, J. Biol. Chem., 264 (1989) 13963.

[62] J. M. Berg, Science, 232 (1986) 485.

[63] A. Aubry and M. Marraud, Biopolymers, 22 (1983) 341.

[64] J. Kraut, Annu. Rev. Biochem., 46 (1977) 331.

[65] G. D. Schulz and R. H. Schirmer, *Principles of Protein Structure*, p 72-73, Springer Verlag Inc. New York, 1979.

[66] M. MacArthur and J. M. Thornton, J. Mol. Biol., 218 (1991) 397.

[67] C. Brandl and C. M. Deber, Proc. Natl. Acad. Sci. (U. S. A), 83 (1986) 917.

[68] K. J. Rothschild, Y. He, T. Mogi, T. Marti, L. J. Stern and H. G. Khorana, Biochemistry, 29 (1990) 5954.

[69] J. B. Dame, J. L. Williams, T. F. McCutchan, J. L. Weber, R. A. Wirtz, W. T. Hockmeyer, W. L. Malory, J. D. Haynes, I. Schneider, D. Roberts, G. S. Sanders, E. P. Reddy, C. L. Diggs and L. H. Miller, Science, 225 (1984) 593.

[70] (a) D. Kauffman, T. Hofmann, A. Bennick and P. Keller, Biochemistry, 25 (1986) 2387; (b) R. W. Frank, R. Gennaro, K. Schneider, M. Przybylski and D. Romeo, J. Biol. Chem., 265 (1990) 18871; (c) B. Agerberth, J. Lee, T. Bergman, M. Carlquist, H. G. Boman, V. Mutt and H. Jörnvall, Eur. J. Biochem. 202 (1991) 849.

[71] E. A. Stroev, *Biochemistry*, Mir Publishers, Moscow, 1989.

Chapter 2

Methodology

The literature on ab initio calculations and normal coordinate analysis is vast and extensive. Hence this chapter does not purport to be a review of these methods. A flavour of the various theories and nuances underlying these methods are however presented in this chapter. The vital links between these methods are also described. Detailed description of these methods is given in references [1–19].

2.1 Ab Initio Methods

2.1.1 Hartree Fock Theory

In molecular orbital theory, the individual molecular orbitals can be expressed as a linear combination of the one electron basis functions Φ_μ centered on the atomic nucleus such that

$$\Psi_i = \sum_{\mu=1}^{N} C_{\mu_i} \Phi_\mu. \tag{2.1}$$

The wave function can then be represented as a single determinant of the doubly occupied molecular orbitals. The coefficient C_{μ_i} can then be chosen in such a way that the calculated total energy is minimum. This leads to the well known Roothan-Hall equations [20,21].

$$\sum_{\nu=1}^{N} (F_{\mu\nu} - \epsilon_i S_{\mu\nu})\, C_{\nu i} = 0, \qquad \mu = 1, 2, \ldots N \tag{2.2}$$

Here N is the total number of basis functions. ϵ_i is the orbital energy of the i^{th} molecular orbital Ψ_i. $S_{\mu\nu} = \langle \Phi_\mu \mid \Phi_\nu \rangle$ are the overlap integrals and $F_{\mu\nu}$ are the elements of the Fock

matrix given by

$$F_{\mu\nu} = H_{\mu\nu}^{core} + \sum_{\lambda=1}^{N}\sum_{\sigma=1}^{N} P_{\lambda\sigma}\left[(\mu\nu \mid \lambda\sigma) - \frac{1}{2}(\mu\lambda \mid \nu\sigma)\right] \tag{2.3}$$

where

$$H_{\mu\nu}^{core} = \left\langle \Phi_\mu \mid -\frac{1}{2}\nabla^2 - \sum_A V_A \mid \Phi_\nu \right\rangle$$

is the one electron integral.

$$P_{\lambda\sigma} = 2\sum_{i=1}^{OCC} C_{\lambda_i}^* C_{\sigma_i} \tag{2.4}$$

is the density matrix. The summation in equation (2.4) is over the occupied molecular orbitals only. Here $P_{\lambda\sigma}$ represents the total electron population existing in the overlap region of the basis functions Φ_μ and Φ_ν. The factor 2 indicates that two electrons occupy each molecular orbital and the asterisk denotes complex conjugation.

The electron energy E^{ee} is given by

$$E^{ee} = \frac{1}{2}\sum_{\mu=1}^{N}\sum_{\nu=1}^{N} P_{\mu\nu}(F_{\mu\nu} + H_{\mu\nu}^{core}) \tag{2.5}$$

The internuclear repulsion is given by

$$E^{nr} = \sum_{A<B}^{M}\sum \frac{Z_A Z_B}{R_{AB}} \tag{2.6}$$

where Z_A and Z_B are the atomic numbers of A and B and R_{AB} is their seperation. The total energy is then the sum of E^{ee} and E^{nr}.

The Roothan-Hall equations (2.2) are not linear since the Fock matrix depends on the molecular orbital coefficients $C_{\mu i}$ through the density matrix expression (2.4). The solution involves an iterative process and the resulting orbitals are derived from their own effective potential.

2.1.2 Electron Correlation

The inability of the Hartree Fock procedures to adequately account for the correlation between motions of electron can be corrected by using more elaborate models comprising a

(a) Configuration interaction [22]
(b) Moller Plesset perturbation theory [23]
The first method is variational but not size consistent but the second is size consistent but not variational. Variational implies that the calculated electronic energy should correspond to an upper bound to the energy that would result from the exact solution of the Schrödinger equation. Size consistency means that the method must give additive results when applied to an assembly of isolated molecules.

Thus the exact energy (nonrelativistic) which includes the effect of electron correlation would be

$$E_{(exact)} = E_{(HartreeFock)} + E_{(correlation)} \tag{2.7}$$

A full configuration interaction is generally not feasible. Partial configuration interaction calculations include the Configuration Interaction Singles (CIS), Configuration Interaction Doubles (CID), and the Configuration Interaction Singles and Doubles (CISD) calculations. A detailed account of configuration interaction and its applications is given in reference [24]. The size consistency of these methods can also be improved by coupled cluster methods [24].

Since we have only employed the second order Moller Plesset theory in our calculations, we briefly discuss the features of Moller Plesset calculations.

The final energy E_λ and Ψ_λ the exact or full CI (within a given basis set) ground state wave function for a system described by the Hamiltonian H_λ can be expanded in powers of λ according to the Rayleigh-Schrödinger perturbation theory [25].

$$\Psi_\lambda = \Psi^{(0)} + \lambda\Psi^{(1)} + \lambda^2\Psi^{(2)} + \cdots$$

$$E_\lambda = E^{(0)} + \lambda E^{(1)} + \lambda^2 E^{(2)} + \cdots \tag{2.8}$$

For practical purposes $\lambda = 1$. The method is denoted by the highest order energy term allowed. Thus truncation after the second order term is denoted as MP2. Here

$$E^{(0)} = \sum_i^{OCC} \epsilon_i \tag{2.9}$$

$$E^{(0)} + E^{(1)} = \int\cdots\int \Psi_o \hat{H} \Psi_o \partial\tau_1 \partial\tau_2 \cdots \partial\tau_n \tag{2.10}$$

where Ψ_o is the Hartree-Fock wave function. ϵ_i are the one electron energies defined by equation (2.2).

The second order contribution to the energy is then given as

$$E^{(2)} = -\sum_{i<j}^{OCC}\sum_{a<b}^{virt}(\epsilon_a + \epsilon_b - \epsilon_i - \epsilon_j)^{-1} \mid (ij \mid\mid ab) \mid^2 \tag{2.11}$$

where

$$(ij \mid\mid ab) = \int\int \chi_i^*(1)\chi_j^*(2)\left(\frac{1}{r_{12}}\right)[\chi_a(1)\chi_b(2) - \chi_b(1)\chi_a(2)]\partial\tau_1\partial\tau_2 \tag{2.12}$$

is the two electron integral integrated over all coordinates (cartesian and spin) for both the electrons.

2.1.3 Basis Sets

It can be seen from the previous sections that basis sets play an important role in the evaluation of the energies. Excellent reviews exist on basis sets [19,26,27] and their properties. Methods to construct new basis sets are described in reference [19] We discuss briefly the salient features of the basis sets employed in the present study.

STO-3G

The STO-3G minimal basis set was developed by Pople and co-workers for first row elements [28]. It was later extended to the second row [29], third row [30] and fourth row [31] elements. It has also been applied to first and second row transistion metals [32]. It is characterized by its small size and effectiveness in predicting geometries [33]. The remarakable agreement of the STO-3G geometries to the experimental geometries is due to the large basis set superposition error which helps cancel other defects to produce reasonable bond parameters. It can be expressed as

$$\Phi_{nl}(\zeta = 1, r) = \sum_{k=1}^{3} d_{nl,k}\ g_l(\alpha_n, k, r) \tag{2.13}$$

where the subscripts n and l define the specific principal and angular quantum numbers and g_l are the normalized gaussian functions. α is the gaussian component and d is the linear expansion coefficient. Their values are determined by minimizing the error in the fit of the gaussian expansion to the exact Slater orbital. The STO-3G basis description of conjugated systems, polar molecules is far from satisfactory. This is due to the fact that all the elements of a single row of the periodic table have the same description. This implies that smaller the basis set, the more the ab initio calculation assumes an empirical flavour.

3-21G/4-21G

These split valence basis sets are a compromise between the speed obtained using a STO-3G basis and the accuracy of the larger computationally slower sets. The 4-21G [33] basis is extremely suitable for geometry optimizations utilizing the analytic gradients. A reduced version of the 4-21G basis set, the 3-21G basis set [34,35] is also used in routine calculations. The characterstics of both the basis sets are similar. The prominent features of these basis sets are that they are both of double zeta quality in the valence shell and exploit the equality of the s and p components. Two further extensions of the 3-21G basis set are the inclusion of polarization functions [36] for second row elements and diffuse functions [37] to improve the description of anion geometries.

4-31G/6-31G

These bases are generated by increasing the number of primitives devoted to the core and first valence electron functions. The 4-31G [38] and 6-31G [39] bases improve upon 3-21G energetics at the expense of increased computer time. Adding all the six components of a cartesian d function to the first row elements gives the 6-31G* basis. Further addition of p functions to the hydrogen results in the 6-31G** basis. The 4-31G and 6-31G* have been extended to the second row elements [40,41]. Replacement of the six component cartesian d's with their five component spherical counterparts give the 6-31+G [42]. A similar strategy employed on the 4-31G with the addition of diffuse s and p functions gives the 4-31+G basis set [43]. However the 4-31+G basis does not give improved anion geometries.

2.1.4 Energies and Geometries

Energies and hence the geometries, calculated by ab initio methods are extremely dependent on the basis set used in the calculation [44]. Structural parameters like bond lengths and bond angles can be reasonably estimated using a good basis set. Thus carbon-hydrogen bond lengths calculated at the RHF/6-31G* are shorter than experimental values by 0.008 to 0.010 A°. Similarly calculated bond lengths for carbonyl bonds of small organic molecules are shorter than the experimental values. Inclusion of electron correlation at the MP2 level using the 6-31G* basis set gives a good match for the carbon-hydrogen bond lengths but the carbonyl bonds are longer. However bond angles are less sensitive to basis set variations. Eventhough absolute values for structural parameters are not very reliable,

relative values between two conformers of the same molecule using the same basis set are useful. As far as conformational analysis of molecules is concerned, the relative energies and hence the conformational stability predicted from ab initio results are consistent with the conclusions arrived from experimental conformational preferences.

2.1.5 Force Constants

The starting point of all force field evaluations is the harmonic approximation.

Harmonic Approximation

The Schrödinger equation for a polyatomic molecule with M nuclei and N electrons is

$$\left[\sum_{\alpha=1}^{M} -\frac{h^2}{2m_\alpha}\nabla_\alpha^2 + \sum_{i=1}^{N} -\frac{h^2}{2m_e}\nabla_i^2 - \sum_{i=1}^{N}\sum_{\alpha=1}^{M}\frac{Z_\alpha e^2}{r_{i\alpha}} + \sum_{\beta>\alpha}^{M}\sum_{\alpha=1}^{M}\frac{Z_\alpha Z_\beta e^2}{r_{\alpha\beta}} + \sum_{j<i}^{N}\sum_{i=1}^{N}\frac{e^2}{r_{ij}}\right]\Psi = E\Psi \tag{2.14}$$

where m_α and Z_α are the mass and charge of nucleus α, m_e and e are the electronic mass and charge, $r_{i\alpha}$ is the distance between electron i and nucleus α, r_{ij} is the distance between electron i and electron j, $r_{\alpha\beta}$ is the distance between the nucleus α and nucleus β respectively. The left hand side of equation (2.14) gives the kinetic energy of the nuclei, the electrons, the potential energy due to the electron-nuclear attraction, nuclear-nuclear repulsion and electron-electron repulsion. The wave function Ψ therefore depends upon 3(M+N) coordinates of the electrons and nuclei. Since the nuclei are heavier and move slowly than the electrons, the nuclear kinetic energy term in equation (2.14) can be neglected, thereby the nuclei can be held stationary. Thus the resulting equation would describe the motion of N electrons in the field of fixed nuclei and the energy E would depend upon the chosen nuclear position. Thus for a polyatomic molecule the electronic energy in the fixed nuclear approximation will depend on all the nuclear positions such that $E = E(R_1, \ldots R_M)$ though E would be constant for those combinations of nuclear displacement that give translation or rotation of a molecule as a whole.

Within the Born-Oppenheimer's approximation [45], if the nuclear kinetic energy can be treated as a perturbation in the fixed nuclear Hamiltonian, the first order correction would vanish at all positions of nuclear equilibrium.

The second order correction would then be given by the following equation

$$\left[\sum_{\alpha=1}^{M} -\frac{h^2}{2m_\alpha}\nabla_\alpha^2 + V(R_1, \ldots R_M)\right]\Psi_{nucl} = E_{nucl}\Psi_{nucl} \tag{2.15}$$

In equation (2.15) which describes the nuclear motion the first term in the left hand side is the kinetic energy operator of the nuclei. E_{nucl} is the second order energy correction that gives the energy of the nuclear motion. The potential $V(R_1, \ldots R_M)$ consists of the quadratic terms in a power series expansion of $E(R_1, \ldots R_M)$ about the equilibrium position.

$$E = E(X_1^o, \ldots X_{3M}^o) + \sum_{i=1}^{3M} \frac{\partial E}{\partial X_i} \mid_o \Delta X_i + \frac{1}{2} \sum_{y=1}^{3M} \frac{\partial^2 E}{\partial X_i \partial X_j} \mid_o \Delta X_i \Delta X_j + \cdots \tag{2.16}$$

where $X_1, X_2, \ldots X_{3M}$ are the cartesian coordinates of the M nuclei. The first term in the L. H. S of equation (2.16) is constant for all E_{nucl} and hence can be ignored. Since E is a minimum at the equilibrium geometry

$$\frac{\partial E}{\partial X_i} \mid_o = 0 \tag{2.17}$$

Here the second term in equation (2.16) vanishes. If all terms of order higher than second are neglected, the potential is a quadratic function of the nuclear displacements ΔX_i

$$E(X_1, \ldots X_M) \equiv \frac{1}{2} \sum_{j=1}^{3M} F_{ij} \Delta X_i \Delta X_j = V(R_1, \ldots R_M) \tag{2.18}$$

where the force constants F_{ij} are given by

$$F_{ij} = \frac{\partial^2 E}{\partial X_i \partial X_j} \mid_o \tag{2.19}$$

Equation (2.18) represents the harmonic approximation. For small displacements about the equilibrium position, equation (2.18) is valid, but it is not accurate for large distortions.

A transformation to mass weighted coordinates $\rho_i = (m_i)^{\frac{1}{2}} \Delta X_i$ followed by rotation of the coordinates to coincide with the principal axes of the quadratic form in equation (2.18) gives an expression for V containing only squared terms.

$$V = \frac{1}{2} \sum_{i=1}^{3M} \lambda_i Q_i^2 \tag{2.20}$$

where Q_i's are coordinates relative to the principal axes and hence called "normal coordinates". As a result of this transformation equation (2.15) which depends on 3M variables separates into 3M equations; each depending upon a single Q_i. Further each of these is a harmonic oscillator equation with force constant λ_i.

For non-linear molecules six (for linear five) of the λ_i which correspond to three translational and three rotational motions of the entire molecule, are zero. These six λ_i's can be removed by working in a coordinate frame having the origin at the center of mass and rotating with the molecule. The remaining 3M-6 degrees of freedom are usually specified by internal coordinates such as bond lengths, bond angles and torsional angles. Though the harmonic approximation is good enough for most vibrational calculations, recent studies indicate that the inclusion of anharmonicity leads to a better agreement of the computed wave numbers with the experimental wave numbers.

Anharmonicity

Most of the vibrational calculations to date have used the harmonic approximation of equation (2.18) but with the progress in ab initio calculations, cubic and quartic force constants can be evaluated. These are the third and fourth order terms in equation (2.16). The inclusion of them in equation (2.18) allows the possibility of including anharmonicity. Perturbation theory yields the following formula for anharmonicity [17].

$$\chi_{rr} = \frac{1}{16}\Phi_{rrrr} - \frac{1}{16}\sum_s \Phi^2_{rrs}\frac{[8\omega_r^2 - 3\omega_s^2]}{\omega_s(4\omega_r^2 - \omega_s^2)} \tag{2.21}$$

Equation (2.21) contains the quadratic, diagonal and semi-diagonal quartic force constants. The ω_k's are the harmonic frequencies. The evaluation of the quartic force constant Φ_{rrrr} is given in reference [46]. A detailed treatment of anharmonicity and its inclusion in force field calculations is given in references [47–49].

Though inclusion of anharmonicity leads to more accurate frequencies the calculations are still not computationally feasible for large molecules. Moreover non-inclusion of anharmonicity leads to errors which can be minimized through proper scaling. The decisive factor in the evaluation of accurate vibrational frequencies is the evaluation of an accurate potential using a reasonably large basis set. The effect of basis set on force constants of small molecules has been recently studied [50].

2.2 Normal Coordinate Analysis

In the previous section we have looked at the evaluation of the ab initio potential and hence ab initio force constants. These cartesian force constants are non-informative for detailed vibrational studies though they are easier to compute. The force constants evaluated with

respect to the internal coordinates are more useful because of the following reasons:
(a) These coordinates make it easier to compare and transfer force constants between related molecules.
(b) Systematic errors in the calculations are easily detectable.
(c) Beyond the harmonic approximation, the expansion of the potential in a power series will be rapidly convergent.
Before we discuss the conversion of cartesian coordinate force constants into internal coordinate force constants a summary of the conventional methods of evaluation of force constants, potential energy distributions are given. Detailed treatment of these methods are given in references [10–15].

2.2.1 Internal Coordinates

The description of the motions of a polyatomic molecule having N nuclei requires 3N cartesian coordinates represented by the column matrix X. Of these six for a non linear molecule and five for a linear correspond to translational and rotational motions. The remaining 3N-6 or 3N-5 coordinates are called "internal coordinates" represented by the column matrix R. The vibrational energy of a polyatomic molecule which is a sum of the kinetic energy T and potential energy V can be expressed in different ways. The kinetic energy is easier to express in terms of the cartesian coordinates while the potential energy is easier to express in terms of internal coordinates. The relationship between the two coordinate sets $R = BX$, where B is the transformation matrix, is linear only in the harmonic approximation. The Eliashevich coordinates R_m [51] correspond to the linear part of this relation.

2.2.2 Potential Functions

The potential energy function can be written as a Taylor series expansion of the internal coordinates. Two types of potential functions are generally employed to calculate the normal modes of vibrations.

The "Generalized Valence Force Field" (GVFF)

$$V = V(0) + \frac{1}{2}\sum_{mm'} f_{mm'} R_m R_{m'} + \frac{1}{6}\sum_{mm'm''} f_{mm'm''} R_m R_{m'} R_{m''} + \cdots \qquad (2.22)$$

The harmonic approximation means that the terms of higher order than quadratic are neglected. The quadratic force constants are then defined as

$$f_{mm'} = \frac{\partial^2 V}{\partial R_m \partial R_{m'}} \tag{2.23}$$

The coordinates used are only the bond stretching Δr_{ij} and the valence angle variations $\Delta\Theta_{jk}$. f_{mm} are stretching or bending principal force constants, while $f_{mm'}$ are interaction force constants.

The "Urey-Bradley Force Field" (UBFF)

This force field [52] uses not only bond length and valence angle variations, but also the variations Δq_{jk} of the q_{jk} distances between non bonded atoms.

$$V = \sum_i V(\Delta r_i) + \sum_{i>j} V(\Delta\Theta_{jk}) + \sum_{ij}(\Delta q_{jk}) + \cdots \tag{2.24}$$

where

$$V(\Delta r_i) = K_i' r_{ij} \Delta r_{ij} + \frac{1}{2} K_i (\Delta r_{ij})^2$$

$$V(\Delta\Theta_{jk}) = H_{jk}' r_{ij} r_{jk} \Delta\Theta_{jk} + \frac{1}{2} H_{jk} r_{ij} r_{ik} (\Delta\Theta_{jk})^2$$

$$V(\Delta q_{jk}) = F_{jk}' q_{jk} \Delta q_{jk} + \frac{1}{2} F_{jk} (\Delta q_{jk})^2$$

where K_i, K_i' are stretching force constants, H_{jk}, H_{jk}' are bending force constants, F_{jk}, F_{jk}' are repulsive force constants. F' is usually taken as $0.1F$.

2.2.3 Equations of Motion

Using the Wilson's method [11], which defines a G matrix with elements g_{mm}, the kinetic energy matrix can than be written as

$$2T = \dot{R}^{\dagger} G^{-1} \dot{R}$$

or

$$2T = \sum_{mm'} g^{-1}_{mm'} \dot{R}_m \dot{R}_{m'} \tag{2.25}$$

(where $\dot{R}^{\dagger}$ is the transpose of matrix $\dot{R}$ and ($\dot{R}_m = \frac{\partial R_m}{\partial t}$) and the potential energy

$$2V = R^{\dagger} F R$$

or

$$2V = \sum_{mm'} f_{mm'} R_m R_{m'}. \tag{2.26}$$

The Lagrange equations of motion are then written as

$$\frac{\partial}{\partial t}\left(\frac{\partial U}{\partial \dot{R}}\right) + \left(\frac{\partial U}{\partial R}\right) = 0 \tag{2.27}$$

with

$$U = T - V.$$

We get 3N-6 second order differential equations of the form

$$\sum_m g^{-1}_{mm'} \ddot{R}_m + \sum_m f_{mm'} R_m = 0. \tag{2.28}$$

The solutions are

$$R_{ms} = a_{ms} \cos(\lambda_s^{\frac{1}{2}} t + \Phi_s) \tag{2.29}$$

where a_{ms} is the maximum vibration amplitude corresponding to the coordinate R_{ms}, Φ_s the phase factor and $\lambda_s = 4\pi^2 \nu_s^2$ the frequency factor.

After differentiating R_m twice and replacing $\ddot{R}_m$ in equation (2.28), we get the homogenous linear equations

$$\sum_m (f_{mm'} - \lambda_s g^{-1}_{mm'}) a_{ms} = 0 \tag{2.30}$$

or written under a matrix form and after multiplying by G

$$\mid FG - E\lambda_s \mid A_s = 0 \tag{2.31}$$

where A_s is the column matrix of maximum vibration amplitudes a_{ms} corresponding to the ν_s frequency. The frequency factors λ_s are then the solutions of the secular determinant

$$\mid FG - E\Lambda \mid = 0 \tag{2.32}$$

where E is the identity matrix and Λ the diagonal matrix of frequency parameters λ_s. Equation (2.31) can be written as

$$\mid FG - E\Lambda \mid A = 0$$

where A is the square matrix of the 3N-6 over 3N-6 amplitude vectors A_s from equation (2.31) for each λ_s; the a_{ms} values may be calculated, assuming their normalization such as

$$\sum_m (a_{ms})^2 = 1. \tag{2.33}$$

The normalized vibration amplitudes x_{ms} are then

$$x_{ms} = \frac{a_{ms}}{(\sum_m (a_{ms})^2)^{\frac{1}{2}}}. \tag{2.34}$$

2.2.4 Vibrational Normal Modes and Potential Energy Distributions

In the harmonic approximation, all the vibration modes are orthogonal, which mean that they do not exchange energy.

A system of coordinates Q_s called "normal coordinates" may then be found such that the kinetic and potential energy may be written:

$$2T = \sum_{s=1}^{3N-6} (\dot{Q}_s)^2 \qquad 2V = \sum_{s=1}^{3N-6} \lambda_s (Q_s)^2 \tag{2.35}$$

or with the matrix notation

$$2T = \dot{Q}^\dagger E Q \qquad 2V = Q^t \Lambda Q. \tag{2.36}$$

The Lagrange equations of motion correspond then to the 3N-6 independent equations

$$\ddot{Q}_s + \lambda_s Q_s = 0.$$

Their solutions being written

$$Q_s = Q_s^o \cos(\lambda_s^{\frac{1}{2}} t + \phi_s). \tag{2.37}$$

If we call L the transformation matrix from normal to internal coordinates,

$$R_m = \sum_s L_{ms} Q_s$$

or

$$R = LQ \tag{2.38}$$

it can then be shown that

$$Q_s^o = \sum_m L_{ms}^{-1} a_{ms}. \tag{2.39}$$

This means considering the preceding normalization condition equation (2.33)

$$Q_s^o = 1$$

and

$$L_{ms}^{-1} = a_{ms}.$$

The L_{ms}^{-1} elements are the vibration amplitudes of the R_m internal coordinates for the vibration mode ν_s. The potential energy for the normal mode ν_s will be written according to equation (2.36) as

$$V_s = \frac{1}{2}\lambda_s Q_s^2$$

The equations (2.29) may then be written as

$$\lambda_s = \sum_m L_{ms}^2 f_{mm} + \sum_{m' \neq m} L_{ms} L_{m's} f_{mm'}$$

or

$$\sum_m \left(\frac{L_{ms}^2}{\lambda_s}\right) f_{mm} + \sum_{m' \neq m} \left(\frac{L_{ms} L_{m's}}{\lambda_s}\right) f_{mm'} = 1. \tag{2.40}$$

The terms $\frac{L_{ms}^2}{\lambda_s}$ and $\frac{L_{ms}L_{m's}}{\lambda_s}$ are called "potential energy distribution". The first term corresponds to the potential energy of the normal mode ν_s of the principal force constant f_{mm}; the second represents the contribution of the interaction force constant $f_{mm'}$. In general, $\frac{L_{ms}^2}{\lambda_s}$ terms are larger and provide a reasonable measure of the contribution of the internal coordinate R_m to the normal coordinate Q_s.

2.2.5 Symmetry Coordinates

The difficult computational problem [12,53,54] encountered in calculating force constants direct from vibrational frequencies may be simplified with symmetry coordinates. These coordinates S_k take into account the fact that vibrational modes belonging to different symmetry classes of the symmetry point group of the considered molecular entity are

orthogonal to each other. The secular determinant equation (2.32) using these coordinates may be factored in sub-determinants of lower dimensions, corresponding to the different symmetry classes

$$| FG - E\Lambda | = 0.$$

These "symmetry coordinates" are linearly related to the internal coordinates through the matrix U

$$S = UR. \tag{2.41}$$

The F_s and G_s matrices expressed with symmetry coordinates are then related to the internal F and G matrices by the relations

$$F_s = UFU' \tag{2.42}$$

$$G_s = UGU'. \tag{2.43}$$

The vector (Q) consisting of normal coordinates Q_i and S are linked by L_s as $S = L_s Q$. The elements of the potential energy distribution (PED) for the a-th normal frequency ν_a correspond to

$$\left[(F_s)_{ii}\frac{(L_s)^2_{ia}}{\lambda_a}\right] \times 100$$

where i refers to the i-th symmetry coordinates.

2.3 Conversion and Scaling of Force Constants

In the previous sections we have discussed the salient features of ab initio methods and normal coordinate analysis. Generally the force constants calculated quantum mechanically are with respect to the cartesian coordinates. So it has to be converted to internal coordinate force constants. Furthermore due to the non-inclusion of anharmonicity, and electron correlation for large molecules, the force constants calculated are generally too high by about 10-15%. So a suitable scaling procedure has to be employed to relate the calculated force constants to the experimental force constants. Before we delve into the intricacies of scaling we discuss the methods of converting cartesian force constants to internal force constants.

2.3.1 Conversion of Cartesian Force Constants to Internal Force Constants

The main bottleneck in the conversion of the cartesian force constants to internal force constants is that the force field matrix in cartesian coordinates spans a 3N dimensional space, with N being the number of atoms, while the number of non-redundant internal coordinates is only 3N-6 (or 3N-5 for linear molecules). The transformation from cartesian to internal coordinates can be described as follows [55]:

The potential-energy surface of a given state can be described in cartesian coordinates

$$E(x) = E_o(x) + f_x.x + 0.5.x.F_x.x + \cdots \tag{2.44}$$

and in internal coordinates as

$$E(r) = E_o(r) + f_r.r + 0.5.r.F_r.r + \cdots \tag{2.45}$$

where $r = B.x$ is the internal coordinate vector, x is the cartesian vector, f_x and f_r are gradients, F_x and F_r are the second derivative matrices in the two frameworks and B is the Wilson's B matrix [10] which transforms cartesian into internal coordinates. By inspection

$$F_r = B^{-1\dagger}.F_x.B^{-1} \tag{2.46}$$

where $\dagger$ means transpose. Since B is a rectangular matrix, to invert it, it is necessary to use the notion of a generalized inverse matrix.

$$B^{-1\dagger} = (BB^{\dagger})^{-1}.B \tag{2.47}$$

However $BB^{\dagger}$ can be singular so that the inversion is always not possible. The symmetric G is non-singular [56] and can be inverted

$$G = Bm^{-1}B^{\dagger}.$$

If A is the inverse of B then we have

$$\begin{aligned} AB &= E \\ ABm^{-1}B^{\dagger} &= Em^{-1}B^{\dagger} \\ AG &= m^{-1}B^{\dagger} \\ A &= m^{-1}B^{\dagger}G^{-1} \end{aligned}$$

as given in [57]. Since we need the inverse of symmetric G, we have

$$A^{sym}B^{sym} = E$$

where,

$$B^{sym} = UB.$$

Postmultiplying by $m^{-1}B^{\dagger sym}$ on both sides we have

$$\begin{aligned} A^{sym}B^{sym}m^{-1}B^{\dagger sym} &= m^{-1}B^{\dagger sym} \\ A^{sym}G^{sym} &= m^{-1}B^{\dagger sym} \\ A^{sym} &= m^{-1}B^{\dagger sym}G^{-1sym}. \end{aligned}$$

Using Equation (2.46),

$$\begin{aligned} F^{sym} &= A^{\dagger sym}F_{cart}A^{sym} \\ F^{int} &= U^{\dagger}f^{sym}U. \end{aligned}$$

Here A^{sym}, G^{sym}, F^{sym} are the symmetric A, G and F matrices, respectively. U is the U matrix which contains the description of the symmetric coordinates in terms of internal coordinates.

2.3.2 Scaling

Generally SCF force constants obatined with *sp* basis sets are overestimated. The overestimation is of the order of 10-15% for diagonal stretching force constants and 20-30% for diagonal bending force constants. The off diagonal force constants are overestimated by orders between 10-30%. The vibrational frequencies obtained are determined mainly by the diagonal terms. The overestimation is fairly systematic and hence the relative values are more or less accurate. The best way to scale down is to combine the theory and the experiment. This has been the method proposed by Pulay [58–59]. They scaled down the stretching force constants by 10%, the bending force constants by 20% and obtained fairly accurate numbers for most of the frequencies. In the above case the interaction force constants are not scaled. This was taken care of in other scaling procedures employed by Botschwina and co-workers [60,61,64], Fogarasi et al. [65] and Pouchan et al. [62,63,66].

In our calculations we have employed the scaling procedure adopted by Durig et al. [67]. In this scaling procedure the stretching force constants are scaled by a factor of 0.8, the bending force constants by a factor of 0.9, and a geometric mean of them is employed to scale the other force constants. Thus, if C_i is a scale factor assigned to group i, the diagonal terms F_{ii} and F_{jj} are scaled by C_i and C_j, for F_{ij} the geometric mean $(C_iC_j)^{\frac{1}{2}}$ is used. i. e. the coupling terms are not independently scaled. In matrix notation the theoretical force constant matrix F^u is scaled accordingly as

$$F^s = C^{\frac{1}{2}} F^u C^{\frac{1}{2}} \tag{2.48}$$

where C is the diagonal matrix of the scale factors. The best approach to scaling would be to obtain a reliable match by optimizing the calculated force constants to the experimental force constants; but necessarily it requires reliable gas phase experimental wave numbers. This is the principle behind the Scaled Quantum Mechanical (SQM) force field approach proposed by Pulay [68] and others [69,70].

2.4 Intensities

A number of molecular properties can be calculated from ab initio calculations. Detailed reviews of the various properties which can be calculated are given in references [4,5,71]. In this section we briefly mention the methods available for the calculation of theoretical IR and Raman intensities. The importance of the prediction of IR intensities and Raman intensities has been discussed extensively in references [72,73]

2.4.1 Raman Intensities

Komornicki and McIver [74] reported the first efficient method for the prediction of Raman intensities [75]. Their method required double numerical differentiation, a procedure which was computationally difficult [76] especially when one had to retain precision in the final results. Raman intensities are obtained theoretically from the first derivatives of the polarizability with respect to the nuclear coordinates [77]. However, since the applied polarizability itself is a second derivative of energy with respect to an applied electric field, the Raman intensity is a third derivative property. Thus the analytical expression for the calculation of Raman intensities can be written as follows [80]:

The polarizability derivatives are evaluated analytically using the expression [78–79]

$$\frac{\partial \alpha_{fg}}{\partial x} = \frac{\partial^3 E}{\partial f \partial g \partial x} = \left\langle \frac{\partial D^f}{\partial x} \frac{\partial P}{\partial g} \right\rangle = \left\langle \frac{\partial P}{\partial f} G^x \left(\frac{\partial P}{\partial g} \right) \right\rangle + \left\langle \frac{\partial^2 P}{\partial f \partial g} G^x \left(P^o \right) \right\rangle - \left\langle \frac{\partial S}{\partial x} \frac{\partial^2 W}{\partial f \partial g} \right\rangle + \left\langle \frac{\partial^2 P}{\partial f \partial g} \frac{\partial h}{\partial x} \right\rangle + \left\langle \frac{\partial P}{\partial f} \frac{\partial D^g}{\partial x} \right\rangle \quad (2.49)$$

In the above equation f and g are electric field directions, x is a nuclear coordinate, $\langle\rangle$ denote matrix trace, $D^f_{\mu\nu} = \langle \mu \mid f \mid \nu \rangle$ are the dipole integrals, P is the density matrix, G^x () denotes the contraction of the integral derivatives with a matrix, S is the overlap matrix, W is the energy weighted density matrix (Lagrangian) and h is the core hamiltionian. It should be noted that the above Raman intensities are predicted within the harmonic approximation.

2.4.2 IR Intensities

As in the case of Raman intensities Komornicki and McIver [74] had reported the first efficient numerical method towards the prediction of IR intensities. Unlike Raman intensities, IR intensities are easier to evaluate because only the first derivative of the energy has to be calculated. Yamaguchi et al. [81] have reported the expressions for the analytical evaluation of the dipole derivatives. Thus the the derivation of the analytical expression for the dipole moment derivative in the Restricted Closed Shell approximation is given below [81]

The electronic energy for a closed-shell SCF wave function is given by [82]

$$E_{SCF} = 2 \sum_{i}^{d.o} h_{ii} + \sum_{i,j}^{d.o} \{2(ii \mid jj) - (ij \mid ij)\}. \quad (2.50)$$

The first order derivative with respect to a nuclear coordinate (a) is given by

$$\frac{\partial E_{SCF}}{\partial a} = 2 \sum_{i}^{d.o} h^a_{ii} + \sum_{i,j}^{d.o} \{2(ii \mid jj)^a - (ij \mid ij)^a\} - 2 \sum_{i}^{d.o} S^a_{ii} \epsilon_i, \quad (2.51)$$

and the expression for the electronic dipole moment (derivative of energy with respect to an external electric field (f)) would be given by

$$\frac{\partial E_{SCF}}{\partial f} = 2 \sum_{i}^{d.o} h^f_{ii}, \quad (2.52)$$

and the expression for the dipole derivative can be obtained by taking the derivative of equation (2.51) with respect to an electric field (f)

$$\frac{\partial}{\partial f}\left(\frac{\partial E_{SCF}}{\partial a}\right) = 2\sum_{i}^{d.o} h_{ii}^{af} + 4\sum_{i}^{d.o}\sum_{j}^{all} U_{ji}^{f} F_{ij}^{a} - 2\sum_{i}^{d.o} \epsilon_i^f S_{ii}^a - 4\sum_{i}^{d.o}\sum_{j}^{all} \epsilon_i U_{ji}^f S_{ij}^a \tag{2.53}$$

where

$$h_{ii}^{af} = \sum_{\mu\nu}^{AO} C_{\mu}^{i0} C_{\nu}^{i0}\left(\frac{\partial^2 h_{\mu\nu}}{\partial a \partial f}\right) = -e\sum_{\mu\nu}^{AO} C_{\mu}^{i0} C_{\nu}^{i0} \frac{\partial}{\partial a}\langle \mu \mid r_f \mid \nu\rangle\,, \tag{2.54}$$

and the $\epsilon_i^{(f)}$ are derivatives of orbital energies. Equation (2.53) can also be obtained by taking a derivative of equation (2.52) with respect to a nuclear coordinate (a).

In this thesis, except for the Moller Plesset calculations all the calculated Raman and IR intensities have been evaluated analytically.

2.5 Computational details

All ab initio calculations were done using the Gaussian 90 suite of programs [83] installed on a Convex C-220 system. The normal coordinate analysis were done using a modified version of the program of Schachtschneider [84]. The conversion of force constants to symmetric force constants were done using a modified version of the program VECEIG kindly provided by Mr. Amarendra Vijay and Professor D. N. Satyanarayana.

2.6 References

[1] N. G. Richards and D. L. Cooper, *Ab Initio Molecular Orbital Calculations for Chemists*, 2nd edn., Clarendon Press, Oxford, 1983.

[2] S. Wilson, *Electron Correlation in Molecules*, Clarendon Press, Oxford, 1984.

[3] W. J. Hehre, L. Radom, P. v. R. Schleyer and J. A. Pople, *Ab Initio Molecular Orbital Theory*, Wiley, New York, 1986.

[4] Advances in Chemical Physics, *Ab Initio Methods in Quantum Chemistry*, Vol. 67: Vol. 69, Wiley, New York, 1987.

[5] G. Naray-Szabo, P. Surjan and J. A. Angyan, *Applied Quantum Chemistry*, Akademiai Kiado, Budapest, 1987.

[6] D. M. Hirst, *A Computational approach to Chemistry*, Blackwell Scientific, London, 1990.

[7] A. Szabo and N. S. Ostlund, *Modern Quantum Chemistry*, Mc Graw Hill, New York, 1989.

[8] C. E. Dykstra, *Quantum Chemistry and Molecular Spectroscopy*, Prentice Hall, Englewood Cliffs., N. J., 1992.

[9] G. C. Schatz and M. A. Ratner, *Quantum Mechanics in Chemistry*, Prentice Hall, Englewood Cliffs., N. J., 1993.

[10] E. B. Wilson, J. C. Decius and P. C. Cross, *Molecular Vibrations*, Mc Graw Hill, New York, 1955.

[11] G. Herzberg, *Infrared and Raman Spectra of Polyatomic Molecules*, D. van Nostrand, New York, 1945.

[12] T. Shimanouchi, in *Physical Chemistry an Advanced Treatise*, Vol. IV, Moleculr Properties, Ed. D. Henderson, Ch. 6, Academic Press, New York, 1970

[13] L. M. Sverdlov, M. A. Kovner and E. P. Krainiv, *Vibrational Spectra of Polyatomic Molecules*, Halsted Press, Wiley, New York, 1974.

[14] P. Bauschewitz, *Spectroscopic Infrarouge*, Vols. 1 and 2, Gauthier Villars, Paris, 1961, 1967.

[15] S. J. Cyvin, *Molecular Vibrations and Mean Square Amplitudes*, Elsevier, Amsterdam, 1968.

[16] J. A. Pople, in *Modern Theoretical Chemistry*, Ed. H. F. Schaefer III, Vol. 4, Plenum, New York, 1977.

[17] I. M. Mills, in *Molecular Spectroscopy*, Eds. K. N. Rao and C. W. Mathews, Academic Press, New York, 1972.

[18] G. Fogarasi and P. Pulay, in *Vibrational Spectra and Structure*, A series of Advances, Ed. J. R. Durig, Vol. 14, Elsevier, Amsterdam, 1985.

[19] R. Poirier, R. Kari and I. G. Csizamadia, *Handbook of Gaussian Basis sets*, Elsevier Science, New York, 1985.

[20] C. C. J. Roothan, Rev. Mod. Phys., 23 (1951) 69.

[21] G. Hall, Proc. Roy. Soc. (London), A205 (1951) 541.

[22] (a) L. Salem and C. Rowland, Angew. Chem. Int. Edn. Engl., 11 (1972) 92. (b) W. J. Hehre, L. Salem and M. R. Wilcott, J. Am. Chem. Soc., 96 (1974) 4328. (c) R. E. Townshend, G. Ramuni, G. Segal, W. J. Hehre and L. Salem, J. Am. Chem. Soc., 98 (1976) 2190. (d) S. R. Langhoff and E. R. Davidson, Int. J. Quant. Chem., 8 (1974) 61. (e) J. A. Pople, R. Seeger and R. Krishnan, Int. J. Quant. Chem. Symp., 11 (1977) 149.

[23] (a) C. Moller and M. S. Plesset, Phys. Rev., 46 (1934) 618. (b) J. A. Pople, J. S. Binkley and R. Seeger, Int. J. Quant. Chem. Symp., 10 (1976) 1.

[24] C. W. Bauschlicher, S. R. Lanhoff and P. R. Taylor, Adv. Chem. Phys., 77 (1990) 103.

[25] I. N. Levine, *Quantum Chemistry*, p 222ff, 4^{th} edn., Prentice Hall, Englewood Cliffs., N. J., 1991.

[26] E. R. Davidson and D. Feller, Chem. Rev., 86 (1986) 681.

[27] H. Setters and J. Almlöf, J. Phys. Chem., 93 (1989) 5136.

[28] W. J. Hehre, R. F. Stewart and J. A. Pople, J. Chem. Phys., 51 (1969) 2657.

[29] W. J. Hehre, R. Ditchfield, R. F. Stewart and J. A. Pople, J. Chem. Phys., 52 (1970) 2769.

[30] W. J. Pietro, B. A. Levi, W. J. Hehre and R. F. Stewart, Inorg. Chem., 19 (1980) 2225.

[31] W. J. Pietro, F. S. Blurock, R. S. Hout, W. J. Hehre, D. J. Defrees and R. F. Stewart, Inorg. Chem., 20 (1981) 3650.

[32] W. J. Pietro and W. J. Hehre, J. Comput. Chem., 4 (1983) 241.

[33] P. Pulay, G. Fogarasi, F. Pang and J. E. Boggs, J. Am. Chem. Soc., 101 (1979) 2550.

[34] J. S. Binkley, J. A. Pople and W. J. Hehre, J. Am. Chem. Soc., 102 (1980) 939.

[35] M. S. Gordon, J. S. Binkley, J. A. Pople, W. J. Pietro and W. J. Hehre, J. Am. Chem. Soc., 104 (1982) 2797.

[36] W. J. Pietro, M. M. Francl, W. J. Hehre, J. A. Pople and J. S. Binkley, J. Am. Chem. Soc., 104 (1982) 5048.

[37] T. Clark, J. Chandrasekhar, G. Spitznagel and P. v. R. Schleyer, J. Comput. Chem., 4 (1983) 294.

[38] R. Ditchfield, W. J. Hehre and J. A. Pople, J. Chem. Phys., 54 (1971) 724.

[39] W. J. Hehre, R. Ditchfield and J. A. Pople, J. Chem. Phys., 56 (1972) 2257.

[40] W. J. Hehre and W. A. Latham, J. Chem. Phys., 56 (1972) 5225.

[41] M. M. Francl, W. J. Pietro, W. J. Hehre, J. S. Binkley, M. S. Gordon, D. J. Defrees and J. A. Pople, J. Chem. Phys., 77 (1982) 3654.

[42] R. H. Nobes, W. R. Rodwell and L. Radom, J. Comput. Chem., 3 (1982) 561.

[43] J. Chandrasekhar, J. G. Andrade and P. v. R. Schleyer, J. Am. Chem. Soc., 103 (1981) 5609.

[44] J. R. Durig and A. Wang, J. Mol. Str. (Theochem), 294 (1993) 13.

[45] M. Born and R. Oppenheimer, Ann. Phys. (Leipzig), 84 (1927) 457.

[46] P. Pulay, G. Fogarasi, F. Pang and J. E. Boggs, J. Am. Chem. Soc., 101 (1979) 256.

[47] (a) P. Botschwina, Chem. Phys. Lett., 29 (1974) 98. (b) P. Botschwina, Chem. Phys., 40 (1979) 33. (c) P. Botschwina, H. Härtner and W. Sawodny, Chem. Phys. Lett., 74 (1980) 156. (d) P. Botschwina, Chem. Phys., 68 (1982) 41. (e) P. Botschwina, Mol. Phys., 47 (1982) 241.

[48] (a) P. Pulay, A. Ruoff and W. Sawodny, Mol. Phys., 30 (1975) 1123. (b) P. Pulay, W. Meyer and J. E. Boggs, J. Chem. Phys., 68 (1978) 5077. (c) P. Pulay, J. G. Lee and J. E. Boggs, J. Chem. Phys., 79 (1983) 3382. (d) see reference 17, p 198ff

[49] (a) H. B. Schlegel, S. Wolfe and F. Bernardi, J. Chem. Phys., 67 (1977) 4194, 63 (1975) 3632, 67 (1977) 4181. (b) C. W. Bock, M. Trachtman and P. George, J. Mol. Spectrosc., 84 (1980) 256. (c) C. W. Bock, M. Trachtman and P. George, J. Mol. Str., 89 (1981) 76. (d) D. Steel, W. B. Person and K. G. Brown, J. Phys. Chem., 85 (1981) 2007.

[50] J. R. Durig, T. J. Geyer and Y. H. Kim, J. Mol. Str., 244 (1991) 103.

[51] M. Eliashevich, C. R. Acad. Sci., U. S. S. R., 28 (1940) 605.

[52] H. C. Urey and C. A. Bradley, Phys. Rev., 38 (1931) 1969.

[53] D. E. Munn, T. Shimanouchi, J. H. Meal and L. Fano, J. Chim. Phys., 27 (1957) 43.

[54] J. H. Schachtschneider and R. G. Snyder, Spectrochim. Acta., 19 (1963) 117.

[55] P. Pulay, Mol. Phys., 17 (1969) 197.

[56] D. Papoušek and J. Plíva, Czech. Chem. Commun., 28 (1963) 755.

[57] B. L. Crawford and W. H. Fletcher, J. Chem. Phys., 19 (1951) 141.

[58] P. Pulay and W. Meyer, J. Mol. Spectrosc., 40 (1971) 58.

[59] P. Pulay and W. Meyer, Mol. Phys., 27 (1974) 473.

[60] P. Botschwina, Chem. Phys. Lett., 29 (1974) 580.

[61] P. Botschwina, Chem. Phys. Lett., 41 (1976) 486.

[62] C. Pouchan, A. Dargelos and M. Chaillet, J. Mol. Spectrosc., 76 (1979) 118.

[63] J. P. Dognon, C. Pouchan, A. Dargelos and J. P. Flament, Chem. Phys. Lett., 109 (1984) 492.

[64] (a) W. Bleicher and P. Botschwina, Mol. Phys., 30 (1975) 1029. (b) P. Botschwina, W. Meyer and A. M. Semkow, Chem. Phys., 15 (1976) 25.

[65] (a) G. Fogarasi, P. Pulay, K. Molt and W. Sawodny, Mol. Phys., 33 (1977) 1565. (b) K. O. Christie, E. C. Curtis, W. Sawodny, H. Härtner and G. Fogarasi, Spectrochim. Acta, 37A (1981) 549.

[66] C. Pouchan, D. Liotand, A. Dargelos and M. Chaillet, J. Chim. Phys., 73 (1976) 1046.

[67] J. R. Durig, A. Y. Wang, J. S. Little and P. A. Brletic, J. Chem. Phys., 93 (1990) 905.

[68] P. Pulay, G. Fogarasi, G. Pongor, J. E. Boggs and A. Vargha, J. Am. Chem. Soc., 105 (1983) 7037.

[69] P. Botschwina, Chem. Phys. Lett., 29 (1974) 98.

[70] C. E. Blom and C. Altona, Mol. Phys., 31 (1976) 1377.

[71] C. E. Dykstra, S. Y. Liu and D. J. Malik, in "Advances in Chemical Physics", Vol 75, Wiley, New York, 1989.

[72] P. Pulay, G. Fogarasi and J. E. Boggs, J. Chem. Phys., 74 (1981) 3999.

[73] R. D. Amos, Chem. Phys. Lett., 114 (1985) 10.

[74] A. Komoronicki and W. J. McIver, J. Chem. Phys., 70 (1979) 2014.

[75] G. B. Bacskay, S. Saebo and P. R. Taylor, Chem. Phys., 90 (1984) 215.

[76] D. R. Hartree, *Numerical Analysis*, Oxford University Press, New York, 1968.

[77] W. B. Person and G. Zerbi, Eds., *Vibrational intensities in Infrared and Raman Spectroscopy*, Elsevier, Amsterdam, 1982.

[78] R. McWeeny, Phys. Rev., 126 (1961) 1028.

[79] R. McWeeny, Rev. Mod. Phys., 32 (1960) 335.

[80] M. J. Frisch, Y. Yamaguchi, J. F. Gaw, H. F. Schaefer III and J. S. Binkley, J. Chem. Phys., 84 (1986) 531.

[81] Y. Yamaguchi, M. J. Frisch, J. F. Gaw, H. F. Schaefer III and J. S. Binkley, J. Chem. Phys., 84 (1986) 2262.

[82] W. A. Goddard and F. W. Bobrowicz, in *Modern Theoretical Chemistry*, Ed. H. F. Schaefer III, Vol. 3, Plenum, New York, 1977.

[83] Gaussian 90, Revision I, M. J. Frisch, M. Head Gordon, G. W. Trucks, J. B. Foresman, H. B. Schlegel, K. Raghavachari, M. Robb, J. S. Binkley, C. Gonzalez, D. J. Defrees, D. J. Fox, R. A. Whiteside, R. Seeger, C. F. Melius, J. Backer, R. L. Martin, L. R. Kahn, J. J. P. Stewart, S. Topiol and J. A. Pople, Gaussian Inc., Pittsburgh PA, 1990.

[84] J. H. Schachtschneider, *Vibrational Analysis of Polyatomic Molecules*, Parts-V and VI, Technical Report No. 23164, Shell Development Company, Emeryville CA, 1964.

Chapter 3

The Pyruvate system

In this chapter the results of our studies on two systems, pyruvic acid and pyruvate anion are presented.

A number of theoretical studies exist for pyruvic acid because of its small size and more so because of its interesting structure and properties. It has been studied at the semi empirical INDO level [1,2] and also at the AM1 level [3]. At the ab initio level studies of pyruvic acid range from the calculation of energies at the STO-3G level [4] to the more recent calculations of energies using the HF/3-21G [3], HF/4-21G [5], HF/4-31G, HF/6-31G** and MP2/4-31G [6] methods. Except for the study of Murto et al. [6] all the studies have exclusively focussed on the energies and geometries of pyruvic acid.

On the other hand, the only theoretical study on the pyruvate anion has been the AM1 and 3-21G study of the keto and enol forms [3]. In general, very few theoretical studies exist on the geometries and vibrational spectra of anions of polyatomic molecules. The focus of the few existing studies has been at the evaluation of electron affinities [7,8]. Ab initio studies of anions are difficult because the diffuse spatial extent of outermost orbitals in anions should be taken into account in all calculations.

The normal coordinate analysis of pyruvic acid has been done by Hollenstein et al. [9] based on the microwave structure of pyruvic acid [10]. They had assigned the gas phase frequencies of pyruvic acid. A normal coordinate analysis of the pyruvate anion has been done by Kakihana et al. [11]. In their study the solid state IR spectra of sodium pyruvate and four of its isotopomers were used to generate the force constants. The X-Ray structures of sodium pyruvate [12,13], potassium pyruvate [13] and benzamidinium pyruvate [14] have also been elucidated.

3.1 Pyruvic acid

The vibrational frequencies of four conformations of pyruvic acid were evaluated using the 4-21G, 6-31G* and 6-31G** basis sets. The starting structures were obtained from the optimized conformations of Alsenoy et al. [5]. The 6-31G** optimized conformations are plotted in Figure 3.1. It was observed that conformations II and IV gave negative frequencies inspite of their low energy differences relative to the minimum energy conformation (I). In both conformation II and IV the methyl group is staggered with respect to the carbonyl oxygen.

Since Murto et al. [6] have calculated the geometries of pyruvic acid at the MP2/4-21G level and also assigned the HF/4-31G frequencies to the corresponding experimental spectra, we do not discuss these aspects here. The symmetry coordinates, calculated frequencies, potential energy distributions and the calculated force constants are given in Tables 3.1 to 3.6.

3.1.1 Staggered vs Eclipsed Conformations

Studies on $CH_3C(=X)Y$ systems like acetic acid, acetaldehyde and isobutene had highlighted the structural consequences of the so called methyl hyperconjugation [15]. These studies which included geometry optimizations at the HF/4-21G level had calculated the energy differences for the staggered and eclipsed conformations and on the basis of the energetic differences and the resulting structural changes, had attributed the stability of the eclipsed conformation to methyl hyperconjugation.

Pyruvic acid due to the presence of a strong intramolecular hydrogen bond involving the carbonyl oxygen and the carboxyl hydrogen should prove to be the right candidate to study the effect of methyl hyperconjugation. Previous studies by Cordell and Boggs [16] on the electron density distributions of furan, pyrrole and thiophene had recommended the use of polarization functions on the heavy atoms to obtain reasonable maps. Hence we used the 6-31G* basis set optimized geometries to obtain the electron density distributions. Plotting the valence electron density distribution using the 6-31G** basis set proved to be cumbersome because of the size of the molecule and the basis.

The resulting electron distributions are plotted in Figures 3.2 and 3.3 [17]. It can be easily seen from the plot that the delocalization of the electron density is profound in case of conformation I compared to that in conformation II. The plots clearly indicate that methyl conjugation plays an important role in the stabilization of conformation I. Thus

the orientation of the methyl group plays an important role in maximizing or minimizing the extent of electron delocalization in pyruvic acid. The extent of delocalization eventually translates itself into the existence of conformation II as a transition state in the potential surface of pyruvic acid calculated at all these levels. These observations can be supplemented by the values of the force constants which indicate that the bond between the methyl and the carbonyl groups has significant double bond character. This could also be the reason for the stability of the resulting enol form of pyruvic acid.

3.2 Pyruvate anion

A recent study of the oxalate dianion by Dewar et al. [18] using the AM1 semiempirical method had indicated that the two carboxylate groups are perpendicular to each other. Calculations at the ab initio level using the 6-31G* and 6-31+G basis corroborated their findings at the AM1 level. Calculations on the oxalate dianion at the 3-21G and 4-21G level by us indicated that the two carboxylate groups were in the same plane. Similarly the AM1 study of pyruvate anion indicated that the carboxylate group was perpendicular to the $CH_3C = O$ group [3]. On the other hand the 3-21G study of the pyruvate anion indicated that the carboxylate group was in the same plane as the $CH_3C = O$ group [3]. The X-Ray structures of sodium pyruvate, potassium pyruvate and benzamidinium pyruvate indicated that the carboxylate group was nearly in the same plane as the $CH_3C = O$ group. Understandably either the AM1 calculation with its inherent approximations or the inadequacy of the 3-21G and 4-21G basis in the description of the anion geometries was responsible for the widely conflicting results on the exact structure of the oxalate dianion and the pyruvate anion.

We initially employed the 6-31G** and 6-31++G** basis sets and performed calculations at the Hartree Fock level on the pyruvate anion and our calculations indicated that the carboxylate group was perpendicular to the $CH_3C = O$ group. However the calculations at the HF/4-21G level showed that the planar form was more stable. Hence we performed calculations using the 4-31G* and 6-31G** basis at the second order Moller Plesset level of theory and in this process tried to resolve the issue of the minimum energy orientation of the carboxylate group. The structure of pyruvate anion was optimized at all the levels and the vibrational frequencies were calculated at all levels except the MP2/6-31G** level. The calculated vibrational frequencies alongwith the calculated IR intensities, potential energy distributions were used as aids in assigning the solid state IR

spectra of sodium pyruvate. Vibrational frequencies at the Moller Plesset level reveal some interesting deviations for which we have proposed an explanation.

The geometry of the pyruvate anion was the X-Ray structure of sodium pyruvate [12]. An alternate structure of the pyruvate anion was also obtained by abstracting the carboxyl hydrogen in pyruvic acid. Optimizations at the 4-21G level indicated that the two structures converged to the same structure. We performed optimizations employing two different point group symmetries C_1 and C_s. Since calculations using the C_1 symmetry involve the variation of all the variables, we found it to be useful in isolating the global minima. The vibrational frequencies at the Hartree Fock level were evaluated analytically while at the Moller Plesset level they were evaluated numerically.

The energies and relative energies of the two sets of calculations are given in Table 3.7. The optimized geometries at all the levels of calculation alongwith the corresponding X-Ray data of sodium pyruvate, potassium pyruvate and benzamidinium pyruvate are given in Table 3.8. An optimized structure of the pyruvate anion at the MP2/6-31G** level is given in Figure 3.4.

3.2.1 Geometries and Energies

It can be seen from Table 3.7 that the C_s and C_1 forms have the same energy at the HF/4-21G, MP2/4-31G* and MP2/6-31G** levels. At the HF/6-31G** level the C_s is nearly 1.57 kJ/mol more energetic than the corresponding C_1 form. The energy difference increases to nearly 7.56 kJ/mol at the HF/6-31++G** level. Negative frequencies are obtained for the C_s structure at both the HF/6-31G** and HF/6-31++G** levels indicating that it is a transition state structure.

Since the geometries of the C_s and C_1 structures are same at the HF/4-21G, MP2/4-31G* and MP2/6-31G** levels the geometries of only the C_s structure are given in Table 3.8. At the MP2/6-31G** level the $C - COO^-$ distance is $1.565A^o$while the $CH_3 - C$ distance is $1.520A^o$. Thus the $C - COO^-$ distance is slightly longer than a normal $C - C$ bond and significantly longer than a $C - COOH$ distance (the MP2/4-31G distance is pyruvic acid is $1.535A^o$), a finding which has implications for the tendency of α-keto acids to decarboxylate. The corresponding experimental values given in Table 3.8 also support these findings. The $O5 - C3 - O6$ angle is 131.6°in the MP2/6-31G** optimized structure. Surprisingly, the value of this angle does not change with basis sets. Moreover in all the experimental data (X-Ray crystallography) the value of this angle is around 127^o. On the

other hand the lengths of the $C-O$ bonds change considerably as different basis sets are used.

The orientation of the carboxylate group is of particular interest in the present study. Dewar's ab initio calculations on oxalate dianion using the HF/6-31G* and HF/6-31+G basis sets indicated that the structure in which the two carboxylate groups were perpendicular to each other(D_{2d}) was about 4.88 kcal/mol more stable than the corresponding planar (D_{2h}) structure at the HF/6-31G* level. The use of the HF/6-31+G basis set increases this energy difference to 6.31 kcal/mol. Our calculations on the pyruvate anion using the HF/6-31G** and HF/6-31++G** basis sets indicate a similar trend though the energy differences are small. The experimental structures of sodium pyruvate, potassium pyruvate and benzamidinium pyruvate clearly indicate that the carboxylate group is nearly in the same plane as the $CH_3C=O$ group. The calculations at the Moller Plesset level using the 4-31G* and 6-31G** substantiate the fact that the carboxylate group is in the same plane as the $CH_3C=O$ group.

We have calculated the barrier heights of the carboxylate group rotation and the methyl group rotation. The results are plotted in Figures 3.5 and 3.6. The carboxylate group rotation has been carried out on a single orientation of the methyl hydrogen (cis to the keto oxygen). The barrier height is around 6.2 kJ/mol at the MP2/6-31G** level. At the MP2/4-31G* the barrier height is about 7.6 kJ/mol. The low barrier height energies are in accordance with the observations made earlier. This also implies that the out of plane twists of the carboxylate group are energetically accessible. This is in conformance with the earlier calculations on the carboxylate group rotation by Umeyama et al. [19] and Norris et al. [3]. In case of the methyl hydrogen the calculations were carried out on the two different orientations of the carboxylate oxygen. Since the calculations were done using different bond lengths for the carboxylate oxygens, we obtain different plots for the different orientations. The difference in energies in the two conformations having different orientations of the carboxylate oxygen is about 2.6 kJ/mol. The barrier height to the methyl group rotation is about 7.7 kJ/mol at the MP2/6-31G** level. It increases to about 9.1 kJ/mol at the MP2/4-31G* level. Three distinct minima are observed at 0°, 120°, and 240°. Maxima are observed at 60°, 180°and 300°. The maxima at 180°is lower than the maxima at either 60°or 300°.

3.2.2 Vibrational Frequencies

The vibrational frequencies have been calculated on all the optimized geometries. Since the calculations indicate that the C_s and C_1 forms possess the same structure at the HF/4-21G, MP2/4-31G* and the MP2/6-31G** levels the frequencies of the C_s form calculated at the HF/4-21G and MP2/4-31G* level are used in the assignments. Frequency calculations at the HF/6-31G** and HF/6-31++G** levels give negative frequencies for the C_s form. This indicates that the C_s form is a transition state in the potential energy surface of the pyruvate anion calculated at these levels. It is of interest to note that the energy of the C_s form is only about 1.57kJ/mol higher than the C_1 form at the HF/6-31G** level but even then negative frequencies are obtained.

The earlier vibrational analysis of Kakihana et al. [11] was done using the X-Ray parameters of Tavale et al. [12]. The force fields for the $CH_3C = O$ group were transferred from the calculation of pyruvic acid and for the carboxylate group the parameters were transferred from sodium acetate. We assigned the spectra of sodium pyruvate using the ab initio frequencies calculated at the HF/4-21G and MP2/4-31G* levels. The symmetry coordinates of pyruvate anion in the C_s form is given in Table 3.9. The calculated frequencies and assignments alongwith the corresponding experimental frequencies and assignments are given in Table 3.10. The calculated potential energy distributions are given in Table 3.11. In case of the frequencies of the A" species the ab initio assignments are in agreement with the earlier NCA assignments of Kakihana et al. [11]. Moreover the assignments at the HF/4-21G level agree with the assignments at the MP2/4-31G* level. The salient points of the assignment are that the out of plane $C = O_k$ bend comes lower than the corresponding out of plane COO bend.

In case of the A' species the current assignments are in agreement with the earlier assignments of Kakihana et al. [11] for frequencies above $1406cm^{-1}$but there are a number of deviations in the lower frequencies. Our calculations both at the HF/4-21G and MP2/4-31G* level indicate that the $\delta_s(CH_3)$ mode comes higher than the $\nu_s(COO^-)$ mode in contrast to the observations made earlier. In the formate ion the $\nu_s(COO^-)$ mode has been assigned to the frequencies at 1360.6 and $1357cm^{-1}$in the IR and Raman spectra of sodium formate respectively [20]. This is in accordance with the present ab initio assignment of $\nu_s(COO^-)$ at $1353.9cm^{-1}$rather than at $1405.9cm^{-1}$as assigned earlier. However, in the acetate ion this mode has been assigned to the frequencies at around 1440 and 1423.7 in the IR spectra of sodium acetate recorded at two different temperatures 290K and 80K

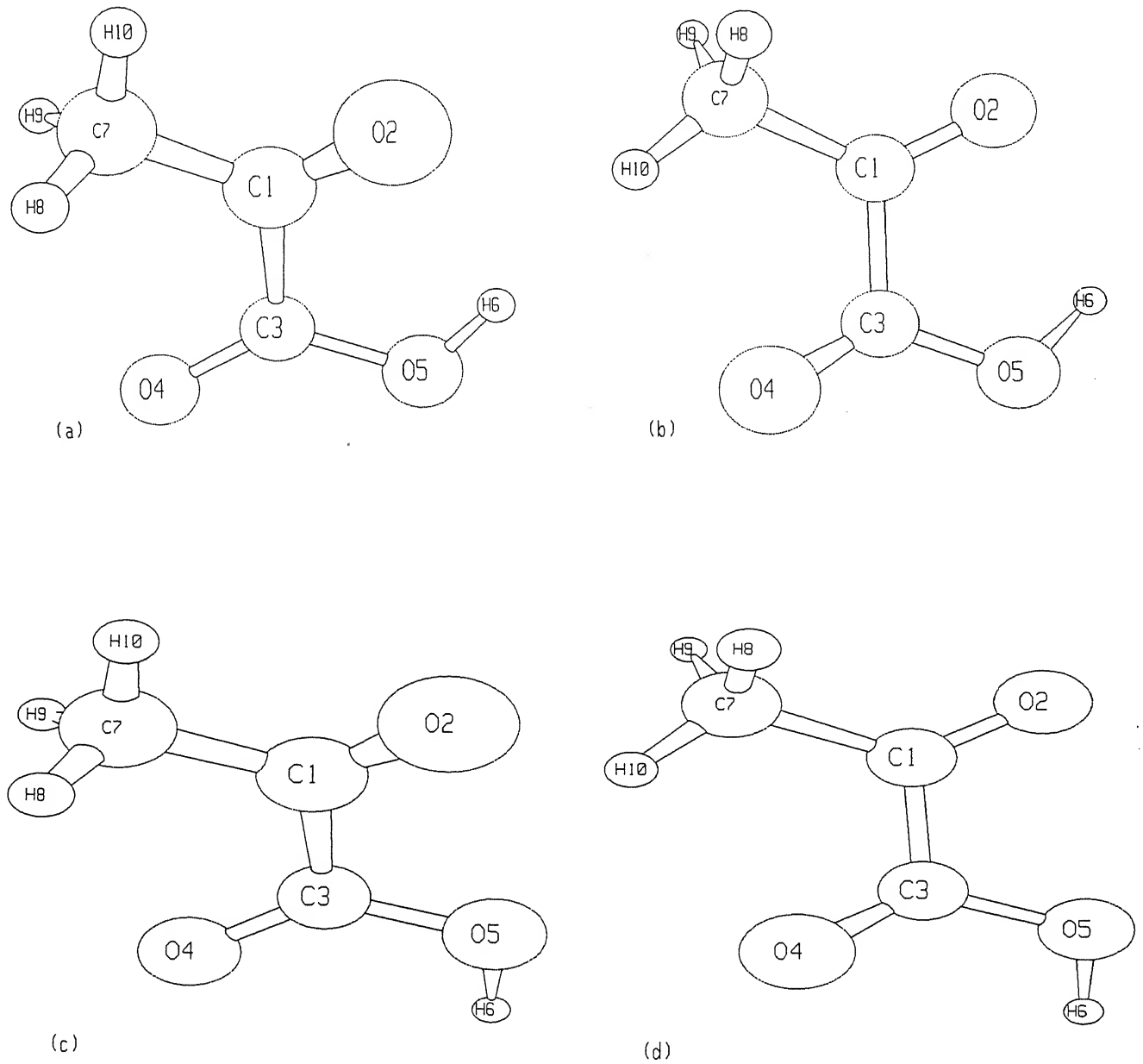

Figure 3.1: 6-31G** optimized structures of all the conformations of Pyruvic acid. (a) I, (b) II, (c) III and (d) IV.

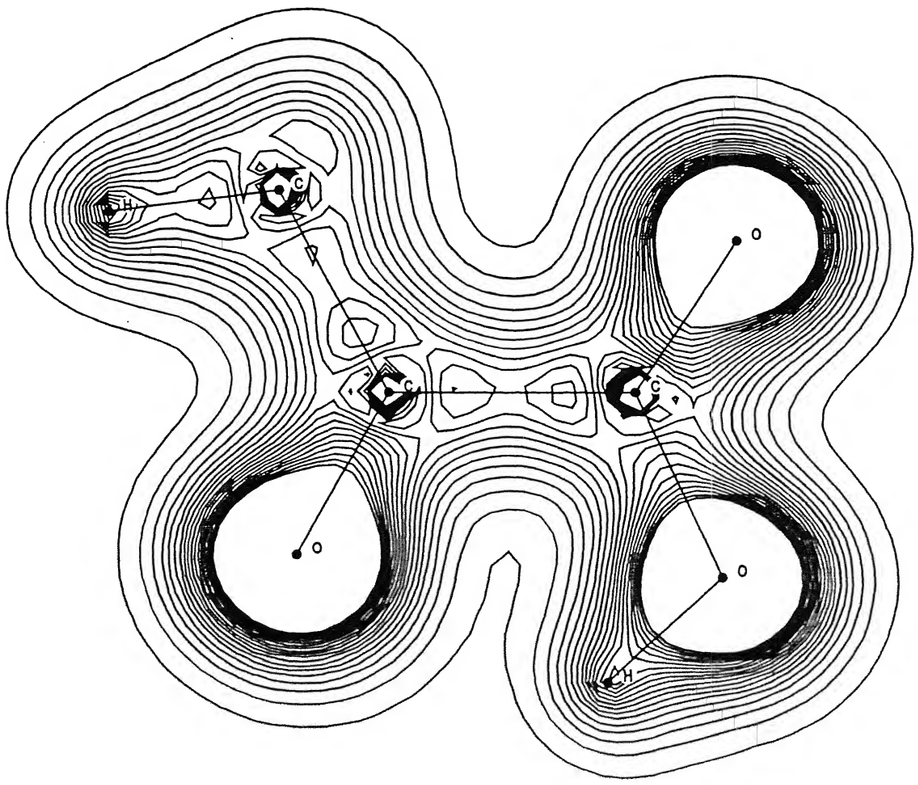

CONTOUR	VALUE
1	0.02500
2	0.05000
3	0.07500
4	0.10000
5	0.12500
6	0.15000
7	0.17500
8	0.20000
9	0.22500
10	0.25000
11	0.27500
12	0.30000
13	0.32500
14	0.35000
15	0.37500
16	0.40000
17	0.42500
18	0.45000
19	0.47500

Figure 3.2: Valence electron density map of conformation I of pyruvic acid evaluated using the 6-31G* basis set. Interval between contours is 0.02500 electrons per cubic a. u..

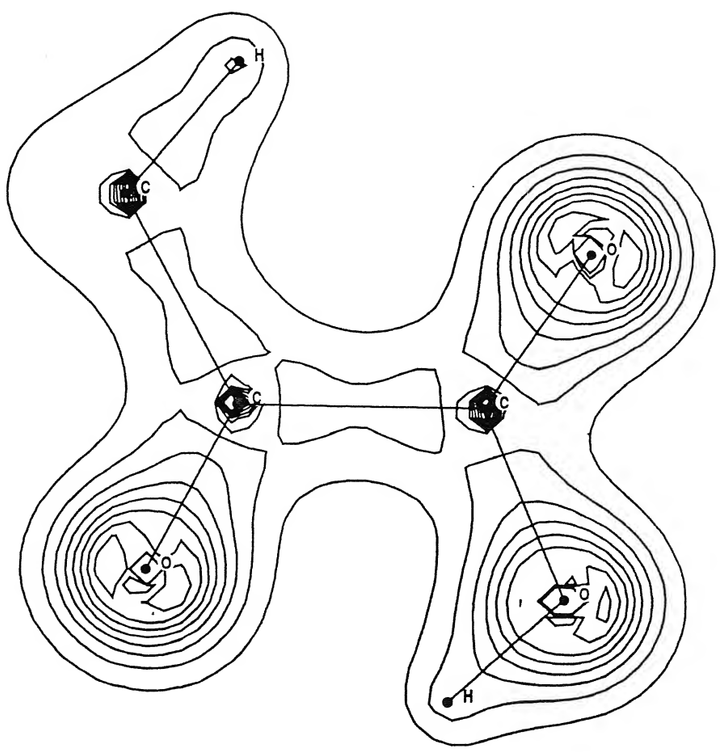

CONTOUR	VALUE
1	0.12500
2	0.25000
3	0.37500
4	0.50000
5	0.62500
6	0.75000
7	0.87500
8	1.00000
9	1.12500

Figure 3.3: Valence electron density map of conformation III of pyruvic acid evaluated using the 6-31G* basis set. Interval between contours is 0.12500 electrons per cubic a. u..

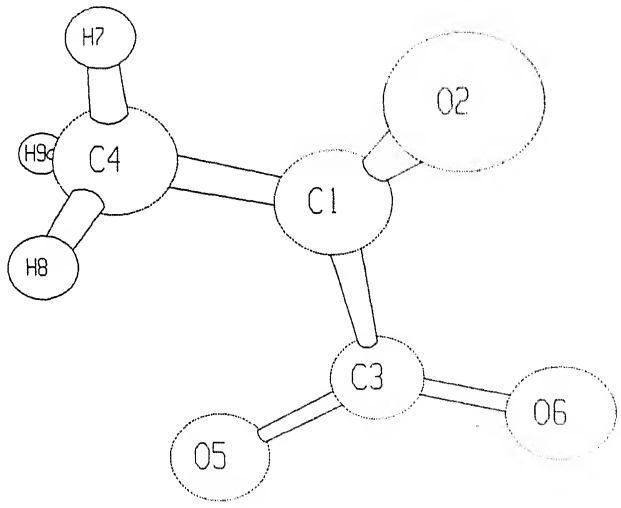

Figure 3.4: MP2/6-31G** optimized structure of the Pyruvate anion.

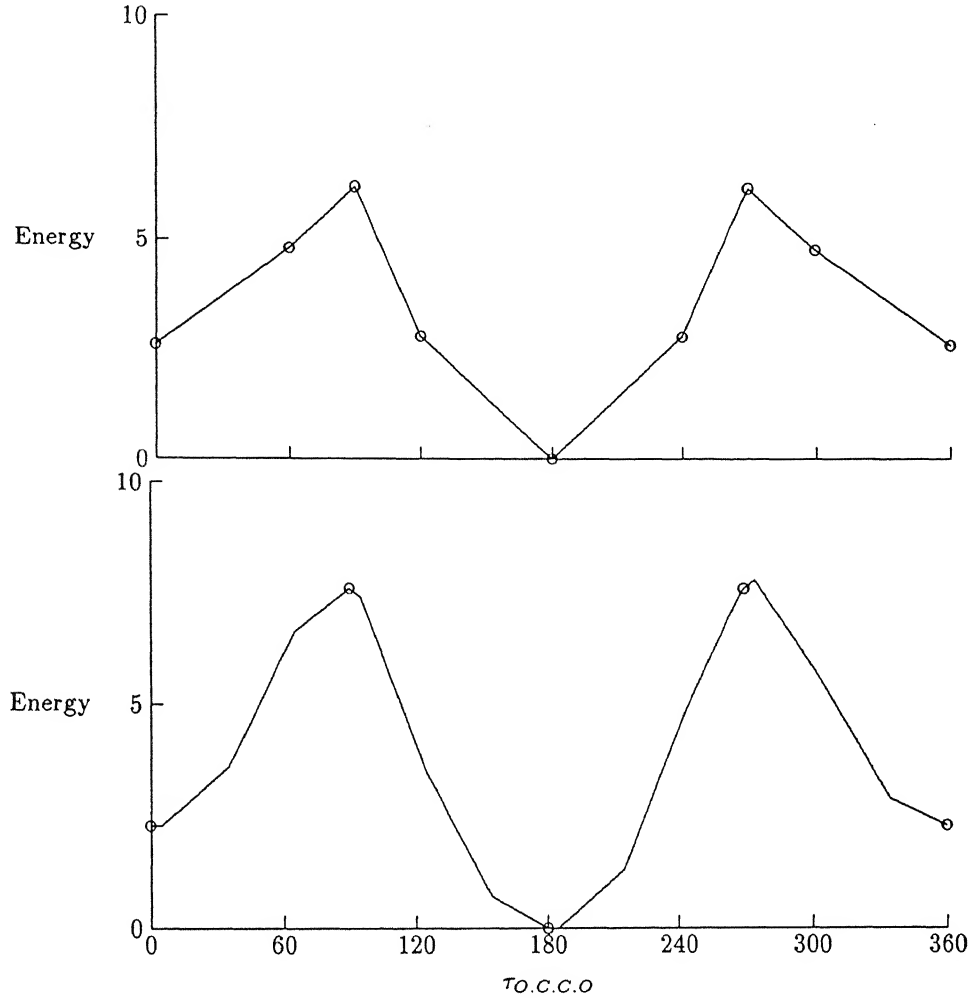

Figure 3.4: Variation of Energy with the torsional angle $\tau[O5.C3.C1.O2]$ in pyruvate anion. The lower plot corresponds to the MP2/4-31G* results. Energy is in kJ/mol.

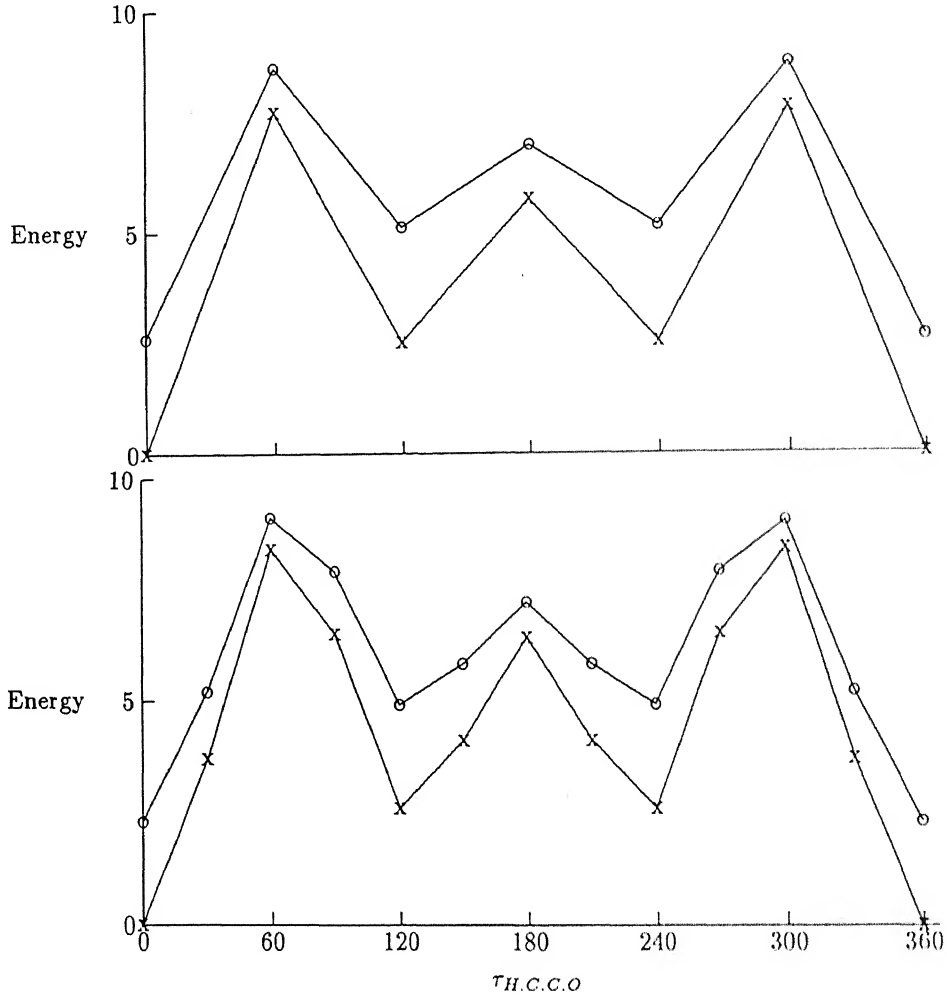

Figure 3.5: Variation of Energy with the torsional angle $\tau[H7.C4.C2.O1]$ in pyruvate anion. The lower plot corresponds to the MP2/4-31G* results. x corresponds to O1.C2.C3.O5. angle of 180° and o corresponds to O1.C2.C3.O5 angle of 0° Energy is in kJ/mol.

Table 3.1: Symmetry coordinates of pyruvic acid

Coordinate	Notation	Description
A' species		
$S_1 = (1/\sqrt{6})(2R_{7.10} - R_{7.8} - R_{7.9})$	$\nu_a(CH_3)$	asym. CH_3 stretch
$S_2 = (1/\sqrt{3})(R_{7.10} + R_{7.8} + R_{7.9})$	$\nu_s(CH_3)$	sym. CH_3 stretch
$S_3 = R_{5.6}$	$\nu(OH)$	OH stretch
$S_4 = R_{3.4}$	$\nu(C = O_a)$	acid $C = O$ stretch
$S_5 = R_{1.2}$	$\nu(C = O_k)$	keto $C = O$ stretch
$S_6 = R_{3.5}$	$\nu(C - O)$	$C - O$ stretch
$S_7 = R_{1.3}$	$\nu(C_aC_k)$	acid C-keto C stretch
$S_8 = R_{1.7}$	$\nu(C_kC_m)$	keto C-methyl C stretch
$S_9 = (1/\sqrt{6})(2\alpha_{8.7.9} - \alpha_{8.7.10} - \alpha_{9.7.10})$	$\delta_a(CH_3)$	asym. CH_3 deformation
$S_{10} = (1/\sqrt{6})(\alpha_{8.7.9} + \alpha_{8.7.10} + \alpha_{9.7.10} - \beta_{1.7.8} - \beta_{1.7.9} - \beta_{1.7.10})$	$\delta_s(CH_3)$	sym. CH_3 deformation
$S_{11} = (1/\sqrt{6})(2\beta_{1.7.10} - \beta_{1.7.8} - \beta_{1.7.9})$	$\gamma_{\parallel}(CH_3)$	in plane CH_3 rock
$S_{12} = \alpha_{3.5.6}$	$\delta(COH)$	COH bend
$S_{13} = 2\alpha_{1.3.4} - \alpha_{1.3.5} - \alpha 4.3.5$	$\delta(O - CC)$	$O - CC$ bend
$S_{14} = 2\alpha_{2.1.7} - \alpha_{2.1.3} - \alpha 3.1.7$	$\delta(CCC)$	CCC bend
$S_{15} = \alpha_{1.3.5} - \alpha_{4.3.5}$	$\gamma_{\parallel}(C = O_a)$	in plane acid $C = O$ wag
$S_{16} = \alpha_{2.1.3} - \alpha_{3.1.7}$	$\gamma_{\parallel}(C = O_k)$	in plane keto $C = O$ wag
$S_{17} = (1/\sqrt{6})(\alpha_{9.7.10} + \alpha_{8.7.10} + \alpha_{8.7.9} + \beta_{1.7.8} + \beta_{1.7.9} + \beta_{1.7.10})$		redundant
A" species		
$S_1 = (1/\sqrt{2})(R_{7.8} - R_{7.9})$	$\nu_a(CH_3)$	CH_3 stretch
$S_2 = (1/\sqrt{2})(\alpha_{8.7.10} - \alpha_{9.7.10})$	$\delta(CH_3)$	CH_3 deformation
$S_3 = (1/\sqrt{2})(\beta_{1.7.8} - \beta_{1.7.9})$	$\gamma_{\perp}(CH_3)$	out of plane CH_3 rock
$S_4 = \tau_{5.3.1.4}$	$\gamma_{\perp}(C = O_a)$	out of plane acid $C = O$ wag
$S_5 = \tau_{2.1.3.7}$	$\gamma_{\perp}(C = O_k)$	out of plane keto $C = O$ wag
$S_6 = \tau_{1.3.5.6} + \tau_{4.3.5.6}$	$\tau(CO)$	OH torsion
$S_7 = \tau_{2.1.3.4} + \tau_{2.1.3.5} + \tau_{7.1.3.4} + \tau_{7.1.3.5}$	$\tau(C_kC_a)$	skeletal torsion
$S_8 = \tau_{2.1.7.8} + \tau_{2.1.7.9} + \tau_{2.1.7.10} + \tau_{3.1.7.8} + \tau_{3.1.7.9} + \tau_{3.1.7.10}$	$\tau(C_kC_m)$	CH_3 torsion

Atom numbering is given in Figure 3.1.

Table 3.2: Assignment of the calculated frequencies of conformation I of pyruvic acid to the gas phase IR spectra of pyruvic acid

No.	4-21G		6-31G*		6-31G**		Exp.	OD	I. I.	R. A.
	Uns	Sca	Uns	Sca	Uns	Sca				
A' species										
1	274	245	277	248	276	247	258.0	48	.0	9.0
2	424	384	431	390	429	388	388.4	41	.1	.4
3	584	530	582	528	582	528	534.7	8	.2	26.0
4	638	580	655	594	655	595	603.8	72	1.3	10.9
5	799	743	849	789	850	790	762.4	30	.3	31.6
6	1065	981	1078	985	1072	978	968.6	53	2.3	3.3
7	1249	1153	1274	1178	1271	1176	1136.7	75	2.8	30.5
8	1322	1203	1374	1248	1366	1239	1214.4	298	1.3	151.8
9	1429	1312	1541	1389	1528	1377	1354.8	644	1.1	2.1
10	1573	1408	1574	1448	1566	1444	1384.4	82	8.2	12.1
11	1617	1447	1601	1432	1583	1416	1424.4	24	2.8	12.6
12	1930	1824	2024	1916	2023	1915	1729.4	89	1.8	.7
13	2007	1893	2084	1967	2083	1967	1799.7	345	1.9	72.3
14	3219	3054	3230	3064	3209	3045	2936.0	2	4.6	153.5
15	3321	3152	3338	3167	3321	3151	3032.5?	2	2.0	263.1
16	3825	3629	4015	3809	4090	3880	3432.2	100	2.1	129.8
A" species										
1	92	83	92	83	91	81	119.5	-	12.4	12.1
2	136	122	132	118	129	115	-	-	14.5	10.1
3	453	405	440	393	439	393	394.4	39	10.4	276.1
4	656	587	688	616	682	610	664.3	293	20.1	215.0
5	799	714	797	713	794	711	720	2	107.4	.7
6	1175	1051	1149	1027	1141	1021	1017.8	16	58.1	3.7
7	1631	1459	1607	1437	1591	1423	1405.9	8	61.1	7.6
8	3274	3107	3295	3127	3278	3111	3032.5?	2	24.2	147.7

Uns : Unscaled, Sca : Scaled, Exp. : Experimental gas phase values from reference [9], OD : experimental relative optical density, I. I : IR intensities in units of KM/mol, R. A : Raman activities in units of A^4/AMU.

Table 3.3: Assignment of the calculated frequencies of conformation III of pyruvic acid to the gas phase IR spectra of pyruvic acid

No.	4-21G		6-31G*		6-31G**		Exp.	OD	I. I.	R. A.
	Uns	Sca	Uns	Sca	Uns	Sca				
A' species										
1	271	242	270	241	269	241	258.0	48	.0	7.9
2	420	380	421	381	421	381	388.4	41	.1	.0
3	570	518	571	518	571	518	534.7	8	.0	11.3
4	627	567	644	582	644	583	603.8	72	1.8	.6
5	778	725	821	764	821	764	762.4	30	.9	.1
6	1054	975	1074	983	1068	976	968.6	53	2.3	2.1
7	1218	1116	1269	1171	1265	1167	1136.7	75	1.4	102.3
8	1301	1184	1366	1236	1355	1225	1214.4	298	2.6	143.6
9	1506	1386	1538	1389	1527	1376	1354.8	644	1.3	51.0
10	1573	1409	1574	1453	1567	1451	1384.4	82	11.7	21.4
11	1621	1451	1605	1435	1587	1419	1424.4	24	3.0	26.2
12	1945	1842	2031	1922	2030	1922	1729.4	89	2.0	.4
13	1965	1854	2063	1948	2062	1948	1799.7	345	1.2	237.9
14	3221	3056	3229	3063	3208	3044	2936.0	2	3.3	71.8
15	3318	3149	3335	3164	3318	3148	3032.5?	2	3.2	64.2
16	3855	3657	4052	3844	4130	3918	3432.2	100	1.2	12.4
A" species										
1	79	70	42	37	41	36	119.5	-	12.3	11.3
2	135	120	145	129	141	126	-	-	15.1	9.3
3	437	391	423	379	422	378	394.4	39	.3	534.1
4	633	566	662	592	655	586	664.3	293	31.3	5.1
5	806	721	813	727	810	725	720	2	107.0	1.7
6	1180	1056	1154	1032	1146	1025	1017.8	16	58.1	6.9
7	1637	1464	1611	1441	1595	1426	1405.9	8	63.1	9.2
8	3277	3109	3293	3124	3276	3108	3032.5?	2	79.4	131.2

Uns : Unscaled, Sca : Scaled, Exp. : Experimental gas phase values from reference [9]. OD : experimental relative optical density, I. I : IR intensities in units of KM/mol, R. A : Raman activities in units of A^4/AMU.

Table 3.4: Calculated potential energy distributions of conformation I of pyruvic acid using different basis sets

	HF/4-21G		*HF/6-31G**		*HF/6-31G***	
	Freq.	PED	Freq.	PED	Freq.	PED
A' species						
1	274	16(49.4),13(26.1),15(12.0)	277	16(51.6),13(24.1),14(11.7)	276	16(51.6),13(24.1),14(11.4)
2	424	14(44.4),15(30.5), 7(11.5)	431	14(40.4),15(32.1), 7(12.5)	429	14(40.4),15(31.9), 7(12.5)
3	584	13(41.7),16(23.7), 7(17.4)	582	13(44.4),16(22.9), 7(18.4)	582	13(44.3),16(22.7), 7(18.5)
4	638	14(36.0), 8(21.4),15(20.9)	655	14(36.3),15(24.3), 8(19.2)	655	14(36.4),15(24.0), 8(19.2)
5	799	7(32.6),15(29.0)	849	7(30.3),15(29.4), 8(14.6)	850	7(30.2),15(29.4), 8(14.6)
6	1065	8(35.2),11(34.0)	1078	11(49.1), 8(25.5)	1072	11(50.1), 8(24.7)
7	1249	6(41.2),11(25.4)	1274	6(37.8),11(20.3), 8(12.7) ,14(11.4)	1271	6(37.3),11(19.0), 8(13.3) ,14(11.8)
8	1322	12(38.7), 7(14.6), 8(11.6) ,11(10.0)	1374	12(47.8), 7(14.0) -	1366	12(51.1), 7(12.7) -
9	1429	12(38.6), 6(24.8), 7(14.1)	1541	10(50.4),12(19.3), 6(16.5)	1528	10(59.0),12(14.9), 6(13.9)
10	1573	10(93.6) -	1574	10(33.9), 6(17.8),12(14.0) ,7(11.4), 8(10.5)	1566	10(25.2), 6(21.5),12(14.9) , 7(13.2), 8(10.1)
11	1617	9(89.1)	1601	9(89.3)	1583	9(87.2)
12	1930	5(83.4)	2024	5(84.2)	2023	5(84.3)
13	2007	4(78.1)	2084	4(76.4)	2083	4(76.5)
14	3219	2(96.4)	3230	2(97.4)	3209	2(97.8)
15	3321	1(96.8)	3338	1(97.7)	3321	1(98.0)
16	3825	3(99.9)	4015	3(99.9)	4090	3(99.9)
A" species						
1	92	8(56.0), 7(20.1)	92	7(73.8), 6(13.5)	91	7(69.9), 6(12.5), 8(11.3)
2	136	7(65.7), 8(20.1), 6(10.2)	132	8(73.0), 3(10.3)	129	8(70.7)
3	453	5(56.5), 4(33.6)	440	5(59.9), 4(28.8)	439	5(59.9), 4(28.5), 3(10.2)
4	656	6(98.2)	688	6(94.6)	682	6(95.5)
5	799	4(55.9), 5(22.8), 3(20.2)	797	4(58.2), 3(23.2), 5(15.9)	794	4(58.2), 3(24.1), 5(15.4)
6	1175	3(72.2), 5(14.3)	1149	3(70.0), 5(16.4)	1141	3(68.9), 5(17.1)
7	1631	2(91.8)	1607	2(93.5)	1591	2(93.4)
8	3274	1(99.8)	3295	1(99.8)	3278	1(99.8)

Freq. : Frequencies, PED : Potential energy distributions, Symmetry coordinate numbering is given in Table 3.1.

Table 3.5: Calculated potential energy distributions of conformation III of pyruvic acid using different basis sets

	HF/4-21G		*HF/6-31G**		*HF/6-31G***	
	Freq.	PED	Freq.	PED	Freq.	PED
A' species						
1	271	16(43.7),13(33.8),15(18.6)	270	16(48.4),13(31.4),15(14.6)	269	16(48.4),13(31.4),15(14.4)
2	420	14(48.3),15(23.5), 7(14.0)	421	14(45.0),15(25.8), 7(14.6)	421	14(44.8),15(25.8), 7(14.6)
3	570	13(39.9),16(29.1), 7(15.5)	571	13(42.2),16(26.1), 7(18.0)	571	13(42.2),16(25.9), 7(18.1)
4	627	14(35.5),15(25.0), 8(13.4)	644	14(34.9),15(27.6), 8(13.1)	644	14(34.8),15(27.5), 8(13.2)
5	778	7(33.6),15(23.8), 8(15.5) , 6(10.5)	821	7(30.3),15(23.4), 8(18.4) , 6(10.2)	821	7(30.1),15(23.6), 8(18.3) -
6	1054	8(38.3),11(27.3), 6(11.9)	1074	11(45.1), 8(29.0)	1068	11(46.3), 8(28.1)
7	1218	6(35.5),12(29.4),11(19.6) -	1269	6(29.3),11(24.4), 8(14.5) ,14(13.1)	1265	6(29.3),11(22.7), 8(14.7) ,14(13.2)
8	1301	12(25.4),11(19.2), 8(16.0) ,14(13.9), 7(13.1)	1366	12(61.7) -	1355	12(63.1) -
9	1506	6(30.5),12(27.5), 7(16.3) ,13(12.3)	1538	10(52.3), 6(18.5) -	1527	10(66.1), 6(13.1) -
10	1573	10(93.6) -	1574	10(39.6), 6(17.1), 7(13.0) , 8(11.0)	1567	10(25.5), 6(23.1), 7(16.1) -
11	1621	9(90.0)	1605	9(90.0)	1587	9(87.4)
12	1945	4(60.0), 5(29.1)	2031	4(64.9), 5(23.1)	2030	4(65.6), 5(22.4)
13	1965	5(52.3), 4(24.7)	2063	5(60.3), 4(19.4)	2062	5(61.0), 4(18.9)
14	3221	2(96.9)	3229	2(97.2)	3208	2(97.6)
15	3318	1(97.2)	3335	1(97.5)	3318	1(97.8)
16	3855	3(99.9)	4052	3(99.9)	4130	3(99.9)
A" species						
1	79	7(77.9), 8(15.0)	42	7(91.0)	41	7(89.2)
2	135	8(77.1)	145	8(78.2), 3(11.7)	141	8(77.8), 3(11.4)
3	437	5(51.4), 4(33.2)	423	5(54.9), 4(29.8)	422	5(54.7), 4(29.5)
4	633	6(85.3)	662	6(80.0), 5(11.8)	655	6(80.1), 5(11.9)
5	806	4(55.3), 5(20.8), 3(19.4) -	813	4(57.1), 3(19.5), 5(11.8) , 6(10.6)	810	4(57.1), 3(20.4), 5(11.5) -
6	1180	3(71.9), 5(15.0)	1154	3(69.8), 5(16.9)	1146	3(68.6), 5(17.5)
7	1637	2(92.2)	1611	2(93.7)	1595	2(93.6)
8	3277	1(99.8)	3293	1(99.8)	3276	1(99.8)

Freq. : Frequencies, PED : Potential energy distributions, Symmetry coordinate numbering is given in Table 3.1.

Table 3.6: Calculated diagonal force constants of the two conformations of pyruvic acid using different basis sets

	Sym. Cor.	*4-21G*				*6-31G*				*6-31G*			
		CI		CIII		CI		CIII		CI		CIII	
		Uns	Sca	Uns	Sca	Uns	Sca	Uns	Sca	Uns	Sca	Uns	Sca
A' species													
1	$\nu_a(CH_3)/\nu_a(CH_3)$	5.9323	5.3390	5.9266	5.3340	5.9745	5.3770	5.9663	5.3697	5.9149	5.3234	5.9069	5.3163
2	$\nu_s(CH_3)/\nu_s(CH_3)$	6.0064	5.4057	6.0103	5.4093	6.0377	5.4339	6.0327	5.4294	5.9596	5.3636	5.9548	5.3593
3	$\nu(OH)/\nu(OH)$	8.1812	7.3630	8.3126	7.4813	9.0134	8.1120	9.1864	8.2677	9.3527	8.4174	9.5430	8.5887
4	$\nu(C=O_a)/\nu(C=O_a)$	15.3907	13.8516	15.0882	13.5794	16.9241	15.2317	16.4970	14.8473	16.9148	15.2233	16.4983	14.8484
5	$\nu(C=O_k)/\nu(C=O_k)$	14.5735	13.1161	15.1363	13.6227	16.3109	14.6798	16.8734	15.1860	16.3085	14.6776	16.8718	15.1847
6	$\nu(C-O)/\nu(C-O)$	7.4310	6.6879	7.3748	6.6373	8.3805	7.5425	8.2936	7.4642	8.4163	7.5747	8.3324	7.4992
7	$\nu(C_aC_k)/\nu(C_aC_k)$	4.2978	3.8680	4.3038	3.8734	4.7144	4.2430	4.6291	4.1662	4.7122	4.2410	4.6195	4.1576
8	$\nu(C_kC_m)/\nu(C_kC_m)$	4.8296	4.3466	4.7081	4.2373	5.1217	4.6095	5.0497	4.5448	5.1155	4.6039	5.0346	4.5311
9	$\delta_a(CH_3)/\delta_a(CH_3)$	0.6456	0.5165	0.6520	0.5216	0.6328	0.5063	0.6391	0.5113	0.6175	0.4940	0.6225	0.4980
10	$\delta_s(CH_3)/\delta_s(CH_3)$	0.7293	0.5834	0.7266	0.5813	0.6923	0.5539	0.6904	0.5523	0.6766	0.5413	0.6761	0.5409
11	$\gamma_{\parallel}(CH_3)/\gamma_{\parallel}(CH_3)$	0.7980	0.6384	0.8011	0.6408	0.7683	0.6146	0.7718	0.6174	0.7548	0.6038	0.7581	0.6064
12	$\delta(COH)/\delta(COH)$	0.9360	0.7488	0.8472	0.6777	0.9831	0.7864	0.8722	0.6977	0.9628	0.7702	0.8450	0.6760
13	$\delta(O-CC)/\delta(O-CC)$	1.2221	0.9777	1.1392	0.9113	1.2497	0.9998	1.1732	0.9386	1.2491	0.9993	1.1735	0.9388
14	$\delta(CCC)/\delta(CCC)$	1.1252	0.9002	1.1287	0.9030	1.1662	0.9330	1.1481	0.9184	1.1679	0.9343	1.1489	0.9191
15	$\gamma_{\parallel}(C=O_a)/\gamma_{\parallel}(C=O_a)$	1.4022	1.1218	1.3459	1.0768	1.4313	1.1451	1.3812	1.1049	1.4273	1.1419	1.3832	1.1065
16	$\gamma_{\parallel}(C=O_k)/\gamma_{\parallel}(C=O_k)$	1.2886	1.0309	1.2514	1.0011	1.2495	0.9996	1.1756	0.9405	1.2471	0.9977	1.1762	0.9410
A" species													
1	$\nu_a(CH_3)/\nu_a(CH_3)$	5.8019	5.2217	5.8088	5.2279	5.8645	5.2780	5.8549	5.2694	5.8055	5.2249	5.7961	5.2165
2	$\delta(CH_3)/\delta(CH_3)$	0.6590	0.5272	0.6655	0.5324	0.6437	0.5149	0.6488	0.5191	0.6305	0.5044	0.6347	0.5078
3	$\gamma_{\perp}(CH_3)/\gamma_{\perp}(CH_3)$	0.7439	0.5952	0.7423	0.5939	0.6727	0.5381	0.6733	0.5386	0.6591	0.5273	0.6609	0.5288
4	$\gamma_{\perp}(C=O_a)/\gamma_{\perp}(C=O_a)$	0.5163	0.4130	0.5191	0.4152	0.5406	0.4325	0.5442	0.4354	0.5409	0.4327	0.5454	0.4363
5	$\gamma_{\perp}(C=O_k)/\gamma_{\perp}(C=O_k)$	0.5995	0.4796	0.6411	0.5129	0.5483	0.4386	0.5767	0.4613	0.5489	0.4391	0.5766	0.4613
6	$\tau(CO)/\tau(CO)$	0.0969	0.0776	0.0803	0.0642	0.1075	0.0860	0.0932	0.0745	0.1054	0.0843	0.0900	0.0720
7	$\tau(C_kC_a)/\tau(C_kC_a)$	0.0627	0.0502	0.0235	0.0188	0.0373	0.0298	0.0063	0.0050	0.0369	0.0295	0.0061	0.0049
8	$\tau(C_kC_m)/\tau(C_kC_m)$	0.0045	0.0036	0.0065	0.0052	0.0066	0.0053	0.0080	0.0064	0.0064	0.0051	0.0076	0.0061

All force constants are in units of $mdynes/A^o$. Uns : Unscaled, Sca : Scaled, CI : conformation I, CIII : conformation III.

Table 3.7: Absolute and relative energies of the pyruvate anion after various levels of optimization

Level		C_1 *species*		C_s *species*	
		Energy(a.u)	$\Delta E(kJ/mol)$	Energy(a.u)	$\Delta E(kJ/mol)$
I	4-21G	-339.1486	-0.0001	-339.1486	0.0
II	6-31G**	-339.9736	-1.5675	-339.9730	0.0
III	6-31++G**	-340.0006	-7.5378	-339.9977	0.0
IV	MP2/4-31G*	-340.5757	-0.0003	-340.5757	0.0
V	MP2/6-31G**	-340.9285	0.0	-340.9285	0.0

Table 3.8: Calculated and experimental geometrical parameters of the pyruvate anion

				C_s species				*C_1 species*			*Experimental*	
			TI	TII	TIII	TIV	TV	TII	TIII	EI	EII	EIII
Bond length(A^o)												
	1	2	1.216	1.196	1.196	1.229	1.232	1.199	1.201	1.207(3)	1.203(7)	1.196(3)
	1	3	1.569	1.572	1.574	1.563	1.565	1.550	1.537	1.559(3)	1.550(7)	1.532(3)
	1	4	1.518	1.519	1.517	1.518	1.520	1.518	1.516	1.498(4)	1.486(8)	1.488(4)
	3	5	1.252	1.234	1.236	1.263	1.266	1.234	1.231	1.239(3)	1.240(6)	1.246(2)
	3	6	1.242	1.221	1.222	1.251	1.254	1.224	1.231	1.255(3)	1.248(6)	1.241(2)
	4	7	1.083	1.085	1.085	1.093	1.089	1.085	1.084	0.98(5)	1.027(7)	0.971(c)
	4	8	1.082	1.084	1.084	1.090	1.087	1.083	1.086	0.97(4)	1.004(6)	0.940(c)
	4	9	1.082	1.084	1.084	1.090	1.087	1.088	1.086	0.91(5)	0.981(7)	0.950(c)
Bond angle(^{o})												
1	3	5	112.697	112.701	112.774	112.631	112.561	112.090	114.234	116.5(2)	116.4(4)	117.1(2)
1	3	6	115.912	115.765	116.181	115.703	115.884	116.239	114.233	116.2(2)	116.9(4)	116.9(2)
5	3	6	131.391	131.534	131.045	131.666	131.555	131.660	131.449	127.3(2)	126.7(5)	126.0(2)
2	1	3	124.178	123.652	123.271	124.159	124.227	124.209	124.104	119.6(2)	119.2(4)	119.2(2)
2	1	4	122.224	120.306	120.345	120.427	120.257	120.561	121.021	123.5(2)	123.3(5)	121.8(2)
3	1	4	113.598	116.041	116.384	115.414	115.516	115.186	114.876	116.9(2)	117.4(5)	119.0(2)
7	4	1	110.646	109.841	109.506	109.931	109.977	110.301	110.307	109.0(3)	110.6(7)	109.9(c)
8	4	1	109.093	109.817	109.870	109.507	109.438	108.923	109.200	109.0(3)	109.4(6)	106.7(c)
9	4	1	109.093	109.817	109.870	109.507	109.438	109.829	109.204	113.0(3)	106.7(5)	108.8(c)
7	4	8	110.822	110.551	110.607	110.884	110.908	110.904	110.219	108.6(c)	107.2(c)	102.8(c)
7	4	9	110.822	110.551	110.607	110.884	110.908	109.800	110.220	101.9(c)	110.6(c)	112.1(c)
8	4	9	106.247	106.204	106.337	106.047	106.088	107.021	107.638	114.4(c)	112.4(c)	116.0(c)
Dihedral angle(^{o})												
2	1	3	5	180.000	180.000	180.000	180.000	180.000	128.408	-91.479	-	-	-
2	1	3	6	.000	.000	.000	.020	.000	-52.657	91.478	-16.1(3)	20.9(7)	5.8(3)
4	1	3	5	.000	.000	.000	.000	.000	-49.202	88.522	-16.4(3)	22.4(7)	-5.2(c)
4	1	3	6	180.000	180.000	180.000	180.000	180.000	129.734	-88.521	-	-	-
2	1	4	7	.000	.000	.000	.000	.000	3.404	.000	1.0(3)	1.6(9)	-2.5(c)
2	1	4	8	-122.167	-121.784	-121.672	-122.056	-122.070	-118.534	-121.258	-	-	-
2	1	4	9	122.167	121.784	121.672	122.056	122.070	124.557	121.286	-	-	-
3	1	4	7	180.000	180.000	180.000	180.000	180.000	-178.892	180.000	179.0(3)	-178.1(5)	177.4(c)
3	1	4	8	57.833	58.216	58.328	57.944	57.930	59.170	58.741	-	-	-
3	1	4	9	-57.833	-58.216	-58.328	-57.944	-57.930	-57.738	-58.714	-	-	-

TI, TII, TIII, TIV, TV are the optimized structures at the HF/4-21G, HF/6-31G**, HF/6-31++G**, MP2/4-31G* and MP2/6-31G** levels respectively. EI, EII, EIII are the X-Ray structures of sodium pyruvate, potassium pyruvate and benzamidinium pyruvate respectively. EI and EII are from reference [13]. EIII is from reference [14].(c) indicates that the parameters were calculated from the X-Ray coordinates.

Table 3.9: Symmetry coordinates of pyruvate anion

Coordinate	Notation	Description
A' species		
$S_1 = (1/\sqrt{6})(2R_{4.7} - R_{4.8} - R_{4.9})$	$\nu_a(CH_3)$	asym. CH_3 stretch
$S_2 = (1/\sqrt{3})(R_{4.7} + R_{4.8} + R_{4.9})$	$\nu_s(CH_3)$	sym. CH_3 stretch
$S_3 = R_{1.2}$	$\nu(C = O_k)$	keto $C = O$ stretch
$S_4 = R_{3.5} - R_{3.6}$	$\nu_a(COO)$	asym. COO stretch
$S_5 = R_{3.5} + R_{3.6}$	$\nu_s(COO)$	sym. COO stretch
$S_6 = R_{1.3}$	$\nu(C_aC_k)$	acid C-keto C stretch
$S_7 = R_{1.4}$	$\nu(C_kC_m)$	keto C-methyl C stretch
$S_8 = (1/\sqrt{6})(2\alpha_{8.4.9} - \alpha_{7.4.8} - \alpha_{7.4.9})$	$\delta_a(CH_3)$	asym. CH_3 deformation
$S_9 = (1/\sqrt{6})(\alpha_{8.4.9} + \alpha_{7.4.8} + \alpha_{7.4.9} - \beta_{1.4.7} - \beta_{1.4.8} - \beta_{1.4.9})$	$\delta_s(CH_3)$	sym. CH_3 deformation
$S_{10} = (1/\sqrt{6})(2\beta_{1.4.7} - \beta_{1.4.8} - \beta_{1.4.9})$	$\gamma_{\parallel}(CH_3)$	in plane CH_3 rock
$S_{11} = 2\alpha_{1.3.5} - \alpha_{1.3.6} - \alpha 5.3.6$	$\delta(OCO)$	OCO bend
$S_{12} = 2\alpha_{2.1.4} - \alpha_{2.1.3} - \alpha 3.1.4$	$\delta(CCC)$	CCC bend
$S_{13} = \alpha_{1.3.6} - \alpha_{5.3.6}$	$\gamma_{\parallel}(COO)$	in plane acid COO wag
$S_{14} = \alpha_{2.1.3} - \alpha_{3.1.4}$	$\gamma_{\parallel}(C = O_k)$	in plane keto $C = O$ wag
$S_{15} = (1/\sqrt{6})(\alpha_{8.4.9} + \alpha_{7.4.8} + \alpha_{7.4.9} + \beta_{1.4.7} + \beta_{1.4.8} + \beta_{1.4.9})$		redundant
A" species		
$S_1 = (1/\sqrt{2})(R_{4.8} - R_{4.9})$	$\nu_a(CH_3)$	CH_3 stretch
$S_2 = (1/\sqrt{2})(\alpha_{7.4.8} - \alpha_{7.4.9})$	$\delta(CH_3)$	CH_3 deformation
$S_3 = (1/\sqrt{2})(\beta_{1.4.8} - \beta_{1.4.9})$	$\gamma_{\perp}(CH_3)$	out of plane CH_3 rock
$S_4 = \tau_{6.3.1.5}$	$\gamma_{\perp}(COO)$	out of plane acid COO wag
$S_5 = \tau_{2.1.3.4}$	$\gamma_{\perp}(C = O_k)$	out of plane keto $C = O$ wag
$S_6 = \tau_{2.1.3.5} + \tau_{2.1.3.6} + \tau_{4.1.3.5} + \tau_{4.1.3.6}$	$\tau(C_kC_a)$	skeletal torsion
$S_7 = \tau_{2.1.4.7} + \tau_{2.1.4.8} + \tau_{2.1.4.9} + \tau_{3.1.4.7} + \tau_{3.1.4.8} + \tau_{3.1.4.9}$	$\tau(C_kC_m)$	CH_3 torsion

Atom numbering is given in Figure 3.4

Table 3.10: Assignment of the calculated frequencies of pyruvate anion at the HF/4-21G and MP2/4-31G* to the solid state IR spectra of sodium pyruvate

No.	4-21G S.I	Ass.	MP2/4-31G* US.IV	Ass.	Exp. Obsd.	Ass.[a]
A' species						
1	266(11.4)	$\gamma_{\parallel}(C=O_k)$	280(7.5)	$\gamma_{\parallel}(C=O_k)$	298.9	$\gamma_{\parallel}(COO)$
2	379(1.1)	$\delta(CCC)$	403(1.7)	$\delta(CCC)$	396.0	$\gamma_{\parallel}(C=O_k)$
3	500(2.24)	$\delta(OCO)$	525(1.5)	$\delta(OCO)$	545.5	$\delta(CCC)$
4	590(16.9)	$\delta(CCC)$	629(22.0)	$\delta(CCC)$	631.2	$\gamma_{\parallel}(C=O_k)$
5	777(111.7)	$\gamma_{\parallel}(COO)$	821(59.6)	$\gamma_{\parallel}(COO)$	834.1	$\delta(OCO)$
6	949(16.5)	$\nu(C_kC_m)$	987(8.3)	$\gamma_{\parallel}(CH_3)$	981.8	$\gamma_{\parallel}(CH_3)$
7	1140(83.2)	$\gamma_{\parallel}(CH_3)$	1206(78.6)	$\nu(C_kC_m)$	1188.4	$\nu(C_kC_m)$
8	1345(206.6)	$\nu_s(COO)$	1372(98.3)	$\nu_s(COO)$	1353.9	$\delta_s(CH_3)$
9	1372(46.2)	$\delta_s(CH_3)$	1417(37.5)	$\delta_s(CH_3)$	1405.9[b]	$\nu_s(COO)$
10	1448(19.6)	$\delta_a(CH_3)$	1527(14.3)	$\delta_a(CH_3)$	1425.8	$\delta_a(CH_3)$
11	1769(443.3)	$\nu_a(COO)$	1764(72.3)	$\nu(C=O_k)$	1633.0	$\nu_a(COO)$
12	1807(107.8)	$\nu(C=O_k)$	1811(333.4)	$\nu_a(COO)$	1709.0	$\nu(C=O_k)$
13	3045(27.4)	$\nu_s(CH_3)$	3105(20.8)	$\nu_s(CH_3)$	2932.0	$\nu_s(CH_3)$
14	3118(35.7)	$\nu_a(CH_3)$	3207(36.1)	$\nu_a(CH_3)$	3024.2	$\nu_a(CH_3)$
A" species						
1	67(2.0)	$\tau(C_kC_a)$	34(1.6)	$\tau(C_kC_a)$	-	$\tau(C_kC_a)$
2	126(0.0)	$\tau(C_kC_m)$	149(0.1)	$\tau(C_kC_m)$	-	$\tau(C_kC_m)$
3	406(24.7)	$\gamma_{\perp}(C=O_k)$	408(15.5)	$\gamma_{\perp}(C=O_k)$	432.3	$\gamma_{\perp}(C=O_k)$
4	727(14.4)	$\gamma_{\perp}(COO)$	743(5.1)	$\gamma_{\perp}(COO)$	749.6	$\gamma_{\perp}(COO)$
5	1016(2.1)	$\gamma_{\perp}(CH_3)$	1039(2.4)	$\gamma_{\perp}(CH_3)$	1017.5	$\gamma_{\perp}(CH_3)$
6	1464(2.7)	$\delta(CH_3)$	1531(1.9)	$\delta(CH_3)$	1406	$^c\delta(CH_3)$
7	3118(13.6)	$\nu_a(CH_3)$	3211(12.0)	$\nu_a(CH_3)$	2988.5	$\nu_a(CH_3)$

S.I and US.IV are the scaled 4-21G and unscaled MP2/4-31G* frequencies. The parameters given in parantheses are the calculated IR intensities in units of KM/mol.(a) The assignments are of reference 11. (b) This frequency is approximate. All frequencies are in cm^{-1}.

Table 3.11: Calculated frequencies and potential energy distributions of the pyruvate anion at the 4-21G and MP2/4-31G* levels

No.	*4-21G*			*MP2/4-31G**	
	US.I	S.I	PED.I	US.IV	PED.IV
A' species					
1	297	266	14(46.8),11(31.4),13(18.7)	280	14(50.0),11(31.0),13(17.0)
2	415	379	12(52.4), 6(30.7)	403	12(51.5), 6(26.2),13(10.7)
3	551	500	11(41.0),14(25.5), 6(14.3)	525	11(44.2),14(25.1), 6(14.6)
4	640	590	12(33.7), 7(27.5), 6(17.5),10(10.0)	629	12(35.2), 7(23.7),13(13.8), 6(12.3)
5	852	777	13(54.0), 6(17.0),11(11.7)	821	13(47.5), 6(22.0), 7(10.5)
6	1033	949	7(34.9),10(33.1)	987	10(48.3), 7(25.1)
7	1248	1140	10(35.4),12(20.5), 7(20.4)	1206	7(26.0),10(22.4),12(20.1)
8	1429	1345	5(71.4), 6(11.8),13(10.2)	1372	5(67.4), 6(15.0)
9	1533	1372	9(94.1)	1417	9(87.2), 7(10.9)
10	1617	1448	8(90.8)	1527	8(91.5)
11	1869	1769	4(89.7)	1764	3(82.3)
12	1913	1807	3(83.6)	1811	4(91.0)
13	3209	3045	2(93.0)	3105	2(95.6)
14	3286	3118	1(93.4)	3207	1(95.9)
A' species					
1	75	67	6(83.9)	34	6(83.8)
2	141	126	7(75.7), 2(15.2)	149	7(77.1), 2(13.2)
3	454	406	5(62.0), 4(29.0)	408	5(63.3), 4(26.9)
4	813	727	4(60.4), 3(22.8), 5(15.8)	743	4(60.8), 3(25.6), 5(13.1)
5	1137	1016	3(73.2), 5(15.4)	1039	3(72.2), 5(16.9)
6	1636	1464	2(94.3)	1531	2(95.9)
7	3286	3118	1(99.8)	3211	1(99.8)

US.I, S.I and US.IV are the unscaled,scaled 4-21G and unscaled MP2/4-31G* frequencies. PED.I and PED.IV are the potential energy distributions corresponding to the HF/4-21G and MP2/4-31G* calculated frequencies. All frequencies are in cm^{-1}.

3.4 References

[1] M. S. Gordon and D. E. Tallman, Chem. Phys. Lett., 17 (1974) 385.

[2] C. A. Ponce and F. Tomas Vert, An. Quin., Ser. A, 78 (1982) 53.

[3] K. E. Norris and J. E. Gready, J. Mol. Str., 258 (1992) 109.

[4] D. M. Hayes, G. L. Kenyon and P. A. Kollman, J. Am. Chem. Soc., 100 (1978) 4331.

[5] C. Van Alsenoy, L. Schäffer, K. Siam and J. D. Ewbank, J. Mol. Str., 187 (1989) 271.

[6] J. Murto, T. Raaska, H. Kunttu and M. Räsänen, J. Mol. Str., 200 (1989) 93.

[7] J. Simons and K. D. Jordan, Chem. Rev., 87 (1987) 535.

[8] J. Baker, R. H. Nobes and L. Radom, J. Comput. Chem., 7 (1986) 349.

[9] H. Hollenstein, F. Akermann and Hs. H. Günthard, Spectrochim. Acta., 34A (1978) 1041.

[10] C. E. Dyllick-Brenzinger, A. Bauder and Hs. H. Günthard, Chem. Phys., 23 (1977) 195.

[11] M. Kakihana and M. Okamoto, J. Phys. Chem., 88 (1984) 1797.

[12] S. S. Tavale, L. M. Pant and A. B. Biswas, Acta Crystallogr., 11 (1961) 1281.

[13] W. Rach, G. Kiel and G. Gattow, Z. Anorg. Allg. Chem., 563 (1988) 87.

[14] B. Kratochvíl, J. Ondŕacek, J. Krechl and J. Hasek, Acta Crystallogr., Sect. C, 43 (1987) 2182.

[15] J. O. Williams, C. van Alsenoy, J. N. Scarsdale and L. Schäffer, J. Mol. Str., 86 (1981) 103.

[16] MOLDEN, QCPE 619, Department of Chemistry, Indiana University, Bloomington, U. S. A.

[17] F. R. Cordell and J. E. Boggs, J. Mol. Str., 85 (1981) 163.

[18] M. J. S. Dewar and Y. S. Zheng, J. Mol. Str., 209 (1990) 157.

[19] H. Umeyama, S. Nakagawa and T. Nomoto, Chem. Pharm. Bull., 28 (1980) 2874.

[20] K. G. Kidd and H. M. Mantisch, J. Mol. Spectrosc., 85 (1981) 375.

[21] M. Kakihana, M. Kotaka and M. Okamoto, J. Phys. Chem., 87 (1983) 2526.

[22] J. de Villepin and A. Novak., Spectrochim. Acta, 27A (1971) 1259.

[23] P. Beak, Acc. Chem. Res., 10 (1977) 186.

[24] V. I. Danilov, J. S. Kwiatkowski, B. Lesyng and V. I. Poltev, Int. J. Quant. Chem., Quant. Biol. Symp., 8 (1981) 359.

[25] H. B. Schlegel, P. Gund and E. M. Flueder, J. Am. Chem. Soc., 104 (1982) 5347.

[26] J. E. Gready, J. Comput. Chem., 6 (1985) 377.

[27] M. Becker, Ber. Bunsenges. Phys. Chem., 68 (1964) 669.

[28] Y. Pocker, J. E. Meany, B. J. Nist and C. Zadorojny, J. Phys. Chem., 75 (1969) 2879.

[29] J. Fournier, Stud. Biophys., 113 (1986) 105.

[30] K. Ohwada, Spectrochim. Acta., 34A (1978) 141.

Chapter 4

Dicarboxylic acids

In the previous chapter our studies on pyruvic acid and the pyruvate anion clearly indicate the nature of the problems which have to be encountered in a theoretical study of carboxylic acids. In pyruvic acids the availability of gas phase data and the fundamental frequencies made the assignment of experimental frequencies from the calculations fairly straight forward. In pyruvate anion although the gas phase data is not available, the fundamental frequencies in the solid state were known and hence the assignment of experimental frequencies from the calculated frequencies and PED's is not very difficult. However when we have a new molecule for which only solid and/or solution state frequencies are available, the assignment with the help of calculated ab initio frequencies, PED's, IR and Raman intensities is a very difficult task and to a certain extent is arbitrary. The first problem is to decide on the fundamentals and the second to justify the deviations in frequencies from the calculated values when going to solid and/or solution state from the gas phase. In this chapter and the following chapters we address these two problems with reference to a number of dicarboxylic, tricarboxylic and amino acids.

The systems which we would be discussing in this chapter are the higher dicarboxylic acids malonic, hydroxymalonic, succinic, glutaric and adipic. The physical studies of these dicarboxylic acids show that the addition of a CH_2 group changes their properties dramatically [1] in comparison to oxalic acid. Thus oxalic acid crystallizes in α and β forms while the higher dicarboxylic acids crystallize only in the β form. The presence of intramolecular hydrogen bonds in the higher dicarboxylic acids has been observed by the FTIR spectra of these acids in solution. The unusually high k1/k2 ratio which is generally observed in the lower dicarboxylic acids is not observed in the higher dicarboxylic acids. This has been attributed to the stability of the monoanion through intramolecular hydrogen

bonding [1].

A scan of the literature indicates that though oxalic acid has been extensively studied there have been no detailed calculations on the higher dicarboxylic acids. Though there has been a CNDO/2 study of these acids [2], the input structures were taken from the X-Ray structures which have since been improved. We have found considerable difference in the structures obtained in the X-Ray study and the subsequent neutron diffraction data. An STO-3G calculation was done on malonic acid by Merchàn et al. [3]. More recently a HF/3-21G* [4] calculation has been done on some of the conformations of glutaric acid and it has been shown that the intramolecularly hydrogen bonded U conformation is more stable than the linear conformation. To our knowledge there has been no other calculation on the conformations of higher acids or on hydroxymalonic acid.

A number of studies exist on the IR and Raman spectra of dicarboxylic acids. A vibrational study of succinic acid and adipic acid was done by Suzuki et al. [5,6] but they assumed a C_{2h} point group instead of a C_i point group and more recently there has been a vibrational study of malonic acid [7] using normal coordinate analysis.

The aims of the present investigation include the study of the energetics of the different conformations of dicarboxylic acids and to obtain the most stable conformation as predicted by Hartree Fock theory. The structures of malonic, hydroxy malonic and succinic acids were taken from the neutron diffraction studies of the compounds [7–9]. In case of adipic acid the starting structure was taken from the X-Ray study [10]. Since the existing X-Ray structure of glutaric acid [11,12] did not have hydrogens the structure was assumed to be of C_{2h} point group, but on addition of hydrogens the structure no longer belonged to a C_{2h} group. Hence a model of glutaric acid was built assuming the linear conformation to possess C_s symmetry. In case of succinic and adipic acids a C_i point group was assumed while in case of the other acids a C_1 point group was assumed. All the structures were optimized and the frequencies were calculated at the HF/4-21G level. Since acids are electron rich species, we used the HF/6-31G** basis set to study the smaller acids and hence the effect of basis sets on geometries and frequencies can be highlighted. All the potential scans were done at the HF/4-21G level. The vibrational frequencies, Raman activities, and IR intensities were calculated analytically. The symmetry coordinates for all the acids studied are listed in Tables 4.1 to 4.5.

The optimized geometries and the corresponding neutron diffraction or X-ray parameters are given in Tables 4.6 to 4.10. The vibrational frequencies and the corresponding Raman activities and IR intensities are given in Tables 4.11 to 4.17. Raman activities and

IR intensities calculated at the 6-31G** level are more reliable than those calculated at the 4-21G level. Hence intensities and activities calculated at this level are displayed in Tables 4.13 to 4.15. The potential energy distributions are given in Tables 4.18 to 4.22. The optimized structures are shown in Figure 4.1. The frequencies of the isotopomers and the corresponding assignments of malonic acid, hydroxymalonic acid and succinic acids are given in Tables 4.23 to 4.24. Table 4.25 lists some of the values of the force constants used in the vibrational analysis of malonic, succinic and adipic acids. The diagonal force constants of all the acids are given in Tables 4.26 to 4.30. The geometries of all the acids are discussed followed by the assignment of the vibrational frequencies and then the overall trends are highlighted.

4.1 Geometries

The geometries and the potential energy scans of all the dicarboxylic acids have been evalulated at the 4-21G level which is a split valence basis set. Generally the use of polarisation functions have been recommended for electron rich species because they give accurate geometries and energies. The use of higher levels of theory which explicitly include correlation like the second order Moller Plesset theory(MP2) might give more accurate results, but given the size and number of systems involved, the use of such high levels of theory would be prohibitive. The study of pyruvic acid [13] and subsequently oxalic acid [14] which are both electron rich species have shown that the barrier heights as calculated by the 6-31G* basis set was not as accurate as those calculated at higher levels of theory. Surprisingly, the use of a HF/4-21G basis set gives accurate enough barrier heights. Hence the potential energy scans have been done with the HF/4-21G basis set. The geometries of the smaller systems have been calculated at the HF/6-31G** basis set also to indicate the effect of basis set on the geometries.

The energies of the optimized geometries of all the acids at the 4-21G level were plotted against the number of CH_2 groups present. The plot shown in Figure 4.2 indicates that the correlation of the energy to the number of CH_2 groups is linear.

4.1.1 Malonic acid

Malonic acid and its monoanion had been the subject of an ab initio calculation using the STO-3G set [3]. The aim of the earlier study has been to explain the k1/k2 ratio

observed in malonic acid and hence the focus was on the stability of the monoanion rather than the acid. In the present study the focus however is on the acid itself. The potential energy scan for the rotation of one of the carboxyl groups in malonic acid at the HF/4-21G level is shown in Figure 4.3. The dihedral angle $O7.C3.C1.C2$ gives a distinct minimum around 120°(The optimized structure has $O7.C3.C1.C2$ dihedral angle as 117.964°). There is another minimum between 260°-310°. A single maxmimum occurs at 180°. At the maximum energy conformation the oxygens of the two terminal carboxyl groups are close to each other. In the minimum energy conformation they are nearly perpendicular to each other(see Figure 4.1a). The flat space around 260°-310°indicates that a large portion of the conformational space is accessible through low energy barriers. These results are in agreement with an earlier study [3].

The optimized geometry and the corresponding neutron diffraction data are given in Table 4.6. The optimized structure is shown in Figure 4.1a. The optimized geometries are similar to the neutron diffraction structure. There is a shortening of the $O-H$ and $C=O$ bonds on optimization with the 4-21G basis set. The distances are further shortened on optimization with the 6-31G** basis set. On the other hand there is an increase in the $C-O$ bond lengths as compared to the experiment. The previous studies on pyruvic acid [13] and oxalic acid [14] are in accordance with these results. Even at the MP2/6-31G** level there was a distinct decrease in the $O-H$ bond length as compared to the experiment in oxalic acid. The $O-H$ and $C=O$ bonds are non equivalent in the experimental structure. In the neutron diffraction structure, the two carboxyl groups are not symmetry related and there are different types of hydrogen bonding in the chain [7].

4.1.2 Hydroxymalonic acid

The substitution of an hydroxyl group in place of the methylene hydrogen leads to some interesting changes. In the optimized geometries the two carboxyl groups are nearly in the same plane. Though there is no intramolecular hydrogen bonding in the neutron diffraction structure, there is a distinct formation of an intramolecular hydrogen bond between the hydroxyl hydrogen and the carboxyl oxygen in the optimized structure. The neutron diffraction study was done at two temperatures [8]. The structure at room temperature and liquid nitrogen temperature differed in the orientation of the carboxyl groups to the plane of the molecule. The optimization of both the structures led to the same structure thereby indicating that the minima obtained is not local. Eventhough the 4-21G basis is

said to be unsuitable for reproducing intramolecular interactions especially hydrogen bonding, we found that hydrogen bonding is described well in the 4-21G optimized structure. Thus, given a favourable geometry, the 4-21G basis is adequate to represent and reproduce intramolecular interactions. The fully optimized structure at the HF/4-21G level is shown in Figure 4.1b. The optimized geometries at the HF/4-21G and HF/6-31G** levels are shown in Table 4.7.

4.1.3 Succinic acid

The introduction of an additional methylene group in malonic acid brings in a lot of symmetry into the molecule. The earlier X-Ray structure of Suzuki et al. [5] which was based on Broadley's study of the same [12] had assumed succinic acid, to be of C_{2h} symmetry and they performed the normal coordinate analysis of succinic acid based on that assumption. The neutron diffraction work of succinic acid proved that it belongs to the C_i point group [9] and not to the C_{2h} point group as reported earlier. To resolve the problem of the point groups we built a structure of succinic acid having a C_1 point group and optimized the same. The C_1 structure converged to the C_i structure. The neutron diffraction of succinic acid was also reported at two temperatures viz. liquid nitrogen and room temperature. The optimization of both the structures yielded the same optimized structure. A significant feature of the optimized geometry is that the $C1 - C2$ distance increases on optimization at the 4-21G and 6-31G** level. The salient features of the optimization are similar to those discussed in malonic and hydroxymalonic acid. The potential energy scans for different changes in the torsion angle $O.C.C.C$ (both $O7.C3.C1.C2$ and $O11.C6.C2.C1$) and the $C.C.C.C$ are shown in Figure 4.4. There are three distinct minima at the $C.C.C.C$ torsion values around 60°, 180°and 300°. Two maxima are found at values around 120°and 240°. The minimum energy curve corresponds to the $O.C.C.C$ torsion value of around 0°. The scan indicates that the stability of the succinic acid is maintained when the two carboxylic ends are in the gauche or trans conformation and the hydroxyl group of the carboxylate moiety is trans to the central methylene groups. The fully optimized structure ($O.C.C.C$ = 0°and $C.C.C.C$ = 180°) shown in Figure 4.1c corresponds to the lowest central minima in the potential energy scan diagram given in Figure 4.4 with symmetry C_i. The other two minima correspond to C_1 symmetry. The optimized geometries are shown in Table 4.8.

4.1.4 Glutaric acid

The X-Ray study of β-glutaric acid by Morrison [11] indicated that it either belonged to the C_s or C_{2h} point group. They analysed the crystal structure of glutaric acid assuming a C_{2h} point group. In the absence of hydrogens such an analysis might give meaningful results. The addition of hydrogens could lead to either a C_s or a C_{2v} point group. The C_{2v} symmetry could not be imposed on the molecule because it is very much dependent on the orientation of the central methylene group. So a model of glutaric acid in the C_s symmetry was built based on the X-Ray parameters of Morrison [11]. The stability of our model was tested by constructing another model having the C_1 point group symmetry. The C_s point group model possesed the same energy as the C_1 point group model. As the molecule possesed the C_s symmetry both the carboxyl groups lie in the same plane. The potential energy scans for different changes in the torsion angle $O.C.C.C$ (both $O12.C6.C2.C1$ and $O14.C7.C3.C1$) and $C6.C2.C1.C3$ are shown in Figures 4.5 and 4.6. $C2.C1.C3.C7$ was fixed at 180°. There are three distinct minima at the $C6.C2.C1.C3$ torsion values around 60°, 180°and 300°. Two maxima are found at values around 120°and 240°respectively. The minimum energy curve corresponds to the $O.C.C.C$ torsion value of 0°. A scan was also done in which the $C2.C1.C3.C7$ was fixed at 90°. In this case the rotation around the $C1.C2$ bond is more hindered more beyond 180°and hence the minima around 240°is higher than the minima around 120°. The two potential energy scans of succinic acid and glutaric acid indicate similar trends. The barrier height of rotation in glutaric acid is lower than that of succinic acid. This indicates that the rotation about the CC bonds is more facile and hence glutaric acid can easily change conformations depending on the medium. This also confirms the findings of Takasuka et al. [4] who found that the intramolecularly hydrogen bonded conformation is more stable than the linear conformation. The frequencies were however not calculated for the intramolecularly hydrogen bonded conformation because the linear conformation posseses a C_s symmetry. The fully optimized structure shown in Figure 4.1d corresponds to a conformation in which the $O.C.C.C$ torsion angle is 0°, the $C6.C3.C2.C1$ torsion is 180°and the $C2.C1.C3.C7$ corresponds to 180°and thus the resulting structure belongs to the C_s point group. The optimized geometry is compared with the available experimental data in Table 4.9.

4.1.5 Adipic acid

The X-Ray structure of Housty et al. [10] was taken as the input for the optimization of adipic acid. The molecule belongs to the C_i point group. It very much resembles succinic acid. In this case also the earlier vibrational analysis of Suzuki et al. [6] assumed the structure to belong to the C_{2h} point group and not to the C_i point group. The trends in the geometry of adipic acid is similar to that of the previously discussed molecules. In light of the above studies no scans were done on adipic acid. The optimized geometry is compared with the available X-Ray data in Table 4.10.

4.2 Vibrational frequencies

The vibrational frequencies were calculated on the optimized geometries of the dicarboxylic acids. The frequencies have been calculated at the HF/4-21G level for all the acids. For the lower acids the frequencies were also calculated at the HF/6-31G** level to see the effect of basis set on the frequencies and assignments. The calculated frequencies at the HF/6-31G** level are too high even after scaling. This is in accordance with the earlier study of oxalic acid [14]. The assignments of both the basis sets agree in general except for a few alterations in some acids. Hence in all the cases the unscaled HF/4-21G frequencies and the corresponding potential energy distributions were used for the assignments. The other frequencies have been arranged in such a way that their potential energy distributions correspond to those of the unscaled 4-21G frequencies.

Since the gas phase spectra of these acids were not available we used the solid state IR and Raman spectra for the assignments. A number of factors have to be taken into consideration before we proceed with such an assignment. The major difference between the calculated and solid state spectra is that computations are done on an isolated molecule, while in the solid state the molecules are held together by intermolecular forces. These intermolecular forces in acids are predominantly due to hydrogen bonding. The influence of hydrogen bonding is that the $O-H$ and $C=O$ stretching frequencies decrease while the $\delta(COH)$ and out of plane OH bending ($\tau(CO)$ in our nomencalture) frequencies increase [15]. An increase in the strength of the hydrogen bond leads to further decrease of the $\nu(OH)$ and $\nu(C=O)$ frequencies and increase in the bending frequencies. The other fundamentals appear at slightly higher frequencies as in case of solid acetic acid [16]. So in going from gas to solid state, what one might expect is a decrease in the $\nu(OH)$ and

$\nu(C=O)$ and an increase in the OH bending frequencies. If we compare the acetic acid gas phase and solid state spectra as shown in Table 4.11, $\nu(OH)$ and $\nu(C=O)$ decrease as expected. The major difference in the other peaks occur for the $(\delta(COH)+\nu(CO))$ and the out of plane OH bend modes. All the other modes are in the same range of frequencies. Gasesous and solid state spectra of oxalic acid also exhibit similar trends (see Table 4.12).

Hence our strategy of assigning the calculated ab initio frequencies to the experimental solid state spectra is to expect a major shift in the experimental peaks corresponding to $\nu(CO)$, $\delta(COH)$ and $\gamma(OH)$ ($\tau(CO)$ in our nomenclature) and a much smaller deviation in the other frequencies from the calculated ones.

Dicarboxylic acids exist as dimers in the solid state. The presence of the dimer has been taken into account in the existing normal coordinate calculations of malonic acid [7], succinic acid [5] and adipic acid [6]. Most of our calculated frequencies and the corresponding assignments are in agreement with the existing NCA calculations after taking into account the effect of hydrogen bonding as explained. Our emphasis here is to explain the deviations and test the applicability of ab initio calculations in the evaluation of force fields for these molecules. Since the existing normal coordinate analyses were done on the solid state Raman and IR spectra of the dicarboxylic acids only the solid state data are given for them. In hydroxymalonic acid eventhough no previous calculations have been done we have been able to assign the solid state spectra owing to its similarity with glycolic acid [17]. In case of glutaric acid we faced a number of problems in the assignment owing to the lack of sufficient solid state data. Hence we had to take into account the solution spectra and also had to rely on the experimental intensities [18] to get a meaningful assignment. Thus in case of glutaric acid our assignments are based both on the solid state and the solution spectra. We discuss some of the important frequencies of these acids with reference to the ab initio assignments of formic acid [19], acetic acid [19], glycolic acid [20], oxalic acid [14] and tartaric acid [21].

4.2.1 COOH frequencies

Comparsions of the $\nu(OH)$ mode can be made with the spectra of oxalic acid [22] (the simplest dicarboxylic acid) and the effect of the methylene group if any on this mode can be made by comparison with the gas phase spectra of acetic acid [23]. The comparison of the calculated frequencies is however valid only if the appearence of the $\nu(OH)$ mode of an isolated molecule is independent of other factors (except that of intramolecular hy-

drogen bonding). The observed gas phase frequencies of oxalic acid appear at 3576 and $3498cm^{-1}$for the cTt conformer and at $3472cm^{-1}$for the cTc conformer [14]. In acetic acid the gas phase frequency was observed at $3583cm^{-1}$[23]. The decrease in frequency both in gas phase as well as the in the solid state from the calculated frequencies can be taken as a rough measure of H-bonding, keeping in mind that the calculated frequencies do not include the effect of anharmonicity and electron correlation. Although the structures of these molecules are very different, the calculated OH frequency appears in the narrow range 3850-$3860cm^{-1}$in all the cases. Correspondingly in the solid state spectra of these acids the $\nu(OH)$ frequency wherever observed falls in a narrow range around $3000cm^{-1}$. However hydroxymalonic acid an α-hydroxy carboxylic acid is an exception to this rule. Kanters et al. [24] had observed that the $\nu(OH)_{alc}$ frequency of α-carboxylic acids is largely independent of the medium in which the spectra are taken. Their inference was based on the fact that the X-Ray data of hydroxymalonic acid does not indicate the involvement of the alcoholic OH in any sort of hydrogen bonding [25]. The $\nu(OH)_{(alc)}$ value reported by them was $3500cm^{-1}$in the IR spectra of anhydrous hydroxymalonic acid. The free $\nu(OH)$ value also appears around $3500cm^{-1}$. This gives credence to their inference but our calculated frequencies for hydroxymalonic acid indicates the presence of an intramolecular hydrogen bond in the optimized structure.

As in the case of the $\nu(OH)$ mode, comparisons for the $\nu(C=O)$ mode are made with the experimental spectra of oxalic acid and acetic acid. This mode occurs at 1800 and $1817cm^{-1}$in the gas phase spectra of oxalic acid [22] and at $1788cm^{-1}$in the gas phase spectra of acetic acid [23]. Eventhough the calculated $\nu(C=O)$ frequencies are generally high even after scaling the trends exhibited by them are observed in the experimental spectra. Thus two distinct bands corresponding to the two carboxyl groups are present in the lower dicarboxylic acids but as we proceed towards higher dicarboxylic acids the peaks merge and only a single peak is observed. In case of hydroxymalonic acid the presence of a hydroxyl group in the α position increases the frequency of the $\nu(C=O)$ mode. Thus eventhough the $C=O4$ is involved in hydrogen bonding the frequency corresponding to this mode appears at a higher frequency. In glycolic acid (hydroxyacetic acid) the gas phase IR spectrum indicates that this mode appears at $1806cm^{-1}$[20]. This is about $18cm^{-1}$higher when compared to acetic acid.

$\nu(CO)$ and $\delta(COH)$ modes are usually coupled and give rise to two frequencies in monocarboxylic acids. In case of dicarboxylic acids the assignment of these two modes with some certainty was difficult from the calculated ab initio values due to large shifts

in the solid state. Hence in all the cases these modes have been left unassigned. Based on the intensity profiles one can however speculate on the position of the experimental peaks. In doing this we should keep in mind that the $\delta(COH)$ undergoes a blue shift under the influence of hydrogen bonding. The magnitude and factors governing this shift are dependent on a number of factors. Our observations indicate that the amount of shift depends on the corresponding contribution to the PED and the modes with which this frequency is coupled. In most cases this mode gets coupled with the $\nu(C-O)$ mode but there is a propensity of it getting coupled either with the $\omega(CH_2)$ or $t(CH_2)$ modes. The coupling with the CH_2 bending modes changes the characterstics of the corresponding CH_2 bending mode [26]. In the experimental solid state spectra the presence of this mode can be traced to the sudden increase in the intensity of the IR peaks in the range 1100-1500cm^{-1}. Studies of a number of carboxylic acids indicate that a peak around 1250$cm^{-1}$is the strongest IR peak and they have attributed its origin to the coupled $\delta(COH)$ and $\nu(CO)$ modes [27]. The corresponding peaks in the gas phase spectra of acetic acid for these modes are 1340 and 1192cm^{-1}[23]. In oxalic acid these modes have been assigned to the frequencies at (1423,1195) and (1330,1176)cm^{-1}[14]. In the β form of oxalic acid these mode appear at (1475,1209) and (1381,1181)cm^{-1}[28]. The values of the beta form are particularly given because we presume that the higher dicarboxylic acids which also crystallize in the beta form may have values close to those given for this form [1]. An examination of the frequencies of oxalic acid in the gas phase and solid state indicate that only two of the frequencies increase while the other two have similar values in the gas phase and solid state spectra. The two frequencies which do not change much are those in which the dominant contributor to the PED is the $\nu(CO)$ mode. A noticeable fact is that in all the higher dicarboxylic acids the $\nu(C-O)$ mode appears at frequencies > 1200$cm^{-1}$and hence distinguishes the higher dicarboxylic acids from oxalic acid. However in the α form of oxalic acid frequencies corresponding to this mode appear above 1200cm^{-1}. Thus in malonic acid a plausible assignment would be to attribute the peaks at 1312, 1294 and 1318, 1289cm^{-1}in the IR and Raman spectra of solid sample to this coupled mode [7]. Similar kind of assignments for all the other acids would be to attribute the peaks at (1130,1205,1380) and (1135,1212,1365/1425)cm^{-1}in the IR and Raman spectra of the solid state hydroxymalonic acid, peaks at (1289,1419) and 1418cm^{-1}in the Raman and the IR spectra of solid state succinic acid, peaks at (1306,1409,1434) and (1240,1420)cm^{-1}in the IR spectra of solid and aqueous glutaric acid, peak at 1429cm^{-1}in the IR spectra of adipic acid to these coupled modes.

The next set of frequencies are the $\delta(C-O)$ and $\delta(C=O)$ bending modes. These frequencies are not influenced by hydrogen bonding and hence can easily be assigned in most of the acids. Mostly they appear coupled with the out of plane CO bend ($\gamma(COO)$ in our nomenclature). In cases where they are coupled with the out of plane OH bend ($\tau(CO)$ in our nomenclature) they shift towards higher frequencies. These three modes occur as coupled modes. In solid monocarboxylic acids $\gamma(COO)$ and $\delta(COO)$ are assigned to the frequencies at 550 and $683cm^{-1}$[19]. In the higher dicarboxylic acids these modes appear around the frequencies given for monocarboxylic acids. Our results for these modes are mostly in accordance with the existing normal coordinate analysis of malonic, succinic and adipic acids [5–7].

As has already been said, the out of plane CO bend is not affected much by the presence of hydrogen bonding and hence the assignment of this mode did not pose any problem. On the other hand, the out of plane OH bend($\tau(CO)$) is another frequency which is extensively affected by hydrogen bonding. In the β form of oxalic acid the solid state frequencies for this mode occur at 792 and $828cm^{-1}$[28]. The corresponding gas phase frequency is $664cm^{-1}$[14]. Thus the peak corresponding to this mode should be found between 800-950cm^{-1}in the vibrational spectra of the solid state samples. As in the case of the coupled $\delta(COH)$ and $\nu(CO)$ mode plausible assignments for this mode would be to attribute the peaks at (770,900) and $765cm^{-1}$in the IR and Raman spectra of malonic acid, peaks at (700,900) and $697cm^{-1}$in the IR and Raman spectra of hydroxymalonic acid, peak at $914cm^{-1}$in the IR spectra of succinic acid, peaks at (922,792) and (762,785)cm^{-1}in the IR and Raman spectra of solid state and aqueous glutaric acid, peaks at 897 and $928cm^{-1}$in the Raman and IR spectra of adipic acid to it. The peak at $900cm^{-1}$in the Raman spectra of malonic acid has a significant contribution from the $\delta(CCC)$ mode. The presence of hydrogen bonding in the solution may be responsible for the appearence of the peaks in aqueous glutaric acid around the same region as in the solid state.

In case of the lower acids some of the assignments for these modes were supported by matching the corresponding deuterium shifts. Tables 4.23 and 4.24 list the assignments for some of the isotopomers of malonic, hydroxymalonic and succinic acids.

The calculated frequencies indicate that the appearence of the $COOH$ frequencies in the higher dicarboxylic acids follow certain trends. Thus the frequencies of an unknown dicarboxylic acid can be assigned from ab initio frequencies using these trends.

4.2.2 CH frequencies

The $\nu(CH_2)$ regions in most of the higher dicarboxylic acids are obscured by the presence of the OH stretch frequencies in the solid state spectra. Hence for most cases the peaks corresponding to this region are not clear. However on the basis of our calculations we have assigned these frequencies in all the acids. In hydroxymalonic acid only a single CH stretch is present and in case of glutaric acid we have taken recourse to the calculated intensities to assist us in our assignments.

The $\delta(CH_2)$ mode could easily be assigned in most of the dicarboxylic acids because this frequency is not affected by the medium in which the spectra are recorded. Moreover unlike other CH_2 bending modes it is not coupled with other modes. In succinic acid in the A_u species this mode gets coupled with the $\nu(CC)$ and $\nu(CO)$ modes on using the 6-31G** basis set. Surprisingly, the normal coordinate analysis of malonic acid indicates that this mode gets coupled with other modes [7]. The normal coordinate analysis of succinic acid also indicates that the CH_2 bending modes are coupled to a limited extent [5].

The $\omega(CH_2)$ mode on the other hand is extensively coupled with other modes notably the $\delta(COH)$ mode. The use of the 6-31G** basis set gives rise to a frequency higher than the $\delta(CH_2)$ mode in which the principal contributors to the PED are the $\omega(CH_2)$, $\nu(CC)$ and $\nu(CO)$ modes. This effect is observed in both succinic and malonic acids. The improved description (addition of d orbitals to oxygen and p orbitals to hydrogen) may be responsible for this change. This mode could however be assigned. This kind of coupling in acids has been extensively observed [26]

The other CH_2 bending modes appear at lower frequencies. The $t(CH_2)$ mode is also coupled to the other modes but the intensities associated with these peaks are very small. Moreover in the solid state the coupling with the $\delta(COH)$ mode may result in some misassignments of this mode. The last CH_2 bending mode the $\rho(CH_2)$ bending mode is either coupled with the $\nu(CC)$ or the CO bending modes. In the solid state it gets coupled with the $\tau(CO)$ mode and shifts to higher frequencies. In this case also the assignments are very much dependent on the nature of the coupling and are prone to vary from the gas phase to the solid state. In some cases peaks associated with this mode cannot be observed in the experimental vibrational spectra because of the low intensity. The $\delta(CCC)$ and $\tau(CC)$ modes are low frequency modes and in most cases they could not be assigned.

It can be observed that the methylene group frequencies are not very informative in case of dicarboxylic acids. Some of the specific features of our calculation are that in the

C_s model of glutaric acid the $t(CH_2)$ and $\rho(CH_2)$ modes are a part of the A" species which makes glutaric acid unique with respect to the methylene group frequencies. Moreover the 6-31G** basis set gives more reasonable frequencies as far as the CH_2 group are concerned. But 4-21G potential energy distributions appear to be more reasonable than those evaluated using a 6-31G** basis set.

4.2.3 CC frequencies

The $\nu(CC)$ frequency characterized by the strong intensity in the Raman spectrum could be easily assigned in most cases except in glutaric acid. The $\nu(CC)$ bands distinguish bonds of the type $HOOC-CH_2$ and H_2C-CH_2. Thus the frequencies associated with the former appear around $900cm^{-1}$while those associated with the latter bonds appear around $1050cm^{-1}$. The presence of the carboxyl group induces a strong polarity in the C-C bonds along the chain such that induced polarity progressively decreases with increasing distance from the carboxyl group [29]. Use of the 6-31G** basis set however gives a better description of the modes associated with CC.

Thus it can be seen that the presence of the methylene group does not affect many of the vibrational frequencies substantially. Hence these frequencies cannot be employed to distinguish between the various acids, but the similarity of these frequencies and hence probably the force constants can be harnessed in the development of a common force field for all the dicarboxylic acids. A number of notable differences exist however, with respect to monocarboxylic acids and hence force constants transferred from monocarboxylic acids may not describe the features of dicarboxylic acids adequately.

4.3 Force constants

Some of the diagonal force constants which were employed to perform the normal coordinate analysis of malonic acid and succinic acid are given in Table 4.25 [5–7]. They were determined from experimental frequencies. The normal coordinate analysis of adipic acid was performed with the same set of force constants employed in succinic acid [5]. It can be seen that a number of differences exist in the force constants used for both malonic and succinic acid. The calculated force constants displayed in Tables 4.26 to 4.30 however indicate a trend in which the frequencies gradually change. Hollenstein and Günthard had developed a transferable force field for molecules containing the $C=O$ group [30]. The

salient features of the criteria for transferability of the force field include the exclusion of interaction force constants and the congruency of the nuclei involved, for the transferability of diagonal force constants. Recently Williams and Lowrey had developed a scheme for the scaling of the force constant of formic acid and acetic acid to account for the effect of hydration on these acids [19]. Such a scheme would help one to have further faith in the values of the force constants, but given the size of these systems and the number of water molecules needed to completely hydrate these acids, calculations at the present level of sophistication are not feasible for such large systems. A fit of the calculated force constants would be able to provide a set of transferable force constants which could be applied for all dicarboxylic acids.

4.4 Conclusions

The study of the conformation and geometry of the higher dicarboxylic acids gives an insight into the diverse structural forms accessible to them. The decrease of the barrier heights of carboxyl group rotation as the number of intervening methylene groups increase could indicate the ease at which the higher dicarboxylic acids can form different hydrogen bonded structures. It could also explain the typical behaviour of the higher dicarboxylic acids as far as their pK_a values are concerned.

The salient features of the study of the vibrational frequencies of higher dicarboxylic acids are given. The calculated $\nu(OH)$ frequency occurs over a narrow range of frequencies indicating that the structure of the acid has little effect on the frequency for isolated molecules. The exact $\nu(C=O)$ is dependent on the actual structure of the molecule, though the frequency mode is localized. The frequency around $1150cm.^{-1}$in the calcuations is due to the coupled $\nu(C-O)+\delta(COH)$ mode. The other coupled mode comes much higher. The calculated $\tau(CO)$ occurs over a narrow range of frequencies indicating that the structure has little effect on this frequency also. Methylene groups adjacent to the carboxyl group and those far off can be easily distinguished on the basis of the $\nu(CH_2)$ and $\nu(CC)$ frequencies. As far as the CO bending modes are concerned they appear at frequencies characterstic of monocarboxylic acids.

The study of the force constants clearly indicates that a comprehensive force field specific for dicarboxylic acid can be developed. The effect of the change of basis set gives results which give an overall agreement but differ in specific details for certain frequencies specially for the CH_2 bending modes.

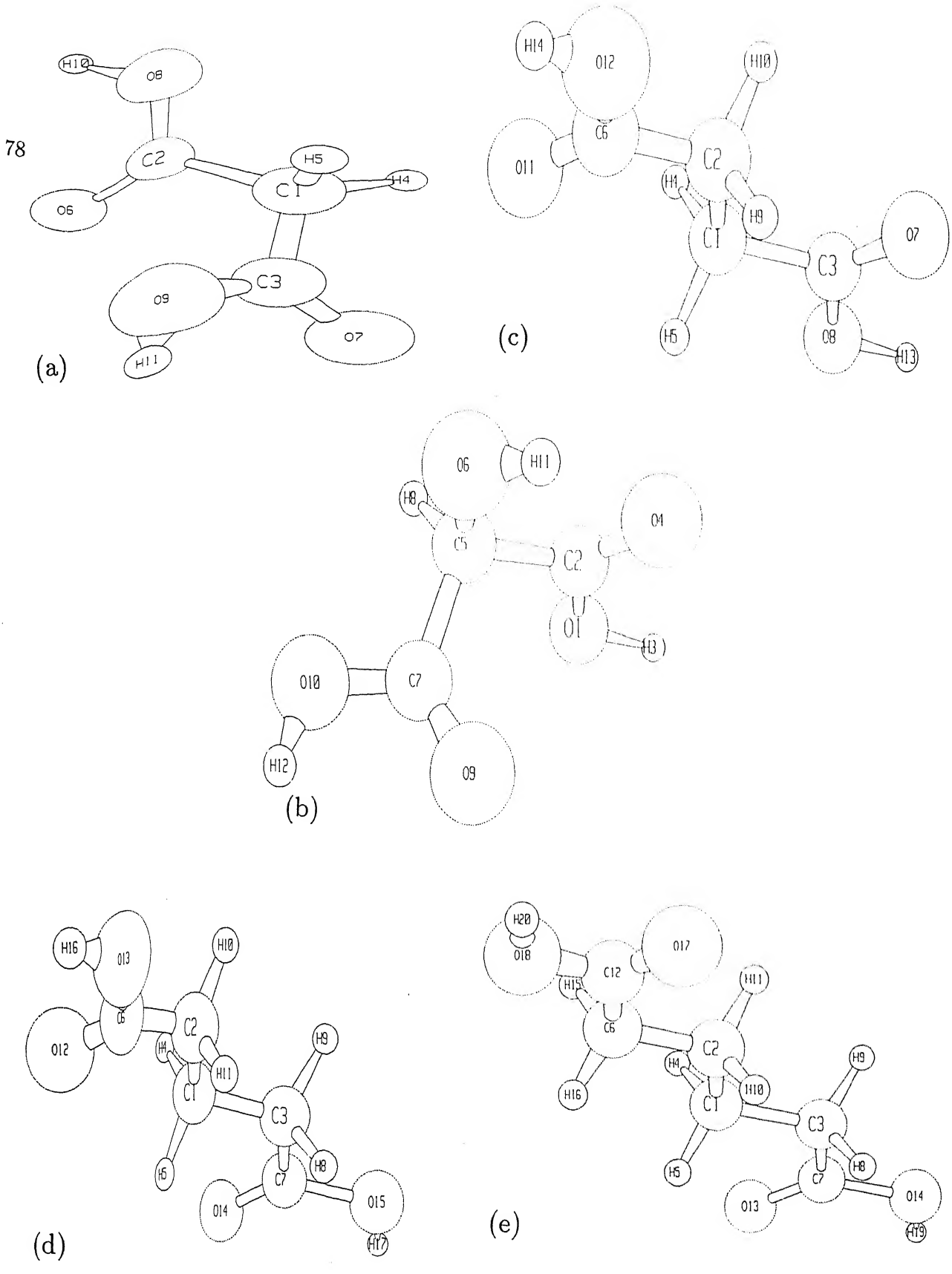

Figure 4.1: 4-21G optimized structures of (a) Malonic acid, (b) Hydroxymalonic acid, (c) Succinic acid, (d) Glutaric acid and (e) Adipic acid.

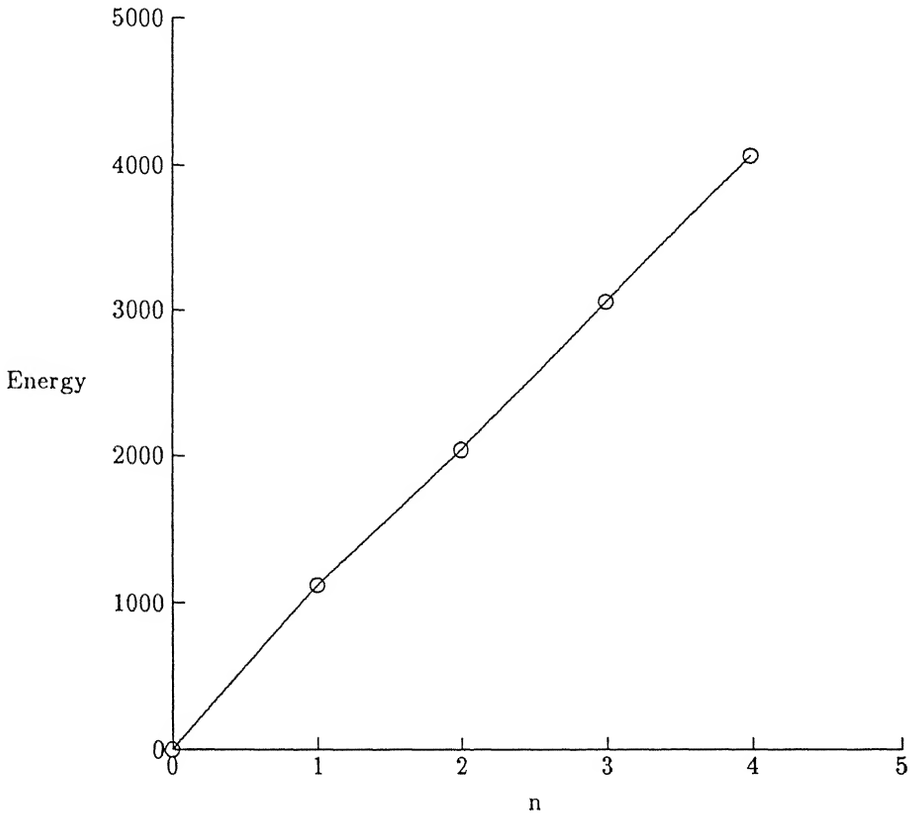

Figure 4.2: Variation of Energy with the increase in n (number of CH_2) groups. All energies relative to the E(RHF) of oxalic acid -987125.2425 kJ/mol. Energy is in 1/100(kJ/mol).

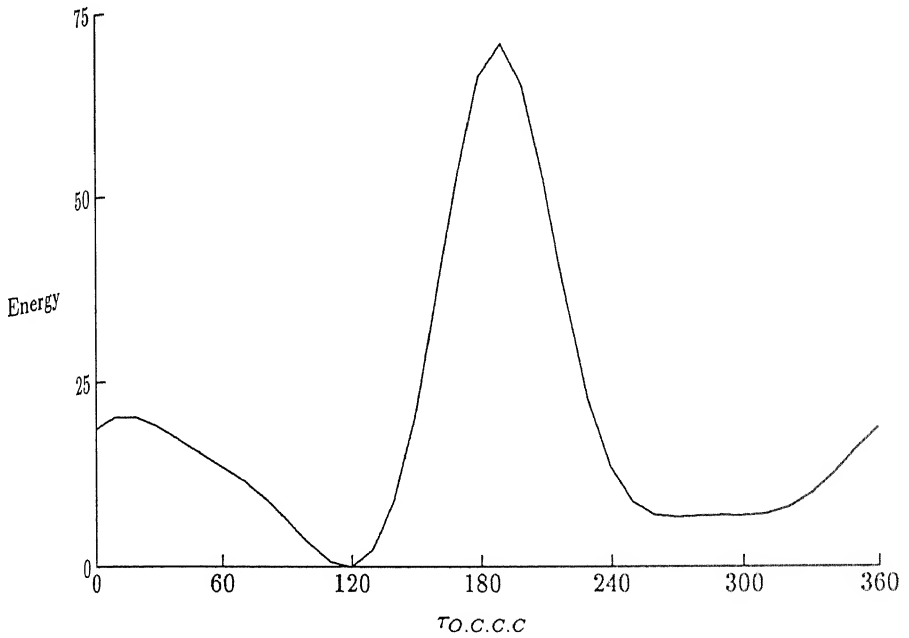

Figure 4.3: Variation of Energy with the torsional angle $\tau_1[O.C.C.C]$ in malonic acid. Energy is in kJ/mol

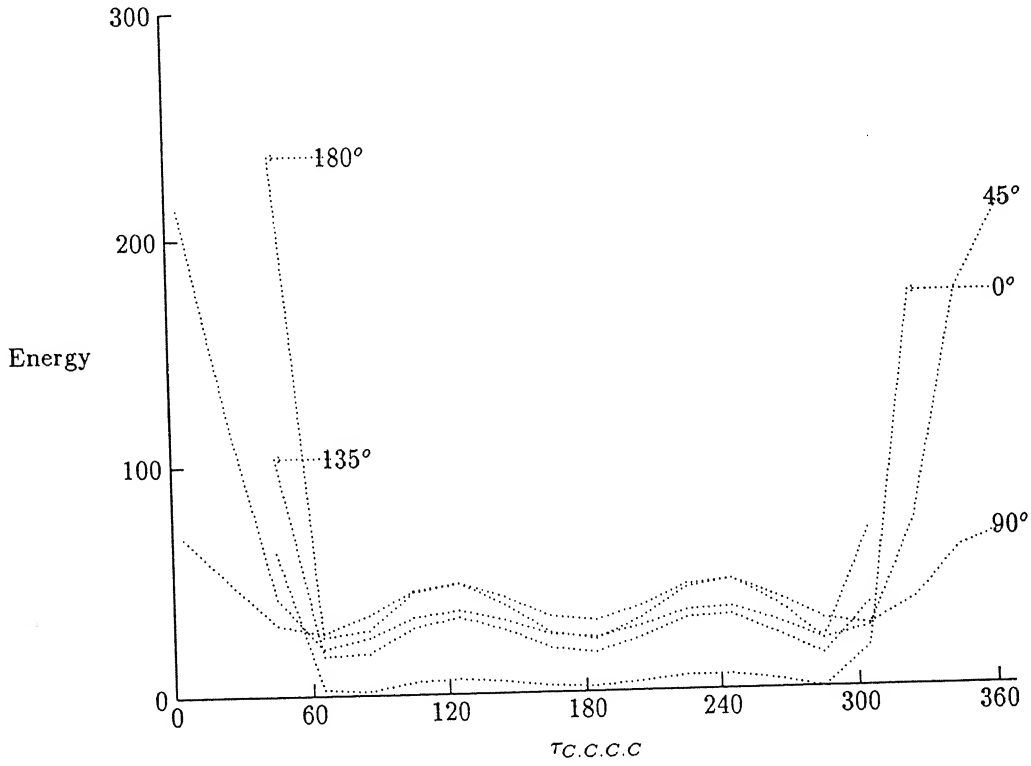

Figure 4.4: Variation of Energy with the torsional angle $\tau_2[C.C.C.C]$ at specific values of the torsional angle $\tau_1[O.C.C.C]$ in succinic acid. Energy is in kJ/mol.

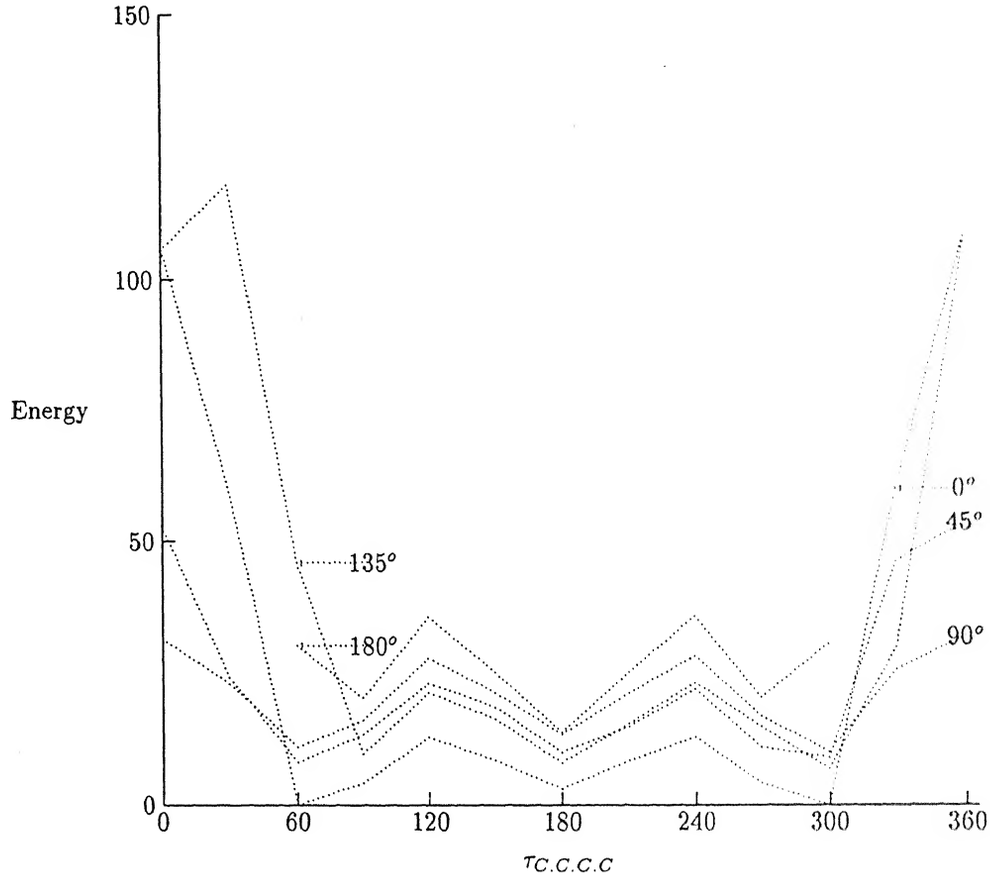

Figure 4.5: Variation of Energy with the torsional angle $\tau_2[C.C.C.C]$ at specific values of the torsional angle $\tau_1[O.C.C.C]$ in glutaric acid. $\tau_3[C.C.C.C]$ is 180°. Energy is in kJ/mol.

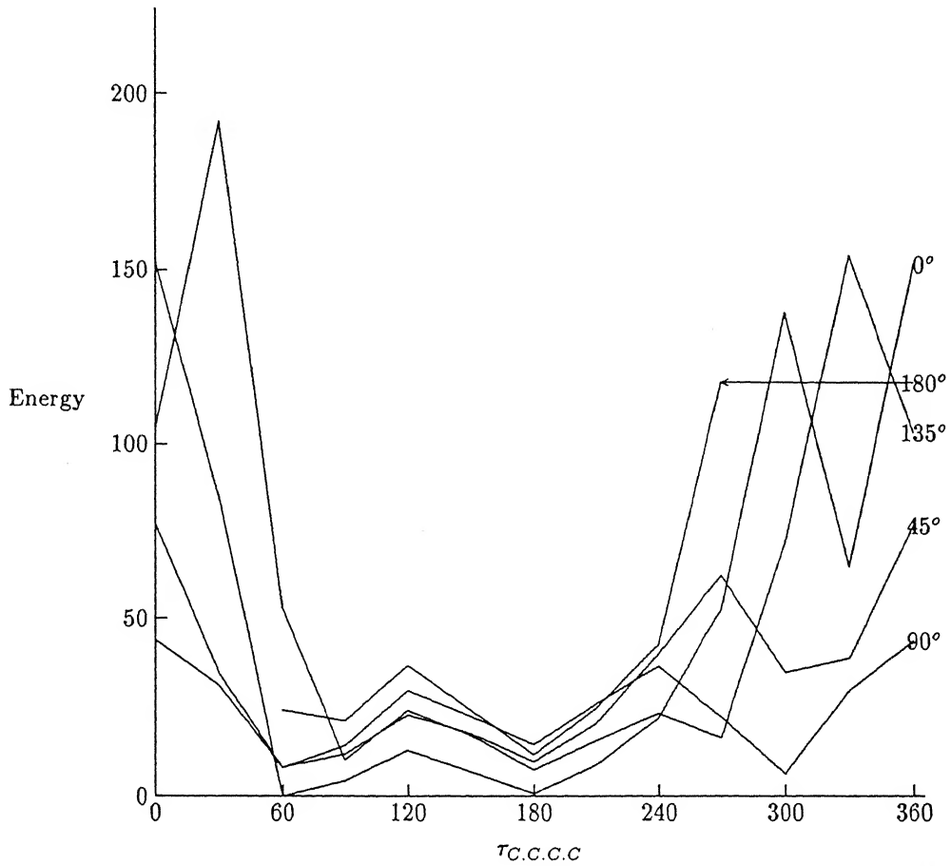

Figure 4.6: Variation of Energy with the torsional angle $\tau_2[C.C.C.C]$ at specific values of the torsional angle $\tau_1[O.C.C.C]$ in glutaric acid. $\tau_3[C.C.C.C]$ is 90°. Energy is in kJ/mol.

Table 4.1: Symmetry coordinates of Malonic acid

Coordinate	Description
$S_1 = R_{8.10}$	$\nu(OH)$
$S_2 = R_{9.11}$	$\nu(OH)$
$S_3 = R_{1.4} - R_{1.5}$	$\nu_a(CH_2)$
$S_4 = R_{1.4} + R_{1.5}$	$\nu_s(CH_2)$
$S_5 = R_{2.6}$	$\nu(C=O)$
$S_6 = R_{3.7}$	$\nu(C=O)$
$S_7 = R_{2.8}$	$\nu(C-O)$
$S_8 = R_{3.9}$	$\nu(C-O)$
$S_9 = R_{1.2}$	$\nu(C''C)$
$S_{10} = R_{1.3}$	$\nu(C'C)$
$S_{11} = 2\alpha_{1.2.8} - \alpha_{1.2.6} - \alpha_{6.2.8}$	$\delta(C-O)$
$S_{12} = \alpha_{1.2.6} - \alpha_{6.2.8}$	$\delta(C=O)$
$S_{13} = 2\alpha_{1.3.9} - \alpha_{1.3.7} - \alpha_{7.3.9}$	$\delta(C-O)$
$S_{14} = \alpha_{1.3.7} - \alpha_{7.3.9}$	$\delta(C=O)$
$S_{15} = 4\alpha_{4.1.5} - \alpha_{2.1.4} - \alpha_{2.1.5} - \alpha_{3.1.4} - \alpha_{3.1.5}$	$\delta(CH_2)$
$S_{16} = \alpha_{2.1.4} + \alpha_{2.1.5} - \alpha_{3.1.4} - \alpha_{3.1.5}$	$\omega(CH_2)$
$S_{17} = \alpha_{2.1.4} - \alpha_{2.1.5} - \alpha_{3.1.4} + \alpha_{3.1.5}$	$t(CH_2)$
$S_{18} = \alpha_{2.1.4} - \alpha_{2.1.5} + \alpha_{3.1.4} - \alpha_{3.1.5}$	$\rho(CH_2)$
$S_{19} = 5\alpha_{2.1.3} - \alpha_{4.1.5} - \alpha_{2.1.4} - \alpha_{2.1.5} - \alpha_{3.1.4} - \alpha_{3.1.5}$	$\delta(CC'C)$
$S_{20} = \alpha_{2.8.10}$	$\delta(COH)$
$S_{21} = \alpha_{3.9.11}$	$\delta(COH)$
$S_{22} = \tau_{8.2.1.6}$	$\gamma(COO)$
$S_{23} = \tau_{9.3.1.7}$	$\gamma(COO)$
$S_{24} = \tau_{1.2.8.10} + \tau_{6.2.8.10}$	$\tau(CO)$
$S_{25} = \tau_{1.3.9.11} + \tau_{7.3.9.11}$	$\tau(CO)$
$S_{26} = \tau_{3.1.2.6} + \tau_{3.1.2.8} + \tau_{4.1.2.6} + \tau_{4.1.2.8} + \tau_{5.1.2.6} + \tau_{5.1.2.8}$	$\tau(C'C)$
$S_{27} = \tau_{2.1.3.7} + \tau_{2.1.3.9} + \tau_{4.1.3.7} + \tau_{4.1.3.9} + \tau_{5.1.3.7} + \tau_{5.1.3.9}$	$\tau(C'C)$

Atom numbering is given in Figure 4.1(a).

Table 4.2: Symmetry coordinates of Hydroxymalonic acid

Coordinate	Description
$S_1 = R_{6.11}$	$\nu(OH)_{alc}$
$S_2 = R_{1.3}$	$\nu(OH)_{ac}$
$S_3 = R_{10.12}$	$\nu(OH)_{ac}$
$S_4 = R_{5.8}$	$\nu(CH)$
$S_5 = R_{2.4}$	$\nu(C=O)$
$S_6 = R_{7.9}$	$\nu(C=O)$
$S_7 = R_{5.6}$	$\nu(C-O)_{alc}$
$S_8 = R_{1.2}$	$\nu(C-O)$
$S_9 = R_{7.10}$	$\nu(C-O)$
$S_{10} = R_{2.5}$	$\nu(C'C)$
$S_{11} = R_{5.7}$	$\nu(C'C)$
$S_{12} = 2\alpha_{1.2.5} - \alpha_{4.2.5} - \alpha_{1.2.4}$	$\delta(C-O)$
$S_{13} = \alpha_{4.2.5} - \alpha_{1.2.4}$	$\delta(C=O)$
$S_{14} = 2\alpha_{5.7.10} - \alpha_{5.7.9} - \alpha_{9.7.10}$	$\delta(C-O)$
$S_{15} = \alpha_{5.7.9} - \alpha_{9.7.10}$	$\delta(C=O)$
$S_{16} = \alpha_{2.1.3}$	$\delta(COH)_{ac}$
$S_{17} = \alpha_{7.10.12}$	$\delta(COH)_{ac}$
$S_{18} = \alpha_{5.6.11}$	$\delta(COH)_{alc}$
$S_{19} = \alpha_{2.5.8} - \alpha_{7.5.8}$	$\rho(OC'H)$
$S_{20} = 2\alpha_{6.5.8} - \alpha_{2.5.8} - \alpha_{7.5.8}$	$\delta(OC'H)$
$S_{21} = \alpha_{2.5.6} - \alpha_{6.5.7}$	$\rho(OC'C)$
$S_{22} = 2\alpha_{2.5.7} - \alpha_{2.5.6} - \alpha_{6.5.7}$	$\delta(OC'C)$
$S_{23} = \alpha_{2.5.6} + \alpha_{2.5.7} + \alpha_{6.5.7} - \alpha_{2.5.8} - \alpha_{6.5.8} - \alpha_{7.5.8}$	$\delta(CC'C)$
$S_{24} = \tau_{1.2.5.4}$	$\gamma(COO)$
$S_{25} = \tau_{9.5.7.10}$	$\gamma(COO)$
$S_{26} = \tau_{2.5.6.11} + \tau_{8.5.6.11}$	$\tau(C'O)$
$S_{27} = \tau_{3.1.2.4} + \tau_{3.1.2.5}$	$\tau(CO)$
$S_{28} = \tau_{5.7.10.12} + \tau_{9.7.10.12}$	$\tau(CO)$
$S_{29} = \tau_{1.2.5.6} + \tau_{4.2.5.6} + \tau_{1.2.5.7} + \tau_{4.2.5.7} + \tau_{1.2.5.8} + \tau_{4.2.5.8}$	$\tau(C'C)$
$S_{30} = \tau_{2.5.7.9} + \tau_{2.5.7.10} + \tau_{6.5.7.9} + \tau_{6.5.7.10} + \tau_{8.5.7.9} + \tau_{8.5.7.10}$	$\tau(C'C)$

Atom numbering is given in Figure 4.1(b).

Table 4.3: Symmetry coordinates of Succinic acid

Coordinate	Description
A_g species	
$S_1 = R_{8.13} + R_{12.14}$	$\nu(OH)$
$S_2 = R_{1.4} + R_{1.5} + R_{2.9} + R_{2.10}$	$\nu_s(CH_2)$
$S_3 = R_{1.4} - R_{1.5} + R_{2.9} - R_{2.10}$	$\nu_a(CH_2)$
$S_4 = R_{3.7} + R_{6.11}$	$\nu(C=O)$
$S_5 = R_{3.8} + R_{6.12}$	$\nu(C-O)$
$S_6 = R_{1.3} + R_{2.6}$	$\nu(CC')$
$S_7 = R_{1.2}$	$\nu(C'C')$
$S_8 = \alpha_{3.8.13} + \alpha_{6.12.14}$	$\delta(COH)$
$S_9 = 2\alpha_{1.3.8} - \alpha_{1.3.7} - \alpha_{7.3.8} + 2\alpha_{2.6.12} - \alpha_{2.6.11} - \alpha_{11.6.12}$	$\delta(C-O)$
$S_{10} = \alpha_{1.3.7} - \alpha_{7.3.8} + \alpha_{2.6.11} - \alpha_{11.6.12}$	$\delta(C=O)$
$S_{11} = 4\alpha_{4.1.5} - \alpha_{3.1.4} - \alpha_{3.1.5} - \alpha_{2.1.4} - \alpha_{2.1.5} + 4\alpha_{9.2.10} - \alpha_{6.2.9} - \alpha_{6.2.10} - \alpha_{1.2.9} - \alpha_{1.2.10}$	$\delta(CH_2)$
$S_{12} = \alpha_{3.1.4} + \alpha_{3.1.5} - \alpha_{2.1.4} - \alpha_{2.1.5} + \alpha_{6.2.9} + \alpha_{6.2.10} - \alpha_{1.2.9} - \alpha_{1.2.10}$	$\omega(CH_2)$
$S_{13} = \alpha_{3.1.4} - \alpha_{3.1.5} - \alpha_{2.1.4} + \alpha_{2.1.5} + \alpha_{6.2.9} - \alpha_{6.2.10} - \alpha_{1.2.9} + \alpha_{1.2.10}$	$t(CH_2)$
$S_{14} = \alpha_{3.1.4} - \alpha_{3.1.5} + \alpha_{2.1.4} - \alpha_{2.1.5} + \alpha_{6.2.9} - \alpha_{6.2.10} + \alpha_{1.2.9} - \alpha_{1.2.10}$	$\rho(CH_2)$
$S_{15} = 5\alpha_{3.1.2} - \alpha_{4.1.5} - \alpha_{3.1.4} - \alpha_{3.1.5} - \alpha_{2.1.4} - \alpha_{2.1.5} + 5\alpha_{1.2.6} - \alpha_{9.2.10} - \alpha_{6.2.9} - \alpha_{6.2.10} - \alpha_{1.2.9} - \alpha_{1.2.10}$	$\delta(C'C'C)$
$S_{16} = \tau_{8.3.1.7} - \tau_{12.6.2.11}$	$\gamma(COO)$
$S_{17} = \tau_{1.3.8.13} + \tau_{7.3.8.13} - \tau_{2.6.12.14} - \tau_{11.6.12.14}$	$\tau(CO)$
$S_{18} = \tau_{2.1.3.7} + \tau_{4.1.3.7} + \tau_{5.1.3.7} + \tau_{2.1.3.8} + \tau_{4.1.3.8} + \tau_{5.1.3.8} - \tau_{1.2.6.11} - \tau_{9.2.6.11} - \tau_{10.2.6.11} - \tau_{1.2.6.12} - \tau_{9.2.6.12} - \tau_{10.2.6.12}$	$\tau(C'C)$

Table 4.3. (Continued): Symmetry coordinates of Succinic acid

Coordinate	Description
A_u species	
$S_1 = R_{8.13} - R_{12.14}$	$\nu(OH)$
$S_2 = R_{1.4} + R_{1.5} - R_{2.9} - R_{2.10}$	$\nu_s(CH_2)$
$S_3 = R_{1.4} - R_{1.5} - R_{2.9} + R_{2.10}$	$\nu_a(CH_2)$
$S_4 = R_{3.7} - R_{6.11}$	$\nu(C=O)$
$S_5 = R_{3.8} - R_{6.12}$	$\nu(C-O)$
$S_6 = R_{1.3} - R_{2.6}$	$\nu(CC')$
$S_7 = \alpha_{3.8.13} - \alpha_{6.12.14}$	$\delta(COH)$
$S_8 = 2\alpha_{1.3.8} - \alpha_{1.3.7} - \alpha_{7.3.8} - 2\alpha_{2.6.12} + \alpha_{2.6.11} + \alpha_{11.6.12}$	$\delta(C-O)$
$S_9 = \alpha_{1.3.7} - \alpha_{7.3.8} - \alpha_{2.6.11} + \alpha_{11.6.12}$	$\delta(C=O)$
$S_{10} = 4\alpha_{4.1.5} - \alpha_{3.1.4} - \alpha_{3.1.5} - \alpha_{2.1.4} - \alpha_{2.1.5} - 4\alpha_{9.2.10} + \alpha_{6.2.9} + \alpha_{6.2.10} + \alpha_{1.2.9} + \alpha_{1.2.10}$	$\delta(CH_2)$
$S_{11} = \alpha_{3.1.4} + \alpha_{3.1.5} - \alpha_{2.1.4} - \alpha_{2.1.5} - \alpha_{6.2.9} - \alpha_{6.2.10} + \alpha_{1.2.9} + \alpha_{1.2.10}$	$\omega(CH_2)$
$S_{12} = \alpha_{3.1.4} - \alpha_{3.1.5} - \alpha_{2.1.4} + \alpha_{2.1.5} - \alpha_{6.2.9} + \alpha_{6.2.10} + \alpha_{1.2.9} - \alpha_{1.2.10}$	$t(CH_2)$
$S_{13} = \alpha_{3.1.4} - \alpha_{3.1.5} + \alpha_{2.1.4} - \alpha_{2.1.5} - \alpha_{6.2.9} + \alpha_{6.2.10} - \alpha_{1.2.9} + \alpha_{1.2.10}$	$\rho(CH_2)$
$S_{14} = 5\alpha_{3.1.2} - \alpha_{4.1.5} - \alpha_{3.1.4} - \alpha_{3.1.5} - \alpha_{2.1.4} - \alpha_{2.1.5} - 5\alpha_{1.2.6} + \alpha_{9.2.10} + \alpha_{6.2.9} + \alpha_{6.2.10} + \alpha_{1.2.9} + \alpha_{1.2.10}$	$\delta(C'C'C)$
$S_{15} = \tau_{8.3.1.7} + \tau_{12.6.2.11}$	$\gamma(COO)$
$S_{16} = \tau_{1.3.8.13} + \tau_{7.3.8.13} + \tau_{2.6.12.14} + \tau_{11.6.12.14}$	$\tau(CO)$
$S_{17} = \tau_{2.1.3.7} + \tau_{4.1.3.7} + \tau_{5.1.3.7} + \tau_{2.1.3.8} + \tau_{4.1.3.8} + \tau_{5.1.3.8} + \tau_{1.2.6.11} + \tau_{9.2.6.11} + \tau_{10.2.6.11} + \tau_{1.2.6.12} + \tau_{9.2.6.12} + \tau_{10.2.6.12}$	$\tau(C'C)$
$S_{18} = \tau_{3.1.2.6} + \tau_{4.1.2.6} + \tau_{5.1.2.6} + \tau_{3.1.2.9} + \tau_{4.1.2.9} + \tau_{5.1.2.9} + \tau_{3.1.2.10} + \tau_{4.1.2.10} + \tau_{5.1.2.10}$	$\tau(C'C')$

Atom numbering is given in Figure 4.1(c).

Table 4.4: Symmetry coordinates of Glutaric acid

Coordinate	Description
A' species	
$S_1 = R_{13.16}$	$\nu(OH)$
$S_2 = R_{15.17}$	$\nu(OH)$
$S_3 = R_{1.4} + R_{1.5}$	$\nu_s(C''H_2)$
$S_4 = R_{3.8} + R_{3.9}$	$\nu_s(C''H_2)$
$S_5 = R_{2.10} + R_{2.11}$	$\nu_s(C''H_2)$
$S_6 = R_{6.12}$	$\nu(C=O)$
$S_7 = R_{7.14}$	$\nu(C=O)$
$S_8 = R_{6.13}$	$\nu(C-O)$
$S_9 = R_{7.15}$	$\nu(C-O)$
$S_{10} = R_{2.6}$	$\nu(CC')$
$S_{11} = R_{3.7}$	$\nu(CC')$
$S_{12} = R_{1.2}$	$\nu(C''C''')$
$S_{13} = R_{1.3}$	$\nu(C''C''')$
$S_{14} = \alpha_{6.13.16}$	$\delta(CCOH)$
$S_{15} = \alpha_{7.15.17}$	$\delta(CCOH)$
$S_{16} = 2\alpha_{2.6.13} - \alpha_{2.6.12} - \alpha_{12.6.13}$	$\delta(C-O)$
$S_{17} = 2\alpha_{3.7.15} - \alpha_{3.7.14} - \alpha_{14.7.15}$	$\delta(C-O)$
$S_{18} = \alpha_{2.6.12} - \alpha_{12.6.13}$	$\delta(C=O)$
$S_{19} = \alpha_{3.7.14} - \alpha_{14.7.15}$	$\delta(C=O)$
$S_{20} = 4\alpha_{4.1.5} - \alpha_{2.1.4} - \alpha_{2.1.5} - \alpha_{3.1.4} - \alpha_{3.1.5}$	$\delta(C''H_2)$
$S_{21} = \alpha_{2.1.4} + \alpha_{2.1.5} - \alpha_{3.1.4} - \alpha_{3.1.5}$	$\omega(C''H_2)$
$S_{22} = 5\alpha_{1.2.3} - \alpha_{4.1.5} - \alpha_{2.1.4} - \alpha_{2.1.5}$ $- \alpha_{3.1.4} - \alpha_{3.1.5}$	$\delta(C''C'''C')$
$S_{23} = 4\alpha_{10.2.11} - \alpha_{1.2.10} - \alpha_{1.2.11} - \alpha_{6.2.10} - \alpha_{6.2.11}$	$\delta(C'H_2)$
$S_{24} = \alpha_{1.2.10} + \alpha_{1.2.11} - \alpha_{6.2.10} - \alpha_{6.2.11}$	$\omega(C'H_2)$
$S_{25} = 5\alpha_{1.2.6} - \alpha_{10.2.11} - \alpha_{1.2.10} - \alpha_{1.2.11}$ $- \alpha_{6.2.10} - \alpha_{6.2.11}$	$\delta(C'''C''C')$
$S_{26} = 4\alpha_{8.3.9} - \alpha_{1.3.8} - \alpha_{1.3.9} - \alpha_{7.3.8} - \alpha_{7.3.9}$	$\delta(C''H_2)$
$S_{27} = \alpha_{1.3.8} + \alpha_{1.3.9} - \alpha_{7.3.8} - \alpha_{7.3.9}$	$\omega(C''H_2)$
$S_{28} = 5\alpha_{1.3.7} - \alpha_{8.3.9} - \alpha_{1.3.8} - \alpha_{1.3.9}$ $- \alpha_{7.3.8} - \alpha_{7.3.9}$	$\delta(C'''C'C)$

Table 4.4. (Continued): Symmetry coordinates of Glutaric acid

Coordinate	Description
A'' species	
$S_1 = R_{1.4} - R_{1.5}$	$\nu_a(C''H_2)$
$S_2 = R_{3.8} - R_{3.9}$	$\nu_a(C'H_2)$
$S_3 = R_{2.10} - R_{2.11}$	$\nu_a(C'H_2)$
$S_4 = \alpha_{2.1.4} - \alpha_{2.1.5} - \alpha_{3.1.4} + \alpha_{3.1.5}$	$t(C''H_2)$
$S_5 = \alpha_{2.1.4} - \alpha_{2.1.5} + \alpha_{3.1.4} - \alpha_{3.1.5}$	$\rho(C''H_2)$
$S_6 = \alpha_{1.2.10} - \alpha_{1.2.11} - \alpha_{6.2.10} + \alpha_{6.2.11}$	$t(C'H_2)$
$S_7 = \alpha_{1.2.10} - \alpha_{1.2.11} + \alpha_{6.2.10} - \alpha_{6.2.11}$	$\rho(C'H_2)$
$S_8 = \alpha_{1.3.8} - \alpha_{1.3.9} - \alpha_{7.3.8} + \alpha_{7.3.9}$	$t(C'H_2)$
$S_9 = \alpha_{1.3.8} - \alpha_{1.3.9} + \alpha_{7.3.8} - \alpha_{7.3.9}$	$\rho(C'H_2)$
$S_{10} = \tau_{13.6.2.12}$	$\gamma(COO)$
$S_{11} = \tau_{15.7.3.14}$	$\gamma(COO)$
$S_{12} = \tau_{2.6.13.16} + \tau_{12.6.13.16}$	$\tau(CO)$
$S_{13} = \tau_{3.7.15.17} + \tau_{14.7.15.17}$	$\tau(CO)$
$S_{14} = \tau_{1.2.6.12} + \tau_{1.2.6.13} + \tau_{10.2.6.12} + \tau_{10.2.6.13} + \tau_{11.2.6.12} + \tau_{11.2.6.13}$	$\tau(C'C)$
$S_{15} = \tau_{1.3.7.14} + \tau_{1.3.7.15} + \tau_{8.3.7.14} + \tau_{8.3.7.15} + \tau_{9.3.7.14} + \tau_{9.3.7.15}$	$\tau(C'C)$
$S_{16} = \tau_{2.1.3.7} + \tau_{2.1.3.8} + \tau_{2.1.3.9} + \tau_{4.1.3.7} + \tau_{4.1.3.8} + \tau_{4.1.3.9} + \tau_{5.1.3.7} + \tau_{5.1.3.8} + \tau_{5.1.3.9}$	$\tau(C''C')$
$S_{17} = \tau_{3.1.2.6} + \tau_{3.1.2.10} + \tau_{3.1.2.11} + \tau_{4.1.2.6} + \tau_{4.1.2.10} + \tau_{4.1.2.11} + \tau_{5.1.2.6} + \tau_{5.1.2.10} + \tau_{5.1.2.11}$	$\tau(C''C')$

Atom numbering is given in Figure 4.1(d).

Table 4.5: Symmetry coordinates of Adipic acid

Coordinate	Description
A_g species	
$S_1 = R_{1.2}$	$\nu(C''C'')$
$S_2 = R_{1.3} + R_{2.6}$	$\nu(C''C')$
$S_3 = R_{3.7} + R_{6.12}$	$\nu(C'C)$
$S_4 = R_{14.19} + R_{18.20}$	$\nu(OH)$
$S_5 = R_{7.13} + R_{12.17}$	$\nu(C=O)$
$S_6 = R_{7.14} + R_{12.18}$	$\nu(C-O)$
$S_7 = R_{3.8} - R_{3.9} + R_{6.15} - R_{6.16}$	$\nu_a(C'H_2)$
$S_8 = R_{3.8} + R_{3.9} + R_{6.15} + R_{6.16}$	$\nu_s(C'H_2)$
$S_9 = R_{1.4} - R_{1.5} + R_{2.10} - R_{2.11}$	$\nu_a(C''H_2)$
$S_{10} = R_{1.4} + R_{1.5} + R_{2.10} + R_{2.11}$	$\nu_s(C''H_2)$
$S_{11} = 2\alpha_{3.7.14} - \alpha_{13.7.14} - \alpha_{3.7.13} + 2\alpha_{6.12.18} - \alpha_{17.12.18} - \alpha_{6.12.17}$	$\delta(C-O)$
$S_{12} = \alpha_{13.7.14} - \alpha_{3.7.13} + \alpha_{17.12.18} - \alpha_{6.12.17}$	$\delta(C=O)$
$S_{13} = \alpha_{7.14.19} + \alpha_{12.18.20}$	$\delta(COH)$
$S_{14} = 4\alpha_{8.3.9} - \alpha_{1.3.8} - \alpha_{1.3.9} - \alpha_{7.3.8} - \alpha_{7.3.9} + 4\alpha_{15.6.16} - \alpha_{2.6.15} - \alpha_{2.6.16} - \alpha_{12.6.15} - \alpha_{12.6.16}$	$\delta(C'H_2)$
$S_{15} = \alpha_{1.3.8} + \alpha_{1.3.9} - \alpha_{7.3.8} - \alpha_{7.3.9} + \alpha_{2.6.15} + \alpha_{2.6.16} - \alpha_{12.6.15} - \alpha_{12.6.16}$	$\omega(C'H_2)$
$S_{16} = \alpha_{1.3.8} - \alpha_{1.3.9} - \alpha_{7.3.8} + \alpha_{7.3.9} + \alpha_{2.6.15} - \alpha_{2.6.16} - \alpha_{12.6.15} + \alpha_{12.6.16}$	$t(C'H_2)$
$S_{17} = \alpha_{1.3.8} - \alpha_{1.3.9} + \alpha_{7.3.8} - \alpha_{7.3.9} + \alpha_{2.6.15} - \alpha_{2.6.16} + \alpha_{12.6.15} - \alpha_{12.6.16}$	$\rho(C'H_2)$
$S_{18} = 5\alpha_{1.3.7} - \alpha_{8.3.9} - \alpha_{1.3.8} - \alpha_{1.3.9} - \alpha_{7.3.8} - \alpha_{7.3.9} + 5\alpha_{2.6.12} - \alpha_{15.6.16} - \alpha_{2.6.15} - \alpha_{2.6.16} - \alpha_{12.6.15} - \alpha_{12.6.16}$	$\delta(C''C'C)$
$S_{19} = 4\alpha_{4.1.5} - \alpha_{2.1.4} - \alpha_{2.1.5} - \alpha_{3.1.4} - \alpha_{3.1.5} + 4\alpha_{10.2.11} - \alpha_{1.2.10} - \alpha_{1.2.11} - \alpha_{6.2.10} - \alpha_{6.2.11}$	$\delta(C''H_2)$
$S_{20} = \alpha_{2.1.4} + \alpha_{2.1.5} - \alpha_{3.1.4} - \alpha_{3.1.5} + \alpha_{1.2.10} + \alpha_{1.2.11} - \alpha_{6.2.10} - \alpha_{6.2.11}$	$\omega(C''H_2)$
$S_{21} = \alpha_{2.1.4} - \alpha_{2.1.5} - \alpha_{3.1.4} + \alpha_{3.1.5} + \alpha_{1.2.10} - \alpha_{1.2.11} - \alpha_{6.2.10} + \alpha_{6.2.11}$	$t(C''H_2)$
$S_{22} = \alpha_{2.1.4} - \alpha_{2.1.5} + \alpha_{3.1.4} - \alpha_{3.1.5} + \alpha_{1.2.10} - \alpha_{1.2.11} + \alpha_{6.2.10} - \alpha_{6.2.11}$	$\rho(C''H_2)$
$S_{23} = 5\alpha_{2.1.3} - \alpha_{4.1.5} - \alpha_{2.1.4} - \alpha_{2.1.5} - \alpha_{3.1.4} - \alpha_{3.1.5} + 5\alpha_{1.2.6} - \alpha_{10.2.11} - \alpha_{1.2.10} - \alpha_{1.2.11} - \alpha_{6.2.10} - \alpha_{6.2.11}$	$\delta(C''C''C')$
$S_{24} = \tau_{14.7.3.13} - \tau_{18.12.6.17}$	$\gamma(COO)$
$S_{25} = \tau_{3.7.14.19} + \tau_{13.7.14.19} - \tau_{6.12.18.20} - \tau_{17.12.18.20}$	$\tau(CO)$
$S_{26} = \tau_{2.1.3.7} + \tau_{2.1.3.8} + \tau_{2.1.3.9} + \tau_{4.1.3.7} + \tau_{4.1.3.8} + \tau_{4.1.3.9} + \tau_{5.1.3.7} + \tau_{5.1.3.8} + \tau_{5.1.3.9} - \tau_{1.2.6.12} - \tau_{1.2.6.15} - \tau_{1.2.6.16} - \tau_{10.2.6.12} - \tau_{10.2.6.15} - \tau_{10.2.6.16} - \tau_{11.2.6.12} - \tau_{11.2.6.15} - \tau_{11.2.6.16}$	$\tau(C''C')$
$S_{27} = \tau_{1.3.7.13} + \tau_{1.3.7.14} + \tau_{8.3.7.13} + \tau_{8.3.7.14} + \tau_{9.3.7.13} + \tau_{9.3.7.14} - \tau_{2.6.12.17} - \tau_{2.6.12.18} - \tau_{15.6.12.17} - \tau_{15.6.12.81} - \tau_{16.6.12.17} - \tau_{16.6.12.18}$	$\tau(C'C)$

Table 4.5. (Continued): Symmetry coordinates of Adipic acid

Coordinate	Description
A_u species	
$S_1 = R_{1.3} - R_{2.6}$	$\nu(C''C')$
$S_2 = R_{3.7} - R_{6.12}$	$\nu(C'C)$
$S_3 = R_{14.19} - R_{18.20}$	$\nu(OH)$
$S_4 = R_{7.13} - R_{12.17}$	$\nu(C=O)$
$S_5 = R_{7.14} - R_{12.18}$	$\nu(C-O)$
$S_6 = R_{3.8} - R_{3.9} - R_{6.15} + R_{6.16}$	$\nu_a(C'H_2)$
$S_7 = R_{3.8} + R_{3.9} - R_{6.15} - R_{6.16}$	$\nu_s(C'H_2)$
$S_8 = R_{1.4} - R_{1.5} - R_{2.10} + R_{2.11}$	$\nu_a(C''H_2)$
$S_9 = R_{1.4} + R_{1.5} - R_{2.10} - R_{2.11}$	$\nu_s(C''H_2)$
$S_{10} = 2\alpha_{3.7.14} - \alpha_{13.7.14} - \alpha_{3.7.13} - 2\alpha_{6.12.18} + \alpha_{17.12.18} + \alpha_{6.12.17}$	$\delta(C-O)$
$S_{11} = \alpha_{13.7.14} - \alpha_{3.7.13} - \alpha_{17.12.18} + \alpha_{6.12.17}$	$\delta(C=O)$
$S_{12} = \alpha_{7.14.19} - \alpha_{12.18.20}$	$\delta(COH)$
$S_{13} = 4\alpha_{8.3.9} - \alpha_{1.3.8} - \alpha_{1.3.9} - \alpha_{7.3.8} - \alpha_{7.3.9} - 4\alpha_{15.6.16} + \alpha_{2.6.15} + \alpha_{2.6.16} + \alpha_{12.6.15} + \alpha_{12.6.16}$	$\delta(C'H_2)$
$S_{14} = \alpha_{1.3.8} + \alpha_{1.3.9} - \alpha_{7.3.8} - \alpha_{7.3.9} - \alpha_{2.6.15} - \alpha_{2.6.16} + \alpha_{12.6.15} + \alpha_{12.6.16}$	$\omega(C'H_2)$
$S_{15} = \alpha_{1.3.8} - \alpha_{1.3.9} - \alpha_{7.3.8} + \alpha_{7.3.9} - \alpha_{2.6.15} + \alpha_{2.6.16} + \alpha_{12.6.15} - \alpha_{12.6.16}$	$t(C'H_2)$
$S_{16} = \alpha_{1.3.8} - \alpha_{1.3.9} + \alpha_{7.3.8} - \alpha_{7.3.9} - \alpha_{2.6.15} + \alpha_{2.6.16} - \alpha_{12.6.15} + \alpha_{12.6.16}$	$\rho(C'H_2)$
$S_{17} = 5\alpha_{1.3.7} - \alpha_{8.3.9} - \alpha_{1.3.8} - \alpha_{1.3.9} - \alpha_{7.3.8} - \alpha_{7.3.9} - 5\alpha_{2.6.12} + \alpha_{15.6.16} + \alpha_{2.6.15} + \alpha_{2.6.16} + \alpha_{12.6.15} + \alpha_{12.6.16}$	$\delta(C''C'C)$
$S_{18} = 4\alpha_{4.1.5} - \alpha_{2.1.4} - \alpha_{2.1.5} - \alpha_{3.1.4} - \alpha_{3.1.5} - 4\alpha_{10.2.11} + \alpha_{1.2.10} + \alpha_{1.2.11} + \alpha_{6.2.10} + \alpha_{6.2.11}$	$\delta(C''H_2)$
$S_{19} = \alpha_{2.1.4} + \alpha_{2.1.5} - \alpha_{3.1.4} - \alpha_{3.1.5} - \alpha_{1.2.10} - \alpha_{1.2.11} + \alpha_{6.2.10} + \alpha_{6.2.11}$	$\omega(C''H_2)$
$S_{20} = \alpha_{2.1.4} - \alpha_{2.1.5} - \alpha_{3.1.4} + \alpha_{3.1.5} - \alpha_{1.2.10} + \alpha_{1.2.11} + \alpha_{6.2.10} - \alpha_{6.2.11}$	$t(C''H_2)$
$S_{21} = \alpha_{2.1.4} - \alpha_{2.1.5} + \alpha_{3.1.4} - \alpha_{3.1.5} - \alpha_{1.2.10} + \alpha_{1.2.11} - \alpha_{6.2.10} + \alpha_{6.2.11}$	$\rho(C''H_2)$
$S_{22} = 5\alpha_{2.1.3} - \alpha_{4.1.5} - \alpha_{2.1.4} - \alpha_{2.1.5} - \alpha_{3.1.4} - \alpha_{3.1.5} - 5\alpha_{1.2.6} + \alpha_{10.2.11} + \alpha_{1.2.10} + \alpha_{1.2.11} + \alpha_{6.2.10} + \alpha_{6.2.11}$	$\delta(C''C''C')$
$S_{23} = \tau_{14.7.3.13} + \tau_{18.12.6.17}$	$\gamma(COO)$
$S_{24} = \tau_{3.7.14.19} + \tau_{13.7.14.19} + \tau_{6.12.18.20} + \tau_{17.12.18.20}$	$\tau(CO)$
$S_{25} = \tau_{2.1.3.7} + \tau_{2.1.3.8} + \tau_{2.1.3.9} + \tau_{4.1.3.7} + \tau_{4.1.3.8} + \tau_{4.1.3.9} + \tau_{5.1.3.7} + \tau_{5.1.3.8} + \tau_{5.1.3.9} + \tau_{1.2.6.12} + \tau_{1.2.6.15} + \tau_{1.2.6.16} + \tau_{10.2.6.12} + \tau_{10.2.6.15} + \tau_{10.2.6.16} + \tau_{11.2.6.12} + \tau_{11.2.6.15} + \tau_{11.2.6.16}$	$\tau(C''C')$
$S_{26} = \tau_{1.3.7.13} + \tau_{1.3.7.14} + \tau_{8.3.7.13} + \tau_{8.3.7.14} + \tau_{9.3.7.13} + \tau_{9.3.7.14} + \tau_{2.6.12.17} + \tau_{2.6.12.18} + \tau_{15.6.12.17} + \tau_{15.6.12.81} + \tau_{16.6.12.17} + \tau_{16.6.12.18}$	$\tau(C'C)$
$S_{27} = \tau_{3.1.2.6} + \tau_{3.1.2.10} + \tau_{3.1.2.11} + \tau_{4.1.2.6} + \tau_{4.1.2.10} + \tau_{4.1.2.11} + \tau_{5.1.2.6} + \tau_{5.1.2.10} + \tau_{5.1.2.11}$	$\tau(C''C'')$

Atom numbering is given in Figure 4.1(e).

Table 4.6: 4-21G and 6-31G** optimized parameters of Malonic acid

				X	I	II
Bond length(A^o)						
1	2			1.503	1.506	1.510
1	3			1.502	1.500	1.508
1	4			1.085	1.081	1.082
1	5			1.086	1.080	1.083
2	6			1.227	1.201	1.185
3	7			1.218	1.201	1.185
2	8			1.291	1.355	1.325
3	9			1.290	1.356	1.324
8	10			.991	.969	.949
9	11			.973	.969	.948
Bond angle(°)						
2	1	3		110.968	110.508	111.570
2	1	4		107.877	109.156	108.528
2	1	5		108.129	108.436	108.727
3	1	4		110.175	109.297	108.967
3	1	5		111.367	110.058	110.380
4	1	5		108.206	109.364	108.603
1	2	6		121.606	126.470	125.464
1	2	8		114.226	110.178	111.124
6	2	8		124.168	123.318	123.404
1	3	7		121.534	126.849	124.628
1	3	9		115.516	109.839	111.812
7	3	9		122.948	123.297	123.546
2	8	10		114.886	111.950	108.620
3	9	11		112.874	112.280	108.727
Dihedral angle(°)						
2	1	3	7	87.121	117.964	106.058
2	1	3	9	-92.426	-63.414	-75.244
3	1	2	6	-6.982	-19.531	-6.928
3	1	2	8	173.116	162.542	174.057
6	2	8	10	4.498	-.086	-.395
7	3	9	11	-3.987	-5.327	-4.090
4	1	2	6	113.794	100.697	113.144
4	1	2	8	-66.108	-77.231	-65.871
4	1	3	7	-32.287	-2.179	-13.755
4	1	3	9	148.166	176.443	164.943

X : Neutron diffraction parameters are from reference [7], I : HF/4-21G optimized parameters, II : HF/6-31G** optimized parameters. Energies of the 4-21G and 6-31G** optimized conformations are -414.430714 and -415.437575 hartrees respectively.

Table 4.7: 4-21G and 6-31G** optimized parameters of Hydroxymalonic acid

				X	I	II
Bond length(A^o)						
1	2			1.299	1.343	1.317
7	10			1.308	1.347	1.319
2	4			1.214	1.203	1.186
7	9			1.219	1.203	1.186
2	5			1.525	1.505	1.518
5	7			1.524	1.515	1.526
5	6			1.391	1.428	1.385
5	8			1.011	1.075	1.083
1	3			.730	.969	.949
6	11			.599	.972	.948
10	12			.851	.969	.949
Bond angle(°)						
1	2	5		113.802	111.009	112.383
5	7	10		112.256	111.297	111.840
4	2	5		120.477	124.025	122.914
5	7	9		122.656	124.707	124.161
1	2	4		125.717	124.966	124.698
9	7	10		125.088	123.956	123.961
2	1	3		115.765	113.222	109.428
7	10	12		114.670	112.325	108.913
2	5	7		109.315	108.235	109.180
2	5	6		111.890	109.660	110.736
2	5	8		109.273	110.647	109.249
7	5	6		112.025	108.781	109.147
7	5	8		110.655	109.536	109.193
6	5	8		103.552	109.939	109.312
5	6	11		112.414	108.843	108.594
Dihedral angle(°)						
4	2	1	3	8.550	4.119	4.036
5	2	1	3	-172.152	-175.675	-176.743
9	7	10	12	-12.027	2.944	2.268
5	7	10	12	167.749	-174.862	-175.564
2	5	6	11	-23.676	-16.461	-20.900
7	5	6	11	99.490	101.733	99.320
1	2	5	7	71.280	65.477	69.844
4	2	5	6	15.305	4.214	9.282
4	2	5	7	-109.381	-114.319	-110.919
4	2	5	8	129.386	125.655	129.730
9	7	5	6	-19.549	-89.333	-96.742
9	7	5	2	105.059	29.758	24.430
10	7	5	2	-74.724	-152.455	-157.744
9	7	5	8	-134.550	150.478	143.815
8	5	6	11	-141.241	-138.327	-141.311

X : Neutron diffraction parameters are from reference [8], I : HF/4-21G optimized parameters, II : HF/6-31G** optimized parameters. Energies of the 4-21G and 6-31G** optimized conformations are -489.093658 and -490.287754 hartrees respectively.

Table 4.8: 4-21G and 6-31G** optimized parameters of Succinic acid

				X	I	II
Bond length($A°$)						
1	2			1.508	1.524	1.521
1	3			1.500	1.499	1.505
1	4			1.087	1.083	1.084
1	5			1.087	1.083	1.084
3	7			1.222	1.205	1.188
3	8			1.305	1.358	1.328
8	13			.994	.969	.948
Bond angle(°)						
2	1	3		113.005	110.989	112.081
2	1	4		110.985	111.229	111.313
2	1	5		112.019	111.261	111.313
4	1	3		107.085	108.580	108.123
5	1	3		107.783	108.544	108.124
1	3	7		123.776	126.402	125.725
1	3	8		113.292	111.063	111.768
7	3	8		122.927	122.534	122.507
3	8	13		112.007	111.736	108.473
Dihedral angle(°)						
2	1	3	7	-10.757	-.056	.000
2	1	3	8	169.975	179.895	180.000
4	1	3	7	111.758	122.495	123.054
4	1	3	8	-67.510	-57.545	-56.946
1	3	8	13	176.967	179.948	180.000
7	3	8	13	-2.308	-.095	.000

X : Neutron diffraction parameters are from reference [9], I : HF/4-21G optimized parameters, II : HF/6-31G** optimized parameters. Energies of the 4-21G and 6-31G** optimized conformations are -453.392742 and -454.483226 hartrees respectively.

Table 4.9: 4-21G optimized parameters of Glutaric acid

				X	I					I
Bond length(A^o)						Bond length(A^o)				
1	2			1.530	1.531	1	3			1.531
1	4			-	1.081	1	5			1.081
2	10			-	1.085	3	8			1.085
2	11			-	1.085	3	9			1.085
2	6			1.530	1.502	3	7			1.502
6	12			1.230	1.204	7	14			1.204
6	13			1.300	1.361	7	15			1.361
13	16			-	.969	15	17			.969
Bond angle(^{o})						Bond angle(^{o})				
1	2	10		-	111.565	1	3	8		111.560
1	2	11		-	111.565	1	3	9		111.560
1	2	6		115.000	111.564	1	3	7		111.584
10	2	11		-	106.617	8	3	9		106.609
2	6	12		123.000	126.754	3	7	14		126.778
2	6	13		115.000	110.864	3	7	15		110.846
12	6	13		122.000	122.382	14	7	15		122.376
6	13	16		-	111.599	7	15	17		111.606
2	1	3		109.000	111.285	2	1	4		109.781
2	1	5		-	109.781					
Dihedral angle(^{o})						Dihedral angle(^{o})				
1	2	6	13		180.000	1	3	7	15	180.000
2	6	13	16		180.000	3	7	15	17	180.000
2	1	3	7		179.972	4	1	3	7	-58.259
5	1	3	7		58.259					

X : X-ray parameters are from reference [11], I : HF/4-21G optimized parameters.
Energy of the 4-21G optimized conformation is -492.344542 hartrees.

Table 4.10: 4-21G optimized parameters of Adipic acid

				X	I
Bond length(A°)					
1	2			1.506	1.537
1	3			1.528	1.532
1	4			.921	1.084
1	5			1.060	1.084
3	7			1.500	1.502
3	8			1.005	1.085
3	9			1.035	1.085
7	13			1.233	1.205
7	14			1.294	1.361
14	19			1.178	.969
Bond angle(°)					
2	1	3		110.367	111.631
2	1	4		108.668	110.065
2	1	5		107.401	110.086
4	1	5		93.873	106.744
1	3	7		114.746	111.675
1	3	8		109.314	111.346
1	3	9		112.531	111.318
8	3	9		111.654	106.608
3	7	13		121.635	126.709
3	7	14		116.146	111.045
13	7	14		122.201	122.246
7	14	19		110.262	111.624
Dihedral angle(°)					
2	1	3	7	-174.385	180.000
1	3	7	13	-8.142	.063
1	3	7	14	173.357	-179.937
4	3	7	13	-24.997	-23.957
4	3	7	14	156.501	156.034
3	7	14	19	-168.844	-179.948
13	7	14	19	12.664	.052

X : X-ray parameters are from reference [10], I : HF/4-21G optimized parameters. Energy of the 4-21G optimized conformation is -531.298409 hartrees.

Table 4.11: Comparison of gas phase and solid state IR frequencies of acetic acid

Freq.	Assignment	Solid State[a]		Gas Phase		
		0^oC	-180^oC	G1	G2	G3
	A' species					
1	$\nu(OH)$	2927	2875	3583	3577	3566
2	$\nu_d(CH_3)$	-	-	3051	2997	3051
3	$\nu_s(CH_3)$	-	-	2944	2961	2941
4	$\nu(C=O)$	-	-	1788	1799	1779
5	$\delta_d(CH_3)$	-	-	1430	1401	1439
6	$\delta_s(CH_3)$	-	-	1382	1340	1380
7	$\delta(COH)+\nu(C-O)$	1411	1418	1264	1279	1280
8	$\nu(C-O)+\delta(COH)$	1268	1284	1182	1192	1181
9	$\rho(CH_3)$	1019	1022	989	990	987
10	$\nu(CC)$	884	908	847	846	847
11	$\rho(CO_2):\delta(C-O)$	629	635	657	654	581
12	$\delta(CO_2):\delta(C=O)$	450	450	581	536	536
	A'' species					
1	$\nu_d(CH_3)$	-	-	2996	3048	2996
2	$\delta_d(CH_3)$	1440	1448	1430	1445	1434
3	$\rho(CH_3)$	1047	1049	1048	1068	1044
4	$\omega(CO_2):\gamma(COO)$	-	592	642	654	639
5	$\pi(OH):\tau(CO)$	906	923	534	582	535
6	$\tau(CC)$	-	-	-	-	-

(a) Solid state frequencies are from reference [16]. G1 : Gas phase frequencies are from reference [31], G2 : Gas phase frequencies are from reference [30], Gas phase frequencies are from reference [23a]. The gas phase frequencies have been arranged according to the assignment of reference [31].

Table 4.12: Comparison of calculated, gas phase and solid state IR frequencies of oxalic acid(cTc conformer)

Freq.	Assignment	Calculated			Gas Phase	Solid State	
		I	II	III	G1	$S1_\alpha$	$S2_\beta$
	A_g species						
1	$\nu(OH)$	3620	3868	3480	-	2887	3110
2	$\nu(C=O)$	1877	1964	1797	1800[a]	1702	1763
3	$\delta(COH)$	1361	1504	1460	1423[a]	1493	1475
4	$\nu(C-O)$	1194	1225	1221	1195[a]	1317	1209
5	$\nu(CC)$	794	861	816	815	852	823
6	$\delta(C-O)$	545	555	562	-	547	560
7	$\delta(C=O)$	404	416	410	405[a]	485	462
	A_u species						
1	$\tau(CO)$	585	615	712	664	907	828
2	$\gamma(COO)$	451	463	455	461[b]	492	506
3	$\tau(CC)$	137	109	133	-	138	-
	B_g species						
1	$\gamma(COO)$	781	803	783	-	-	-
2	$\tau(CO)$	578	608	696	-	885	792
	B_u species						
1	$\nu(OH)$	3621	3871	3485	3472	2915	3157
2	$\nu(C=O)$	1891	1960	1824	1817	1737	1714
3	$\delta(COH)$	1240	1346	1334	1329	1407	1381
4	$\nu(C-O)$	1193	1223	1205	1176	1237	1181
5	$\delta(C=O)$	650	666	649	-	725	674
6	$\delta(C-O)$	249	268	274	264[b]	373	336

(a)Raman frequencies from reference [22], (b) Neon matrix values below $500cm^{-1}$from reference [33], I : HF/4-21G frequencies, II : HF/6-31G** frequencies, III : MP2/4-31G* frequencies from reference [14]. G1 : Gas phase frequencies are from reference [22], S1 : Solid state frequencies of the α form are from reference [32], S2 : Solid state frequencies of the β form are from reference [27].

Table 4.13: Calculated frequencies of Malonic acid

Freq.	Unscaled		Scaled		Exp.		R. A.	I. R.
	I	II	I	II	Ra	Ir		
1	55	48	50	43	-	-	.5	.3
2	85	77	76	69	-	-	1.5	2.4
3	181	172	162	154	-	244	.6	2.2
4	387	397	348	358	407	429	.8	3.0
5	426	440	385	396	432	451	.7	2.0
6	559	561	500	502	578	574	3.1	24.8
7	562	575	505	518	578	574	2.2	21.0
8	632	659	568	592	592	592	3.7	137.7
9	651	681	584	612	-	-	1.7	150.5
10	684	712	612	637	-	-	.7	140.8
11	783	818	715	745	665	655	5.7	15.8
12	960	1002	906	935	923	919	4.3	9.3
13	973	986	895	911	923	919	6.0	13.5
14	1056	1065	952	958	940	935	.6	3.6
15	1222	1306	1125	1199	-	-	1.2	242.9
16	1240	1363	1135	1233	-	-	6.9	108.7
17	1363	1280	1223	1159	1180	1173	2.0	204.7
18	1438	1418	1296	1275	1218	1216	2.2	.8
19	1491	1510	1366	1385	1403	1397	1.9	42.0
20	1525	1570	1430	1428	1427	1414	1.3	215.6
21	1597	1585	1393	1449	1437	1436	7.8	46.5
22	1959	2038	1850	1925	1650	1703	5.9	368.1
23	1972	2054	1862	1940	1686	1735	6.7	470.8
24	3266	3243	3100	3078	2951	2955	84.9	1.1
25	3319	3300	3151	3132	2991	2995	53.6	.8
26	3853	4124	3657	3914	-	2990	75.1	140.3
27	3859	4130	3662	3919	-	2990	78.2	116.5

I : 4-21G frequencies, II : 6-31G** frequencies, Exp. : Experimental frequencies are from reference [7]. R. A. :Raman activities are in units of A^4/AMU, I. R. :IR intensities in units of KM/mol. All frequencies are in units of $cm^{-1}$and arranged so that their corresponding potential energy distribution (PED) matches with the unscaled 4-21G PED's.

Table 4.14: Calculated frequencies of Hydroxymalonic acid

Freq.	Unscaled		Scaled		Exp.		R. A.	I. R.
	I	II	I	II	Ra	Ir		
1	47	32	42	29	-	-	.7	2.4
2	102	94	91	84	-	-	1.1	1.1
3	172	170	154	152	-	-	.7	4.1
4	243	269	218	241	202	-	.6	9.2
5	283	301	254	270	325	325	1.0	13.6
6	357	365	320	327	-	-	.5	103.1
7	409	417	370	377	420	420	1.7	16.4
8	501	512	452	463	-	445	1.4	9.5
9	549	558	495	503	-	-	1.6	18.8
10	631	647	566	580	-	-	3.1	133.5
11	656	678	588	609	-	610	2.2	249.3
12	687	716	620	646	660	660	3.2	56.5
13	782	815	719	745	697	700	6.4	33.2
14	835	866	752	781	790	800	1.4	36.7
15	977	999	889	909	921	920	4.7	31.8
16	1006	1048	940	974	950	-	2.9	23.9
17	1152	1249	1079	1161	1135	1130	3.0	210.2
18	1225	1298	1126	1192	-	-	1.0	255.1
19	1242	1326	1139	1211	-	-	1.8	174.0
20	1380	1388	1287	1256	1240	1250	5.1	57.3
21	1431	1426	1245	1286	1275	1280	3.6	17.6
22	1469	1486	1328	1346	1312	1315	2.6	146.7
23	1523	1566	1395	1442	1365	1380	2.5	86.4
24	1574	1612	1435	1478	1450	1445	1.3	39.4
25	1952	2036	1844	1923	1665	1735	5.7	290.2
26	1956	2046	1848	1933	1665	1735	7.1	477.9
27	3329	3265	3159	3098	2953	2960	73.0	10.5
28	3812	4117	3617	3906	3485	3500	25.4	134.4
29	3851	4122	3655	3911	-	-	72.8	140.3
30	3854	4124	3658	3913	-	-	90.2	116.7

I : 4-21G frequencies, II : 6-31G** frequencies, Exp. : Experimental frequencies are from reference [17]. R. A. :Raman activities are in units of A^4/AMU, I. R. :IR intensities in units of KM/mol. All frequencies are in units of $cm^{-1}$and arranged so that the corresponding potential energy distribution (PED) matches with the unscaled 4-21G PED's.

Table 4.15: Calculated frequencies of Succinic acid

Freq.	Unscaled		Scaled		Exp.	R. A./I. R.
	I	II	I	II		
A_g species						
1	112	94	101	84	157	.3
2	269	268	243	242	-	1.0
3	373	387	340	352	388	1.9
4	552	559	493	501	575	7.1
5	679	712	607	637	-	1.0
6	700	720	635	651	678	7.5
7	985	996	912	923	931	12.5
8	1126	1161	1058	1085	1084	4.7
9	1164	1153	1041	1031	-	1.0
10	1233	1317	1135	1210	-	3.8
11	1440	1423	1289	1273	-	13.7
12	1453	1448	1318	1315	-	4.1
13	1558	1587	1443	1422	1370	16.4
14	1613	1608	1415	1472	1445	.8
15	1947	2030	1837	1916	1652	8.6
16	3246	3229	3080	3065	2925	157.5
17	3272	3261	3106	3094	2966	105.6
18	3853	4130	3656	3919	-	174.2
A_u species						
1	18	26	16	23	-	4.3
2	76	80	68	71	-	.2
3	140	140	125	125	225	5.8
4	555	556	496	498	545	54.2
5	565	574	506	514	584	51.0
6	638	654	576	591	639	115.5
7	671	695	600	622	-	242.9
8	891	887	797	793	802	58.3
9	913	947	863	892	893	2.1
10	1213	1279	1383	1174	-	518.0
11	1325	1294	1185	1157	1175	4.2
12	1411	1396	1117	1253	1203	62.9
13	1511	1538	1267	1408	1308	288.0
14	1615	1594	1445	1437	1418	60.3
15	1940	2025	1832	1913	1739	750.3
16	3252	3233	3086	3069	2930	12.0
17	3293	3279	3125	3112	2980	9.7
18	3852	4129	3656	3919	2990	240.8

I : 4-21G frequencies, II : 6-31G** frequencies, Exp. : Experimental frequencies are from reference [5]. R. A. : Raman activities are in units of A^4/AMU, I. R. :IR intensities in units of KM/mol. All frequencies are in units of $cm^{-1}$and arranged so that the corresponding potential energy distribution (PED) matches with the unscaled 4-21G PED's.

Table 4.16: Calculated frequencies of Glutaric acid

Freq.	Uns.	Sca.	Exp.				R. A.	I. R.
			E1	E2	E3	E4		
	A′ species							
1	101	91	-	-	-	-	.0	.2
2	242	216	-	292(sh)	-	-	.3	5.6
3	286	263	320(m)	325(sh)	-	-	3.4	.3
4	450	404	-	-	-	-	.6	6.3
5	544	491	-	-	481(m)	-	2.9	120.0
6	678	613	587(m)	600(m)	586(m)	-	3.3	.2
7	691	624	680(m)	672(m)	670(vw)	-	4.5	28.8
8	896	843	-	792(m)	762(m)	785(sh)	.1	6.4
9	969	907	852(m)	862(vs)	853(sh)	870(m)	11.5	.1
10	1110	1034	1067(m)	1061(s)	1067(s)	1060(m)	8.0	.4
11	1111	1046	1067(m)	1061(s)	1067(s)	1060(m)	8.4	29.5
12	1206	1114	-	-	-	-	.6	575.9
13	1231	1133	-	-	-	-	7.0	87.3
14	1405	1261	1240(w)	1236(w)	1235(w)	1240(vs)	1.5	20.5
15	1441	1301	-	-	-	-	3.9	2.6
16	1478	1343	-	-	-	-	1.0	144.9
17	1532	1393	-	1335(w)	-	1320(sh)	1.2	.1
18	1546	1396	-	-	1350(m)	-	.3	55.6
19	1618	1449	1445(m)	1440(sh)	-	-	.0	8.9
20	1626	1455	1445(m)	1440(sh)	-	-	35.3	34.0
21	1648	1474	1465(m)	-	1468(m)	1455(sh)	3.6	13.9
22	1948	1839	1647(m)	1707(vs)	1700(vs)	1715(vs)	.2	9.1
23	1952	1842	1647(m)	1707(vs)	1700(vs)	1715(vs)	9.1	483.1
24	3218	3054	-	-	-	-	.2	4.1
25	3220	3056	2905(vs)	2912(vs)	-	-	171.5	7.1
26	3256	3090	2977(vs)	-	2985(m)	2985(sh)	36.5	8.2
27	3851	3655	-	-	-	-	145.1	71.3
28	3854	3657	-	-	-	-	158.8	65.5
	A″ species							
1	28	25	-	-	-	-	.1	.0
2	59	53	-	-	-	-	.0	.0
3	92	83	-	-	-	-	.0	.1
4	126	112	-	-	-	-	.7	.0
5	551	493	442(s)	460(m)	-	-	9.9	.3
6	563	504	-	512(sh)	527(m)	-	2.0	115.0
7	674	603	-	-	-	-	4.2	7.5
8	606	-	-	-	-	.1	274.0	
9	816	730	-	737(m)	695(vw)	-	.2	47.2
10	964	862	852(m)	862(vs)	853(sh)	870(m)	.2	.0
11	1207	1080	1162(w)	1160(m)	1164(m)	1175(m)	.5	10.9
12	1314	1176	1203(w)	1210(vw)	1207(s)	1210(sh)	3.8	.0
13	1426	1276	-	1271(sh)	1281(w)	1270(sh)	.4	1.9
14	1461	1308	1295(m)	1296(m)	1306(vs)	1295(sh)	27.7	.0
15	3248	3082	2950(vs)	2945(vs)	2960(s)	-	148.3	4.6
16	3250	3085	-	-	-	-	.9	.0
17	3299	3131	-	-	-	-	7.7	13.3

I : 4-21G frequencies, (E1, E2), (E3, E4) : Experimental Raman and IR frequencies of the powder and solution are from reference [18], R. A. :Raman activities are in units of A^4/AMU, I. R. :IR intensities in units of KM/mol. All frequencies are in units of $cm^{-1}$and arranged so that the corresponding potential energy distribution (PED) matches with the unscaled 4-21G PED's. (vw) very weak, (w) weak, (sh) shoulder, (m) medium, (s) strong, (vs) very strong

Table 4.17: Calculated frequencies of Adipic acid

	A_g species				A_u species			
Freq.	Uns.	Sca.	Exp.	R. A.	Uns.	Sca.	Exp.	I. R.
1	73	66	-	.5	30	27	-	2.9
2	121	109	-	.5	49	44	-	0.0
3	186	167	-	.7	81	72	-	2.3
4	269	247	-	4.1	143	128	-	.6
5	542	485	514	.4	350	313	-	6.5
6	557	498	575	12.2	503	457	517	94.1
7	663	600	666	10.5	558	499	530	107.1
8	675	604	-	4.1	679	607	-	295.5
9	881	789	800	.5	699	632	690	57.6
10	932	879	920	10.2	795	711	739	29.2
11	1098	1027	1051	10.7	922	861	904	9.6
12	1136	1061	1091	16.1	1023	915	915	17.9
13	1228	1130	-	9.0	1081	1020	1044	25.1
14	1229	1100	-	1.1	1210	1116	-	675.6
15	1399	1251	1224	8.1	1301	1164	1150	4.5
16	1432	1290	1248	5.3	1396	1253	1194	29.5
17	1466	1312	1302	35.5	1465	1311	1316	32.9
18	1507	1390	1383	1.9	1465	1327	-	70.5
19	1538	1364	1413	.9	1539	1393	1357	101.9
20	1623	1453	1436	27.6	1620	1450	1410	45.7
21	1648	1474	1448	23.9	1660	1485	1462	16.4
22	1946	1837	1644	8.9	1945	1836	1697	493.6
23	3216	3052	2875	174.2	3217	3053	-	3.3
24	3222	3058	2890	88.4	3228	3064	-	38.4
25	3236	3072	2919	177.9	3245	3080	-	.4
26	3260	3094	2935	21.9	3278	3111	2978	42.9
27	3853	3656	-	322.9	3852	3656	3000	133.9

I : 4-21G frequencies, Exp. : Experimental frequencies are from reference [6]. R. A. :Raman activities are in units of A^4/AMU, I. R. :IR intensities in units of KM/mol. All frequencies are in units of cm^{-1} and arranged so that the corresponding potential energy distribution (PED) matches with the unscaled 4-21G PED's.

Table 4.18: Potential energy distributions of the frequencies of Malonic acid

No.	I		II	
	Freq.	PED	Freq.	PED
1	55	26(81.9)	48	26(78.9)
2	85	27(67.1),19(15.5)	77	27(81.1)
3	181	19(54.2),11(13.8)	172	19(62.2),11(13.6),23(10.6)
4	387	11(35.5),13(28.1),18(10.1)	397	11(46.1),13(21.2)
5	426	13(30.9),14(23.1),18(11.7)	440	13(39.6),14(20.9),18(17.2)
6	559	22(32.6),24(23.4),27(13.5)	561	22(40.0),24(27.9),18(12.1)
7	562	25(32.6),23(25.0),12(13.5)	575	25(37.1),23(23.6),12(20.3)
8	632	14(45.4),11(14.6)	659	14(42.1),11(15.7),12(13.2)
9	651	25(47.7),12(26.8),23(11.2)	681	25(48.7),12(23.3)
10	685	24(46.1),22(29.4)	712	24(49.2),22(26.9)
11	783	23(24.3), 7(11.0), 9(10.1)	819	23(31.0)
12	960	10(37.5), 8(26.2), 9(16.5)	986	9(48.3),23(14.7)
13	973	9(31.5),23(20.8),19(18.5)	1003	10(36.4), 8(24.5)
14	1057	18(51.1),27(10.9),22(10.2)	1065	18(52.8),22(16.3)
15	1222	7(40.3),20(31.5)	1281	17(41.7), 8(17.1),21(11.0)
16	1240	21(30.5), 8(28.0)	1306	7(38.6),20(29.3)
17	1364	17(74.0),21(15.2)	1363	21(49.1),17(26.9), 8(12.7)
18	1439	16(46.7),20(30.0)	1419	16(39.9),20(38.4)
19	1491	21(26.6), 8(24.3),14(16.9),10(10.3)	1511	8(24.4),14(13.7),21(11.8), 7(10.4)
20	1525	16(39.8), 9(15.3), 7(11.1)	1571	16(27.1), 9(18.0), 7(14.0),10(10.7)
21	1598	15(96.0)	1585	15(82.0)
22	1959	5(80.2)	2038	5(68.3), 6(12.6)
23	1973	6(79.4)	2055	6(68.1), 5(12.5)
24	3267	4(99.0)	3244	4(97.5)
25	3320	3(99.0)	3301	3(97.7)
26	3854	1(99.7)	4126	1(99.3)
27	3860	2(99.7)	4131	2(99.3)

I : 4-21G distributions, II : 6-31G** distributions. Symmetry coordinate numbers given in Table 4.1

Table 4.19: Potential energy distributions of the frequencies of Hydroxymalonic acid

No.	I		II	
	Freq.	PED	Freq.	PED
1	47	30(72.2),29(18.1)	32	30(64.5),29(19.3)
2	102	29(61.6),26(21.5)	94	29(67.5),26(20.7)
3	172	22(57.0)	170	22(59.7),14(10.2)
4	243	23(40.6),26(12.4)	269	23(39.7),12(14.4)
5	283	21(47.9),12(18.1),25(10.7)	301	21(48.5),12(12.6),25(12.4)
6	357	26(71.5)	365	26(69.4),14(10.4)
7	409	14(40.5),13(11.6),26(11.2),10(11.2)	417	14(38.0),13(13.0),26(12.6),10(11.5)
8	501	12(46.8)	513	12(47.1)
9	550	27(37.7),24(21.4),15(20.4),11(10.8)	558	27(40.3),24(19.4),15(18.5),11(11.8)
10	631	28(78.0)	647	28(66.0),27(17.4)
11	656	27(41.6),15(28.0)	679	15(30.0),27(27.8),28(17.0)
12	687	13(41.2)	716	13(40.1),24(10.1)
13	783	24(14.4),11(12.9),13(12.7), 9(10.6) ,15(10.4),10(10.4)	815	24(20.2),13(12.4),10(10.2),11(10.0) -
14	835	25(56.7)	866	25(53.2)
15	977	23(27.2),24(20.7),10(17.0)	999	23(27.5),24(20.2),10(19.9)
16	1006	11(31.7),10(21.2),21(15.3)	1049	11(28.1),10(18.5),21(15.7)
17	1152	7(62.2),18(12.6)	1249	7(65.1),18(12.1)
18	1225	9(22.4),16(18.8),17(18.4), 8(16.3) -	1298	9(21.1),19(18.9), 8(18.3),16(16.2) ,17(13.9)
19	1242	16(22.1),17(21.5), 8(19.2), 9(19.0)	1326	17(24.8),16(22.8), 9(18.4), 8(14.2)
20	1380	20(33.4),19(25.1),18(19.7) -	1388	19(24.9),18(19.7),16(19.4), 7(12.0) ,20(10.4)
21	1431	19(27.9),20(23.4),17(22.8)	1426	17(28.4),20(22.9),19(13.2),18(11.6)
22	1469	18(28.9),16(22.1), 8(17.1),20(11.4) ,13(11.3)	1487	18(27.3), 8(20.4),20(16.0),16(14.2) ,13(11.6)
23	1524	20(19.2), 9(17.3),17(14.2),11(13.0) ,19(10.4)	1566	9(23.4),20(21.3),11(17.5),15(11.0) -
24	1575	18(28.2),19(19.6),10(15.2) -	1612	10(19.5),18(18.2),19(14.2), 8(14.2) ,20(10.4)
25	1953	6(75.6)	2036	6(63.2), 5(17.5)
26	1957	5(75.0)	2046	5(63.6), 6(17.4)
27	3330	4(99.3)	3266	4(99.3)
28	3813	1(99.9)	4118	1(97.9)
29	3852	3(98.6)	4123	3(91.5)
30	3855	2(98.6)	4125	2(93.4)

I : 4-21G distributions, II : 6-31G** distributions. Symmetry coordinate numbers given in Table 4.2

Table 4.20: Potential energy distributions of the frequencies of Succinic acid

No.	I		II	
	Freq.	PED	Freq.	PED
A_g species				
1	113	18(91.1)	94	18(80.8),14(10.1)
2	269	15(42.1),10(22.0), 9(20.8), 6(10.3)	268	15(48.0),10(20.2), 9(15.9), 6(12.0)
3	373	9(66.1), 7(15.0), 6(11.6)	387	9(69.6), 7(14.3)
4	552	16(45.5),17(30.6),14(17.4)	560	16(44.0),17(30.3),14(18.8)
5	679	17(56.6),16(30.8)	712	17(56.8),16(27.2),14(11.8)
6	700	10(57.4), 5(15.6)	720	10(59.0), 5(12.7),15(10.3)
7	986	6(49.9),15(32.1)	997	6(49.4),15(26.6)
8	1126	7(68.7), 5(11.4)	1153	14(73.4),16(22.8)
9	1164	14(78.4),16(18.1)	1161	7(70.4),15(11.0)
10	1234	5(39.7), 8(32.9)	1317	5(43.0), 8(37.2)
11	1441	13(95.5)	1423	13(94.8)
12	1453	8(38.0),12(22.0), 5(16.8),10(11.9)	1449	8(36.7),12(23.5), 5(16.6),10(11.2)
13	1559	12(61.7), 6(15.5)	1587	11(87.8)
14	1613	11(95.1)	1609	12(48.4), 6(15.8), 7(11.7)
15	1948	4(78.7)	2030	4(79.7)
16	3247	2(99.2)	3230	2(99.2)
17	3273	3(99.4)	3262	3(99.4)
18	3854	1(99.9)	4131	1(99.9)
A_u species				
1	18	17(49.7),18(39.8)	26	17(61.4),18(22.0)
2	76	18(56.7),17(37.5)	80	18(82.4),17(11.8)
4	555	15(39.7),13(27.2),16(26.8)	556	15(38.0),13(29.9),16(23.9)
5	565	8(69.2),14(16.8)	574	8(71.8),14(16.3)
6	638	9(76.2)	654	9(76.6), 6(10.8)
7	671	16(62.4),15(18.3),13(17.4)	695	16(64.6),13(22.0),15(10.9)
8	891	13(50.7),15(27.9),12(19.1)	887	13(40.2),15(34.8),12(22.1)
9	913	6(65.7), 5(23.7)	947	6(65.3), 5(18.6)
10	1213	5(42.6), 7(35.6)	1279	5(42.4),11(27.4), 7(22.8)
11	1325	12(89.4)	1294	12(86.4)
12	1412	11(62.7), 7(26.9)	1397	7(50.7),11(41.0)
13	1511	11(28.0), 5(19.2), 6(17.1), 7(17.0), 9(14.7)	1538	5(26.2),11(21.4), 6(17.9) , 9(16.3)
14	1616	10(97.5)	1595	10(91.6)
15	1940	4(80.3)	2025	4(81.1)
16	3253	2(99.8)	3234	2(99.7)
17	3294	3(99.9)	3280	3(99.9)
18	3854	1(99.9)	4131	1(99.9)

I : 4-21G distributions, II : 6-31G** distributions. Symmetry coordinate numbers given in Table 4.3

Table 4.21: Potential energy distributions of the frequencies of Glutaric acid

No.	*A' species*		*A'' species*	
	Freq.	PED	Freq.	PED
1	101	22(30.3),28(26.7),25(26.5)	28	15(27.3),14(27.2),17(18.3),16(18.2)
2	242	25(21.2),28(21.2),17(18.8),16(18.8)	59	15(28.7),14(28.5),16(18.4),17(17.9)
3	286	22(26.2),13(12.1),12(12.1),10(12.1) ,11(12.1)	92	14(24.8),15(24.6),17(17.3),16(17.2) -
4	450	16(30.7),17(30.7),22(18.7)	126	17(32.7),16(32.4),14(15.6),15(15.3)
5	544	17(24.2),16(24.2) -	551	11(23.0),10(19.6),13(16.2),12(13.0) , 9(12.1), 7(10.5)
6	678	19(31.3),18(31.2)	563	10(22.3),12(18.5),11(18.2),13(16.1)
7	692	18(27.2),19(27.0),25(13.1),28(13.0)	674	13(38.4),12(20.4),11(16.9)
8	897	10(29.6),11(29.5)	678	12(36.1),13(17.4),10(16.4)
9	969	11(29.5),10(29.4)	817	5(51.3)
10	1110	12(44.2),13(44.0)	964	7(26.1), 9(26.0), 4(15.5)
11	1111	13(25.1),12(24.9),22(10.2)	1207	5(32.0), 7(24.9), 9(24.8)
12	1206	9(23.5), 8(22.9),15(16.8),14(16.3)	1314	6(30.2), 8(30.1), 4(24.8)
13	1231	8(19.2), 9(18.5),14(15.8),15(15.4)	1426	8(44.1), 6(44.1)
14	1405	27(24.4),24(24.3),21(23.4)	1462	4(69.1), 8(14.4), 6(14.3)
15	1441	15(19.2),14(19.2),24(16.3),27(16.0)	3248	3(44.0), 2(43.5), 1(12.0)
16	1479	21(29.8),14(11.7),15(11.5)	3251	2(50.0), 3(49.6)
17	1532	24(27.6),27(27.4)	3300	1(88.2)
18	1546	21(38.6),27(16.4),24(16.2)		
19	1619	23(47.8),26(47.5)		
20	1627	26(45.2),23(45.0)		
21	1648	20(93.3)		
22	1948	6(43.6), 7(36.4)		
23	1952	7(43.4), 6(36.2)		
24	3218	5(50.8), 4(48.8)		
25	3221	4(49.6), 5(47.6)		
26	3257	3(97.6)		
27	3852	1(99.8)		
28	3855	2(99.8)		

I : 4-21G distributions. Symmetry coordinate numbers given in Table 4.4

Table 4.22: Potential energy distributions of the frequencies of Adipic acid

No.	A_g species		A_u species	
	Freq.	PED	Freq.	PED
1	73	27(82.6)	30	26(49.3),25(33.4)
2	121	26(91.1)	49	25(51.1),27(19.3),26(17.0)
3	186	18(56.6),11(20.3),12(11.6)	81	22(55.1),17(34.1)
4	269	23(31.3), 2(22.7),11(20.1), 3(13.8)	143	27(60.9),26(27.2)
5	542	11(45.5),23(32.8)	350	10(38.2),22(22.9),11(16.8),17(14.6)
6	557	24(40.6),25(31.5),17(20.4)	503	10(45.5), 2(13.9),17(12.0)
7	663	12(67.8)	558	23(42.0),24(33.1),16(18.6)
8	676	25(56.5),24(24.8),17(14.4)	679	24(55.4),23(26.8),16(13.6)
9	882	22(34.1),17(29.0),24(15.4),16(13.7)	699	11(57.5),17(14.5), 5(14.0)
10	932	3(59.8), 6(14.9)	795	21(70.0)
11	1098	1(67.8)	923	2(52.9),17(16.2)
12	1137	2(57.4),23(18.4)	1023	16(44.6),20(26.7),23(12.2)
13	1228	6(38.0),13(30.8)	1081	1(82.6)
14	1230	22(45.7),17(33.5),16(10.5)	1210	5(44.2),12(32.5)
15	1399	16(73.1),22(18.1)	1301	15(48.6),20(32.6),16(10.7)
16	1432	15(43.0),13(32.2)	1397	19(41.8),14(37.0),12(13.8)
17	1467	21(92.1)	1465	15(32.1),20(30.8)
18	1507	20(32.8),15(22.8), 6(10.8)	1465	19(23.5),12(20.7),15(12.1), 5(11.9) ,20(11.6)
19	1538	20(51.7),15(20.9)	1539	14(46.9),19(19.9), 2(11.1)
20	1623	14(95.0)	1621	13(91.6)
21	1649	19(95.7)	1660	18(95.2)
22	1947	5(79.6)	1945	4(79.8)
23	3217	10(95.2)	3218	7(60.4), 9(39.1)
24	3223	8(95.5)	3229	9(60.6), 7(39.3)
25	3237	9(77.4), 7(21.9)	3246	6(71.2), 8(28.4)
26	3261	7(78.0), 9(21.8)	3279	8(71.6), 6(28.3)
27	3854	4(99.9)	3854	3(99.9)

I : 4-21G distributions. Symmetry coordinate numbers given in Table 4.5

Table 4.23: Isotope frequencies of $CD_2(COOD)_2$, $CH_2(C^{18}O^{18}OH)_2$ and $CDOD(COOD)_2$

$CD_2(COOD)_2$					$CH_2(C^{18}O^{18}OH)_2$					$CDOD(COOD)_2$				
I	II	Ra	Ir	Ass.	I	II	Ra	Ir	Ass.	I	II	Ra	Ir	Ass.
46	40	-	-	$\tau(CC')$	48	41	-	-	$\tau(CC')$	41	28	-	-	$\tau(CC')$
74	68	-	-	$\tau(CC')$	72	66	-	-	$\tau(CC')$	89	83	-	-	$\tau(CC')$
155	148	-	-	$\delta(CC'C)$	155	147	-	-	$\delta(CC'C)$	147	146	-	-	$\delta(OC'C)$
308	321	-	-	$\delta(C-O)$	336	344	-	-	$\delta(C-O)$	206	221	-	-	$\tau(C'O)$
360	360	-	-	$\delta(C-O)$	370	384	393	410	$\delta(C-O)$	222	233	200	-	$\delta(CC'C)$
389	395	-	-	$\tau(CO)$	497	500	419	439	$\gamma(COO)$	261	278	-	-	$\rho(OC'C)$
400	410	-	-	$\tau(CO)$	500	511	-	-	$\tau(CO)$	351	358	307	-	$\delta(C-O)$
506	526	405	415	$\delta(C=O)$	551	574	570	567	$\delta(C=O)$	397	401	-	-	$\tau(CO)$
537	546	523	514	$\gamma(COO)$	573	600	-	-	$\tau(CO)$	405	415	-	-	$\tau(CO)$
525	553	567	559	$\delta(C=O)$	606	630	-	-	$\tau(CO)$	450	463	-	-	$\tau(CO)$
655	679	650	669	$\gamma(COO)$	697	729	747	751	$\gamma(COO)$	532	548	510	-	$\delta(C=O)$
765	754	727	744	$\omega(CD_2)$	880	901	906	906	$\nu(CC')$	571	591	580	-	$\delta(C=O)$
819	818	788	790	$t(CD_2)$	889	918	919	914	$\nu(CC')$	656	673	646	-	$\gamma(COO)$
857	863	836	836	$\gamma(COO)$	947	954	955	959	$\rho(CH_2)$	722	728	757	-	$\gamma(COO)$
932	927	878	869	$t(CD_2)$	1218	1150	-	-	$t(CH_2)$	816	836	776	-	$\rho(OC'D)$
984	1014	-	-	$\delta(COD)$	1102	1173	-	-	$\delta(COH)$	826	838	835	830	$\delta(C'OD)$
981	1021	932	932	$\delta(CD_2)$	1106	1213	1216	1203	$\delta(COH)$	878	910	892	890	$\delta(OC'D)$
1056	1064	1041	1032	$\delta(CD_2)$	1291	1269	1265	1278	$\omega(CH_2)$	998	998	-	-	$\delta(COD)$
1093	1123	1082	1057	$\omega(CD_2)$	1358	1378	1417	1424	$\delta(CH_2)$	976	1018	-	-	$\delta(COD)$
1326	1370	1345	1344	$\nu(C-O)$	1430	1424	1429	1429	$\delta(CH_2)$	979	1045	1026	-	$\delta(COD)$
1302	1407	1370	1369	$\nu(C-O)$	1389	1444	1422	1410	$\nu(CC')^{@}$	1102	1135	1070	1060	$\nu(C-O)$
1844	1920	1644	1696	$\nu(C=O)$	1814	1888	1630	1676	$\nu(C=O)$	1145	1223	1162	1155	$\nu(C'-O)$
1857	1933	1669	1727	$\nu(C=O)$	1827	1902	1666	1706	$\nu(C=O)$	1335	1406	1310	1330	$\nu(C-O)$
2253	2242	2155	2145	$\nu_s(CD_2)$	3100	3078	2950	-	$\nu_s(CH_2)$	1356	1426	1365	-	$\nu(C-O)$
2336	2323	2247	2247	$\nu_a(CD_2)$	3151	3132	2990	-	$\nu_a(CH_2)$	1839	1919	1733	1730	$\nu(C=O)$
2661	2848	-	2270	$\nu(OD)$	3645	3901	-	-	$\nu(OH)$	1844	1928	1733	1730	$\nu(C=O)$
2666	2852	-	2270	$\nu(OD)$	3651	3907	-	-	$\nu(OH)$	2326	2282	2177	-	$\nu(CD)$
										2633	2844	-	-	$\nu(OD)_a$
										2660	2847	-	-	$\nu(OD)$
										2663	2848	-	-	$\nu(OD)$

Experimental frequencies for $CD_2(COOD)_2$ and $CH_2(C^{18}O^{18}OH)_2$ are from reference [7] and for $CDOD(COOD)_2$ from reference [17]. (@) indicates coupled mode.

Table 4.24: Isotope frequencies of $(CH_2COOD)_2$, $(CD_2COOH)_2$ and $(CD_2COOD)_2$

$(CH_2COOD)_2$				$(CD_2COOH)_2$				$(CD_2COOD)_2$			
I	II	Exp.	Ass.	I	II	Exp.	Ass.	I	II	Exp.	Ass.
A_g species											
100	84		$\tau(CC')$	85	71		$\tau(CC')$	85	71		$\tau(CC')$
242	241		$\delta(C'C'C)$	238	238		$\delta(C'C'C)$	237	237		$\delta(C'C'C)$
330	343		$\delta(CO)$	339	351		$\delta(CO)$	329	342		$\delta(C-O)$
390	398		$\tau(CO)$	455	459		$\gamma(COO)$	380	387		$\tau(CO)$
564	586		$\gamma(COO)$	587	612		$\tau(CO)$	515	532		$\gamma(COO)$
582	596		$\delta(C=O)$	621	632		$\delta(C=O)$	576	589		$\delta(C=O)$
866	869		$\nu(CC')$	805	802		$\omega(CD_2)$	771	762		$\omega(CD_2)$
1041	1031		$\rho(CH_2)$	922	919		$\delta(CD_2)$	914	911		$\delta(CD_2)$
997	1049		$\delta(COD)$	929	931		$\gamma(COO)$	929	931		$\gamma(COO)$
1065	1087		$\nu(C'C')$	958	950		$t(CD_2)$	958	950		$t(CD_2)$
1289	1273		$t(CH_2)$	1081	1076		$\delta(CD_2)$	988	1022		$\delta(COD)$
1258	1282		$\nu(C-O)$	1117	1197		$\nu(C-O)$	1081	1087		$\delta(CD_2)$
1443	1421		$\delta(CH_2)$	1225	1263		$\delta(COH)$	1181	1225		$\nu(C'C')$
1406	1467		$\nu(CC')^a$	1372	1426		$\nu(C-O)$	1331	1413		$\nu(C-O)$
1833	1911		$\nu(C=O)$	1834	1914		$\nu(C=O)$	1830	1910		$\nu(C=O)$
2661	2852		$\nu(OD)$	2244	2238		$\nu_s(CD_2)$	2244	2238		$\nu_s(CD_2)$
3080	3065		$\nu_s(CH_2)$	2301	2294		$\nu_a(CD_2)$	2301	2294		$\nu_a(CD_2)$
3106	3094		$\nu_a(CH_2)$	3656	3919		$\nu(OH)$	2661	2852		$\nu(OD)$
A_u species											
16	23	-	$\tau(CC')$	15	23	-	$\tau(CC')$	15	23	-	$\tau(CC')$
66	69	-	$\tau(C'C')$	64	66	-	$\tau(C'C')$	62	64	-	$\tau(C'C')$
122	123	-	$\delta(C'C'C)$	123	123	-	$\delta(C'C'C)$	120	120	-	$\delta(C'C'C)$
398	405	-	$\tau(CO)$	420	415	-	$\rho(CD_2)$	376	377	-	$\tau(CO)$
483	496	530	$\delta(C-O)$	473	479	517	$\tau(C-O)$	457	467	518	$\delta(C-O)$
553	564	566	$\rho(CH_2)$	567	582	623	$\delta(C=O)$	474	481	-	$\rho(CD_2)$
557	564	614	$\delta(C=O)$	572	584	-	$\tau(CO)$	543	554	611	$\delta(C=O)$
797	792	807	$\rho(CH_2)$	658	661	665	$t(CD_2)$	654	650	644	$t(CD_2)$
815	828	862	$\nu(CC')$	813	814	848	$\nu(CC')$	766	764	808	$\nu(CC')$
977	1040	1048	$\delta(COD)$	941	937	954	$t(CD_2)$	941	937	948	$t(CD_2)$
1185	1157	1180	$t(CH_2)$	997	1015	1017	$\omega(CD_2)$	1008	994	1012	$\omega(CD_2)$
1222	1199	1214	$\omega(CH_2)$	1063	1049	1058	$\delta(CD_2)$	975	1032	1045	$\delta(CD_2)$
1353	1399	1382	$\nu(C-O)$	1157	1221	-	$\delta(COH)$	1064	1057	1058	$\delta(CD_2)$
1445	1431	1429	$\delta(CH_2)$	1370	1406	-	$\nu(C-O)$	1320	1384	1367	$\nu(C-O)$
1828	1909	1735	$\nu(C=O)$	1830	1913	1710	$\nu(C=O)$	1827	1908	1725	$\nu(C=O)$
2661	2852	2280	$\nu(OD)$	2243	2233	2130	$\nu_s(CD_2)$	2243	2233	2100	$\nu_s(CD_2)$
3086	3069	2945	$\nu_s(CH_2)$	2312	2303	2170	$\nu_a(CD_2)$	2312	2303	2170	$\nu_a(CD_2)$
3125	3112	2990	$\nu_a(CH_2)$	3656	3919	3030	$\nu(OH)$	2661	2852	2287	$\nu(OD)$

Experimental frequencies for $(CH_2COOD)_2$, $(CD_2COOH)_2$ and $(CD_2COOD)_2$ are from reference [5].

Table 4.25: Diagonal force constants used in the normal coordinate analysis of malonic, succinic and adipic acids

Mode	Malonic	Succinic	Adipic
$\nu(CC')$	4.742	3.100	3.100
$\nu(C'C')$	-	2.542	-
$\nu(C''C')$	-	-	2.900
$\nu(C''C'')$	-	-	2.542
$\nu(CH)$	4.796	4.200	4.200
$\nu(C-O)$	6.871	4.900	4.900
$\nu(C=O)$	9.304	9.400	9.400
$\nu(OH)$	4.950	4.400	4.400
$\delta(COH)$	0.946	0.550	0.550

Values of force constants are in units of mdynes/A^o. Values for succinic, adipic and malonic acid are from references [5], [6] and [7].

Table 4.26: Diagonal force constants of malonic acid

	Sym. Cor.[a]	Force Const. ($mdynes/\AA$)			
		USFI	SFI	USFII	SFII
1	$\nu(OH)/\nu(OH)$	8.3122	7.4809	9.5240	8.5716
2	$\nu(OH)/\nu(OH)$	8.3367	7.5030	9.5493	8.5944
3	$\nu_a(CH_2)/\nu_a(CH_2)$	5.9415	5.3473	5.8653	5.2787
4	$\nu_s(CH_2)/\nu_s(CH_2)$	6.0286	5.4257	5.9293	5.3363
5	$\nu(C=O)/\nu(C=O)$	15.0690	13.5621	16.5305	14.8774
6	$\nu(C=O)/\nu(C=O)$	15.1522	13.6370	16.5881	14.9292
7	$\nu(C-O)/\nu(C-O)$	7.0040	6.3036	7.9320	7.1388
8	$\nu(C-O)/\nu(C-O)$	7.0211	6.3190	7.9711	7.1740
9	$\nu(C'C)/\nu(C'C)$	4.8019	4.3217	5.0872	4.5785
10	$\nu(C'C)/\nu(C'C)$	4.9369	4.4432	5.2134	4.6920
11	$\delta(C-O)/\delta(C-O)$	1.1696	0.9357	1.2059	0.9648
12	$\delta(C=O)/\delta(C=O)$	1.2823	1.0259	1.3628	1.0902
13	$\delta(C-O)/\delta(C-O)$	1.1813	0.9450	1.1927	0.9542
14	$\delta(C=O)/\delta(C=O)$	1.2635	1.0108	1.3424	1.0739
15	$\delta(CH_2)/\delta(CH_2)$	0.6712	0.5370	0.6592	0.5274
16	$\omega(CH_2)/\omega(CH_2)$	0.7852	0.6282	0.7249	0.5799
17	$t(CH_2)/t(CH_2)$	0.7981	0.6384	0.7328	0.5862
18	$\rho(CH_2)/\rho(CH_2)$	0.9633	0.7706	0.8691	0.6953
19	$\delta(CC'C)/\delta(CC'C)$	1.1262	0.9010	0.9772	0.7818
20	$\delta(COH)/\delta(COH)$	0.8645	0.6916	0.8541	0.6832
21	$\delta(COH)/\delta(COH)$	0.8583	0.6867	0.8524	0.6820
22	$\gamma(COO)/\gamma(COO)$	0.6056	0.4845	0.6462	0.5169
23	$\gamma(COO)/\gamma(COO)$	0.6834	0.5467	0.6830	0.5464
24	$\tau(CO)/\tau(CO)$	0.0854	0.0683	0.0912	0.0729
25	$\tau(CO)/\tau(CO)$	0.0797	0.0637	0.0876	0.0701
26	$\tau(C'C)/\tau(C'C)$	0.0097	0.0078	0.0087	0.0069
27	$\tau(C'C)/\tau(C'C)$	0.1019	0.0815	0.0680	0.0544

V :indicates units of A^o. USFI and SFI : Unscaled and Scaled 4-21G force constants, USFII and SFII: Unscaled and Scaled 6-31G** force constants.

Table 4.27: Diagonal force constants of hydroxymalonic acid

	Sym. Cor.[a]	Force Const. ($mdynes/V$)			
		USFI	SFI	USFII	SFII
1	$\nu(OH)_{alc}/\nu(OH)_{alc}$	8.1255	7.3129	9.4776	8.5298
2	$\nu(OH)_{ac}/\nu(OH)_{ac}$	8.3141	7.4827	9.5185	8.5667
3	$\nu(OH)_{ac}/\nu(OH)_{ac}$	8.3033	7.4730	9.5116	8.5604
4	$\nu(CH)/\nu(CH)$	6.0958	5.4862	5.8668	5.2801
5	$\nu(C=O)/\nu(C=O)$	14.9271	13.4344	16.4395	14.7956
6	$\nu(C=O)/\nu(C=O)$	14.9899	13.4909	16.4377	14.7939
7	$\nu(C-O)_{alc}/\nu(C-O)_{alc}$	6.2172	5.5955	7.1432	6.4289
8	$\nu(C-O)/\nu(C-O)$	7.4598	6.7138	8.2838	7.4554
9	$\nu(C-O)/\nu(C-O)$	7.2601	6.5341	8.1462	7.3316
10	$\nu(C'C)/\nu(C'C)$	4.9362	4.4426	5.1299	4.6169
11	$\nu(C'C)/\nu(C'C)$	4.5370	4.0833	4.8249	4.3424
12	$\delta(C-O)/\delta(C-O)$	1.1064	0.8851	1.1421	0.9136
13	$\delta(C=O)/\delta(C=O)$	1.3344	1.0676	1.4141	1.1313
14	$\delta(C-O)/\delta(C-O)$	1.1037	0.8830	1.1487	0.9190
15	$\delta(C=O)/\delta(C=O)$	1.2664	1.0131	1.3404	1.0723
16	$\delta(COH)_{ac}/\delta(COH)_{ac}$	0.8426	0.6741	0.8393	0.6715
17	$\delta(COH)_{ac}/\delta(COH)_{ac}$	0.8585	0.6868	0.8500	0.6800
18	$\delta(COH)_{alc}/\delta(COH)_{alc}$	1.0473	0.8378	0.9819	0.7855
19	$\rho(OC'H)/\rho(OC'H)$	0.8277	0.6622	0.7935	0.6348
20	$\delta(OC'H)/\delta(OC'H)$	0.8358	0.6686	0.8828	0.7062
21	$\rho(OC'C)/\rho(OC'C)$	1.2909	1.0327	1.3437	1.0750
22	$\delta(OC'C)/\delta(OC'C)$	1.3063	1.0450	1.1810	0.9448
23	$\delta(CC'C)/\delta(CC'C)$	1.1119	0.8895	1.2041	0.9633
24	$\gamma(COO)/\gamma(COO)$	0.5738	0.4591	0.6127	0.4901
25	$\gamma(COO)/\gamma(COO)$	0.5394	0.4315	0.5863	0.4690
26	$\tau(C'O)/\tau(C'O)$	0.0356	0.0285	0.0338	0.0270
27	$\tau(CO)/\tau(CO)$	0.0775	0.0620	0.0826	0.0661
28	$\tau(CO)/\tau(CO)$	0.0852	0.0681	0.0918	0.0734
29	$\tau(C'C)/\tau(C'C)$	0.0487	0.0390	0.0382	0.0306
30	$\tau(C'C)/\tau(C'C)$	0.0113	0.0090	0.0066	0.0053

V :indicates units of A^o. USFI and SFI : Unscaled and Scaled 4-21G force constants, USFII and SFII: Unscaled and Scaled 6-31G** force constants.

Table 4.28: Diagonal force constants of succinic acid

	Sym. Cor.[a]	Force Const. ($mdynes/\AA$)			
		USFI	SFI	USFII	SFII
A_g species					
1	$\nu(OH)/\nu(OH)$	8.3083	7.4774	9.5491	8.5942
2	$\nu_s(CH_2)/\nu_s(CH_2)$	5.9463	5.3517	5.8670	5.2803
3	$\nu_a(CH_2)/\nu_a(CH_2)$	5.8037	5.2233	5.7566	5.1809
4	$\nu(C=O)/\nu(C=O)$	14.7370	13.2633	16.1995	14.5796
5	$\nu(C-O)/\nu(C-O)$	6.9330	6.2397	7.8508	7.0657
6	$\nu(CC')/\nu(CC')$	4.8962	4.4066	5.2008	4.6807
7	$\nu(C'C')/\nu(C'C')$	4.9389	4.4450	5.1836	4.6652
8	$\delta(COH)/\delta(COH)$	0.8655	0.6924	0.8546	0.6837
9	$\delta(C-O)/\delta(C-O)$	1.1827	0.9462	1.2444	0.9955
10	$\delta(C=O)/\delta(C=O)$	1.3817	1.1054	1.4467	1.1574
11	$\delta(CH_2)/\delta(CH_2)$	0.7125	0.5700	0.6899	0.5519
12	$\omega(CH_2)/\omega(CH_2)$	0.8369	0.6695	0.7982	0.6385
13	$t(CH_2)/t(CH_2)$	0.8613	0.6890	0.8179	0.6543
14	$\rho(CH_2)/\rho(CH_2)$	0.8848	0.7079	0.8751	0.7001
15	$\delta(C'C'C)/\delta(C'C'C)$	1.4014	1.1212	1.2562	1.0050
16	$\gamma(COO)/\gamma(COO)$	0.5492	0.4393	0.5968	0.4775
17	$\tau(CO)/\tau(CO)$	0.0856	0.0685	0.0923	0.0739
18	$\tau(C'C)/\tau(C'C)$	0.0108	0.0086	0.0083	0.0067
A_u species					
1	$\nu(OH)/\nu(OH)$	8.3081	7.4773	9.5480	8.5932
2	$\nu_s(CH_2)/\nu_s(CH_2)$	5.9548	5.3594	5.8756	5.2880
3	$\nu_a(CH_2)/\nu_a(CH_2)$	5.8509	5.2658	5.7978	5.2180
4	$\nu(C=O)/\nu(C=O)$	14.7874	13.3086	16.2745	14.6470
5	$\nu(C-O)/\nu(C-O)$	6.8623	6.1761	7.7817	7.0035
6	$\nu(CC')/\nu(CC')$	4.9122	4.4209	5.1888	4.6700
7	$\delta(COH)/\delta(COH)$	0.8638	0.6910	0.8530	0.6824
8	$\delta(C-O)/\delta(C-O)$	1.1379	0.9103	1.1989	0.9592
9	$\delta(C=O)/\delta(C=O)$	1.3165	1.0532	1.3828	1.1063
0	$\delta(CH_2)/\delta(CH_2)$	0.6903	0.5523	0.6739	0.5391
11	$\omega(CH_2)/\omega(CH_2)$	0.7464	0.5972	0.6941	0.5553
12	$t(CH_2)/t(CH_2)$	0.7201	0.5761	0.6545	0.5236
13	$\rho(CH_2)/\rho(CH_2)$	0.7844	0.6275	0.7535	0.6028
14	$\delta(C'C'C)/\delta(C'C'C)$	1.2064	0.9652	1.0796	0.8637
15	$\gamma(COO)/\gamma(COO)$	0.5447	0.4358	0.5917	0.4734
16	$\tau(CO)/\tau(CO)$	0.0861	0.0689	0.0927	0.0741
17	$\tau(C'C)/\tau(C'C)$	0.0085	0.0068	0.0060	0.0048
18	$\tau(C'C')/\tau(C'C')$	0.0044	0.0035	0.0073	0.0058

V :indicates units of A^o. USFI and SFI : Unscaled and Scaled 4-21G force constants, USFII and SFII: Unscaled and Scaled 6-31G** force constants.

Table 4.29: Diagonal force constants of Glutaric acid

	Sym. Cor.[a]	F. Const. ($mdynes/V$)			Sym. Cor.[a]	F. Const. ($mdynes/V$)	
		USFI	SFI			USFI	SFI
A' species				*A'' species*			
1	$\nu(OH)/\nu(OH)$	8.3033	7.4730	1	$\nu_a(C''H_2)/\nu_a(C''H_2)$	5.8514	5.2663
2	$\nu(OH)/\nu(OH)$	8.3142	7.4828	2	$\nu_a(C'H_2)/\nu_a(C'H_2)$	5.7191	5.1472
3	$\nu_s(C''H_2)/\nu_s(C''H_2)$	5.9778	5.3800	3	$\nu_a(C'H_2)/\nu_a(C'H_2)$	5.7190	5.1471
4	$\nu_s(C'H_2)/\nu_s(C'H_2)$	5.8468	5.2621	4	$t(C''H_2)/t(C''H_2)$	0.8303	0.6642
5	$\nu_s(C'H_2)/\nu_s(C'H_2)$	5.8467	5.2620	5	$\rho(C''H_2)/\rho(C''H_2)$	0.9353	0.7482
6	$\nu(C=O)/\nu(C=O)$	14.8576	13.3718	6	$t(C'H_2)/t(C'H_2)$	0.7834	0.6267
7	$\nu(C=O)/\nu(C=O)$	14.8629	13.3766	7	$\rho(C'H_2)/\rho(C'H_2)$	0.8319	0.6655
8	$\nu(C-O)/\nu(C-O)$	6.7947	6.1153	8	$t(C'H_2)/t(C'H_2)$	0.7834	0.6267
9	$\nu(C-O)/\nu(C-O)$	6.7960	6.1164	9	$\rho(C'H_2)/\rho(C'H_2)$	0.8315	0.6652
10	$\nu(CC')/\nu(CC')$	4.8257	4.3431	10	$\gamma(COO)/\gamma(COO)$	0.5411	0.4329
11	$\nu(CC')/\nu(CC')$	4.8281	4.3452	11	$\gamma(COO)/\gamma(COO)$	0.5405	0.4324
12	$\nu(C'C'')/\nu(C'C'')$	4.7074	4.2367	12	$\tau(CO)/\tau(CO)$	0.0860	0.0688
13	$\nu(C'C'')/\nu(C'C'')$	4.7067	4.2361	13	$\tau(CO)/\tau(CO)$	0.0853	0.0683
14	$\delta(COH)/\delta(COH)$	0.8663	0.6930	14	$\tau(C'C)/\tau(C'C)$	0.0079	0.0063
15	$\delta(COH)/\delta(COH)$	0.8647	0.6918	15	$\tau(C'C)/\tau(C'C)$	0.0078	0.0062
16	$\delta(C-O)/\delta(C-O)$	1.1697	0.9358	16	$\tau(C''C')/\tau(C''C')$	0.0087	0.0070
17	$\delta(C-O)/\delta(C-O)$	1.1692	0.9354	17	$\tau(C''C')/\tau(C''C')$	0.0088	0.0070
18	$\delta(C=O)/\delta(C=O)$	1.3373	1.0699	-	-	-	-
19	$\delta(C=O)/\delta(C=O)$	1.3365	1.0692	-	-	-	-
20	$\delta(C''H_2)/\delta(C''H_2)$	0.7242	0.5794-	-	-	-	
21	$\omega(C''H_2)/\omega(C''H_2)$	0.8253	0.6602	-	-	-	-
22	$\delta(C'C''C')/\delta(C'C''C')$	1.0899	0.8719	-	-	-	-
23	$\delta(C'H_2)/\delta(C'H_2)$	0.7119	0.5695	-	-	-	-
24	$\omega(C'H_2)/\omega(C'H_2)$	0.7915	0.6332	-	-	-	-
25	$\delta(C''C'C)/\delta(C''C'C)$	1.2789	1.0232	-	-	-	-
26	$\delta(C'H_2)/\delta(C'H_2)$	0.7120	0.5696	-	-	-	-
27	$\omega(C'H_2)/\omega(C'H_2)$	0.7914	0.6332	-	-	-	-
28	$\delta(C''C'C)/\delta(C''C'C)$	1.2760	1.0208-	-	-	-	

V :indicates units of A^o. USFI and SFI : Unscaled and Scaled 4-21G force constants.

Table 4.30: Diagonal force constants of Adipic acid

	Sym. Cor.[a]	F. Const. ($mdynes/V$) USFI	SFI		Sym. Cor.[a]	F. Const. ($mdynes/V$) USFI	SFI
$A_g$species				*$A_u$species*			
1	$\nu(C''C'')/\nu(C''C'')$	4.5432	4.0889	1	$\nu(C''C')/\nu(C''C')$	4.6814	4.2132
2	$\nu(C''C')/\nu(C''C')$	4.6681	4.2013	2	$\nu(C'C)/\nu(C'C)$	4.8151	4.3336
3	$\nu(C'C)/\nu(C'C)$	4.8190	4.3371	3	$\nu(OH)/\nu(OH)$	8.3086	7.4777
4	$\nu(OH)/\nu(OH)$	8.3088	7.4779	4	$\nu(C=O)/\nu(C=O)$	14.7921	13.3129
5	$\nu(C=O)/\nu(C=O)$	14.7868	13.3081	5	$\nu(C-O)/\nu(C-O)$	6.7739	6.0965
6	$\nu(C-O)/\nu(C-O)$	6.8040	6.1236	6	$\nu_a(C'H_2)/\nu_a(C'H_2)$	5.7300	5.1570
7	$\nu_a(C'H_2)/\nu_a(C'H_2)$	5.7282	5.1554	7	$\nu_s(C'H_2)/\nu_s(C'H_2)$	5.8555	5.2700
8	$\nu_s(C'H_2)/\nu_s(C'H_2)$	5.8542	5.2688	8	$\nu_a(C''H_2)/\nu_a(C''H_2)$	5.7474	5.1726
9	$\nu_a(C''H_2)/\nu_a(C''H_2)$	5.6899	5.1209	9	$\nu_s(C''H_2)/\nu_s(C''H_2)$	5.8557	5.2702
10	$\nu_s(C''H_2)/\nu_s(C''H_2)$	5.8495	5.2646	10	$\delta(C-O)/\delta(C-O)$	1.1628	0.9302
11	$\delta(C-O)/\delta(C-O)$	1.1697	0.9358	11	$\delta(C=O)/\delta(C=O)$	1.3366	1.0693
12	$\delta(C=O)/\delta(C=O)$	1.3560	1.0848	12	$\delta(COH)/\delta(COH)$	0.8637	0.6910
13	$\delta(COH)/\delta(COH)$	0.8641	0.6913	13	$\delta(C'H_2)/\delta(C'H_2)$	0.7108	0.5687
14	$\delta(C'H_2)/\delta(C'H_2)$	0.7121	0.5697	14	$\omega(C'H_2)/\omega(C'H_2)$	0.7889	0.6311
15	$\omega(C'H_2)/\omega(C'H_2)$	0.7839	0.6271	15	$t(C'H_2)/t(C'H_2)$	0.7838	0.6271
16	$t(C'H_2)/t(C'H_2)$	0.7773	0.6218	16	$\rho(C'H_2)/\rho(C'H_2)$	0.8333	0.6666
17	$\rho(C'H_2)/\rho(C'H_2)$	0.8321	0.6657	17	$\delta(C''C'C)/\delta(C''C'C)$	1.2678	1.0142
18	$\delta(C''C'C)/\delta(C''C'C)$	1.3057	1.0446	18	$\delta(C''H_2)/\delta(C''H_2)$	0.7234	0.5787
19	$\delta(C''H_2)/\delta(C''H_2)$	0.7411	0.5929	19	$\omega(C''H_2)/\omega(C''H_2)$	0.7805	0.6244
20	$\omega(C''H_2)/\omega(C''H_2)$	0.8672	0.6938	20	$t(C''H_2)/t(C''H_2)$	0.7363	0.5890
21	$t(C''H_2)/t(C''H_2)$	0.9106	0.7285	21	$\rho(C''H_2)/\rho(C''H_2)$	0.8666	0.6933
22	$\rho(C''H_2)/\rho(C''H_2)$	1.0054	0.8043	22	$\delta(C''C''C')/\delta(C''C''C')$	0.9093	0.7274
23	$\delta(C''C''C')/\delta(C''C''C')$	1.2491	0.9993	23	$\gamma(COO)/\gamma(COO)$	0.5426	0.4341
24	$\gamma(COO)/\gamma(COO)$	0.5423	0.4338	24	$\tau(CO)/\tau(CO)$	0.0858	0.0686
25	$\tau(CO)/\tau(CO)$	0.0855	0.0684	25	$\tau(C''C')/\tau(C''C')$	0.0090	0.0072
26	$\tau(C''C')/\tau(C''C')$	0.0093	0.0075	26	$\tau(C'C)/\tau(C'C)$	0.0081	0.0065
27	$\tau(C'C)/\tau(C'C)$	0.0085	0.0068	27	$\tau(C''C'')/\tau(C''C'')$	0.0124	0.0099

V :indicates units of A^o. USFI and SFI : Unscaled and Scaled 4-21G force constants.

4.5 References

[1] S. Patai, *The Chemistry of Carboxylic Acids and Esters*, Interscience Publishers, New York, 1969.

[2] S. Lifson, A. T. Hagler and P. J. Dauber, J. Am. Chem. Soc., 101 (1979) 5111.

[3] M. Merchàn, F. Tomàs and I. Nebot-Gil, J. Mol. Str., 109 (1984) 51-60.

[4] M. Takasuka, T. Saito and M. Yamakawa, J. Chem. Soc., Perkin Trans. 2 (1991) 1513-16.

[5] M. Suzuki and T. Shimanouchi, J. Mol. Spectrosc., 28 (1968) 394-410.

[6] (a) M. Suzuki and T. Shimanouchi, J. Mol. Spectrosc., 29 (1969) 415-425; (b) V. Ananthanarayanan, Spectrochim. Acta, 20 (1964) 197; (c) K. Fukushima, K. Adichi and K. Watanabe, Bull. Chem. Soc. Jpn., 61 (1988) 3049-53.

[7] D. Bougeard, J. De Villepin and A. Novak, Spectrochim. Acta, 46A (1988) 1281-86.

[8] G. Roelofsen, J. A. Kanters, J. Kroon, H. M. Doesburg and T. Koops, Acta Crystallogr., 34B (1978) 2565.

[9] J. L. Leviel, G. Auvert and J. M. Savariault, Acta Crystallogr., 37B (1981) 2185.

[10] P. J. Housty and M. Hospital, Acta Crystallogr., 18 (1965) 693.

[11] J. D. Morrison and J. M. Robertson, J. Chem. Soc., (1949) 1001-8.

[12] J. S. Broadley, J. D. Morrison and J. M. Robertson, Proc. Roy. Soc. (London), Ser. A 251 (1959) 441.

[13] J. Murto, T. Raaska, H. Kunttu and M. Räsänen, J. Mol. Str., 200 (1989) 93-101.

[14] J. Nieminen, M. Räsänen and J. Murto, J. Phys. Chem., 96 (1992) 5303-5308.

[15] L. Colombo and J. P. Mathieu, in *Molecular Interactions*, Vol. 1, p.384, (Eds. H. Ratajczak and W. J. Oriville Thomas), John Wiley and Sons Ltd., New York, 1980.

[16] M. Haurie and A. Novak, Spectrochim. Acta., 21 (1965) 1217.

[17] J. L. Delarbre, L. Maury and L. Bardet, J. Raman Spectrosc., 16 (1985) 288-296.

[18] J. L. Delarbe, E. Fabrégue, L. Maury and L. Bardet, J. Raman Spectrosc., 19 (1988) 167-74.

[19] R. W. Wiliams and A. H. Lowrey, J. Comput. Chem., 12 (1991) 761-77.

[20] H. Hollenstein, T. K. Ha and Hs. H. Günthard, J. Mol. Str., 146 (1986) 289-307.

[21] L. D. Barron, A. R. Gargaro, L. Hecht, P. L. Polavarapu and H. Sugeta, Spectrochim. Acta, 48A (1992) 1051-66.

[22] B. C. Stace and C. J. Oralratmanee, J. Mol. Struct., 18 (1973) 339.

[23] (a) C. V. Berney, R. L. Reddington and K. C. Lin, J. Chem. Phys., 53 (1970) 1713. (b) R. Meyer, T. K. Ha, H. Frei and Hs. H. Günthard, Chem. Phys., 9 (1975) 393.

[24] J. A. Kanters, J. Kroon and A. F. Peerdeman and J. A. Vliegenthart, Nature, 222 (1969) 370-1.

[25] G. Zerbi, in *Advances in Infrared and Raman Spectroscopy*, Vol. 11, p.301,(Eds. R. J. H. Clark and R. E. Hester), Wiley-Heyden, New York, 1984.

[26] L. J. Bellamy, *The Infrared Spectra of Complex Molecules*, Metheun and Co. Ltd., London, 1955.

[27] J. de Villepin and A. Novak, Spectrochim. Acta, 34A (1978) 1009-17.

[28] P. Jona, M. Gussoni and G. Zerbi, J. Appl. Phys., 57 (1985) 834.

[29] H. Hollenstein and Hs. H. Günthard, J. Mol. Spectrosc., 84 (1980) 457-77.

[30] J. K. Wilmhurst, J. Mol. Spectrosc., 1 (1957) 201.

[31] T. Shimanouchi, *Tables of Molecular Vibrational Frequencies*, Consolidated Vol. 1, NSRDS-NBS 39, U. S. Dept. of Commerce, 1972.

[32] J. de Villepin and A. Novak, Spectrochim. Acta, 34A (1978) 1019-24.

[33] R. L. Reddington and T. E. Reddington, J. Mol. Struct., 48 (1978) 165.

Chapter 5

The Citrate System

In the preceding chapter our detailed studies on dicarboxylic acids had indicated the effect of the presence of the second carboxyl group and the methylene group in comparison to monocarboxylic and oxalic acids. Our studies on citric acid was spurred by the fact that no theoretical studies had been done on this system or other related systems like substituted citric acids. Our studies on pyruvate anion described in Chapter 3 indicated that the HF/4-21G basis set could describe the frequencies of anions quite well. Based on this observation we carried out studies on the citrate trianion also. We divide this chapter into two seperate sections. In the first, we describe our studies on citric acid and the citrate trianion. In the second, we describe our studies on some of the substituted citric acids.

5.1 Citric Acid and the Citrate Trianion

Spectroscopic studies on citric acid(CA) include solid state NMR, IR and Raman studies [1–9,11]. Passerini [1] and Duval [2] recorded the IR spectra of solid CA but no vibrational analysis was done. Attempts to make empirical assignments of vibrational frequencies have concentrated on some regions or specific bands only [3–6]. Bickley et al. [7] have reported the IR and Raman spectra in solution, which in a way augmented the pioneering work of Edsall [8]. Rao and Swamy [9] have also attempted to assign the IR spectra of anhydrous CA based on the vibrational assignment of adipic acid [10].

As far as the citrate trianion(CTA) is concerned the IR spectrum of trisodium citrate was reported by Edsall [8] and Bickley [7] in solution as well as in the solid state but the vibrational assignment given by the latter was approximate. The Raman spectra of the citrate trianion was reported by Marignan [13], Krishnan [14] and Rao [15] but no

vibrational assignment has been made till this date. A sample of sodium citrate has also been studied by solid state NMR [12]. However, there is no detailed study of the vibrational spectra of CA and its trianion.

The structure of CA was studied by X-ray diffraction by Glusker et al. [16]. In case of CTA, the X-ray structure of sodium citrate pentahydrate was determined by Burns and Iball [17] and Nordman et al. [18]. The structure of magnesium citrate decahydrate was determined by Johnson [19]. The X-ray structure of sodium citrate has been done by Glusker et al. [20]. To our knowledge no ab initio calculation has been done either on CA or CTA.

In an attempt to assign the vibrational spectra of citric acid and the trisodium citrate we have performed ab initio calculations on citric acid and the citrate trianion at the HF/4-21G level. The vibrational frequencies were calculated for the optimized conformations. The vibrational assignments were then made for these systems and compared with the available experimental data.

The optimizations and the calculation of the vibrational frequencies have been done using the HF/4-21G basis set. Results in the previous chapters on various carboxylic acids including α-keto carboxylic and dicarboxylic acids clearly indicate that the HF/4-21G basis describes the salient features of geometry and vibrational frequencies fairly well. Extensive studies on the pyruvate anion described in Chapter 3, based on the conclusions arrived by Simons [21] indicate that the HF/4-21G basis set describes some of the features of anions more accurately than those that include polarization functions like the 6-31G** and 6-31++G** basis sets. The barrier heights calculated using the HF/4-21G basis set is closer to the barrier heights calculated using the Moller Plesset methods. The inclusion of correlation by the use of the Moller Plesset or the CI methods will help improve the results obtained in this study, but considering the size of the systems, such calculations have not been attempted.

The geometries of CA and CTA are compared to the available X-ray data. In case of CA the optimized conformation is compared to the X-ray structure of citric acid [16] while in case of CTA to the X-ray structure of magnesium citrate [19].

In light of the fact that gas phase IR and Raman spectra of citric acid and sodium citrate are not available we have used a number of data collected from various sources in our assignments. In the case of CA, the IR spectrum of anhydrous CA [9], IR and Raman spectra of hydrated CA [22] and the Raman spectrum of CA at pH 1.5 [7] were used for the assignment. At pH 1.5 all the carboxyl groups of CA are in the nonionized form. Similarly

in case of CTA, IR data of sodium citrate [13], ammonium citrate [13], Raman spectra of solid and aqueous sodium citrate [7,14] and that of citric acid at pH 7.5 [7] were used. At pH 7.5 all the carboxyl groups of CA are ionized.

5.1.1 Geometry

The optimized bond lengths, bond angles and dihedral angles of CA and CTA along with the experimentally derived bond parameters of CA and CTA are given in Table 5.3. The optimized structures of both citric acid and citrate trianion are shown in Figure 5.1. There is little change in the structure of the neutral citric acid after the geometry optimization on the X-ray structure. Major changes occur only in the O-H bond distances. While in the X-ray structure the distance is around $0.89A^o$ in the final 4-21G optimized structure the distance increases to $0.970A^o$. The C5-C6 and the C6-C10 bond distances are more than the C2-C5 and C10-C14 distances. This is in accordance with the distances derived from the X-ray structure. Unlike the X-ray structure an intramolecular hydrogen bond between the hydroxyl hydrogen H17 and the terminal carboxyl oxygen O4 is formed during the course of the optimization. The torsion angle O4-C2-C5-C6 is 2.0^o and the torsion angle O19-C14-C10-C6 is 32.3^o compared to the angles 8.2^o and 50.4^o in the X-ray structure. In the central carboxyl group the calculated torsion angle O13-C11-C6-O9 is 15.1^o compared to the X-ray obtained angle of 12.3^o. Most of the geometrical features which are present in the X-ray structure are conserved in the optimized structure.

In case of the citrate trianion a number of changes take place in the structure as compared to the X-ray structure of magnesium citrate [19]. The X-ray struture indicates the presence of an intramolecular hydrogen bond between the hydroxyl hydrogen and the terminal carboxylate oxygen. Though the starting structure was not the X-ray structure the optimized structure indicates the presence of this intramolecular hydrogen bond. A number of changes take place in the backbone geometry. The C4-C5-C9-C13 dihedral in the X-ray structure is -175.7^o while in case of the optimized structure it is 61.0^o. The reason behind such drastic changes is that in the X-ray structure the presence of cations and the neighbouring molecules affect the geometry of the citrate trianion. In case of the optimized conformation an isolated trianion is being considered. This certainly would give rise to certain discrepancies in the torsional frequencies which occur in the lower end of the spectrum. Since the other geometrical features are similar, the calculated frequencies could be used in the description of most part of the experimental spectra.

5.1.2 Vibrational frequencies

The symmetry coordinates of citric acid and the citrate trianion are given in Tables 5.1 and 5.2. The calculated vibrational spectra of citric acid and the citrate trianion along with the experimental assignments and potential energy distributions are given in Tables 5.4 and 5.5. As indicated earlier the gas phase frequencies of CA are not available and hence the assignment of CA and CTA are being made using the vibrational spectra of solid and aqueous CA. The philosophy behind such assignment has been described in detail in Chapter 4. Hence it is not discussed here. In addition to the observed shifts from gas phase to the solid state the various peaks can be easily distinguished by their intensity profiles. Bands associated with CC stretches have high intensity in the Raman spectrum, bands associated with CO stretches have high intensity in the IR spectrum, bands associated with bending modes have moderate intensities in the IR and Raman spectra. The ab initio depolarization data could not be used in the assignments due to the absence of the corresponding experimental depolarization values. All the assignments have been done using the potential energy distributions of the unscaled vibrational frequencies. The scaled frequencies are given to indicate the effect of scaling. The ab initio assignments of acetic acid [23], oxalic acid [24], glycolic acid [25] and tartaric acid [26] were used to check for the consistency of many of the assignments. In case of the methylene frequencies the vibrational assignments of hydroxymalonic acid, succinic acid [27] and adipic acid [28] were used. In case of the citrate trianion the ab initio assignments of acetate anion [23] and the vibrational assignments of sodium formate [29] and sodium acetate [30] were also used as aids in the assignment of the vibrational spectra.

OH frequencies

In citric acid there are two distinct *OH* groups owing to the presence of the alcoholic and carboxyl groups. Further the terminal carboxyl groups are distinctly different from the central carboxyl groups. The assignment of the *OH* frequencies in citric acid poses a lot of problems. As in the case of tartaric acid [26] all the $\nu(OH)$ frequencies generally appear as a broad band and hence the $\nu(OH)$ mode has not been assigned. We however discuss the salient features of the various $\nu(OH)$ modes to indicate how well the experimental features of each of these *OH* modes in different systems conform to the theoretically predicted frequencies in case of citric acid.

Generally $\nu(OH)_{alc}$ occurs at higher frequencies than the corresponding $\nu(OH)_{ac}$. How-

ever in case of α-hydroxy compounds there is a great deal of controversy regarding the appearence of the $\nu(OH)_{alc}$ stretch. After an exhaustive study of a number of α-hydroxy compounds Kanters et al. [31] had concluded that the hydroxyl hydrogen is neither involved in intermolecular nor in intramolecular hydrogen bonding in the solid state. Thus the $\nu(OH)_{alc}$ mode appears at $3500cm^{-1}$, $3480cm^{-1}$, $3450cm^{-1}$, $3620cm^{-1}$, $3500cm^{-1}$in the IR spectra of anhydrous hydroxymalonic acid, isomalic acid, DL-α-methylmalic acid, citric acid and L-ascorbic acid respectively. These values are close to those obtained for the stretching modes of the free OH group which is at $3600cm^{-1}$. Soon after this study the X-Ray and neutron diffraction of glycolic acid, one of the simplest α-hydroxy carboxylic acids indicated that the alcoholic OH is involved in the formation of an intramolecular hydrogen bond [31]. However in the gas phase, the IR spectra of glycolic acid indicates that the alcoholic OH is not involved in the formation of an intramolecular hydrogen bond [32]. In CA the involvement of the hydroxyl hydrogen in the formation of an intramolecular hydrogen bond in the optimized structure lowers the $\nu(OH)_{alc}$ frequency and indicates that it is distinctly different from glycolic acid [25] and tartaric acid [26]. In tartaric acid the $\nu(OH)_{alc}$ mode appears at a higher frequency than the $\nu(OH)_{ac}$ mode in the theoretically predicted vibrational spectrum. The scaled frequency for the $\nu(OH)_{alc}$ mode of CA however indicates that it occurs at a higher frequency than the $\nu(OH)_{ac}$ mode. This is an artifact of the scaling method employed in the calculation as can be seen from Table 5.6.

In carboxylic acids the $\nu(OH)_{ac}$ mode is affected by the vagaries of hydrogen bonding. In the matrix spectra of oxalic acid $\nu(OH)_{ac}$ occurs at 3576 and $3498cm^{-1}$in the cTt conformer and at $3472cm^{-1}$in the cTc conformer [24]. In the solid state (extensively hydrogen bonded) of oxalic acid these modes appear at (2887,2915) and $(3110,3157)cm^{-1}$in the α and β forms respectively [33]. From the calculated vibrational spectra of CA given in Table 5.4, it can be inferred that the frequencies of these modes are in agreement with the gas phase values of oxalic acid. In CA all the three carboxyl groups are not similar. The central carboxyl group behaves differently as compared to the terminal carboxyl groups. Since it is an α-carboxyl group one would expect that the $\nu(OH)_{ac}$ for the central carboxyl group to be higher than that of the terminal carboxyl group [34], which is observed in the calculated vibrational spectra of citric acid. Comparisons for this mode can be made either with the spectra of glycolic acid or hydroxymalonic acid (both are α-carboxylic acids). In the gas phase spectra of glycolic acid $\nu(OH)_{ac}$ appears at $3487.6cm^{-1}$[25]. The lowering in case of glycolic acid is due to the involvement of the carboxyl hydrogen in an intramolecular hydrogen bond.

In case of the $\delta(COH)$ mode the assignment of the calculated frequencies to the corresponding values in the solid state or solution spectra is difficult. After an examination of the gas phase and solid state vibrational frequencies of oxalic acid it can be seen that frequencies which have $\delta(COH)$ mode as a dominant contributor to the potential energy distribution increase in the solid state as compared to the gas phase values [24,33]. At this point it is pertinent to note that the $\delta(COH)$ mode is always coupled with the $\nu(C-O)$ mode. Frequencies which have the $\nu(C-O)$ mode as the dominant contributor to the potential energy distribution do not change much when going from the gas phase to the solid state [32]. Thus the coupled modes appear at (1423,1195), (1330,1176)cm^{-1}in the gas phase and at (1475,1209), (1381,1181)cm^{-1}in the solid state spectra of β oxalic acid respectively [33]. This trend has been seen in the studies on dicarboxylic acids described in Chapter 4. In CA also such trends are observed. We have however attempted to assign some of the calculated frequencies to the corresponding values based on the intensity profiles but the veracity of our assignments can be checked only with the availability of gas phase spectra for citric acid. The calculated frequencies also indicate that the OH bending frequencies cannot be used to distinguish between the central and the terminal carboxyl groups. An interesting offshoot of the calculated potential energy distributions is that the $\nu(C-O)_{alc}$ and $\delta(COH)_{alc}$ mode are not coupled in citric acid. Thus the vibrational frequencies of the hydroxyl group in citric acid are distinctly different from those in glycolic acid [25] and hydroxymalonic acid. In both these acids the two modes connected with the hydroxyl group are coupled.

The appearence of the out of plane OH bend ($\tau(CO)$ in our nomenclature) is also affected by the presence of hydrogen bonding. As in the case of the $\delta(COH)$ mode the hydrogen bonding effect is illustrated in the gas phase and solid state spectra of oxalic acid. $\tau(CO)$ appears at $664cm^{-1}$(the value for the other mode is not given) in the gas phase and at (792,828)cm^{-1}in the solid state spectra of oxalic acid respectively [26,33]. Some of the $\tau(CO)$ modes of CA have been assigned, based on the intensity profiles of the calculated and experimental frequencies. The central carboxyl group can be again distinguished by the appearence of its $\tau(CO)$ mode at a lower frequency as compared to the terminal carboxyl groups. In case of the hydroxyl group there is no frequency corresponding to this mode in the matrix spectra of glycolic acid [25] but the calculated values of $\tau(CO)_{alc}$ however indicate that it appears at a lower frequency than the corresponding mode in the carboxyl group [25]. The involvement of the carboxyl hydrogen in an intramolecular hydrogen bond might be responsible for the appearence of the $\tau(CO)_{ac}$ at a higher frequency. Eventhough

the hydroxyl hydrogen is involved in an intramolecular hydrogen bond in CA, $\tau(CO)_{alc}$ appears at a lower frequency than the corresponding $\tau(CO)_{ac}$ mode.

In case of the citrate trianion, an intramolecular hydrogen bond involving the hydroxyl hydrogen and the terminal carboxylate groups is present in the X-ray structure of sodium citrate [20] and magnesium citrate [19], which is in marked contrast to the absence of the same in the crystal structure of citric acid [16]. In the absence of the carboxyl hydrogens the $\nu(OH)_{alc}$ mode is assigned to the peak at $3030cm^{-1}$in the IR spectra of sodium citrate. In the IR spectra of ammonium citrate the hydrogen bonded OH peak comes in the NH stretch region and hence cannot be identified. The effect of hydrogen bonding has been dealt with extensively in the discussion on CA, and hence the salient features of the OH peaks in CTA can be viewed in that context. The $\delta(COH)$ mode which appears as a strong peak at $1651cm^{-1}$in the calculated spectra can be assigned to the peaks at 1490 and $1481cm^{-1}$in the IR spectra of sodium and ammonium citrate respectively [16]. The $\tau(C''O)$ under the influence of strong hydrogen bonding appears at a higher frequency. The presence of a strong H-bond in the crystal structure of sodium citrate could possibly explain the presence of the strong peaks at 761 and $756cm^{-1}$which have been assigned to the $\tau(C''O)$ mode.

COO frequencies

The differences in the two types of carboxyl groups (central and terminal) are further highlighted by the $\nu(C=O)$ frequencies. In α substituted acids the $\nu(C=O)$ appears at higher frequencies than the corresponding unsubstituted acids. Thus in acetic acid $\nu(C=O)$ appears at $1788cm^{-1}$and in glycolic acid it appears at $1806cm^{-1}$[23]. The calculated frequencies of CA clearly indicate this trend. Thus the central carboxyl $\nu(C=O)$ appears at $1980cm^{-1}$and the terminal carboxyl $\nu(C=O)$ appears at $1932cm^{-1}$and $1944cm^{-1}$. Since the O4 of one of terminal carboxyl groups is involved in an intramolecular hydrogen bonding with the hydroxyl hydrogen, the $\nu(C=O4)$ stretch appears at a lower frequency than the $\nu(C=O19)$ stretch. In gaseous oxalic acid the $\nu(C=O)$ stretch appears at 1826 and $1813cm^{-1}$[24]. Correspondingly in the solid state of citric acid the $\nu(C=O)$ stretch has been assigned to the peaks at 1704, 1695 and $1689cm^{-1}$in the IR spectra of anhydrous citric acid [9]. In glutaric acid a dicarboxylic acid which has the same number of carbon atoms separating the terminal carboxyl groups $\nu(C=O)$ appears at $1700cm^{-1}$in the IR of the solid state and at $1715cm^{-1}$in the IR of the solution [35]. In tartaric acid which is also an α-hydroxy carboxylic acid the $\nu(C=O)$ region appears as a broad band with shoulders

at 1694 and $1720cm^{-1}$and at 1694 and $1742cm^{-1}$in the IR and Raman spectra of solid state tartaric acid [26]. In solution a broad weakly polarized band appears at $1733cm^{-1}$in the Raman spectrum [26]. Unlike the longer dicarboxylic acids which show a single band citric acid behaves more like the lower dicarboxylic acids oxalic and malonic which show distinct bands owing to the two $\nu(C=O)$ present in them.

The $\nu(C-O)$ mode appears as a coupled mode with the $\delta(COH)$ mode. The discussion on the $\delta(COH)$ mode amply illustrates the features of this coupled mode. The other COO frequencies are the bending modes $\delta(C-O)$ and $\delta(C=O)$ and the out of plane CO bend ($\gamma(COO)$ in our nomenclature). These modes are not much affected by hydrogen bonding and hence they have been assigned in most cases. Compared to other carboxylic acids there is not much difference in the position of the frequencies associated with these modes. It is not possible to distinguish the carboxyl bends corresponding to the central carboxyl group and terminal carboxyl groups. In case of the $\gamma(COO)$ mode, however we can distinguish between the central and the terminal carboxyl groups. It comes higher in case of the central carboxyl group. This trend was not observed in the corresponding gas phase spectra of acetic acid and glycolic acid [23,25].

In case of the citrate trianion our calculated frequencies indicate that the strong peaks at 1603 and 1605 in the IR spectra of sodium and ammonium citrate can be attributed to the $\nu_a(COO^-)$ mode [15]. The $\nu_a(COO^-)$ mode has been assigned to the frequencies at 1607.3 and $1583cm^{-1}$in the IR and Raman spectra of sodium formate [29].. It has been assigned to the frequencies at 1583.7 and $1579.5cm^{-1}$in the IR spectra of sodium acetate at two different temperatures 80K and 290K [30]. It has been assigned to the peaks at 1640 and $1550cm^{-1}$in the IR spectra of sodium oxalate [36]. In citric acid the $\nu(C=O)$ frequency of the central carboxyl group appears higher than the $\nu(C=O)$ frequencies of the terminal carboxyl groups but in the citrate trianion the $\nu_a(COO^-)$ of the central carboxyl group comes lower than the $\nu_a(COO^-)$ of the terminal carboxyl groups. $\nu_s(COO^-)$ frequencies appear as mixed modes. They are coupled with the CH_2 bending modes and the medium intensity peaks associated with these modes have been assigned to the peaks at 1304, 1325 and $1333cm^{-1}$in the IR spectra of sodium citrate. This mode has been assigned to the frequencies at 1360.6 and $1357cm^{-1}$in the IR and Raman spectra of sodium formate respectively [29]. It has been assigned to the peaks at around 1440 and $1423.7cm^{-1}$in the IR spectra of sodium acetate recorded at two different temperatures [30]. It has been assigned to the peak at $1402cm^{-1}$in the IR spectra of sodium oxalate [36]. The lowering of the wavenumbers associated with this mode could be due to the presence of

the strong intramolecular hydrogen bonding in the solid phase structure of sodium citrate. The antisymmetric stretch is marginally higher than wave numbers associated with this mode in sodium formate, sodium acetate and sodium oxalate. The other CO bending modes appear at low frequencies and have not been assigned in most cases due to lack of data and moreover when they appear at higher frequencies they are of low intensity (calculated). The out of plane CO ($\gamma(COO)$) modes have been assigned to the peaks in the 500-800cm^{-1}range. The assignments are in agreement with the earlier assignment of this mode in the IR spectra of sodium formate, sodium acetate and sodium oxalate.

CH_2 frequencies

The CH_2 frequencies in CA do not show much deviation from the standard behaviour. Thus in CA we have the stretching frequencies in the 2900-3000cm^{-1}region. In case of the CH_2 bending modes the $\delta(CH_2)$ modes are pure bending modes. They have been assigned to the peak at 1430cm^{-1}in the IR spectra of anhydrous CA. In the Raman spectra of CA the peak at 1425cm^{-1}can be attributed to this mode. The calculated IR and Raman intensities of one of the peaks associated with the $\omega(CH_2)$ mode are very low and hence this peak has not been assigned to the experimental spectra. The other peak can be assigned to the one at 1407cm^{-1}in the IR spectra of anhydrous CA [10]. The $t(CH_2)$ mode can be assigned to the peaks at 1207 and 1342cm^{-1}in the IR spectra of anhydrous CA [9].. The $\rho(CH_2)$ is coupled with other modes and can be assigned to the peak at 960cm^{-1}in the IR spectra of anhydrous CA [9]. The $\delta(CCC)$ modes appear at low frequencies and hence have not been assigned. As we have seen in Chapter 4, in dicarboxylic acids also the CH_2 bending modes appear at nearly the same frequencies. Deviations if any arise due to coupling with CO bending modes.

In case of the citrate trianion the $\nu(CH_2)$ frequencies have been assigned to the peaks in the 2900-3000cm^{-1}range in the IR spectra of sodium and ammonium citrate [15]. The CH_2 bending modes as in citric acid appear as mixed modes but they are less coupled. The assignments are in agreement with the intensities and the positions of the peaks. The $\delta(CCC)$ modes have not been assigned because they appear at very low frequencies.

CC frequencies

The $\nu(CC)$ frequencies associated with the $C-COOH$ and the H_2C-CH_2 bonds can be easily distinguished. In general the frequencies associated with the former bond appear at

lower wavenumbers. In citric acid one of the $\nu(CC')$ modes comes higher than the $\nu(C'C'')$ modes. The other mode comes lower. This could be due to the symmetric nature of the two CH_2 groups. The $\nu(C''C)$ frequency associated with the $C-COOH$ bond of the central carboxylic acid comes higher than the other $\nu(CC')$ frequency. Some of the $\nu(CC)$ modes are associated with the $\nu(C-O)$ bands. As a result of this there is an appreciable fall in the calculated Raman intensities. Evidence for this coupling is the low depolarization ratios (< 0.75), a characterstic of the $\nu(C-O)$ frequency.

The CC frequencies follow the same trend as in citric acid. They can be characterized by the strong Raman intensities. In the citrate trianion they are not mixed with the $\nu(C-O)$ mode but in some cases they appear coupled to the CH_2 bending modes. The $\nu(CC)$ frequencies of bonds connecting a carboxylate group and a methylene group, and methylene group-methylene group can easily be distinguished.

5.1.3 Force Constants

In Table 5.6 the symmetric diagonal force constants of CA and CTA, scaled and unscaled are given. The comparative table clearly indicates the changes occuring in the values of the force constants of the trianion to its parent acid. The overall structural changes can be correlated to the corresponding force constants. We compare our calculated (unscaled) force constants with the unscaled force constants of acetic acid and formic acid calculated at the Hartree Fock level using the 4-31G basis set [23]. The value of the $\nu(C=O)$ mode for acetic acid is 14.607 mdynes/A^owhile in case of formic acid it is 15.064 mdynes/A^o. Use of the 6-31G+ basis set in case of formic acid decreases the value to 14.390 mdynes/A^o. On the other hand, in the force constants given by Suzuki et al. [27] for the normal coordinate analysis of solid state succinic acid, the value for this mode is 9.4 mdynes/A^o. Williams and Lowrey have clearly shown that by using a suitable hydration model, comparable force constants can be evaluated to fit the experimental solid state or solution spectra [23]. Given the size of CA and CTA and the number of water molecules needed to completely hydrate it, calculations at the present level of sophistication are not possible.

5.2 Substituted Citric Acids

The proposed mechanisms of the enzymatic reactions of the enzymes involving citric acid have been well documented [37]. The inhibition of the enzymatic activity of these enzymes

by fluorocitrates have been studied extensively [38] after the pioneering work of Peters [39] on the inhibitory action of fluoroacetates.

Interest in the activity of these compounds has increased after the discovery that they inhibit the production of acetyl-CoA(a product of the ATP-citrate lyase), which plays a central role in the biosynthesis of mammalian fatty acids and cholesterol [40]. One of the interesting aspects of these enzymes has been that they are active against only a few specific stereoisomers of the substrates [41]. Moreover the active stereoisomer against one enzyme is not necessarily the active stereisomer against another enzyme [37,41–43]. The inhibitory activity of the substrates is also dependent on the nature of the substituent. Thus while allohydroxy citrate inhibits the activity of ATP-citrate lyase more than the corresponding monofluorocitrate, the difluoro citrate inhibits the acivity of the enzyme more than the other two [44]. One of the questions raised in an earlier paper [45] on the inihibitory activity of these compounds was whether the differences of activity of these compounds were due to steric or electronic effects. In the absence of any theoretical calculation on substituted citric acids we thought it to be worthwhile to study these tricarboxylic acids theoretically to see the effect of substituents on the structure and electronic properties. This would be useful to know whether the specificity of these enzymes against a particular pair of enantiomers is due to electronic or structural effects or both.

The starting structure for the calculations was the X-Ray structure of citric acid [16]. It was optimized at various levels of sophistication which included the AM1, STO-3G, HF/3-21G and HF/4-21G. The various substituted citric acids were obtained by replacing each of the methylene group hydrogens by either a fluorine atom or an hydroxyl group. Monosubstituted citric acids have two chiral centers giving rise to two pairs of enantiomers. Difluorocitric acid has one chiral center and hence has a single pair of enantiomers. Each of the enantiomers was subjected to a complete geometry optimization at the AM1, STO-3G and the HF/3-21G levels. The 3-21G optimized structures were then subject to a single point calculation at the HF/6-31G* level. It should be noted that the energies, geometries and charges of citric discussed in this section have been evaluated at the HF/3-21G level.

In general theoretical calculations which do not include the effects of parity cannot distinguish between pairs of enantiomers [46,47]. However our procedure of creating the isomers by replacing the hydrogens of citric acid gives rise to different starting geometries for each of the enantiomers. Thus the fact that the two starting structures of a pair of enantiomers converge to the same energy after the optimization, indicates that the approximations of the theory at that level are reasonably good to give quantitative results.

In case of one of the pairs of enantiomers of monofluorocitric acid, the two enantiomers do not converge to the same energy due to the presence of a local minimum. All attempts to achieve the global minimum from that structure failed. The notable fact though is that the energy of this errant structure is higher than the corresponding enantiomer. In all other cases the two pairs of enantiomers at the end of the HF/3-21G optimization converge to the similar structures with the same energies. AM1 and STO-3G optimized structures give different energies for the enantiomers indicating the approximations at these levels are too poor to give reliable results. For the sake of clarity we designate each enantiomer as a particular isomer. Thus in monofluorocitric acid the (2R,3S), (2S,3S), (2S,3R) and (2R,3R) enantiomers are designated as isomers I, II, III and IV and in monohydroxycitric acid the (2R,3R), (2S,3R), (2S,3S) and (2R,3S) enantiomers are designated as isomers I, II, III, IV. In case of difluorocitric acid the two enantiomers 3S and 3R are designated isomers I and II.

5.2.1 Energies

In Table 5.7 the energies of the various isomers are given after each stage of optimization. In case of citric acid, the total electronic energy is -751.74344 hartrees. It can be seen that the energy of the system increases as the level of the basis set increases.

The lowest energy isomer in monofluorocitric acid is IV which has an energy of -850.05446 hartrees. Though the corresponding enantiomer II has 5 kJ/mol more energy at the AM1 level it is equal to the energy of the isomer IV after the 3-21G optimization. The diastereomers I and III are always higher in energy than the II and IV isomers.

The difluorocitric acid isomers have nearly the same energy after the AM1 level. After the STO-3G level the isomer I is higher in energy than the isomer II but as expected for enantiomers the energies are equal after the 3-21G optimization.

In case of the monohydroxycitric acids the isomer IV is energetically most stable after the AM1, STO-3G and 3-21G levels of optimization. Though the corresponding enantiomer II has about 20 kJ/mol more energy after the AM1 optimization, the subsequent optimizations at the STO-3G and 3-21G level give rise to the same energies for the enantiomers. The other pair of diastereomers I and III also have the same energy after the 3-21G optimization but they are 10 kJ/mol higher in energy than the II and IV isomers. As in case of monofluorocitric acid the two low energy isomers are stabilized by the formation of hydrogen bonds between the H17 and O19. Though the other pair of diastereomers

have the propensity to form hydrogen bonds between H17 and O19 the geometry of the two atoms which could involve in hydrogen bond do not possess the right geometry as is discussed in the next section.

Thus on the basis of the energy differences it can be concluded that the II and IV isomers in monofluoro and monohydroxy citric acids are energetically more stable than the other pair of diastercomers.

5.2.2 Geometries

In Tables 5.8, 5.9 and 5.10 the geometries of the 3-21G optimized isomers of citric acid, difluoro, monofluoro and monohydroxy citric acids are given. These structures are shown in Figures 5.1, 5.2 and 5.3. Since the X-Ray structures of the subsituted citric acids are not available we have compared the optimized structures to the X-Ray structure of citric acid [16]. The X-Ray structures of the salts of fluorocitrates are available but comparsions are not made because they are present in their trianionic forms [48].

There is little change in the structure of citric acid evaluated at the HF/3-21G and HF/4-21G levels. Except for some minor changes in the geometry as can be seen in Tables 5.1 and 5.8 the overall features are same. Hence we do not discuss the geometry of citric acid here.

The substitution of fluorine in place of one of the methylene hydrogens leads to some interesting distortions which have a profound effect on the structure of the molecule and its biological activity. Fluorine due to its high electronegative character polarizes the C-F bond [38,49]. Due to this a number of changes takes place in the structure of the citric acid. The terminal carboxyl group which is attached to the methylene group containing the fluorine is twisted in such a way that the C=O bond tends to be trans to the C-F bond. Thus while the O=C2-C5-H7 torsion angle is 125^o in normal citric acid, in the monofluoro citric acid isomer I it is -141^o. In the other isomers the O=C-C-F torsion angle has values of 179^o, -115^o and -179^o respectively. One of the offshoots of the twisting of the C=O group is that in the isomers II and IV the O-C-C-F torsion angle tends to 0^o (angle values are 1.7^o and -1.7^o respectively). There is no notable change in the orientation of the central carboxyl group. In marked contrast to citric acid where the central hydroxyl hydrogen is involoved in a weak intramolecular hydgrogen bond with the terminal carboxyl oxygen, in the substituted citric acids a strong intramolecular hydrogen bond emerges between the central hydroxyl hydrogen and the central or terminal carboxyl oxygens. The length

and the orientaion of the hydrogen bond determine the stablility of the particular isomer. Thus in monofluoro citric acid the distance between H17 and O19 is 2.08 A^o in case of isomers II and IV while it is 2.11 A^o in case of isomer III. In isomer I the hydrogen bond exists with the central carboxyl oxygen. The difference of 3 kJ/mol between the energies of isomer I and isomer III indicates that the hydrogen bond formation with the terminal carboxyl oxygen is favoured. The energy differences also indicate that the formation of a stable hydrogen bond favours the particular conformation. Thus isomers II and IV are more stable than I and III. This is obvious because the formation of a hydrogen bond with the terminal carboxyl oxygen involves the formation a six membered ring system, which is far more stable than the five membered ring system formed due to an hydrogen bond with the central carboxyl group. Another notable feature is the shortening of the O1-C2 and C6-C11 distances in isomers II and IV compared to the observed distances in isomers I and III. In both the isomers II and IV C11 is trans to the fluorine atom. The stablity attained due to the formation of an intramolecular hydrogen bond and the conformational changes occuring due to the substituion of fluorine in a particular pair of diastereisomers may have a profound role in the inhibition of the enzymatic activity.

Once the second fluorine replaces the remaining hydrogen in the methylene group the distortions become more pronounced. As compared to the O1-C2-C5-C6 torsion of -178^o in citric acid, in the difluoro citric acid the angle is $+/ -69^o$. This implies that the carboxyl group has rotated in such a way that the two fluorines always eclipse the two carbon atoms rather than a carbon and an oxygen atom as in the case of citric acid. Though a similar kind of effect is found in the monofluoro case in the difluoro case it is much more pronounced. A feature which can be easily noticed is the distance of the fluorine atoms from the carboxyl oxygen. In both the isomers the O-F distances where the oxygen is either a carbonyl or an hydroxyl oxygen are nearly equal with the carbonyl oxygen a bit more distant than the hydroxyl oxygen. In both the cases the =O-F distance is $2.667A^o$ while the -O-F distance is $2.660A^o$. This indicates that the four atoms(two oxygens and the two fluorines lie on a single plane. In normal citric acid the =O-H for both the terminal carboxylic acids is $3.121A^o$ and $2.904A^o$ respectively, while the -O-H distance for both the terminal carboxylic group is $2.582A^o$ and $2.420A^o$ respectively. When compared to the distances in normal citric acid, the C2-C5 distance is elongated and the C6-C10 distance is shortened. This lengthening of the C2-C5 distances could be due to the repulsion between the lone pairs on the carboxyl oxygen and the lone pairs on the fluorine atom. On the other hand the shortening of the C6-C10 could be due to hyperconjugation [50,51]. In

marked contrast to both monofluoro and monohydroxy citric acids the central hydroxyl hydrogen does not form a hydrogen bond with the terminal carboxyl oxygen but with the central carboxyl oxygen. Thus a five membered ring system is formed and due to this the O9-H17 and C11-O13 bonds become longer. The hydrogen bond distance is $2.09A^o$. In the monofluorocitric acids the C-O bond length of the terminal carboxyl group is shortened, while in the difluorocitric acids the C-O bond length of the central carboxyl group is shortened. In all the cases where there is a shortening of the C-O bond distances, the fluorine atom is close to the carboxyl group. In case of the difluorocitric acid the F7-C5-C6-C11 dihedral is $+/-25^o$. It can clearly be seen that the introduction of a second fluorine drastically changes the conformation of citric acid. Thus the strong inhibitory activity of the difluorocitric acids could be correlated to the conformation and the charge effects discussed later, induced due to the presence of the fluorine atoms.

The substitution of the methylene hydrogen by a hydroxyl group gives rise to some interesting structural facets which are similar to those observed in the monofluoro case. Though the -OH group is a good electron withdrawing group compared to the fluorine atom it is less electronegative despite the fact that it is isoelectronic with fluorine, the reason being that the charge is more delocalized in the -OH than in the -F case. Unlike the monofluoro and difluoro case the O=C2-C5-C6 is -54^o and -65^o in the isomer I and II compared to the angle of 2.3^o for normal citric acid. This clearly shows that the presence of the hydroxyl group changes the orientation of the terminal carboxyl group. An important observation is that in the isomers II and IV the O1-C2-C5-O8 torsion angle is $+/-6^o$. This clearly implies that the substituted hydroxyl group in a way behaves very much like the substituted fluorine group. The implication of the observation would be discussed in detail subsequently. There is no notable change in the geometry of the central carboxyl group. In case of the monohydroxy citric acids also an hydrogen bond is formed between the central hydroxyl hydrogen and the terminal carboxyl oxygen. The H-bond distance of 2.12 A^o or 2.02 A^o in both the diastereomers II and IV indicates that the H-bond formed is strong.

The preference for the fluorine or the hydroxyl oxygen to eclipse the carboxyl oxygen as can be seen from the energy profiles could be due to hyperconjugation. In pyruvic acid (discussed in Chapter 3) we had seen the pictorial representation of this effect in the form of the valence electron density distributions. Similar studies on substituted citric acids could not be done because of the imposing size of these systems.

5.2.3 Charges and Dipoles

Charges and dipole moments are basis set dependent. Hence comparisons are valid only at a given level of theory. So only the overall trends between related molecules are being highlighted. At the AM1 level the dipole moment of citric acid is 1.6564. This increases to 2.4941 at the STO-3G level and to 4.1208 at the 3-21G level. The dipole moment of monofluoro citric acid is comparatively smaller than citric acid in all the isomers. This is due to the fact that a new dipole in the form of C-F is present. Since the dipole moment of the molecule is the vector sum of the individual bond dipoles the overall dipole moment decreases. A noticeable feature is that isomers II and IV have higher dipole moments than isomers I and III. In difluoro citric acid the dipole moment is comparatively more than that of monofluoro citric acid but less than that of citric acid. The presence of two C-F bonds in nearly opposite directions is responsible for the cancellation of the overall change in dipole moment. The dipole moment of the monhydroxy citric acid isomers is the least when compared to that of citric acid, monofluoro citric acid and difluoro citric acid. This is due to the presence of an O-H group. The C-O dipole is not very effective because of the presence of a O-H dipole also. In this case the isomers I and III have higher dipole moments than the isomers II and IV. Thus the dipole moment is not an useful quantity to distinguish the various isomers.

The Mulliken charge distribution for all the atoms of the minimum energy isomers are listed in Table 5.11. The plots of the charges on the atoms to the corresponding atom numbers are shown in Figures 5.4, 5.5 and 5.6. As expected, the changes in charges are visible in atoms 5, 6 and 7. We focus our attention on the charge distribution of atom 5 (The carbon on which the hydrogens are substituted by either a fluorine group or a hydroxyl group). It can be clearly seen that as we progress from citric acid to monohydroxy to monfluoro to difluorocitric acid, there is a gradual increase of the positive charge on this atom. This fact is quite obvious owing to the substitution of electron withdrawing groups on this carbon. This would have far reaching effects on the inhibitory action of the substituted citric acids.

5.2.4 Discussion

Preceding our discussion of results on the inhibitory action of substituted citric acids, we give a brief background to the present day understanding of the mechanism of the enzymes. We focus our attention on one enzyme aconitase because the X-Ray structure of

this enzyme is known [52–54]. Moreover a lot of work has been done on the mechanistic aspects of this enzyme [37,55]. The discussion can be extended to ATP citrate lyase because of the fact that only a particular pair of diastereomers are active inhibitors of these enzymes. One of the enantiomer inhibits aconitase while the other inhibits ATP-citrate lyase.

A number of mechanisms have been proposed on the enzymatic activity of aconitase. Thus we have the Ferrous wheel mechanism of Glusker [56,57], the Bailar twist mechanism [58] and the reverse Ferrous wheel mechanism [37]. The Ferrous wheel mechanism is the simplest of all and we use it in our illustration of the inhibitory activity. The X-Ray structure of inactive aconitase and activated aconitase lend further credence to this mechanism. In the ferrous wheel scheme, the Fe^{II} present in the active site of aconitase binds itself to the terminal carboxyl group, the central carboxyl group and the central hydroxyl group of citric acid. After the binding, a base activated enzyme abstracts a proton from the methylene group thereby producing a carbanion. The resulting carbanion undergoes rearrangement and the central hydroxyl group is expended as OH^- producing cis aconitate. We have indicated only the salient features of this mechanism. Thus we can see that this mechanism involves two important steps: first the binding of the substrate to the enzyme, second the formation of the carbanion. The binding of the substrate and the stability of the carbanion therefore would decide on inhibitory action of the substituted citric acids.

The main difference in the various diasteromers arises in the binding stage itself. It can be seen from our results that only in isomers II and IV of monofluorocitric acid and monohydroxycitric acid the substituted group (-F or -OH) was in the same plane as the terminal carboxyl oxygen. Thus the substituted group owing to its higher electronegativity would enter the coordination sphere of Fe^{II} and would bind to the Fe. Therefore geometrical conditions govern the inhibitory activity of a particular set of diastereomers over the other. As has already been pointed out, that as we progress from citric acid to difluorocitric acid the positive charge on carbon 5 increases. Due to this the carbanion formed during the course of reaction would become more stable. The increased stability of the carbanion would therefore make it difficult for the hydroxyl group to be abstracted and hence the reaction would not proceed in that direction. This could possibly explain the improved inhibitory activity of the difluoro citric acids.

Our results therefore answer the questions raised by Marletta et al. [45] that the inhibitory action of the substituted citric acids is both due to steric and electronic effects.

Though our results do not answer the question of the specificity of a single enantiomer against a particular enzyme, the activity of particular pair of diatereomers has been explained.

5.3 Conclusion

In the first section ab initio calculations of citric acid and the citrate trianion have been performed at the Hartree Fock level using the 4-21G basis set. The calculated vibrational frequencies were assigned to the corresponding experimental vibrational spectra. The results indicate that citric acid and the citrate trianion have some unique features as far as their vibrational spectra is concerned. Thus they are quite different from other dicarboxylic acids and α-carboxylic acids in certain aspects.

In the second section our endeavour had been to explain the inhibitory activity of substituted citric acids. Our results clearly give a theoretical basis for the understanding of the activity of substituted citric acids. We have also explained the reason behind the inhibitory acitivity of a particular pair of diastereomers over the other. Thus our comprehensive study of substituted citric acids would help in the understanding of some of the interesting facets of enzyme activity and mechanisims. Further studies on the actual trianions have also been carried out. It would be interesting to carry out enzyme substrate interaction studies to explain the inhibitory action of a particular enantiomer against a particular enzyme, but owing to the size of the substrates and the number of groups involved in the active site, such a study is more challenging.

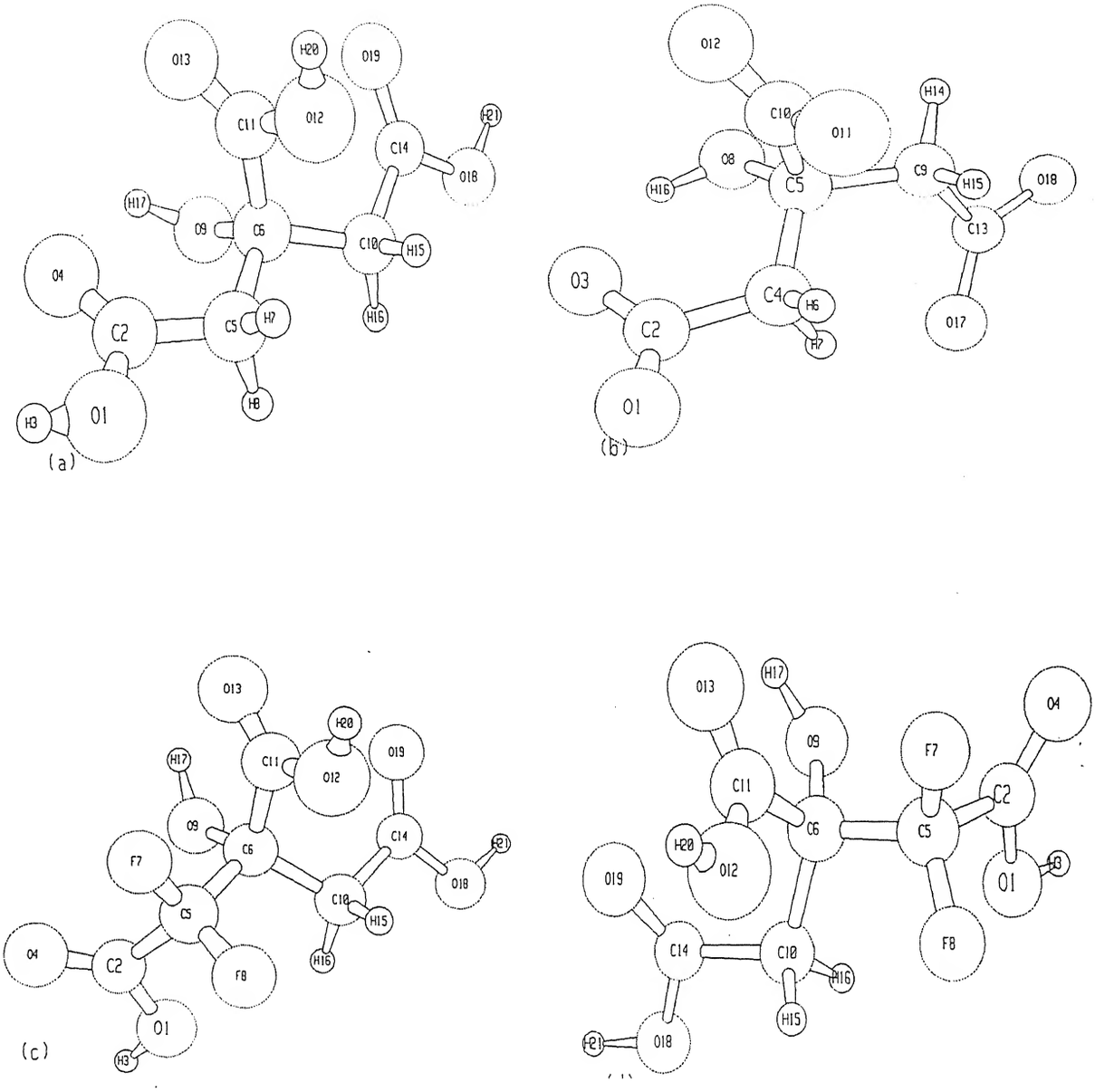

Figure 5.1: Optimized structures of (a) Citric acid (4-21G), (b) Citrate trianion (4-21G), (c) and (d) I(3S) and II(3R) isomers of Difluorocitric acid (3-21G).

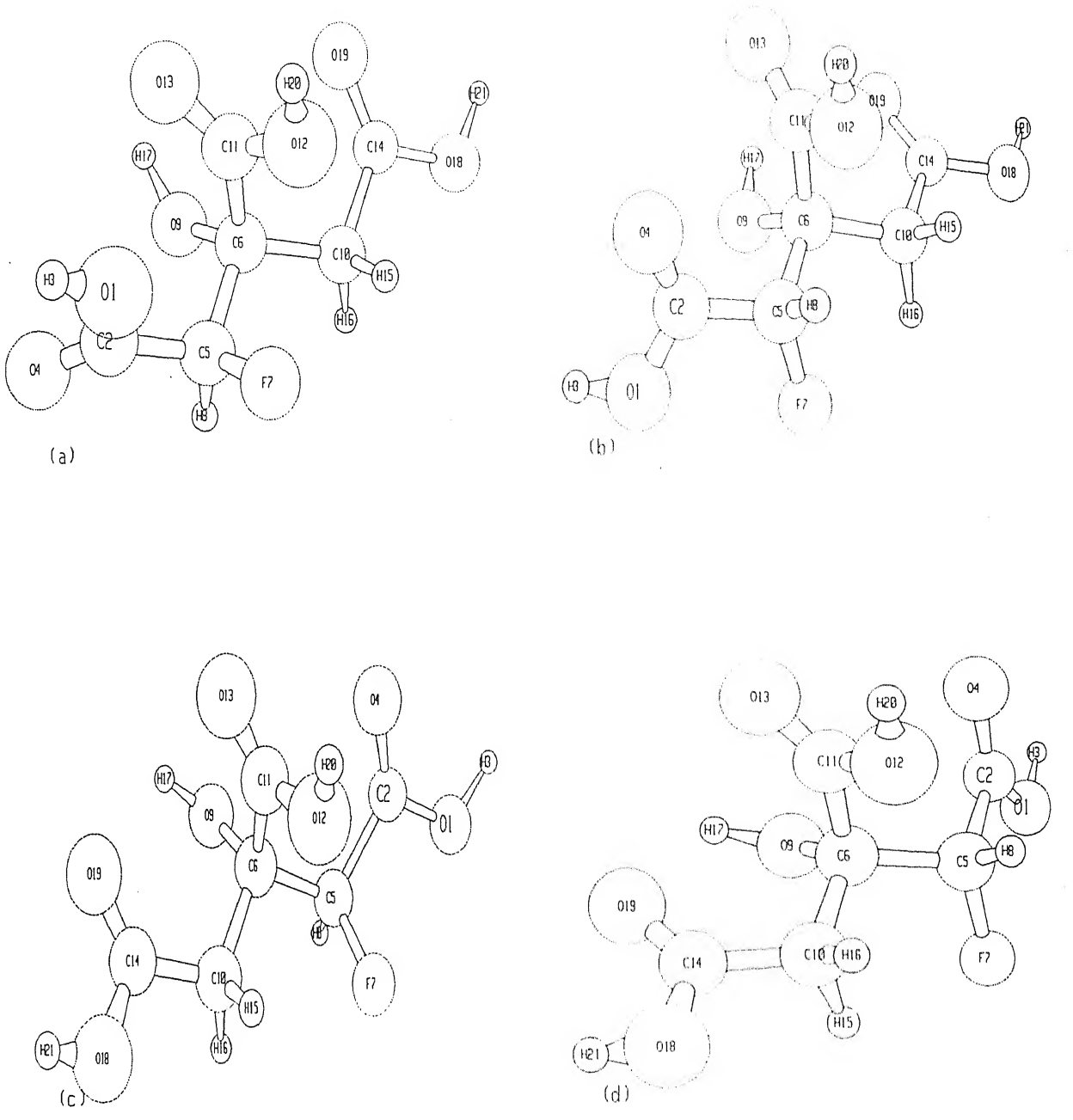

Figure 5.2: 3-21G optimized structures of (a) I(2R,3S), (b) II(2S,3S), (c) III(2S,3R) and (d) IV(2R,3R) isomers of Monofluorocitric acid.

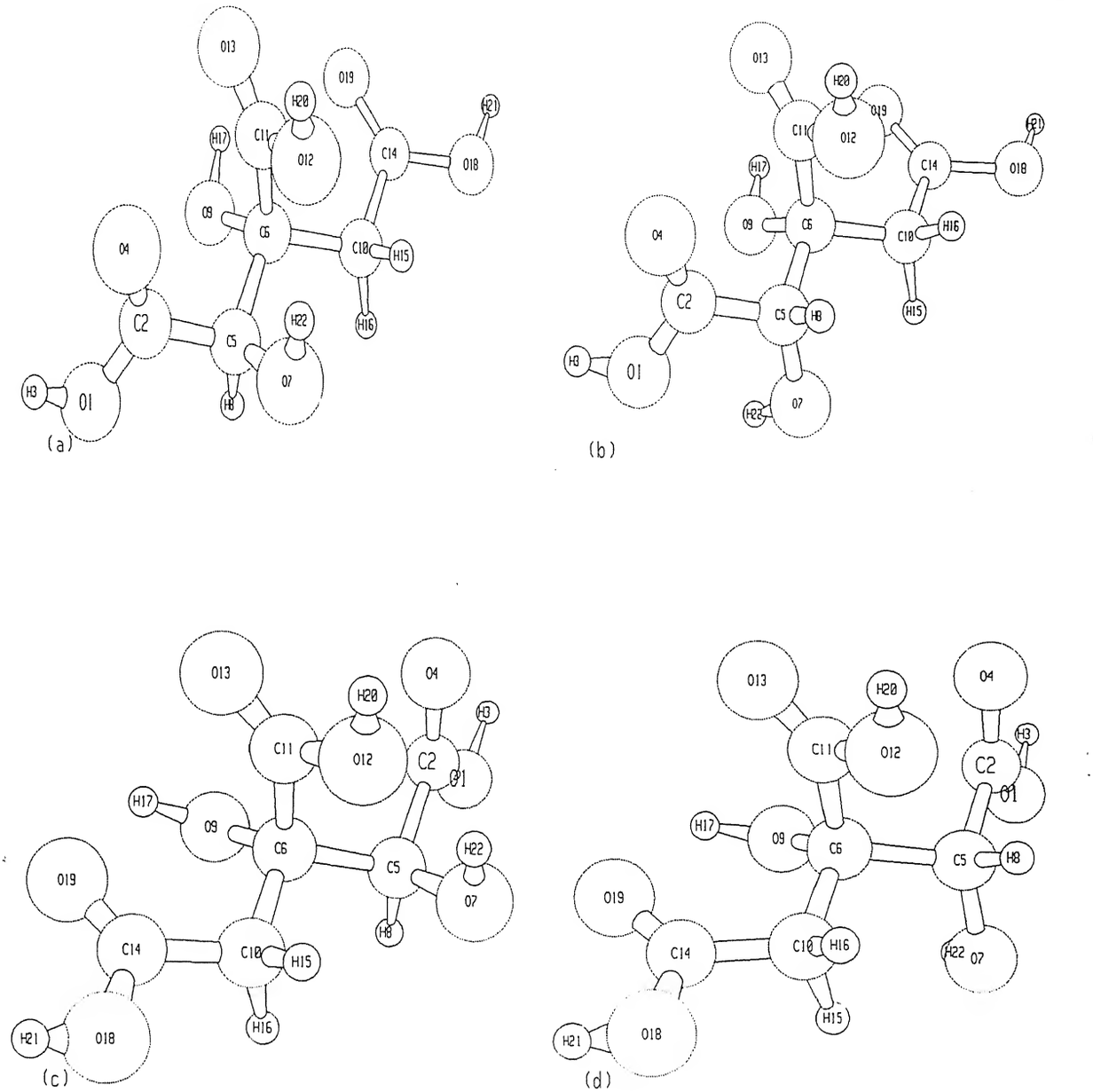

Figure 5.3: 3-21G optimized structures of (a) I(2R,3R), (b) II(2S,3R), (c) III(2S,3S) and (d) IV(2R,3S) isomers of Monohydroxycitric acid.

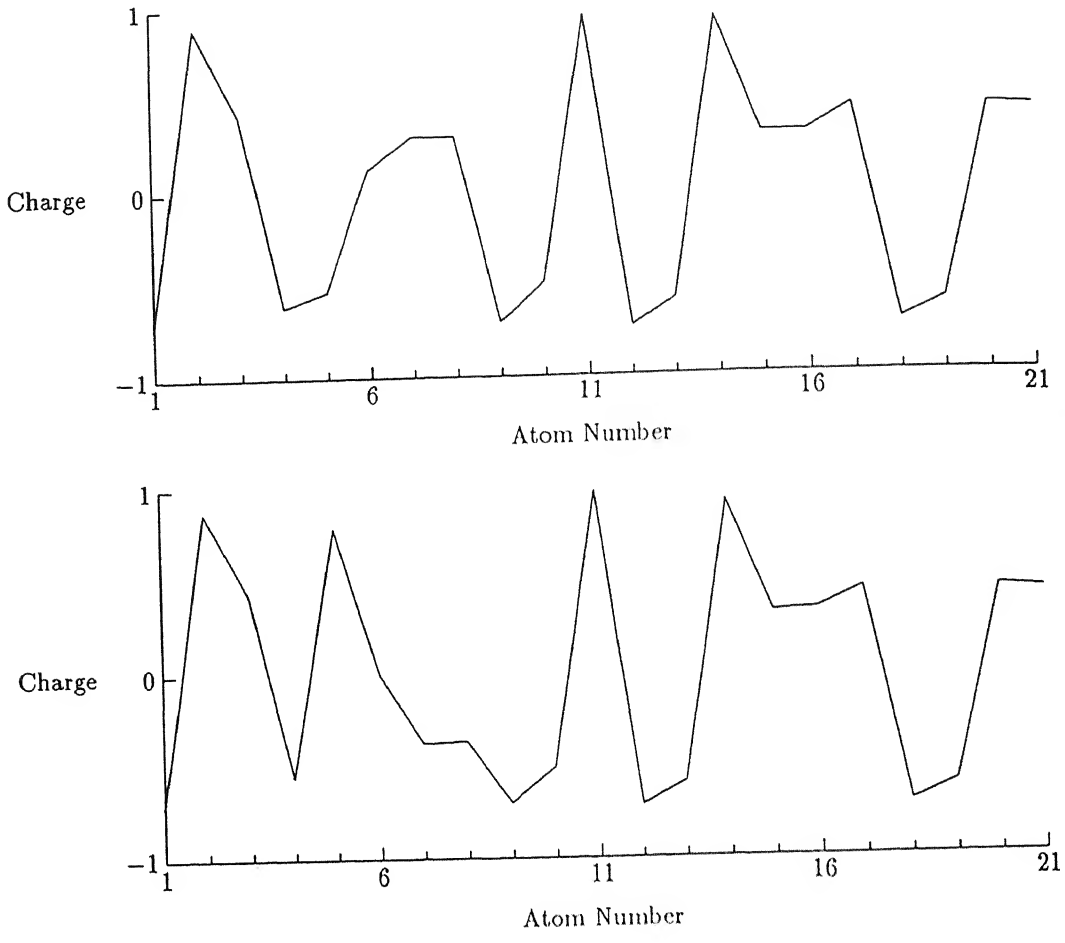

Figure 5.4: Mulliken populations on all the atoms of citric acid and the two conformers of difluorocitric acid

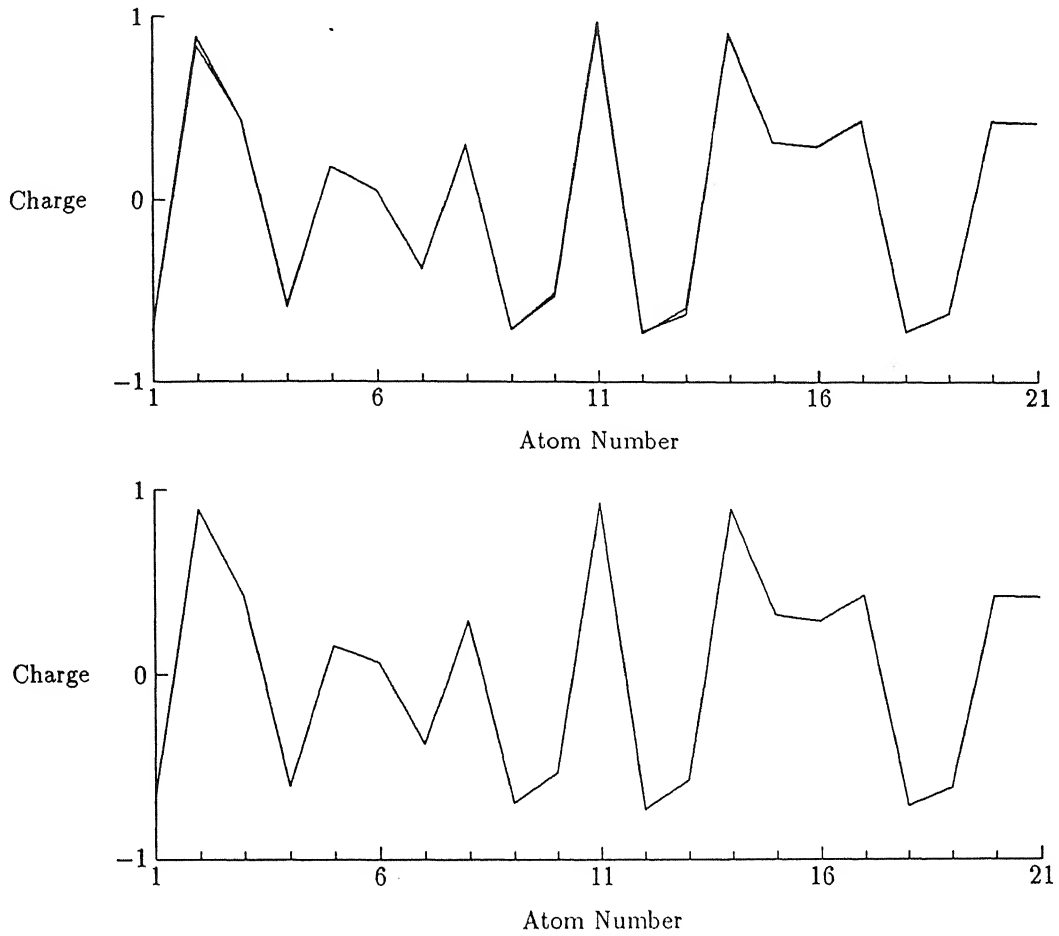

Figure 5.5: Mulliken populations on all the atoms of the four conformers of monofluorocitric acid

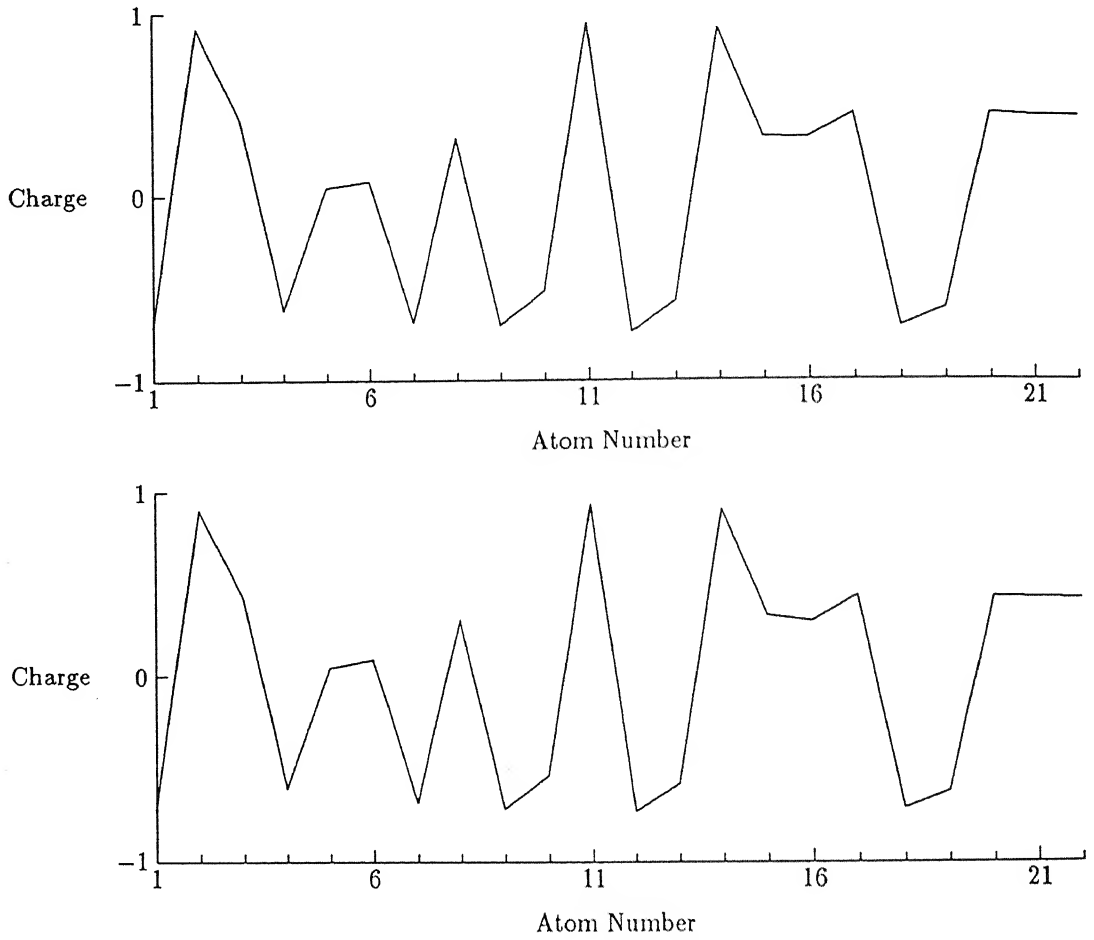

Figure 5.6: Mulliken populations on all the atoms of the four conformers of monohydroxycitric acid

Table 5.1: Symmetry Coordinates of Citric acid

Coordinate	Description
$S_1 = R_{1.2}$	$\nu(C-O)$
$S_2 = R_{2.4}$	$\nu(C=O)$
$S_3 = R_{2.5}$	$\nu(CC')$
$S_4 = R_{5.6}$	$\nu(C'C'')$
$S_5 = R_{5.7} + R_{5.8}$	$\nu_s(CH_2)$
$S_6 = R_{5.7} - R_{5.8}$	$\nu_a(CH_2)$
$S_7 = R_{6.9}$	$\nu(C''O)$
$S_8 = R_{6.10}$	$\nu(C''C)$
$S_9 = R_{6.11}$	$\nu(C''C')$
$S_{10} = R_{11.12}$	$\nu(C-O)$
$S_{11} = R_{11.13}$	$\nu(C=O)$
$S_{12} = R_{10.14}$	$\nu(C'C)$
$S_{13} = R_{10.15} + R_{10.16}$	$\nu_s(CH_2)$
$S_{14} = R_{10.15} - R_{10.16}$	$\nu_a(CH_2)$
$S_{15} = R_{9.17}$	$\nu(OH)$
$S_{16} = R_{14.18}$	$\nu(C-O)$
$S_{17} = R_{14.19}$	$\nu(C=O)$
$S_{18} = 2\alpha_{1.2.5} - \alpha_{4.2.5} - \alpha_{1.2.4}$	$\delta(C-O)$
$S_{19} = \alpha_{4.2.5} - \alpha_{1.2.4}$	$\delta(C=O)$
$S_{20} = 4\alpha_{7.5.8} - \alpha_{2.5.7} - \alpha_{2.5.8} - \alpha_{6.5.7} - \alpha_{6.5.8}$	$\delta(CH_2)$
$S_{21} = \alpha_{2.5.7} + \alpha_{2.5.8} - \alpha_{6.5.7} - \alpha_{6.5.8}$	$\omega(CH_2)$
$S_{22} = \alpha_{2.5.7} - \alpha_{2.5.8} + \alpha_{6.5.7} - \alpha_{6.5.8}$	$\rho(CH_2)$
$S_{23} = \alpha_{2.5.7} - \alpha_{2.5.8} - \alpha_{6.5.7} + \alpha_{6.5.8}$	$t(CH_2)$
$S_{24} = 5\alpha_{2.5.6} - \alpha_{7.5.8} - \alpha_{2.5.7} - \alpha_{2.5.8} - \alpha_{6.5.7} - \alpha_{6.5.8}$	$\delta(CC'C'')$
$S_{25} = 2\alpha_{9.6.11} - \alpha_{5.6.9} - \alpha_{9.6.10}$	$\delta(OC''C)$
$S_{26} = \alpha_{5.6.9} - \alpha_{9.6.10}$	$\rho(OC''C)$
$S_{27} = 2\alpha_{5.6.10} - \alpha_{5.6.11} - \alpha_{11.6.10}$	$\delta(C'C''C)$
$S_{28} = \alpha_{5.6.11} - \alpha_{11.6.10}$	$\rho(C'C''C)$
$S_{29} = \alpha_{6.9.17}$	$\delta(C''OH)$
$S_{30} = 2\alpha_{6.11.12} - \alpha_{6.11.13} - \alpha_{12.11.13}$	$\delta(C-O)$
$S_{31} = \alpha_{6.11.13} - \alpha_{12.11.13}$	$\delta(C=O)$

Table 5.1. (Continued): Symmetry Coordinates of Citric acid

Coordinate	Description
$S_{32} = 4\alpha_{15.10.16} - \alpha_{6.10.15} - \alpha_{6.10.16} - \alpha_{14.10.15} - \alpha_{14.10.16}$	$\delta(CH_2)$
$S_{33} = \alpha_{6.10.15} + \alpha_{6.10.16} - \alpha_{14.10.15} - \alpha_{14.10.16}$	$\omega(CH_2)$
$S_{34} = \alpha_{6.10.15} - \alpha_{6.10.16} + \alpha_{14.10.15} - \alpha_{14.10.16}$	$\rho(CH_2)$
$S_{35} = \alpha_{6.10.15} - \alpha_{6.10.16} - \alpha_{14.10.15} + \alpha_{14.10.16}$	$t(CH_2)$
$S_{36} = 5\alpha_{6.10.14} - \alpha_{15.10.16} - \alpha_{6.10.15} - \alpha_{6.10.16} - \alpha_{14.10.15} - \alpha_{14.10.16}$	$\delta(CC'C'')$
$S_{37} = 2\alpha_{10.14.18} - \alpha_{10.14.19} - \alpha_{18.14.19}$	$\delta(C-O)$
$S_{38} = \alpha_{10.14.19} - \alpha_{18.14.19}$	$\delta(C=O)$
$S_{39} = \tau_{1.2.5.4}$	$\gamma(COO)$
$S_{40} = \tau_{12.11.6.13}$	$\gamma(COO)$
$S_{41} = \tau_{18.14.10.19}$	$\gamma(COO)$
$S_{42} = \alpha_{5.6.10} + \alpha_{5.6.11} + \alpha_{11.6.10} - \alpha_{5.6.9} - \alpha_{9.6.10} - \alpha_{9.6.11}$	$\delta(C'C''C')$
$S_{43} = \tau_{1.2.5.6} + \tau_{1.2.5.7} + \tau_{1.2.5.8} + \tau_{4.2.5.6} + \tau_{4.2.5.7} + \tau_{4.2.5.8}$	$\tau(CC')$
$S_{44} = \tau_{18.14.10.6} + \tau_{18.14.10.15} + \tau_{18.14.10.16} + \tau_{19.14.10.6} + \tau_{19.14.10.15} + \tau_{19.14.10.16}$	$\tau(CC')$
$S_{45} = \tau_{12.11.6.9} + \tau_{12.11.6.5} + \tau_{12.11.6.10} + \tau_{13.11.6.9} + \tau_{13.11.6.5} + \tau_{13.11.6.10}$	$\tau(CC'')$
$S_{46} = \tau_{2.5.6.10} + \tau_{2.5.6.9} + \tau_{2.5.6.11}$	$\tau(C'C'')$
$S_{47} = \tau_{14.10.6.5} + \tau_{14.10.6.9} + \tau_{14.10.6.11}$	$\tau(C'C'')$
$S_{48} = \tau_{5.6.9.17} + \tau_{11.6.9.17} + \tau_{10.6.9.17}$	$\tau(C''O)$
$S_{49} = R_{1.3}$	$\nu(OH)$
$S_{50} = R_{12.20}$	$\nu(OH)$
$S_{51} = R_{18.21}$	$\nu(OH)$
$S_{52} = \alpha_{2.1.3}$	$\delta(C'OH)$
$S_{53} = \alpha_{11.12.20}$	$\delta(C'OH)$
$S_{54} = \alpha_{14.18.21}$	$\delta(C'OH)$
$S_{55} = \tau_{4.2.1.3} + \tau_{5.2.1.3}$	$\tau(CO)$
$S_{56} = \tau_{6.11.12.20} + \tau_{13.11.12.20}$	$\tau(CO)$
$S_{57} = \tau_{10.14.18.21} + \tau_{19.14.18.21}$	$\tau(CO)$

Atom numbering is given in Figure 5.1(a).

Table 5.2: Symmetry Coordinates of Citrate trianion

Coordinate	Description
$S_1 = R_{1.2} + R_{2.3}$	$\nu_s(COO)$
$S_2 = R_{1.2} - R_{2.3}$	$\nu_a(COO)$
$S_3 = R_{2.4}$	$\nu(CC')$
$S_4 = R_{4.5}$	$\nu(C'C'')$
$S_5 = R_{4.6} + R_{4.7}$	$\nu_s(CH_2)$
$S_6 = R_{4.6} - R_{4.7}$	$\nu_a(CH_2)$
$S_7 = R_{5.8}$	$\nu(C''O)$
$S_8 = R_{5.9}$	$\nu(C''C)$
$S_9 = R_{5.10}$	$\nu(C''C')$
$S_{10} = R_{10.11} + R_{10.12}$	$\nu_s(COO)$
$S_{11} = R_{10.11} - R_{10.12}$	$\nu_a(COO)$
$S_{12} = R_{9.13}$	$\nu(C'C)$
$S_{13} = R_{9.14} + R_{9.15}$	$\nu_s(CH_2)$
$S_{14} = R_{9.14} - R_{9.15}$	$\nu_a(CH_2)$
$S_{15} = R_{8.16}$	$\nu(OH)$
$S_{16} = R_{13.17} + R_{13.18}$	$\nu_s(COO)$
$S_{17} = R_{13.17} - R_{13.18}$	$\nu_a(COO)$
$S_{18} = 2\alpha_{1.2.3} - \alpha_{1.2.4} - \alpha_{3.2.4}$	$\delta(COO)$
$S_{19} = \alpha_{1.2.4} - \alpha_{3.2.4}$	$\rho(COO)$
$S_{20} = 4\alpha_{6.4.7} - \alpha_{2.4.6} - \alpha_{2.4.7} - \alpha_{5.4.6} - \alpha_{5.4.7}$	$\delta(CH_2)$
$S_{21} = \alpha_{2.4.6} + \alpha_{2.4.7} - \alpha_{5.4.6} - \alpha_{5.4.7}$	$\omega(CH_2)$
$S_{22} = \alpha_{2.4.6} - \alpha_{2.4.7} + \alpha_{5.4.6} - \alpha_{5.4.7}$	$\rho(CH_2)$
$S_{23} = \alpha_{2.4.6} - \alpha_{2.4.7} - \alpha_{5.4.6} + \alpha_{5.4.7}$	$t(CH_2)$
$S_{24} = 5\alpha_{2.4.5} - \alpha_{6.4.7} - \alpha_{2.4.6} - \alpha_{2.4.7} - \alpha_{5.4.6} - \alpha_{5.4.7}$	$\delta(CC'C'')$
$S_{25} = 2\alpha_{8.5.10} - \alpha_{4.5.8} - \alpha_{8.5.9}$	$\delta(OC''C)$
$S_{26} = \alpha_{4.5.8} - \alpha_{8.5.9}$	$\rho(OC''C)$
$S_{27} = 2\alpha_{4.5.9} - \alpha_{4.5.10} - \alpha_{9.5.10}$	$\delta(C'C''C)$
$S_{28} = \alpha_{4.5.10} - \alpha_{9.5.10}$	$\rho(C'C''C)$
$S_{29} = \alpha_{5.8.16}$	$\delta(C''OH)$
$S_{30} = 2\alpha_{11.10.12} - \alpha_{5.10.11} - \alpha_{5.10.12}$	$\delta(COO)$
$S_{31} = \alpha_{5.10.11} - \alpha_{5.10.12}$	$\rho(COO)$
$S_{32} = 4\alpha_{14.19.15} - \alpha_{5.9.14} - \alpha_{5.9.15} - \alpha_{13.9.14} - \alpha_{13.9.15}$	$\delta(CH_2)$
$S_{33} = \alpha_{5.9.14} + \alpha_{5.9.15} - \alpha_{13.9.14} - \alpha_{13.9.15}$	$\omega(CH_2)$
$S_{34} = \alpha_{5.9.14} - \alpha_{5.9.15} + \alpha_{13.9.14} - \alpha_{13.9.15}$	$\rho(CH_2)$
$S_{35} = \alpha_{5.9.14} - \alpha_{5.9.15} - \alpha_{13.9.14} + \alpha_{13.9.15}$	$t(CH_2)$
$S_{36} = 5\alpha_{5.9.13} - \alpha_{14.19.15} - \alpha_{5.9.14} - \alpha_{5.9.15} - \alpha_{13.9.14} - \alpha_{13.9.15}$	$\delta(CC'C'')$
$S_{37} = 2\alpha_{17.13.18} - \alpha_{10.13.17} - \alpha_{10.13.18}$	$\delta(COO)$
$S_{38} = \alpha_{10.13.17} - \alpha_{10.13.18}$	$\rho(COO)$
$S_{39} = \tau_{1.2.4.3}$	$\gamma(COO)$
$S_{40} = \tau_{11.10.5.2}$	$\gamma(COO)$
$S_{41} = \tau_{17.13.9.18}$	$\gamma(COO)$
$S_{42} = \alpha_{4.5.9} + \alpha_{4.5.10} + \alpha_{9.5.10} - \alpha_{4.5.8} - \alpha_{8.5.9} - \alpha_{8.5.10}$	$\delta(C'C''C')$
$S_{43} = \tau_{1.2.4.6} + \tau_{1.2.4.7} + \tau_{1.2.4.5} + \tau_{3.2.4.6} + \tau_{3.2.4.7} + \tau_{3.2.4.5}$	$\tau(CC')$
$S_{44} = \tau_{17.13.9.14} + \tau_{17.13.9.15} + \tau_{17.13.9.5} + \tau_{18.13.9.14} + \tau_{18.13.9.15} + \tau_{18.13.9.5}$	$\tau(CC')$
$S_{45} = \tau_{11.10.5.4} + \tau_{11.10.5.8} + \tau_{11.10.5.9} + \tau_{12.10.5.4} + \tau_{12.10.5.8} + \tau_{12.10.5.9}$	$\tau(CC'')$
$S_{46} = \tau_{2.4.5.8} + \tau_{2.4.5.9} + \tau_{2.4.5.10}$	$\tau(C'C'')$
$S_{47} = \tau_{13.9.5.4} + \tau_{13.9.5.8} + \tau_{13.9.5.10}$	$\tau(C'C'')$
$S_{48} = \tau_{4.5.8.16} + \tau_{10.5.8.16} + \tau_{9.5.8.16}$	$\tau(C''O)$

Atom numbering is given in Figure 5.1(b).

Table 5.3: 4-21G optimized parameters of citric acid and citrate trianion

Bond length(A°)		Citric acid		Bond length(A°)		Citrate trianion	
		X	OPT			X	OPT
1	2	1.298	1.354	1	2	1.245	1.259
1	3	1.070	.970	2	3	1.266	1.276
2	4	1.239	1.206	2	4	1.515	1.554
2	5	1.497	1.502	4	5	1.541	1.550
5	6	1.544	1.539	4	6	.993	1.080
5	7	.994	1.081	4	7	1.001	1.084
5	8	.931	1.084	5	8	1.442	1.440
6	9	1.407	1.421	5	9	1.532	1.547
6	10	1.532	1.524	5	10	1.555	1.570
6	11	1.535	1.516	8	16	.829	.984
9	17	.840	.970	9	13	1.518	1.562
10	14	1.508	1.501	9	14	1.008	1.084
10	15	.986	1.082	9	15	.978	1.085
10	16	.980	1.078	10	11	1.260	1.271
11	12	1.316	1.361	10	12	1.251	1.255
11	13	1.202	1.198	13	17	1.254	1.262
12	20	.922	.969	13	18	1.259	1.268
14	18	1.310	1.354			-	-
14	19	1.210	1.205			-	-
18	21	.892	.969			-	-

Table 5.4: Calculated and Experimental frequencies of Citric acid

F	U	S	IR			Raman			Dep	PED
			E1	E2	I1	E3	E4	I2		
1	44	39	-	-	.6	-	-	.6	0.7453	43(33.7),44(23.0),47(13.2)
2	49	44	-	-	2.3	-	-	1.4	0.7477	44(34.4),43(27.7)
3	76	68	-	-	.3	-	-	.3	0.7462	46(43.7),45(27.2)
4	98	88	-	-	1.2	-	-	.8	0.7396	47(40.3),46(28.6)
5	117	105	-	-	3.1	-	-	.1	0.7265	36(24.4),45(19.4),28(17.3),24(10.1)
6	156	140	-	-	.6	-	-	.5	0.7313	45(35.4),46(20.0)
7	208	187	-	-	4.8	-	-	.5	0.7248	27(19.5),24(17.4),36(13.8)
8	249	223	-	-	9.7	-	-	.7	0.5926	27(21.0),30(13.2)
9	272	245	-	-	.6	-	-	.5	0.6760	42(14.8),27(14.3),30(13.8)
10	278	255	-	-	9.2	-	-	1.2	0.2332	28(23.4),24(12.3),19(10.2)
11	351	320	-	-	1.4	-	-	.7	0.6412	25(37.9),18(18.3),26(10.4)
12	366	334	-	-	24.9	-	-	2.8	0.1900	37(14.1),31(13.2),26(10.7),18(10.1), 9(10.0)
13	397	358	-	-	6.9	-	-	.6	0.6753	37(24.2),26(14.7),25(13.6),42(11.6),34(10.1)
14	476	427	-	392(s)	218.7	383(11)	401(w)	3.4	0.7407	48(84.3)
15	526	473	-	420(w)^f	1.3	-	440(w)	1.7	0.6868	30(30.8),42(12.8)
16	538	487	-	-	12.3	-	-	3.3	0.7265	56(21.6),18(10.9)
17	556	499	-	503(w)^f	4.5	495(sh)^f	498(vw)	8.0	0.7318	41(23.0),39(17.2),57(14.4),55(11.5)
18	582	524	-	-	104.0	510(m)^f	520(w)	5.6	0.7367	57(15.5),41(12.6),55(12.2),39(10.5),30(10.3)
19	609	553	-	-	375.9	556(7)	569(w)	2.8	0.7454	56(52.7),38(11.8),19(11.4)
20	646	584	-	-	96.8	-	-	2.8	0.4772	31(29.1),26(12.7),55(11.9)
21	678	613	-	-	53.4	598(5)	595(w)	5.4	0.6294	57(27.7),38(18.2),19(16.0)
22	687	617	-	598(s)	158.8	-	-	1.3	0.6871	55(39.0),39(22.3)
23	704	646	-	645(w)^f	48.0	645(w)^f	653(w)	3.8	0.2737	57(21.3),19(19.8),41(12.6)
24	746	674	687(sh)	690(sh)^f	45.2	687(6.5)	679(w)	1.5	0.7070	40(23.6),38(11.7)
25	805	749	-	-	46.1	786(29)	782(vs)	8.3	0.0924	9(34.0)
26	878	802	-	810(w)^f	18.9	-	817(w)	1.3	0.3248	40(33.0),27(11.8)
27	908	852	-	-	8.3	-	-	1.7	0.5979	3(27.1),12(17.5),24(12.9)
28	979	920	928(w)	-	1.9	900(m)^f	903(m)	5.3	0.2550	12(17.6), 3(17.0), 7(14.4)
29	993	911	937(w)	943(m)	8.1	943(20)	943(vs)	9.8	0.0965	7(22.0),12(11.7)

Table 5.4. Continued: Calculated and Experimental frequencies of Citric acid

F	U	S	IR			Raman			Dep	PED
			E1	E2	I1	E3	E4	I2		
30	1054	944	960(w)	-	8.4	-	-	1.6	0.7496	34(37.0),22(23.4)
31	1163	1073	1044(w)	1053(m)	148.9	1053(6.5)	1058(s)	6.2	0.7462	4(18.8),10(13.5), 8(10.3)
32	1177	1085	1073(w)	1090(w)[f]	17.3	1080(s)[f]	1077(s)	5.9	0.7478	8(28.0)
33	1200	1111	-	-	234.7	-	1108(m)	2.1	0.6534	10(16.7),53(15.7),16(10.6)
34	1222	1126	-	1141(s)	508.9	1141(3.5)	-	4.0	0.6146	1(31.5),52(25.7)
35	1252	1147	-	1175(s)	170.7	-	1167(m)	6.2	0.3838	54(19.1),16(18.4)
36	1274	1166	-	1195(w)[f]	57.6	-	-	1.6	0.7458	7(25.2),42(11.3)
37	1365	1223	1207(m)	1210(w)[f]	.3	1205(s)[f]	1228(w)	16.5	0.7335	23(50.0),35(38.6)
38	1430	1294	1280(m)[a]	1280(w)[f]	10.7	-	1298(w)	.9	0.4176	21(33.0),52(24.1),29(10.2)
39	1439	1298	1280(m)[a]	1280(w)[f]	27.3	-	1298(w)	1.4	0.7321	53(25.3),33(13.3),54(10.2)
40	1468	1326	1328(m)	1325(vw)[f]	3.2	-	1319(w)	1.7	0.6968	33(26.1),35(17.2),54(15.0)
41	1476	1348	1342(m)	1350(w)[f]	44.9	1350(w)[f]	1353(w)	2.3	0.6278	23(11.3)
42	1521	1396	1407(m)	1389(s)	126.8	1389(9)	1395(w)	2.6	0.7168	21(24.9), 1(11.8), 3(11.3),19(10.2)
43	1538	1396	1407(m)	1389(s)	128.9	1389(9)	1395(w)	6.1	0.6697	29(26.0),33(24.9), 8(12.9)
44	1556	1413	-	-	4.3	-	-	.7	0.3433	21(22.4),33(19.6),29(13.9)
45	1604	1437	1430(m)	1427(s)	15.3	1425(m)[f]	1438(w)	1.5	0.7495	20(49.3),32(43.3)
46	1618	1451	1430(m)	1427(s)	50.5	1425(m)[f]	1438(w)	19.9	0.7497	32(47.8),20(43.1)
47	1932	1825	1689(m)	-	124.5	-	-	2.9	0.7321	2(75.0)
48	1944	1834	1695(m)	1695(sh)[f]	204.2	1693(11)	-	3.8	0.7207	17(76.4)
49	1980	1871	1704(vs)[a]	1706(s)	382.9	1736(10)	-	8.2	0.4844	11(75.4)
50	3243	3077	2885(s)	-	1.7	2934(21)	-	58.4	0.1405	5(87.8), 6(10.6)
51	3263	3096	2920	-	.7	2950[f]	-	70.5	0.0964	13(88.8)
52	3300	3131	2948(mbr)	-	.2	2975[f]	-	43.3	0.6040	6(88.5), 5(10.3)
53	3328	3157	-	-	.8	3000[f]	-	56.4	0.6196	14(90.2)
54	3843	3646	-	-	110.2	-	-	46.8	0.2449	15(99.0)
55	3851	3444	-	-	80.8	-	-	34.5	0.3598	49(99.0)
56	3853	3446	-	-	75.5	-	-	59.6	0.3425	51(99.5)
57	3860	3452	-	-	91.7	-	-	26.6	0.2879	50(99.6)

(f) Values read from the spectra of reference [22] F : Frequency, U : Unscaled, S : Scaled, E1 : IR frequencies from reference [9], E2 : IR frequencies from reference [22], I1 : IR intensities in units of KM/mol, E3 : Raman frequencies from reference [22], E4 : Raman frequencies of citric acid at pH 1.5 from reference [7], I2 : Raman activities in units of A^4/AMU, Dep : Raman depolarization ratios, PED : Potential energy distributions. All frequencies in units of cm^{-1}.

Table 5.5: Calculated and Experimental frequencies of Citrate trianion

F	U	S	IR			Raman					Dep	PED
			E1	E2	I1	E3	E4	E5	E6	I2		
1	44	39	-	-	1.1	-	-	-	-	1.1	0.7493	44(57.0),38(12.1)
2	60	53	-	-	1.1	-	-	-	-	1.3	0.7472	43(56.3),48(22.2)
3	77	69	-	-	2.4	-	-	-	-	1.3	0.7495	45(41.3),47(19.8)
4	88	78	-	-	.8	-	-	-	-	.4	0.7343	46(57.1),48(21.8)
5	108	97	-	-	7.8	-	-	-	-	.4	0.6497	47(49.4),36(19.3)
6	158	142	-	-	14.1	-	-	-	-	.5	0.6839	27(29.5),36(14.8),46(11.3)
7	239	214	-	-	1.1	-	-	-	-	.8	0.6040	28(31.0),24(14.3),26(11.6)
8	253	229	-	-	3.0	-	-	-	-	1.2	0.1850	46(25.3),36(13.9),27(13.5)
9	298	267	-	-	6.1	-	-	-	-	1.3	0.6377	42(31.4),31(21.6)
10	323	292	-	-	16.7	-	-	-	-	1.7	0.2907	24(26.0),38(15.2),28(14.8),19(14.5)
11	360	327	-	-	8.7	-	-	-	-	2.3	0.2274	26(28.9),46(13.6), 9(13.3)
12	396	360	-	-	2.5	-	-	-	-	4.1	0.2543	19(46.0), 4(12.5)
13	403	362	-	-	16.0	-	-	-	-	1.4	0.6117	25(37.5),38(23.0)
14	543	493	-	-	11.4	-	-	-	-	1.5	0.7303	31(28.9),42(12.0), 9(10.8)
15	583	526	-	-	28.4	-	546(w)	544(w)	542(w)	4.2	0.6952	25(19.3),19(11.9)
16	619	560	-	-	35.7	-	-	576(w)	-	2.4	0.1241	39(28.3),22(18.3)
17	645	585	-	-	39.4	-	597(w)	-	-	3.1	0.5074	41(32.0),12(11.3),34(10.5)
18	709	644	-	-	29.4	-	676(w)	-	-	1.6	0.6547	37(14.6),30(10.7)
19	795	715	737(kink)	727(vvw)	10.3	-	729(w)	-	-	2.3	0.7214	39(21.7),18(20.9),24(15.8)
20	837	752	756(s)	751(vvw)	83.7	-	-	-	-	2.5	0.5888	48(20.7),18(12.9),41(10.1)
21	839	755	761(s)	-	143.9	-	-	-	-	2.3	0.6000	48(54.3),37(16.9)
22	861	781	-	-	32.0	-	-	800(s)	805(w)	7.1	0.0819	40(18.4),48(16.4),30(12.7)
23	883	808	-	-	43.7	-	-	-	-	3.9	0.3800	30(24.0),40(12.5)
24	942	871	-	-	15.4	842(m)	839(s)	841(s)	840(s)	6.6	0.1088	3(25.1),18(13.3),24(11.4)
25	945	877	846(s)	844(w)	45.4	-	-	-	-	.7	0.2655	3(11.4),12(11.4)
26	994	917	948(msh)	924	6.5	968(s)	943(s)	954(s)	954(s)	10.2	0.7319	7(16.0),22(13.6),12(11.8)
27	1027	932	956(msh)	976(wbr)	.2	-	-	-	-	3.4	0.4779	34(31.4),41(16.3), 4(12.3)
28	1152	1051	1062(w)	1076(kink)	17.5	1069(w)	1064(w)	1042(w)	1042(w)	4.6	0.7322	8(28.7),22(16.2)
29	1179	1079	1085(w)	1095(m)	25.4	1084(w)	1082(w)	1095(w)	1092(w)	4.3	0.7148	4(19.3),22(18.6)

Table 5.5. Continued: Calculated and Experimental frequencies of Citrate trianion

F	U	S	IR			Raman					Dep	PED
			E1	E2	I1	E3	E4	E5	E6	I2		
30	1218	1120	1155(wsh)	1144(vvw)	52.6	1140(w)	1156(w)	-	-	4.6	0.6335	7(29.2),42(12.9),35(10.2)
31	1345	1213	1193(w)	-	32.9	1206(w)	-	1214(vw)	1211(w)	12.4	0.7170	23(30.4),35(25.5),33(11.8)
32	1390	1258	1270(m)	-	129.8	1267(vw)	1272(w)	1264(vw)	1260(vw)	3.4	0.4451	35(22.8),23(20.9),33(12.0)
33	1427	1290	1304(m)	-	75.9	-	1290(w)	-	-	1.0	0.7467	21(34.3), 1(19.7),10(12.9)
34	1433	1300	1304(m)	-	81.2	1299(w)	1308(w)	1302(vw)	1296(vw)	4.5	0.3906	16(38.0),33(27.6),37(10.5)
35	1447	1357	1325(m)	-	465.3	-	-	-	-	4.7	0.6840	16(24.5),10(16.6),33(15.8)
36	1457	1361	1333(m)	1333(m)	294.4	-	-	-	-	4.8	0.3305	1(35.7), 3(13.1),18(11.0)
37	1488	1386	-	1399(w)	13.7	-	1391(w)	-	-	4.9	0.3514	10(25.7), 9(12.3),21(11.3)
38	1631	1459	1418(w)	-	23.6	1408(vs)	1406(w)	-	-	13.4	0.7479	32(92.6)
39	1638	1468	1439(s)	1435(s)	140.7	1430(ms)	1431(m)	-	-	9.6	0.7485	20(83.1)
40	1651	1491	1490(kink)	1481(s)	381.3	1476(w)	1440(s)	-	-	6.8	0.5882	29(65.0), 2(14.7)
41	1761	1668	1587(m)	1580(w)	307.2	1589(w)	1585(w)	-	-	1.5	0.3043	11(51.7),17(28.5)
42	1766	1661	1603(s)	1605(s)	500.7	-	1604(w)	-	-	.2	0.5575	17(51.8),11(31.2)
43	1779	1657	1603(s)	1605(s)	214.3	-	1604(w)	-	-	1.5	0.6650	2(59.0),29(17.3)
44	3205	3041	2882(s)	2882(sbr)	53.8	-	-	-	-	75.9	0.1226	13(98.6)
45	3240	3074	-	-	6.3	-	-	-	-	57.9	0.1524	5(60.6),14(33.5)
46	3242	3076	2941(s)	2941(sbr)	57.6	-	-	-	-	64.6	0.4450	14(65.1), 5(29.7)
47	3299	3130	-	-	18.7	-	-	-	-	42.8	0.6740	6(90.9)
48	3516	3335	3030(s)	-	377.0	-	-	-	-	50.3	0.2728	15(99.8)

F : Frequency, U : Unscaled, S : Scaled, E1 : IR frequencies of sodium citrate from reference [15], E2 : IR frequencies of ammonium citrate from reference [15], I1 : IR intensities in units of KM/mol E3 : Raman frequencies of sodium citrate from reference [14], E4 : Raman frequencies of solid sodium citrate from reference [7],E5 : Raman frequencies of aqueous sodium citrate from reference [7], E6 : Raman frequencies of citric acid at pH 7.5, I2 : Raman activities in units of A^4/AMU, Dep : Raman depolarization ratios, PED : Potential energy distributions. All frequencies in units of cm^{-1}.

Table 5.6: Diagonal force constants of citric acid and citrate trianion

	Citric acid				Citrate trianion		
	Sym. Cor.[a]	F. Const. ($mdynes/A°$)			Sym. Cor.[a]	F. Const. ($mdynes/A°$)	
		USFI	SFI			USFI	SFI
1	$\nu(C-O)/\nu(C-O)$	7.0115	6.3103	1	$\nu_s(COO)/\nu_s(COO)$	11.5854	10.4269
2	$\nu(C=O)/\nu(C=O)$	14.5621	13.1059	2	$\nu_a(COO)/\nu_a(COO)$	8.7873	7.9085
3	$\nu(CC')/\nu(CC')$	4.8616	4.3755	3	$\nu(CC')/\nu(CC')$	3.8974	3.5077
4	$\nu(C'C'')/\nu(C'C'')$	4.6546	4.1891	4	$\nu(C'C'')/\nu(C'C'')$	4.5943	4.1348
5	$\nu_s(CH_2)/\nu_s(CH_2)$	5.9560	5.3604	5	$\nu_s(CH_2)/\nu_s(CH_2)$	5.9513	5.3562
6	$\nu_a(CH_2)/\nu_a(CH_2)$	5.8606	5.2745	6	$\nu_a(CH_2)/\nu_a(CH_2)$	5.8629	5.2766
7	$\nu(C''O)/\nu(C''O)$	6.3397	5.7058	7	$\nu(C''O)/\nu(C''O)$	5.9409	5.3468
8	$\nu(C''C)/\nu(C''C)$	4.9707	4.4736	8	$\nu(C''C)/\nu(C''C)$	4.2784	3.8505
9	$\nu(C''C')/\nu(C''C')$	4.7227	4.2505	9	$\nu(C''C')/\nu(C''C')$	3.6468	3.2821
10	$\nu(C-O)/\nu(C-O)$	6.7798	6.1018	10	$\nu_s(COO)/\nu_s(COO)$	11.8527	10.6674
11	$\nu(C=O)/\nu(C=O)$	15.2846	13.7561	11	$\nu_a(COO)/\nu_a(COO)$	9.0968	8.1871
12	$\nu(C'C)/\nu(C'C)$	4.9166	4.4249	12	$\nu(C'C)/\nu(C'C)$	3.5769	3.2192
13	$\nu_s(CH_2)/\nu_s(CH_2)$	6.0355	5.4319	13	$\nu_s(CH_2)/\nu_s(CH_2)$	5.8013	5.2212
14	$\nu_a(CH_2)/\nu_a(CH_2)$	5.9489	5.3540	14	$\nu_a(CH_2)/\nu_a(CH_2)$	5.6828	5.1145
15	$\nu(OH)/\nu(OH)$	8.2601	7.4341	15	$\nu(OH)/\nu(OH)$	6.8674	6.1807
16	$\nu(C-O)/\nu(C-O)$	7.0155	6.3139	16	$\nu_s(COO)/\nu_s(COO)$	11.7462	10.5716
17	$\nu(C=O)/\nu(C=O)$	14.7783	13.3004	17	$\nu_a(COO)/\nu_a(COO)$	8.9568	8.0612
18	$\delta(C-O)/\delta(C-O)$	1.1822	1.0640	18	$\delta(COO)/\delta(COO)$	1.7936	1.4349
19	$\delta(C=O)/\delta(C=O)$	1.4376	1.2939	19	$\rho(COO)/\rho(COO)$	1.5100	1.2080
20	$\delta(CH_2)/\delta(CH_2)$	0.6955	0.5564	20	$\delta(CH_2)/\delta(CH_2)$	0.7427	0.5942
21	$\omega(CH_2)/\omega(CH_2)$	0.7966	0.6373	21	$\omega(CH_2)/\omega(CH_2)$	0.7373	0.5899
22	$\rho(CH_2)/\rho(CH_2)$	0.8865	0.7092	22	$\rho(CH_2)/\rho(CH_2)$	1.1808	0.9447
23	$t(CH_2)/t(CH_2)$	0.7990	0.6392	23	$t(CH_2)/t(CH_2)$	0.7674	0.6139
24	$\delta(CC'C'')/\delta(CC'C'')$	1.8650	1.4920	24	$\delta(CC'C'')/\delta(CC'C'')$	2.6212	2.0970
25	$\delta(OC''C)/\delta(OC''C)$	1.4816	1.1853	25	$\delta(OC''C)/\delta(OC''C)$	1.9964	1.5971
26	$\rho(OC''C)/\rho(OC''C)$	1.4028	1.1222	26	$\rho(OC''C)/\rho(OC''C)$	1.4020	1.1216
27	$\delta(C'C''C)/\delta(C'C''C)$	1.6751	1.3401	27	$\delta(C'C''C)/\delta(C'C''C)$	1.3875	1.1100
28	$\rho(C'C''C)/\rho(C'C''C)$	1.4502	1.1602	28	$\rho(C'C''C)/\rho(C'C''C)$	1.7493	1.3994
29	$\delta(C''OH)/\delta(C''OH)$	1.0513	0.8410	29	$\delta(C''OH)/\delta(C''OH)$	1.4796	1.1837
30	$\delta(C-O)/\delta(C-O)$	1.3271	1.0617	30	$\delta(COO)/\delta(COO)$	1.6670	1.3336

Table 5.6. Continued: Diagonal force constants of citric acid and citrate trianion

	Citric acid				Citrate trianion		
	Sym. Cor.[a]	F. Const. ($mdynes/A°$)			Sym. Cor.[a]	F. Const. ($mdynes/A°$)	
		USFI	SFI			USFI	SFI
31	$\delta(C=O)/\delta(C=O)$	1.2395	0.9916	31	$\rho(COO)/\rho(COO)$	1.2652	1.0122
32	$\delta(CH_2)/\delta(CH_2)$	0.6806	0.5445	32	$\delta(CH_2)/\delta(CH_2)$	0.7578	0.6063
33	$\omega(CH_2)/\omega(CH_2)$	0.8218	0.6574	33	$\omega(CH_2)/\omega(CH_2)$	0.6974	0.5579
34	$\rho(CH_2)/\rho(CH_2)$	0.8621	0.6897	34	$\rho(CH_2)/\rho(CH_2)$	1.1016	0.8813
35	$t(CH_2)/t(CH_2)$	0.8350	0.6680	35	$t(CH_2)/t(CH_2)$	0.7212	0.5770
36	$\delta(CC'C'')/\delta(CC'C'')$	1.6649	1.3319	36	$\delta(CC'C''')/\delta(CC'C'')$	1.4053	1.1242
37	$\delta(C-O)/\delta(C-O)$	1.1778	0.9422	37	$\delta(COO)/\delta(COO)$	1.7076	1.3660
38	$\delta(C=O)/\delta(C=O)$	1.3716	1.0973	38	$\rho(COO)/\rho(COO)$	1.2815	1.0252
39	$\gamma(COO)/\gamma(COO)$	0.5532	0.4426	39	$\gamma(COO)/\gamma(COO)$	0.8153	0.6523
40	$\gamma(COO)/\gamma(COO)$	0.5818	0.4655	40	$\gamma(COO)/\gamma(COO)$	0.7847	0.6277
41	$\gamma(COO)/\gamma(COO)$	0.5531	0.4425	41	$\gamma(COO)/\gamma(COO)$	0.8427	0.6742
42	$\delta(C'C''C')/\delta(C'C''C')$	1.5153	1.2123	42	$\delta(C'C'''C')/\delta(C'C''C')$	1.8482	1.4785
43	$\tau(CC')/\tau(CC')$	0.0220	0.0176	43	$\tau(CC')/\tau(CC')$	0.0411	0.0329
44	$\tau(CC')/\tau(CC')$	0.0201	0.0161	44	$\tau(CC')/\tau(CC')$	0.0143	0.0114
45	$\tau(CC'')/\tau(CC'')$	0.0619	0.0495	45	$\tau(CC'')/\tau(CC'')$	0.0338	0.0270
46	$\tau(C'C'')/\tau(C'C'')$	0.1644	0.1315	46	$\tau(C'C'')/\tau(C'C'')$	0.3421	0.2737
47	$\tau(C'C'')/\tau(C'C'')$	0.1352	0.1082	47	$\tau(C'C'')/\tau(C'C'')$	0.1423	0.1139
48	$\tau(C''O)/\tau(C''O)$	0.0342	0.0274	48	$\tau(C''O)/\tau(C''O)$	0.1227	0.0982
49	$\nu(OH)/\nu(OH)$	8.2959	6.6367	-	-	-	-
50	$\nu(OH)/\nu(OH)$	8.3330	6.6664	-	-	-	-
51	$\nu(OH)/\nu(OH)$	8.3059	6.6447	-	-	-	-
52	$\delta(COH)/\delta(COH)$	0.8636	0.6909	-	-	-	-
53	$\delta(COH)/\delta(COH)$	0.8530	0.6824	-	-	-	-
54	$\delta(COH)/\delta(COH)$	0.8707	0.6965	-	-	-	-
55	$\tau(CO)/\tau(CO)$	0.0870	0.0696	-	-	-	-
56	$\tau(CO)/\tau(CO)$	0.0782	0.0625	-	-	-	-
57	$\tau(CO)/\tau(CO)$	0.0882	0.0706	-	-	-	-

(a) Symmetry Coordinate descriptions given in Tables 5.1 and 5.2.

Table 5.7: Absolute and relative energies of Citric, Difluorocitric, Monofluorocitric and Monohydroxycitric acids after the various levels of optimization

System	AM1[a]	ΔE^a	STO-3G[b]	ΔE^a	3-21G[b]	ΔE^a	6-31G*/3-21G[b]	ΔE^a
Citric	-1378.1931	0.0	-745.9697	0.0	-751.7434	0.0	-755.9533	0.0
Difluorocitric								
I(3S)	-1706.7462	1.3814	-940.8720	11.0521	-948.3856	0.0013	-953.6511	0.0
II(3R)	-1708.1276	0.0	-940.8728	0.0	-948.3856	0.0	-953.6511	0.1668
Monofluorocitric								
I(2R,3S)	-1533.6329	4.5097	-843.4129	2.5696	-850.0512	8.4649	-854.7939	0.6429
II(2S,3S)	-1532.6262	5.5164	-843.4127	3.0311	-850.0545	0.0006	-854.7941	0.1277
III(2S,3R)	-1531.9688	6.1738	-843.4131	1.8791	-850.0501	11.3478	-854.7907	8.9575
IV(2R,3R)	-1538.1426	0.0	-843.4138	0.0	-850.0545	0.0	-854.7941	0.0
Monohydroxycitric								
I(2R,3R)	-1533.7768	29.1562	-819.7922	18.3636	-826.1795	10.5527	-830.7987	6.4616
II(2S,3R)	-1542.0057	20.9273	-819.7992	0.0	-826.1835	0.0010	-830.8012	0.0
III(2S,3S)	-1538.6833	24.2498	-819.7948	11.5183	-826.1795	10.5522	-830.7987	6.4553
IV(2R,3S)	-1562.9330	0.0	-819.7992	0.0049	-826.1835	0.0	-830.8011	0.7610

(a) The AM1 energies and the the relative energies are in units of kJ/mol. (b) The energies at the STO-3G, 3-21G and 6-31G* levels are in units of hartrees. The levels shown indicate that the energies are of the optimized structures optimized at that level. In case of 6-31G* energies the energies have been calculated on the 3-21G optimized structures.

Table 5.8: 3-21G optimized parameters of citric acid and two isomers of difluorocitric acid

Bond length(A^o)		Citric acid		Difluorocitric acid	
		X	OPT	I(3R)	II(3S)
1	2	1.298	1.350	1.345	1.345
1	3	1.070	.969	.969	.969
2	4	1.239	1.205	1.191	1.191
2	5	1.497	1.500	1.511	1.511
5	6	1.544	1.537	1.533	1.533
5	7	.994	1.081	1.367	1.367
5	8	.931	1.084	1.366	1.366
6	9	1.407	1.418	1.418	1.418
6	10	1.532	1.522	1.513	1.513
6	11	1.535	1.514	1.514	1.514
9	17	.840	.970	.972	.972
10	14	1.508	1.499	1.494	1.494
10	15	.986	1.082	1.079	1.079
10	16	.980	1.078	1.077	1.077
11	12	1.316	1.358	1.337	1.337
11	13	1.202	1.196	1.199	1.198
12	20	.922	.969	.969	.969
14	18	1.310	1.350	1.346	1.346
14	19	1.210	1.203	1.205	1.205
18	21	.892	.969	.969	.969

Table 5.8. Continued: 3-21G optimized parameters of citric acid and two isomers of difluorocitric acid

Bond angle(°)			Citric acid		Difluorocitric acid	
			X	OPT	I(3R)	II(3S)
2	4	17	99.839	102.032	63.498	63.470
4	17	9	114.549	117.643	52.997	52.916
2	1	3	114.385	112.267	113.116	113.110
1	2	4	123.414	122.466	125.301	125.290
1	2	5	114.106	110.603	108.544	108.536
4	2	5	122.479	126.930	126.153	126.171
2	5	6	116.188	112.324	109.851	109.846
2	5	7	108.898	108.965	108.186	108.167
2	5	8	104.653	106.924	109.941	109.960
6	5	7	111.215	110.610	109.668	109.652
6	5	8	109.061	109.788	111.108	111.130
7	5	8	106.180	108.075	108.020	108.018
5	6	9	112.061	112.385	107.059	107.028
5	6	10	107.854	109.337	110.085	110.103
5	6	11	109.794	108.127	108.016	108.024
9	6	10	106.375	106.422	110.623	110.622
9	6	11	109.910	109.715	108.283	108.274
10	6	11	110.789	110.876	112.581	112.593
6	9	17	105.776	109.685	110.007	110.000
6	10	14	112.024	110.787	109.930	109.942
6	10	15	111.905	110.322	109.941	109.934
6	10	16	109.380	109.205	109.415	109.434
14	10	15	106.857	108.297	108.946	108.940
14	10	16	108.519	108.450	109.614	109.610
15	10	16	108.009	109.749	108.978	108.964
6	11	12	112.478	109.734	111.258	111.249
6	11	13	123.063	126.616	123.285	123.296
12	11	13	124.456	123.492	125.409	125.409
11	12	20	110.998	112.117	113.341	113.360
10	14	18	111.402	111.374	111.642	111.638
10	14	19	125.686	125.809	125.351	125.357
18	14	19	122.912	122.755	122.967	122.964
14	18	21	106.889	112.089	112.338	112.357

Table 5.8. Continued: 3-21G optimized parameters of citric acid and two isomers of difluorocitric acid

Dihedral angle(°)				Citric acid		Difluorocitric acid	
				X	OPT	I(3R)	II(3S)
3	1	2	4	-.230	.480	3.951	-4.176
3	1	2	5	-179.835	-179.107	-176.557	176.384
1	2	5	6	-172.154	-178.156	69.688	-69.705
1	2	5	7	-45.670	-55.235	-170.625	170.643
1	2	5	8	67.531	61.348	-52.878	52.898
4	2	5	6	8.237	2.280	-110.824	110.862
4	2	5	7	134.721	125.201	8.862	-8.791
4	2	5	8	-112.079	-118.216	126.609	-126.535
2	5	6	9	-57.935	-50.060	27.688	-27.723
2	5	6	10	-174.686	-168.000	-92.609	92.564
2	5	6	11	64.503	71.186	144.103	-144.116
7	5	6	9	176.750	-172.050	-91.090	91.019
7	5	6	10	59.999	70.010	148.613	-148.694
7	5	6	11	-60.813	-50.804	25.325	-25.374
5	6	9	17	85.114	75.086	111.184	-111.262
5	6	10	14	171.130	-174.817	-178.889	178.898
5	6	10	15	-68.883	-54.905	-58.960	58.973
5	6	10	16	50.766	65.797	60.688	-60.665
5	6	11	12	67.982	67.739	72.123	-72.166
5	6	11	13	-111.395	-107.779	-105.482	105.467
6	10	14	18	-129.568	-150.562	-159.144	159.315
6	10	14	19	50.420	32.253	23.092	-22.949
6	11	12	20	-179.972	177.403	-178.349	178.396
10	14	18	21	175.729	-178.734	-177.890	177.920

X : X-Ray parameters of citric acid from reference [16].

Table 5.9: 3-21G optimized parameters of four isomers of monofluorocitric acid

Bond length(A°)					
		I(2R,3S)	II(2S,3S)	III(2S,3R)	IV(2R,3R)
1	2	1.350	1.333	1.343	1.333
1	3	.969	.969	.969	.969
2	4	1.196	1.203	1.199	1.203
2	5	1.507	1.503	1.509	1.503
5	6	1.534	1.527	1.518	1.527
5	7	1.391	1.390	1.397	1.390
5	8	1.076	1.076	1.076	1.076
6	9	1.417	1.415	1.415	1.415
6	10	1.517	1.532	1.533	1.532
6	11	1.516	1.510	1.513	1.510
9	17	.971	.970	.970	.970
10	14	1.496	1.498	1.498	1.498
10	15	1.080	1.080	1.078	1.082
10	16	1.081	1.082	1.084	1.080
11	12	1.334	1.357	1.352	1.358
11	13	1.202	1.194	1.196	1.194
12	20	.968	.969	.968	.969
14	18	1.347	1.347	1.349	1.346
14	19	1.204	1.206	1.206	1.207
18	21	.969	.969	.969	.969

Table 5.9. Continued: 3-21G optimized parameters of four isomers of monofluorocitric acid

Bond angle(°)			I(2R,3S)	II(2S,3S)	III(2S,3R)	IV(2R,3R)
2	4	17	68.262	69.307	83.404	69.314
4	17	9	69.445	43.081	49.422	43.043
2	1	3	112.837	112.276	112.854	112.273
1	2	4	124.142	124.789	123.865	124.790
1	2	5	110.083	114.116	110.127	114.101
4	2	5	125.762	121.068	126.008	121.082
2	5	6	110.947	108.042	113.170	108.044
2	5	7	110.119	111.104	108.708	111.120
2	5	8	108.114	109.238	107.974	109.231
6	5	7	109.274	109.333	111.108	109.341
6	5	8	107.603	109.613	106.840	109.586
7	5	8	110.753	109.486	108.907	109.494
5	6	9	105.865	106.145	103.855	106.121
5	6	10	109.167	109.239	108.288	109.254
5	6	11	110.513	109.033	113.184	109.038
9	6	10	111.210	112.866	113.471	112.881
9	6	11	108.637	109.713	109.826	109.704
10	6	11	111.314	109.729	108.268	109.727
6	9	17	110.064	109.821	109.626	109.814
6	10	14	110.264	111.617	111.736	111.637
6	10	15	109.745	110.959	110.261	108.338
6	10	16	109.937	108.357	109.996	110.959
14	10	15	109.438	109.194	110.112	108.126
14	10	16	108.269	108.130	107.061	109.197
15	10	16	109.159	108.488	107.539	108.487
6	11	12	112.496	109.787	109.656	109.790
6	11	13	122.477	126.506	126.069	126.522
12	11	13	125.017	123.621	124.112	123.603
11	12	20	113.004	112.469	112.580	112.474
10	14	18	111.431	110.928	110.784	110.944
10	14	19	125.582	126.438	126.709	126.437
18	14	19	122.972	122.632	122.502	122.617
14	18	21	112.405	112.495	112.332	112.500

Table 5.9. Continued: 3-21G optimized parameters of four isomers of monofluorocitric acid

Dihedral angle(°)							
				I(2R,3S)	II(2S,3S)	III(2S,3R)	IV(2R,3R)
3	1	2	4	-2.108	4.067	2.294	-4.017
3	1	2	5	176.647	-177.842	-177.889	177.879
1	2	5	6	-81.106	121.640	-171.221	-121.677
1	2	5	7	40.001	1.711	64.826	-1.727
1	2	5	8	161.124	-119.179	-53.178	119.178
4	2	5	6	97.624	-60.190	8.591	60.142
4	2	5	7	-141.269	179.880	-115.362	-179.909
4	2	5	8	-20.146	58.990	126.634	-59.004
2	5	6	9	-64.694	-47.840	78.068	47.858
2	5	6	10	175.506	-169.811	-161.031	169.841
2	5	6	11	52.760	70.281	-40.986	-70.241
7	5	6	9	173.702	73.197	-159.303	-73.204
7	5	6	10	53.903	-48.774	-38.402	48.779
7	5	6	11	-68.843	-168.682	81.643	168.697
5	6	9	17	118.006	170.550	-168.422	-170.612
5	6	10	14	-178.917	169.027	-165.668	-169.055
5	6	10	15	-58.292	-68.935	71.530	-50.103
5	6	10	16	61.782	50.070	-46.905	68.889
5	6	11	12	78.200	54.387	-52.111	-54.414
5	6	11	13	-100.703	-128.898	132.392	128.881
6	10	14	18	-163.766	175.464	-176.444	-175.470
6	10	14	19	17.661	-5.020	4.351	5.048
6	11	12	20	-178.023	-177.780	177.327	177.798
10	14	18	21	-178.722	178.576	-178.930	-178.506

Table 5.10: 3-21G optimized parameters of four isomers of monohydroxycitric acid

Bond length($A°$)					
		I(2R,3R)	II(2S,3R)	III(2S,3S)	IV(2R,3S)
1	2	1.340	1.345	1.340	1.345
1	3	.969	.969	.969	.969
2	4	1.205	1.202	1.205	1.202
2	5	1.511	1.511	1.511	1.511
5	6	1.530	1.534	1.530	1.534
5	7	1.426	1.417	1.426	1.417
5	8	1.073	1.076	1.073	1.076
6	9	1.416	1.420	1.416	1.420
6	10	1.532	1.531	1.532	1.531
6	11	1.516	1.508	1.516	1.508
9	17	.970	.970	.970	.970
10	14	1.499	1.498	1.498	1.498
10	15	1.078	1.082	1.078	1.082
10	16	1.084	1.080	1.084	1.080
11	12	1.367	1.357	1.367	1.357
11	13	1.193	1.196	1.193	1.196
12	20	.970	.969	.970	.969
14	18	1.347	1.347	1.347	1.347
14	19	1.207	1.208	1.207	1.208
18	21	.969	.969	.969	.969
7	22	.970	.968	.970	.968

Table 5.10. Continued: 3-21G optimized parameters of four isomers of monohydroxycitric acid

Bond angle(°)						
			I(2R,3R)	II(2S,3R)	III(2S,3S)	IV(2R,3S)
2	4	17	67.104	62.206	67.102	62.179
4	17	9	45.941	40.663	46.010	40.494
2	1	3	112.552	112.563	112.566	112.570
1	2	4	123.455	123.829	123.452	123.833
1	2	5	112.858	112.549	112.850	112.523
4	2	5	123.640	123.616	123.652	123.637
2	5	6	109.017	106.464	109.020	106.446
2	5	7	110.291	112.318	110.291	112.309
2	5	8	108.716	109.328	108.735	109.329
6	5	7	112.496	109.991	112.488	109.999
6	5	8	108.018	109.897	108.003	109.898
7	5	8	108.207	108.812	108.210	108.829
5	6	9	104.335	104.148	104.333	104.172
5	6	10	109.210	109.479	109.206	109.480
5	6	11	111.613	110.473	111.614	110.448
9	6	10	113.574	113.050	113.554	113.058
9	6	11	108.997	110.074	109.019	110.060
10	6	11	109.085	109.512	109.088	109.517
6	9	17	109.914	109.949	109.928	109.936
6	10	14	111.652	111.775	111.658	111.787
6	10	15	110.838	108.056	110.864	108.035
6	10	16	109.471	110.729	109.451	110.729
14	10	15	109.977	108.577	109.984	108.579
14	10	16	107.277	109.234	107.263	109.246
15	10	16	107.471	108.379	107.465	108.373
6	11	12	110.334	109.476	110.336	109.479
6	11	13	126.864	126.863	126.855	126.869
12	11	13	122.715	123.594	122.723	123.583
11	12	20	112.043	112.414	112.051	112.417
10	14	18	111.186	111.216	111.172	111.223
10	14	19	126.239	126.456	126.256	126.447
18	14	19	122.570	122.325	122.568	122.326
14	18	21	112.458	112.415	112.456	112.416
5	7	22	108.996	109.020	108.984	109.021

Table 5.10. Continued: 3-21G optimized parameters of four isomers of monohydroxycitric acid

Dihedral angle(°)							
				I(2R,3R)	II(2S,3R)	III(2S,3S)	IV(2R,3S)
3	1	2	4	1.260	2.897	-1.229	-2.933
3	1	2	5	178.850	-176.216	-178.815	176.150
1	2	5	6	128.660	114.155	-128.669	-114.080
1	2	5	7	-107.359	-6.288	107.358	6.356
1	2	5	8	11.130	-127.177	-11.146	127.261
4	2	5	6	-53.756	-64.961	53.750	65.006
4	2	5	7	70.225	174.597	-70.223	-174.558
4	2	5	8	-171.286	53.707	171.274	-53.653
2	5	6	9	-62.756	-54.480	62.794	54.377
2	5	6	10	175.497	-175.642	-175.486	175.562
2	5	6	11	54.801	63.680	-54.788	-63.769
7	5	6	9	174.577	67.450	-174.542	-67.537
7	5	6	10	52.830	-53.711	-52.822	53.649
7	5	6	11	-67.866	-174.390	67.875	174.318
5	6	9	17	170.682	175.650	-170.588	-175.855
5	6	10	14	168.100	165.785	-168.066	-165.820
5	6	10	15	-68.916	46.375	68.919	-46.413
5	6	10	16	49.462	-72.178	-49.455	72.120
5	6	11	12	55.472	56.349	-55.435	-56.328
5	6	11	13	-127.876	-126.585	127.908	126.621
6	10	14	18	175.955	173.300	-175.955	-173.194
6	10	14	19	-4.833	-7.379	4.798	7.506
6	11	12	20	-176.487	-176.293	176.517	176.355
10	14	18	21	178.517	178.630	-178.579	-178.630
2	5	7	22	-69.646	39.874	69.665	-39.536
6	5	7	22	52.301	-78.507	-52.280	78.824

Table 5.11: Mulliken charges of citric acid, diflurocitric acid, monofluorocitric acid and monohydroxycitric acid

No.	A	Citric		Difluoro (3R)		Monofluoro (2S,3R)		(2R,3R)		Monohydroxy (2S,3S)		(2R,3S)
1	O	-0.716721	O	-0.716996	O	-0.712216	O	-0.695999	O	-0.710270	O	-0.720035
2	C	0.894662	C	0.876123	C	0.881024	C	0.891224	C	0.917457	C	0.902591
3	H	0.419649	H	0.435153	H	0.425634	H	0.424814	H	0.419883	H	0.427987
4	O	-0.609306	O	-0.560404	O	-0.584797	O	-0.609333	O	-0.620118	O	-0.607611
5	C	-0.529237	C	0.788054	C	0.175179	C	0.156395	C	0.041718	C	0.045904
6	C	0.122361	C	0.002718	C	0.047275	C	0.064504	C	0.074646	C	0.091520
7	H	0.292284	F	-0.382804	F	-0.374829	F	-0.383214	O	-0.688276	O	-0.683850
8	H	0.289942	F	-0.373906	H	0.296273	H	0.293372	H	0.305280	H	0.305012
9	O	-0.703541	O	-0.706345	O	-0.704694	O	-0.699898	O	-0.705222	O	-0.717534
10	C	-0.492375	C	-0.516692	C	-0.527827	C	-0.537320	C	-0.519518	C	-0.541348
11	C	0.931238	C	0.970719	C	0.934803	C	0.930473	C	0.930551	C	0.926298
12	O	-0.734262	O	-0.722384	O	-0.727273	O	-0.732363	O	-0.744190	O	-0.729903
13	O	-0.588737	O	-0.598864	O	-0.586204	O	-0.575861	O	-0.575182	O	-0.583082
14	C	0.911537	C	0.910641	C	0.896317	C	0.899828	C	0.895231	C	0.898285
15	H	0.284972	H	0.312961	H	0.314669	H	0.325599	H	0.302977	H	0.326562
16	H	0.287996	H	0.325118	H	0.295343	H	0.294066	H	0.299846	H	0.295954
17	H	0.425898	H	0.434437	H	0.433822	H	0.432857	H	0.430625	H	0.434144
18	O	-0.718874	O	-0.717502	O	-0.715097	O	-0.714304	O	-0.714479	O	-0.713528
19	O	-0.607235	O	-0.615162	O	-0.612972	O	-0.616432	O	-0.616647	O	-0.622989
20	H	0.423440	H	0.435759	H	0.425167	H	0.429007	H	0.433650	H	0.426523
21	H	0.416310	H	0.419375	H	0.420402	H	0.422585	H	0.421420	H	0.420941
22	-	-	-	-	-	-	-	-	H	0.420618	H	0.418160

5.4 References

[1] L. Passerini, Gazz. Chim. Ital., 65 (1935) 502.

[2] C. Duval, Anal. Chim. Acta, 13 (1955) 427.

[3] H. Nisi, Jpn. J. Phys., 7 (1931) 1.

[4] V. N. Thatte and W. Askhedar, Z. Phys., 100 (1936) 146.

[5] S. Canal and P. Peyrot, C. R. Acad. Sci., 206 (1936) 1179.

[6] D. Hazdi, Pure Appl. Chem., 11 (1965) 435.

[7] R. I. Bickley, H. G. M. Edwards, R. Gustar and S. J. Rose, J. Mol. Str., 210 (1991) 229.

[8] J. T. Edsall, J. Chem. Phys., 5 (1937) 508.

[9] K. M. Rao and N. Swamy, Indian J. Phys., 44 (1970) 34-38.

[10] V. Anantanarayanan, Spectrochim. Acta, 20 (1964) 210.

[11] R. Tabeta and H. Saito, Chem. Lett., (1984) 293-96.

[12] S. F. Dec, C. E. Bronniman, R. A. Wind and G. E. Maciel, J. Magn. Reson., 82 (1989) 454-66.

[13] R. Marignan, Bull. Soc. Chim. Fr., (1948) 315.

[14] T. S. Krishnan, J. Indian Inst. Sci., 36 (1954) 101-103.

[15] K. M. Rao and N. Swamy, Indian J. Phys., 45 (1971) 455-460.

[16] J. P. Glusker, J. A. Minkin and A. L. Patterson, Acta Crystallogr., 25B (1969) 1066.

[17] D. M. Burns and J. Iball, Acta Crystallogr., 7 (1954) 137.

[18] C. E. Nordman, A. S. Weldon and A. L. Patterson, Acta Crystallogr., 13 (1960) 418.

[19] C. K. Johnson, Acta Crystallogr., 18 (1965) 1004.

[20] J. P. Glusker, D. van der Helm, W. E. Love, M. L. Dornberg, J. A. Minkin, C. K. Johnson and A. L. Patterson, Acta Crystallogr., 19 (1965) 561.

[21] (a)J. Simons, Ann. Rev. Phys. Chem., 28 (1977) 17. (b)J. Simons, Chem. Rev., 87 (1987) 535.

[22] B. Schrader, *Raman/Infrared Atlas of Organic Compounds*, VCH Publishers, Weinheim, 1989.

[23] R. W. Williams and A. H. Lowrey, J. Comput. Chem., 12 (1991) 761-77.

[24] J. Nieminen, M. Räsänen and J. Murto, J. Phys. Chem., 96 (1992) 5303.

[25] H. Hollenstein, T. K. Ha and H. H. Günthard, J. Mol. Str., 146 (1986) 289-307.

[26] L. D. Barron. A. R. Gargaro, L. Hecht, P. L. Polavarapu and H. Sugeta, Spectrochim. Acta, 48A (1992) 1051-66.

[27] M. Suzuki and T. Shimanouchi, J. Mol. Spectrosc., 28 (1968) 394-410.

[28] M. Suzuki and T. Shimanouchi, J. Mol. Spectrosc., 29 (1969) 415-25.

[29] K. G. Kidd and H. M. Mantisch, J. Mol. Spectrosc., 85 (1981) 375-389.

[30] M. Kakihana, M. Kotaka and M. Okamoto, J. Phys. Chem., 87 (1983) 2526-35.

[31] A. Kanters, J. Kroon, A. F. Peerdeman and J. A. Vliegenthalt, Nature, 222 (1969) 370-1.

[32] (a) W. P. Pijper, Acta Crystallogr., 27B (1971) 344-48. (b) R. D. Ellison, C. K. Johnson and H. A. Levy, Acta Crystallogr., 27B (1971) 333-44.

[33] J. de Villepin and A. Novak, Spectrochim. Acta, 34A (1978) 1009, 1019.

[34] L. J. Bellamy, *The Infrared Spectra of Complex Molecules*, Metheun and Co. Ltd., London, 1958.

[35] J. L. Delarbre, E. Fabrègue, L. Maury and E. Baudet, J. Raman Spectrosc., 19 (1988) 167-74.

[36] J. de Villepin and A. Novak, Spectrochim. Acta, 27A (1971) 1259-70.

[37] C. Walsh, *Enzymatic Reaction Mechanisms*, W. H. Freeman and Company, San Francisco, 1979.

[38] R. H. Abeles and T. A. Alston, J. Biol. Chem., 265 (1990) 16705.

[39] R. Peters, Endeavour, 13 (1954) 147.

[40] A. C. Sullivan, J. Triscari, J. G. Hamilton, O. Miller and V. R. Wheatley, Lipids, 9 (1973) 121.

[41] W. L. Alworth, *Stereochemistry and its Applications in Biochemistry*, pp123-126, Wiley, New York, 1972.

[42] P. A. Srere and A. Bhaduri, J. Biol. Chem., 239 (1964) 714.

[43] S. Englard, J. Biol. Chem., 235 (1960) 1510.

[44] B. A. Saxty, R. Novelli, R. E. Dolle, L. I. Kruse, D. G. Reid, P. Camilleri and T. N. C. Wells, Eur. J. Biochem., 202 (1992) 889.

[45] M. A. Marletta, P. A. Srere and C. Walsh, Biochemistry, 20 (1981) 3719.

[46] G. E. Tranter, Mol. Phys., 4 (1985) 825.

[47] G. E. Tranter, J. Theor. Biol., 119 (1986) 467.

[48] (a) P. M. Rust, W. C. Stallings, C. T. Monti, R. K. Preston and J. P. Glusker, J. Am. Chem. Soc., 105 (1983) 3206; (b) H. L. Carrell, J. P. Glusker, J. J. Villafranca, A. S. Mildvan, R. J. Dunnel and E. Kun, Science, 170 (1970) 142; (c) T. J. Hurley, H. L. Carrell, R. K. Gupta, J. Schwartz and J. P. Glusker, Arch. Biochem. Biophys., 193 (1979) 478; (d) W. C. Stallings, C. T. Monti, J. E. Belvedere, R. K. Preston, J. P. Glusker, Arch. Biochem. Biophys., 203 (1980) 65.

[49] L. Pauling, J. Am. Chem. Soc., 51 (1929) 1010.

[50] D. Holtz, Prog. Phys. Org. Chem., 8 (1971) 1.

[51] D. A. Dixon, T. Fukunaga and B. E. Smart, J. Am. Chem. Soc., 108 (1986) 4027.

[52] A. H. Robbins and C. D. Stout, Proc. Natl. Acad. Sci. (U. S. A), 86 (1989) 3639.

[53] A. H. Robbins and C. D. Stout, Proteins Struct. Funct. Genet., 5 (1989) 289.

[54] A. H. Robbins and C. D. Stout, J. Biol. Chem., 260 (1985) 2328.

[55] J. A. Goldstein, Y. F. Cheung, M. A. Marletta and C. Walsh, Biochemistry, 17 (1978) 5567.

[56] J. P. Glusker, J. Mol. Biol., 38 (1968) 149.

[57] J. P. Glusker, in *The Enzymes*, 3^{rd} Edn., (Ed. P. Boyer), Academic Press, New York, Vol. 5, p 413, 1971.

[58] J. Bailar, Inorg. Nucl. Chem., 8 (1958) 165.

Chapter 6

Cysteine and Serine

In the previous chapters the conformations and vibrations of a number of carboxylic acids have been studied. In this chapter the vibrational spectra of cysteine and serine in the ionized (zwitterionic) and nonionized (gas phase) forms are studied using the 4-31G* basis set. The experimental vibrational spectra are assigned using the calculated frequencies and PED's.

There have been a number of ab initio studies of glycine [1–7] and alanine [8–11]. Thus the vibrational frequencies for glycine in the gas phase have been evaluated [3–5] and assigned [5]. In the zwitterionic form a solvated model of glycine was used to obtain the vibrational frequencies and assignments [6,7]. The gas phase frequencies of alanine have been evaluated for a number of conformations [10] and those of zwitterionic alanine have been evaluated and assigned to the corresponding experimental spectra [11].

Previous quantum chemical calculations of serine include studies of protonation [12–14] and lattice energies [15], parity violating energy differences of its enantiomers [16,17], differences in its crystal and peptide structure [18] and studies of its low energy conformations [19,20]. Calculations on cysteine include studies of protonation and ionization potentials [1] and a comparison of some PCILO and SCF results [21] and a study of its minimum energy conformations [22]. Calculations on cysteine and serine have to take into account the presence of the hydroxyl and thiol groups in the side chain. The thiol group in cysteine has been a difficult group to model because earlier force field developers have shown that an inaccurately described *SH* group does not tend to form hydrogen bonds [23]. In the solid state the structures of L-cysteine and L-serine have been determined by neutron diffraction [24,25].

There have been a number of vibrational studies of cysteine, the most recent being

that of Li et al. [26]. The vibrational analysis was based on the Raman spectra of L-cysteine. The earlier vibrational study of Susi et al. was also based on the Raman spectra of L-cysteine [27]. A detailed infrared study of cysteine in its various forms was done by Madec et al. [28]. All the previous vibrational studies of serine have been done on the D,L form. Thus Madec et al. [29] have assigned the IR of D,L-serine and its deuterated derivatives. Machida et al. [30] have done a detailed vibrational analysis of D,L-serine and its d_4 derivative. Susi et al. [27] have done the vibrational analysis of D,L-serine using the experimental data of Madec et al. [29]. A recent Raman optical activity (ROA) study of L-cysteine and L-serine [31] had assigned the resulting ROA spectra on the basis of the assignment of the ROA spectra of L-alanine [32].

6.1 Gas Phase Studies

The starting structures of cysteine and serine in the nonionized form were obtained from the earlier 4-21G optimized studies of cysteine and serine [20,22]. The vibrational frequencies were evaluated on three conformations of cysteine and serine. Our choice of the three conformations was based on the energetics. Thus we chose the lowest energy, second lowest energy and highest energy conformer of the earlier conformational study of cysteine and serine [20,22]. The earlier conformational study of cysteine had utilized the 3-21G basis to describe sulphur in cysteine [22]. All the other atoms in both cysteine and serine were described by the 4-21G basis. The 4-31G* basis set was chosen because of its small size and more so because it had polarization functions, which could be utilized in a better description of sulphur and the hydrogen bonding effects exhibited by these amino acids.

6.1.1 Experimental

The presence of nonionized amino and carboxyl groups in gas phase cysteine and serine leads to some problems with regard to its assignment to the corresponding experimental spectra of L-csyteine and L-serine (the amino and carboxyl groups are ionized in the zwitterionic forms). In order to circumvent these problems we thought it would be useful to obtain the IR spectra of the hydrochlorides and methyl esters of cysteine and serine. While the spectra of the corresponding hydrochlorides would be useful in the assignment of the carboxyl group the spectra of the methyl esters could help resolve the problem of assignment of the amino group. Since the spectra of these compounds are not available in

the literature, the compounds had to be synthesized and the resulting spectra are utilized in the assignments. In this section we briefly describe our synthetic efforts.

Commercial anhydrous cysteine hydrochlroide was used in recording the IR spectra of cysteine hydrochloride. Serine hydrochloride was prepared by placing a saturated solution of serine in 10% HCl for about 24 hrs. It was then dried in vaccuum over P_2O_5. The hydrochloride was recrystallised from water and dried over P_2O_5. The methyl ester hydrochlorides of cysteine and serine were prepared by passing HCl gas to a mixture of the corresponding hydrochloride and methanol. The methanol was then removed by evaporating it under vaccuum. The crude ester hydrochloride was recrystallised from water. The methyl esters were prepared by passing NH_3 to a solution of the methyl ester hydrochlorides in dichloromethane. The NH_4Cl was filtered off and the dichloromethane was evaporated under vaccuum at low temperatures to give the methyl esters as oily liquids. It should be noted that the methyl esters are highly unstable at high temperatures and polymerize on storage. Hence the spectra of freshly prepared samples has to be recorded at low temperatures. All IR spectra were recorded on a Perkin Elmer FT-1600 model

6.1.2 Geometries

The 4-31G* optimized energies, bond lengths, bond angles and dihedral angles of the three conformations of cysteine and serine are given in Table 6.3 and the structures are shown in Figures 6.1 and 6.2.

Geometrically the parameters defining the three starting conformations were $\tau_1[N1 - C2 - C3 = O4]$, $\tau_2[H8 - C2 - C9 - S13]$ and $\tau_3[C2 - C9 - S13 - H14]$. They were (-7°,56°,-8°), (12°,-177°,-120°) and (-8°,-120°,-130°) for the three starting conformations respectively. The optimization at the 4-31G* resulted in a significant change in the energetic and geometrical features. The bond lengths C1-C2, C2-C9, C3-O4, C3-O5, O5-H6 and C9-S13 are significantly shorter while the C2-C3 and S13-H14 are longer. There is a dramatic change in the values of the dihedral angles especially τ_3. These results should be seen in the light that our calculation includes the effect of polarization. The main differences between the three conformations is in the orientation of the SH group. There is no notable difference in the orientation of the other groups.

Differences in geometry between the three starting structures of serine were in terms of the torsion angles $\tau_1[N1 - C2 - C3 = O4]$ and $\tau_2[N1 - C2 - C10 - O13]$. The three 4-21G optimized conformations had the the (τ_1, τ_2) values as (5°,54°),(-151°,57°) and (11°,57°).

After optimization at the 4-31G* level the values are (9^o,57^o),(-151^o,61^o) and (14^o,59^o). In terms of conformational differences the *COOH* group in structure I and III are syn periplanar and in II anti periplanar(see Figure 6.2). As the optimized conformations were chosen on the basis of energetic considerations, we found that structure II was a different enantiomer than I and III. Our results are not affected by this difference. The comparison of the 4-21G optimized structure to the 4-31G* optimized structure are similar to those in cysteine.

6.1.3 Vibrational frequencies

The symmetry coordinates of cysteine and serine are listed in Tables 6.1 and 6.2. The calculated frequencies, IR intensities and Raman activities of the three conformations of cysteine and serine are given in Table 6.4 and Table 6.5. The potential energy distributions obtained for all the three conformations of cysteine and serine are shown in Table 6.6 and Table 6.7. Since the vibrational frequencies of cysteine and serine are not available in the gas phase, assignments have been made using the solid state IR spectra of the methyl ester and the hydrochloride of cysteine and serine. To reinforce the NH_2 and *COOH* assignments comparisons have been made with the IR spectra of glycine in the gas phase [33] and the earlier vibrational assignment of glycine [5]. Generally, gas phase frequencies are higher than the solid state frequencies, but in case of CH_2 they are comparable. The observed IR frequencies of the methyl ester and the hydrochloride along with the assignments are tabulated in Table 6.8 and Table 6.9. The frequencies of the zwitterion [26–29] also have been given. These assignments are valid only for the modes of CH_2 and XH (X=S or O) in case of the zwitterion.

NH_2 frequencies

$\nu_a(NH_2)$ and $\nu_s(NH_2)$ of the three conformations of cysteine occur at (3611,3535), (3613,-3536) and (3610,3538) cm^{-1}respectively. These peaks have been assigned to the peaks at 3360 and 3295 cm^{-1}observed in the methyl ester of cysteine. This compares well with the observed $\nu_s(NH_2)$ of glycine at 3411 cm^{-1}. The theoretically predicted $\nu_a(NH_2)$ and $\nu_s(NH_2)$ of glycine are 3579 and 3490 cm^{-1}respectively. $\delta(NH_2)$ in the three conformations of cysteine occurs at 1655, 1652 and 1656 cm^{-1}respectively. This peak has been assigned to the experimental peak at 1593 cm^{-1}in the methyl ester. In the gas phase spectrum of glycine it has been assigned to the peak at 1632.5 cm^{-1}. $\omega(NH_2)$ has been assigned to

the peak at 882 cm^{-1}in the methyl ester. It is a mixed mode with $\delta(NH_2)$. $\tau(NC_\alpha)$ which is very much dependent on the orientation as well as the nature of the groups bonded to these atoms appears at around 200 cm^{-1}. In the zwitterion this mode has been assigned to the peak at 148 cm^{-1}.

$\nu_a(NH_2)$ and $\nu_s(NH_2)$ in the three conformations of serine can be assigned to the peaks at 3362 and 3280 cm^{-1}in the methyl ester. These frequencies are in the same range as in cysteine. $\delta(NH_2)$ has been assigned to the peak at 1596 cm^{-1}in the ester. $\omega(NH_2)$ and $\rho(NH_2)$ appear as mixed modes. They have been assigned to the peaks at 945 $cm^{-1}$and 1227 cm^{-1}in the ester. $\tau(NC_\alpha)$ in the three conformations of serine occurs at 242,331 and 251 cm^{-1}. It can be clearly seen that the NH_2 frequencies of serine and cysteine are similar.

COOH frequencies

In cysteine the $\nu(OH)$ peak has been assigned to the peak at 3377 cm^{-1}in the hydrochloride. $\nu(OH)$ in glycine occurs at 3561 cm^{-1}. $\nu(C=O)$ has been assigned to the peaks at 1735 cm^{-1}in the ester and 1743 cm^{-1}in the hydrochloride. This compares well with the gas phase frequency in glycine of 1781 cm^{-1}. $\nu(C-O)$ has been assigned to the peaks at 1176 cm^{-1}in the ester and 1141 cm^{-1}in the hydrochloride. $\delta(COH)$ has been assigned to the peak at 1203 cm^{-1}in the hydrochloride. $\delta(C=O)$ has been assigned to the peak at 618 and 596 cm^{-1}in the methyl ester and the hydrochloride respectively. The calculated $\delta(C-O)$ frequency appears as a predominant mode around 490 cm^{-1}. It has been assigned to the peak at 458 cm^{-1}in the hydrochloride. $\gamma(COO)$ has been assigned to the frequency at 868 $cm^{-1}$and $\tau(CO)$ has been assigned to the peak at 524 cm^{-1}in the hydrochloride. In the earlier theoretical study of glycine $\tau(CC)$ frequencies were predicted to occur at 86 cm^{-1}. In all the three conformations of cysteine this frequency occurs around 50 cm^{-1}because torsions are not well reproduced in ab initio calculations.

In serine $\nu(OH)$ has been assigned to the peak at 3385 cm^{-1}in the hydrochloride. $\nu(OH)$ in conformation II is lowered due to the presence of hydrogen bonding of the OH hydrogen with the amino nitrogen. The $COOH$ frequencies should be viewed in light of the fact that in conformation II the $COOH$ group is anti periplanar while in the other conformations it is syn periplanar. $\nu(C=O)$ in the three conformations of serine occurs at 1927, 1933 and 1957 cm^{-1}. They have been assigned to the peak at 1735 cm^{-1}in the methyl ester and the peak at 1734 cm^{-1}in the hydrochloride. $\nu(C-O)$ does not appear as a single strong peak in serine. It always occurs as a mixed mode either in the presence of the stronger $\delta(COH)$ or the $\delta(C_\beta OH)$. $\delta(C=O)$ in all the three conformations of serine occurs

in the range 558-659 cm^{-1}. It has been assigned to the peak at 635 cm^{-1}in the methyl ester. The corresponding $\delta(C-O)$ occurs predominantly around 280 cm^{-1}in all the three conformations of serine. The $\gamma(COO)$ mode has been assigned to the peaks at 778 and 767 cm^{-1}in the methyl ester and the hydrochloride while the $\tau(CO)$ has been assigned to the peaks at 562 and 538 cm^{-1}in the ester and hydrochloride respectively. An important observation has been that in conformation II due to the presence of hydrogen bonding the $\tau(CO)$ frequency is higher than in the other two conformations. Thus the presence of intramolecular hydrogen bonding between the amino group and the carboxyl group in structure II accounts for the differences between it and structures I and III.

CH_2 and CH frequencies

CH freqencies are not sensitive to the phase in which the spectrum is taken i.e. the frequencies exhibited in the solid state IR spectra are comparable to those occuring in the gas phase. Hence the assignments of this mode have been reinforced by comparing our assignments with the IR spectra of cysteine [26–28]. $\nu_a(CH_2)$ has been assigned to the peaks at 3000 and 2998 cm^{-1}. In the three conformations of cysteine the relative order of appearence of $\nu(CH)$ and $\nu_s(CH_2)$ is different. Thus in the lowest energy conformation $\nu(CH)$ occurs intermediate to the $\nu_a(CH_2)$ and the $\nu_s(CH_2)$ bands, while in the other two conformations it occurs lower than the $\nu_s(CH_2)$ band. Thus these two bands can be assigned to the experimental peaks at 2953, 2943 and 2961 cm^{-1}in the ester, hydrochloride and zwitterion respectively. The resonance Raman study of cysteine [26] had observed a weak signal at 2918 cm^{-1}which they attributed to the $\nu(C_\alpha H_\alpha)$. $\delta(CH_2)$ has been assigned to the peaks at 1437, 1428 and 1424 $cm^{-1}$and $\omega(CH_2)$ has been assigned to the peaks at 1313, 1316 and 1303 cm^{-1}in the ester, hydrochloride and zwitterion respectively. $t(CH_2)$ occurs as a mixed mode at 1243 and 1118 in the methyl ester, 1222 and 1108 in the hydrochloride and 1269 and 1106 cm^{-1}in the zwitterion respectively. $\rho(CH_2)$ has been assigned to the peaks at 781, 777 and 773 cm^{-1}in the ester, hydrochloride and zwitterion respectively. $\delta(C_\alpha C_\beta S)$ frequencies has been assigned to the peak at 148 cm^{-1}in the zwitterion. This assignment can be considered as valid because the appearence of this peak is independent of the substituents on the nitrogen of the amino group and the carbon of the carboxyl group.

To confirm our assignments of the CH_2 frequencies the earlier IR spectra of zwitterionic serine were used [27,29]. $\nu_a(CH_2)$ has been assigned to the peak at 2975 cm^{-1}in the zwitterion. $\nu_s(CH_2)$ and $\nu(C_\alpha H_\alpha)$ has been assigned to the peaks at 2956 and 2945 cm^{-1}in

the ester and zwitterion respectively. $\delta(CH_2)$ has been assigned to the peak at 1450 cm^{-1}in the ester and zwitterion. $\omega(CH_2)$ has be assigned to the peaks at 1378 and 1364 cm^{-1}in the ester and zwitterion respectively. A feature which can be easily noticed is that in serine the $\delta(CH_2)$ and $\omega(CH_2)$ appear higher than the corresponding peaks in cysteine. The lowering of frequencies in cysteine may be due to the presence of the thiol group. $t(CH_2)$ has be assigned to the peaks at 1309 and 1312 cm^{-1}in the ester and zwitterion respectively. Generally this mode appears as a mixed mode. $\rho(CH_2)$ has been assigned to the peaks at 900, 903 and 901 cm^{-1}in the ester, hydrochloride and zwitterion respectively. $\nu(C_\alpha C_\beta)$ has been assigned to the peaks at 1044, 1025 and 1030 cm^{-1}in the ester, hydrochloride and zwitterion. $\delta(C_\alpha C_\beta O)$ appears at 337, 215 and 338 cm^{-1}which are lower than the $\delta(C_\alpha C_\beta S)$ mode in cysteine.

SH or *OH* frequencies

$\nu(SH)$ has been assigned to the peaks at 2553 and 2551 cm^{-1}in the hydrochloride and zwitterion respectively. A Raman spectrum of 10% cysteine solution gave a peak at 2582 cm^{-1}which has also been attributed to this mode. It was reported that $\nu(SH)$ frequencies are dependent on the value of the torsion angles $\chi_1[C.C_\alpha.C_\beta.S]$ and $\chi_2[C_\alpha.C_\beta.S.H]$ [26]. We have found no evidence of this dependence because the potential energy distribution of this frequency in all the three conformations indicate that contributions to this frequency entirely comes from the $\nu(SH)$ band. $\nu(C_\beta.S)$ frequency has been assigned to the experimental bands at 637, 646 and 646 cm^{-1}in the ester, hydrochloride and zwitterion respectively. Studies on thioethers [34] and the earlier Raman study of mercaptothiols [26] have reported the dependence of the $\nu(CS)$ frequency on the torsion angle χ_1. We wanted to study this dependence theoretically and account for the shifts of more than 100 cm^{-1}in the three conformations of cysteine. Therefore the torsion angle χ_1 was varied at intervals of 10°in the conformation I. The symmetric scaled F matrix was calculated on the optimized geometry. On varying the torsion angle, only the G matrices were changed. Using these G matrices and the original scaled F matrix we obtained the $\nu(CS)$ frequencies. The $\nu(CS)$ frequencies were then plotted with the torsion angle χ_1 in Figure 6.3. The curve displays all the characterstics of the earlier plot established for mercaptothiols. The maximum of the curve is at 807 $cm^{-1}$and the minimum at 713 cm^{-1}. The $\nu(CS)$ frequency of 813 $cm^{-1}$for conformation I is not observed in the plot because the torsion angle corresponding to this frequency has not been sampled. On the lower side, we have obtained frequencies of 687 $cm^{-1}$and 696 cm^{-1}while the minima is at 713 cm^{-1}. We have

not studied the dependence of this frequency on the torsion angle χ_2 because the frequency varied only by 10 $cm^{-1}$for changes in this torsion angle. In mercaptothiols there is no interaction between the terminal CH_3 and the thiol(SH) group but in cysteine there is a lot of interaction between the $COOH$ group and the SH group. Hence this frequency is also dependent on the orientation of the SH and the $COOH$ group. This would then possibly account for the discrepancy betweeen the minimum frequency observed in our plot and the frequencies in conformation II and III. It can be easily seen that the torsion angle at which the minima occurs in the plot (310^o) and the values of the torsion angle χ_1 in conformation II and III are close. $\delta(C_\beta.S.H)$ has been assigned to the peaks at 942 and 931 cm^{-1}in the ester and hydrochloride respectively. $\tau(C_\beta.S)$ can be assigned to the peak at 268 cm^{-1}in the zwitterion.

$\nu(OH_{alc})$ frequencies generally appear higher than the $\nu(OH_{ac})$ [35]. Our theoretical results also indicate this trend. $\delta(C_\beta OH)$ also appears higher than the corresponding $\delta(COH)$ peak. This mode occurs at a range of frequencies from 1227-1346 cm^{-1}. Since the PED does not indicate a dominant mode, it cannot be assigned to a particular frequency. $\nu(C_\beta O)$ can be assigned to the peaks at (1131,1064), (1132,1077) and (1162,1095) cm^{-1}in the ester, hydrochloride and zwitterion respectively. Since this mode was appearing as a dominant mode in a number of frequencies we wanted to find out whether a similar relationship between the torsion angle ($C.C_\alpha.C_\beta.O$) and the $\nu(C_\beta O)$ exists. A similar methodolgy as explained earlier in case of cysteine was used here. The values of $\nu(C_\beta O)$ are plotted against the torsion angle ($C.C_\alpha.C_\beta.O$) in Figure 6.4. We can easily see that the maxima in this case occurs when the $COOH$ group eclipses the $C_\beta OH$ group. This is contrary to the observation found in cysteine. Moreover the difference between the minima and the maxima is of the order of 40 cm^{-1}which is far less than the corresponding difference in cysteine of 100 cm^{-1}. $\tau(C_\beta O)$ can be assigned to the peaks at 480 and 499 cm^{-1}in the ester and zwitterion respectively.

6.2 Zwitterionic studies

In the previous section the conformational dependence of the vibrational frequencies of the nonionized forms of cysteine and serine was highlighted. In the ionized form the presence of two ionized groups (amino and carboxyl) and an hydrophilic side chain might influence the appearence of vibrational frequencies. Since calculations on the nonionized form were carried out using the 4-31G* basis set, the same basis set was also utilized for the

zwitterionic forms. The calculated vibrational frequencies were then utilized in assigning the vibrational spectra of L-cysteine, D,L-serine and L-serine [26–31].

The neutron diffraction structures of cysteine and serine were used as starting structures [24,25].

The 4-31G* optimized energies, bond lengths, bond angles and dihedral angles of the cysteine and serine zwitterions are given in Table 6.12 and the structures are shown in Figures 6.5 and 6.6. The symmetry coordinates utilized for the zwitterionic forms of cysteine and serine are listed in Tables 6.10 and 6.11. The calculated frequencies, IR intensities and Raman activities of the cysteine and serine zwitterions are listed in Tables 6.13 and 6.14. The potential energy distributions obtained for the cysteine and serine zwitterions are given in Table 6.15. The assignment of the d_4 isotopes of cysteine and serine are given in Tables 6.16 and 6.17.

6.2.1 Cysteine

Two structures were obtained from the neutron diffraction study of cysteine [24] were optimized at the 4-31G* level. The only difference in the two structures in the neutron diffraction study was the orientation of the thiol hydrogen. However as seen from Table 6.15 the difference of this orientation did not produce substantial difference in the potential energy distributions for many peaks and the vibrational assignments are nearly the same for both the conformations. On optimization there is some change in the geometry of the backbone also. This can be due to the ease with which the thiol hydrogen could form hydrogen bonds with the carboxyl oxygen.

The methodology we employ here is slightly different from what was utilized in the asignment of the gas phase forms of cysteine. In this study we assigned the experimental Raman spectra and IR spectra of the orthorhombic crystal of L-cysteine and the wavenumbers obtained in the recent Raman optical activity study of L-cysteine in water. It is well known that ab initio frequencies are 10-20% higher than the experimental frequencies. Hence we correlate some of the frequencies on the basis of the intensity patterns in both the Raman and IR spectra. Since we have not calculated the Raman optical activities we employ the arguments used in the earlier ab initio study of L-alanine to verify our assignments.

We limit ourselves in assigning the spectra of L-cysteine in the 600-1500cm^{-1}range owing to the availability of the experimental ROA wavenumbers in that range The higher

regions are generally a broad band and hence the assignments in that region are subject to doubt. We however assign the thiol (SH) stretching mode owing to its distinct band.

At the lower end of the spectra the peaks at 583 and $588cm^{-1}$in the two conformations of cysteine can be assigned to the bands at 642 in the Raman spectra, 637 in the IR spectra and $615cm^{-1}$in the corresponding ROA spectra in solution. In both the conformations of cysteine the major contributor to the PED is the $\nu(C_\alpha C)$ mode. However, the other contributors to this frequency are the $\delta(C_\beta C_\alpha C)$, $\delta(COO)$ and $\rho(COO)$ modes. Li et al. [27] have assigned this frequency to the $\delta(CCO)$, while Gargaro et al. [31] on the basis of the earlier study of L-alanine attribute this frequency to arise from a COO^- bending mode. The peak at 688 and $697cm^{-1}$has been assigned to the frequencies 696, 692 and $685cm^{-1}$in the Raman, IR and ROA spectra of L-cysteine. All the previous assignments have attributed this frequency to the $\nu(CS)$ mode. Our assignment is in agreement with the previous assignments. In our earlier study on the unionized conformation of cysteine the $\nu(CS)$ mode was the dominant mode contributing to this frequency. The peaks at 765 and $768cm^{-1}$in the two conformations of L-cysteine are assigned to the peaks at 773, 770 and $779cm^{-1}$in the Raman, IR and ROA spectra of L-cysteine respectively. The dominant mode contributing to this frequency is $\rho(CH_2)$. The IR study of Madec et al. [28] have attributed this peak to the $\rho(CH_2)$ mode, while the vibrational assignment of Li et al. [26] have attributed this peak to the $\delta(CSH)$ mode. Our assignment is validated by the fact that in the isotope study of L-cysteine($ND_3^+CH(CH_2SD)COO^-$), $\delta(CSD)$ appears at 625 and $650cm^{-1}$. They have been assigned to the peaks at 628 and $621cm^{-1}$in the Raman and IR spectra of ($ND_3^+CH(CH_2SD)COO^-$) respectively [27,28]. Correspondingly the $\delta(CSH)$ mode is a major contributor to the frequencies at 989 and $1001cm^{-1}$. They have been assigned to the peaks at 1004 and $1003cm^{-1}$in the Raman and IR spectra of L-cysteine respectively. The similarity of the calculated and experimental isotope shifts indicates that the $\delta(CSH)$ mode appears at a higher frequency. Hence our assignment of these frequencies appears to be correct. In case of both the conformations of L-cysteine there is a small contribution of the $\delta(CSH)$ mode to this frequency, while in the isotope studies $\delta(CSD)$ is generally found along with the $\rho(CH_2)$ mode.

The peaks at 790, 802 and 844, $857cm^{-1}$have been assigned to the peaks at 825, 823, 813 and 870, 866, $875cm^{-1}$in the Raman, IR and ROA spectra of L-cysteine. The major modes contributing to this frequency are the $\delta(COO)$ and $\gamma(COO)$ modes. Madec et al. [28] had attributed the peaks at 823 and $866cm^{-1}$to the $\delta(COO)$ and $\nu(CC)$ modes, while Li et al. 25] have attributed the peaks at 825 and $870cm^{-1}$to the $\delta(CSH)$ and $\gamma(COO)$ modes.

On the basis of the ab initio assignment of L-alanine Gargaro et al. 30] have attributed the peaks at 813 and 875 to $\rho(CH_2)$ and $\nu(CC)$ modes. The ROA's associated with both these wave numbers is negative; similar to the ROA associated with the peak at $615cm^{-1}$which has been assigned to $\nu(CC)$ and $\gamma(COO)$ modes.

The peaks at 902, 910 and 989, 1001 have been assigned to the peaks at 943, 941, 936 and 1004, 1003, $990cm^{-1}$in the Raman, IR and ROA spectra of L-cysteine respectively. The major contributors to these frequencies are the stretching modes $\nu(CC)$, $\nu(NC)$ and the $\gamma_{\parallel}(NH_3^+)$ rocking mode. The $\delta(CSH)$ mode also contributes to the frequency at 989 and $1001cm^{-1}$. Our assignments of the stretching modes are in agreement with the assignment of Gargaro et al. 30].

The peaks at 1046, 1034 and 1062, $1061cm^{-1}$are predominantly NH_3^+ rocking modes. They have been assigned to the peaks at 1068, 1063 and $1069cm^{-1}$in the Raman, IR and ROA spectra of L-cysteine. The isotope shifts and the corresponding assignments of these frequencies confirms our assignments of these peaks. Incidentally Gargaro et al. 30] have attributed the frequency at $1069cm^{-1}$to the $\nu(CN)$ mode. The positive ROA similar to the one obtained for the wavenumbers associated with the rocking NH_3^+ mode is in agreement with our assignment. The appearence of these frequencies in L-alanine [32] further reinforces our assignments.

The peaks at 1095, 1101 and 1210, 1198 have been assigned to the peaks at 1110, 1104, $1118cm^{-1}$and 1201, 1195, $1211cm^{-1}$in the Raman, IR and ROA spectra of L-cysteine respectively. The major contributing mode to the peaks at 1095 and 1101 is the $\delta(C_\beta C_\alpha H)$ mode. In L-alanine [32] all the wavenumbers associated with CH bends have positive ROA's. The positive ROA associated with the peak at $1118cm^{-1}$is in agreement with this assignment. The major contributor to the peaks at 1210 and $1198cm^{-1}$is the $t(CH_2)$ mode. Gargaro et al. [31] have attributed the peak at $1211cm^{-1}$to $\omega(CH_2)$ and the peak at 1268 to $t(CH_2)$ but it is well known that $t(CH_2)$ modes are generally lower than $\omega(CH_2)$ modes [6,7,31]. Hence our assignment is valid for this frequency. The major contributor to the peaks at 1298, 1294, 1314 and 1306 are the $\omega(CH_2)$ and $\rho(C_\beta C_\alpha H)$ mode. They have been assigned to the peaks at 1273, 1296 and $1268cm^{-1}$in the Raman, IR and ROA spectra of L-cysteine respectively. The peak at $1268cm^{-1}$was attributed to the $t(CH_2)$ mode by Gargaro et al. [31]. On the basis of our earlier argument our assignment of the frequency is consistent.

The major contributors to the bands at 1346, 1333 and 1372, 1363 $cm^{-1}$are the $\rho(C_\beta$-$C_\alpha H)$, $\delta_s(NH_3^+)$ and $\delta(C_\beta C_\alpha H)$ modes. They have been assigned to the peaks at 1300,

1320, 1312 and 1351, 1348, 1351cm^{-1}in the Raman, IR and ROA spectra of L-cysteine respectively. Madec et al. [28] have attributed the peak at 1348$cm^{-1}$to the CH bending mode. Gargaro et al. [31] have attributed the peak at 1351 to the CH bending mode. It can clearly seen that this mode is mixed with contributtions from both the $\delta_s(NH_3^+)$ and $\rho(C_\beta C_\alpha H)$ modes. The positive ROA at 1351cm^{-1}also is in excellent agreement with our assignment because in L-alanine [32] the wavenumbers associated with both the NH_3^+ rock and CH bending modes have positive ROA's. As an alternative assignment the peaks at 1298 and 1294cm^{-1}could be assigned to the peaks at 1273, 1296, 1278cm^{-1}in the Raman, IR and ROA spectra of L-cysteine respectively. The peaks at 1314 and 1306$cm^{-1}$to the peaks at 1300, 1320 and 1312$cm^{-1}$and the peaks at 1346 and 1333$cm^{-1}$to the peaks at 1351, 1348 and 1351cm^{-1}in the Raman, IR and ROA spectra of L-cysteine respectively. This will be consistent with the assignments of Madec et al. [28] and Gargaro et al. [31] wherein these peaks were associated with $C_\alpha H$ bending modes, but our earlier assignment was based on the relative Raman activities and IR intensities.

The peaks at 1425, 1423cm^{-1}have been assigned to the peaks at 1400, 1394 and 1403cm^{-1}in the Raman, IR and ROA spectra of L-cysteine. The predominant mode contributing to this frequency is the $\nu_s(COO^-)$ mode. Madec et al. [28] have attributed the peak at 1394$cm^{-1}$to the $\nu_s(COO^-)$ mode. Li et al. [26] and Gargaro et al. [31] have attributed the peaks at 1400 and 1403$cm^{-1}$to the $\nu_s(COO^-)$ mode. Thus our assignment of this frequency is in agreement with others. Similarly the peaks at 1446 and 1447cm^{-1}can be assigned to the peaks at 1427, 1424 and 1430cm^{-1}in the Raman, IR and ROA spectra of L-cysteine. $\delta(CH_2)$ is the major mode contributing to this frequency. All the previous assignments have attributed the peaks at the above frequencies to the $\delta(CH_2)$ mode.

The peaks at 2715 and 2706$cm^{-1}$are associated with the $\nu(SH)$ mode and have been assigned to the frequencies at 2550 and 2555cm^{-1}in the Raman and IR spectra of L-cysteine. All the previous assignments attribute these frequencies to this mode.

The orientation of the thiol hydrogen leads to the differences obtained in the potential energy distributions of both the conformations. Thus $\nu(SH)$ in conformation II occurs at a lower frequency than in conformation I. In contrast the $\nu(CS)$ frequency in conformation II occurs at a higher frequency than in conformation I. The $\delta(CSH)$ peak is a major mode contributing to the frequency at 1001cm^{-1}in conformation II, while in conformation I it occurs as mixed mode at 989cm^{-1}along with the $\gamma_\parallel(NH_3^+)$ mode. The conformational dependence of the $\nu(CS)$ frequency has been highlighted in the earlier section on the nonionized forms of cysteine.

6.2.2 Serine

The neutron diffraction study of serine [25] indicates the presence of a single conformation. Our efforts to isolate and optimize a second conformation of serine, wherein the hydroxyl hydrogen is trans to the position of the hydroxyl hydrogen as it exists in the neutron diffraction of serine resulted in a single structure. The main differences between serine and cysteine is the existence of a hydroxyl group in place of the thiol group. The close proximity of the hydroxyl group to the $\beta(C)$ and the improved hydrogen bonding capabilities of this group bestow on serine some unusual conformational traits. The NMR studies of serine and cysteine [36] indicate that serine exists as a single rotamer at different pD's. On the other hand at two different pD's cysteine exists as two different rotamers.

Due to the absence of a detailed vibrational analysis of L-serine we have used the data obtained from the vibrational analysis of D,L-serine to assist us in the assignments. The relative data of L-serine is also given along with the wavenumbers obtained from the ROA spectra of L-serine in water [31]. The corresponding Raman activities and IR intensities have also been tabulated. Our calculations have been done using a 4-31G* basis set, hence the calculated intensities may not match the experimentally obtained intensity profiles in all cases.

As in cysteine we limit ourselves in assigning the spectra of L-serine in the 600-1500cm^{-1}range. The peak at 615cm^{-1}has been assigned to the peaks at 619 and 617cm^{-1}in the Raman and IR spectra of D,L-serine. The previous assignments including that of Gargaro et al. [31] have attributed this frequency to the CO_2^- bend. Our studies indicate that this mode is predominantly a $\tau(C_\beta O)$ mode. There is some contribution from the $\delta(CCO)$ and $\delta(CCC)$ modes also. The strong IR intensity attributed to this peak in our calculations is observed in the experimental IR spectra. The peak at 796cm^{-1}has been assigned to the peaks at 750 and 729cm^{-1}in the Raman and IR spectra of D,L-serine. The previous assignment of Machida et al. [30] and Gargaro et al. [31] have attributed this peak to arise either from a CO_2^- wag or a CO_2^- bend mode. The calculated potential energy distribution indicates that the major contributor to this mode is the $\delta(COO)$ mode, which confirms our assignment.

The peak at 829cm^{-1}has been assigned to the peaks at 815cm^{-1}in the Raman and IR spectra of D,L-serine. The previous assignments have attributed this peak to the $\rho(CH_2)$ mode. Our calculations clearly indicate that the major modes contributing to this frequency are the $\delta(COO)$, $\gamma(COO)$, $\nu(CC)$ and $\gamma_\parallel(NH_3^+)$ modes. The isotope studies

indicate that the $\rho(CH_2)$ mode appears at $1107cm^{-1}$. Our results in the previous section clearly indicate that the frequencies associated with the CH_2 bending modes generally appear at higher frequencies in serine than in cysteine is in accordance with this assignment. The peak at $870cm^{-1}$has been assigned to the peaks at 852 and $848cm^{-1}$in the Raman and IR spectra of D,L-serine. This peak has been attributed to the CC stretch in the vibrational analysis of D,L-serine by Machida et al. [30]. Gargaro et al. [31] have attributed this peak to a CN stretch which agrees well with our calculations indicating the $\nu(NC_\alpha)$ mode to be the dominant mode contributing to this frequency. The peak at $949cm^{-1}$has been assigned to the peaks at 900 and $901cm^{-1}$in the Raman and IR spectra of D,L-serine and to the wavenumber $919cm^{-1}$in the ROA spectra of L-serine in water. The dominant mode contributing to this peak is the $\gamma_\perp(NH_3^+)$ mode. There is some contribution from the $\nu(C_\alpha C_\beta)$ mode. The previous assignments have attributed this frequency to the $\nu(C_\alpha C)$ mode.

The peaks at 1003, 1065, 1076 are predominantly NH_3^+ rocking modes. It can be seen from the potential energy distribution of L-serine that a number of modes contribute to these frequencies. This include the $\rho(CH_2)$, $\rho(C_\beta C_\alpha H)$, $\nu(NC)$ and $\delta(C_\beta C_\alpha H)$ modes. The previous assignments of these frequencies have attributed them to the CN, CO, CCN stretching and NH_3^+ rocking modes.

The peaks at 1154 and $1188cm^{-1}$have been assigned to the peaks at 1156, 1176 and 1149, $1189cm^{-1}$in the Raman and IR spectra of D,L-serine respectively. The previous assignments have attributed these peaks predominantly to the NH_3^+ rocking modes. The potential energy distribution indicates that the dominant modes contributing to these frequencies are the $\nu(C_\beta O)$ and $t(CH_2)$ modes. There is some contribution from the $\delta(COH)$ mode to these frequencies. Machida et al. [30] had assigned the peak at $978cm^{-1}$to the $\nu(CO)$ mode. Our assignment for $\nu(C_\beta O)$ is clear from the isotopic studies of L-serine. The prominent mode contributing to the frequency at $1148cm^{-1}$is the $\nu(C_\beta O)$ mode. It can clearly be seen that the ROA assignments of Gargaro et al. [31] have not considered the existence of the hydroxyl side group in their assignments. Moreover they do not have any conclusive assignment to the peak at $1150cm^{-1}$owing to the lack of any discernible ROA, but they have presumed it to arise from either a CH_2 or NH_3^+ bending mode. Our assignment of the peak at $1188cm^{-1}$therefore confirms their presumption.

The peaks at 1306, 1356 are predominantly CH bending modes while the peak at $1369cm^{-1}$is associated with the NH_3^+ bending mode. There is some contribution from the $\delta(COH)$ mode to this frequency. They have been assigned to the peaks at 1249, 1309

and 1247, 1309cm^{-1}in the Raman and IR spectra of D,L-serine. Machida et al. [30] have attributed this peaks to the OH deformation and CH_2 twisting modes while Gargaro et al. [31] have attributed the peak at 1347$cm^{-1}$to arise from a CH bending mode which confirms our assignment. The calculated and experimental isotope shifts of 302 and 285cm^{-1}in case of the $\delta(NH_3^+/ND_3^+)$ peak agrees well with our assignment of the peak at 1369cm^{-1}.

The peaks at 1383 and 1403cm^{-1}have been assigned to the peaks at 1349, 1368 and 1352, 1377cm^{-1}in the Raman and IR spectra of D,L-serine. The dominant modes contributing to this frequency are the $\omega(CH_2)$ and $\delta_s(NH_3^+)$ mode. The earlier assignment of Machida et al. [30] had attributed the peak to the CH bending mode. The ROA spectra does not have any peaks associated with these modes. Hence our assignments of these frequencies cannot be confirmed.

The peaks at 1444 and 1481$cm^{-1}$are associated with the $\nu_s(COO^-)$ and $\delta(CH_2)$ modes. All the previous assignments have attributed the frequencies assigned to this mode to arise from the $\nu_s(COO^-)$ and $\delta(CH_2)$ modes. Hence our assignments of these frequencies is in accordance with the reported assignments.

6.3 Conclusions

The evaluation of vibrational frequencies of three conformations of cysteine and serine using the 4-31G* basis set leads to some interesting observations regarding the conformational dependence of some of the vibrational frequencies. The strategy of assignment of the IR frequencies of methyl ester, hydrochloride and zwitterion of both the compounds using the calculated frequencies of the nonionized conformations could be useful in assignments where the corresponding gas phase spectra is not available. The dependence of the $\nu(C_\beta X)$ where (X=S or O) on the torsion angle $C.C_\alpha.C_\beta.X$ has been highlighted. The lowering of the CH_2 frequencies in cysteine can indicate the influence of the thiol group on the CH_2 frequencies.

Our assignment of nearly all the frequencies observed in the 600-1500cm^{-1}range of the solid state vibrational spectra of L-cysteine and L-serine have highlighted the major differences arising out of the substitution of the thiol group by the hydroxyl group. The existence of a single stable conformation in case of serine and two stable conformations in case of cysteine indicates the geometrical restrictions imposed by serine in forming hydrogen bonds with its hydroxyl group. Although the assignment of many bands agree with the earlier assignments, there are some new assignments based on the 4-31G* ab

initio force fields.

Thus our vibrational assignments of two amino acids cysteine and serine in the nonionized and ionized conformations using ab initio force fields could be a valuable aid in the assignment of higher homologues of cysteine and serine and also in the assignment of other amino acids. Moreover our studies clearly indicate that these amino acids are in some ways similar but in many ways different from the carboxylic acids studied in the earlier chapters.

In the next chapter we delve into the intricacies of the conformations and vibrations of two imino acids, proline and hydroxyproline.

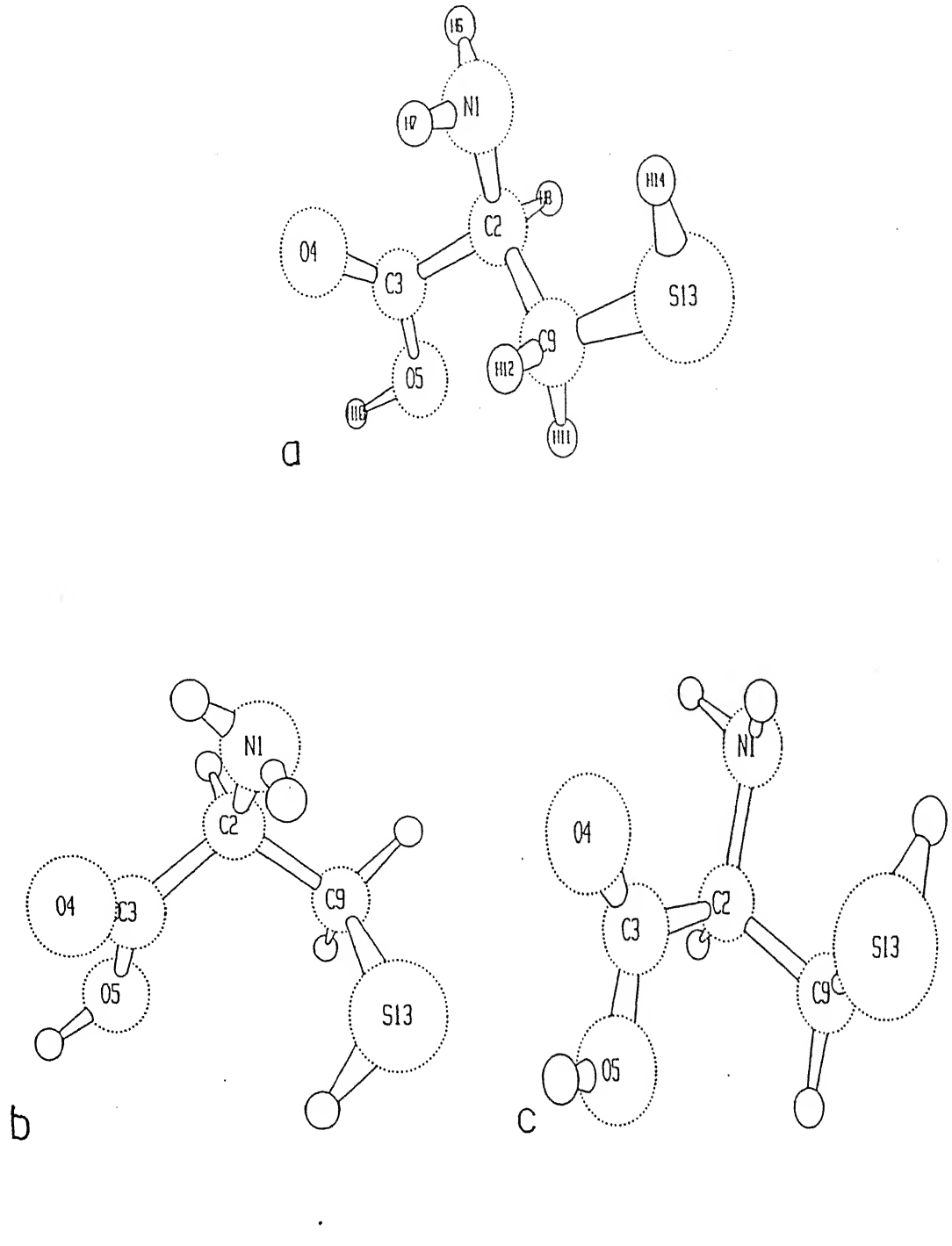

Figure 6.1: 4-31G* optimized structures of the three gas phase conformations (a) I, (b) II and (c) III of Cysteine.

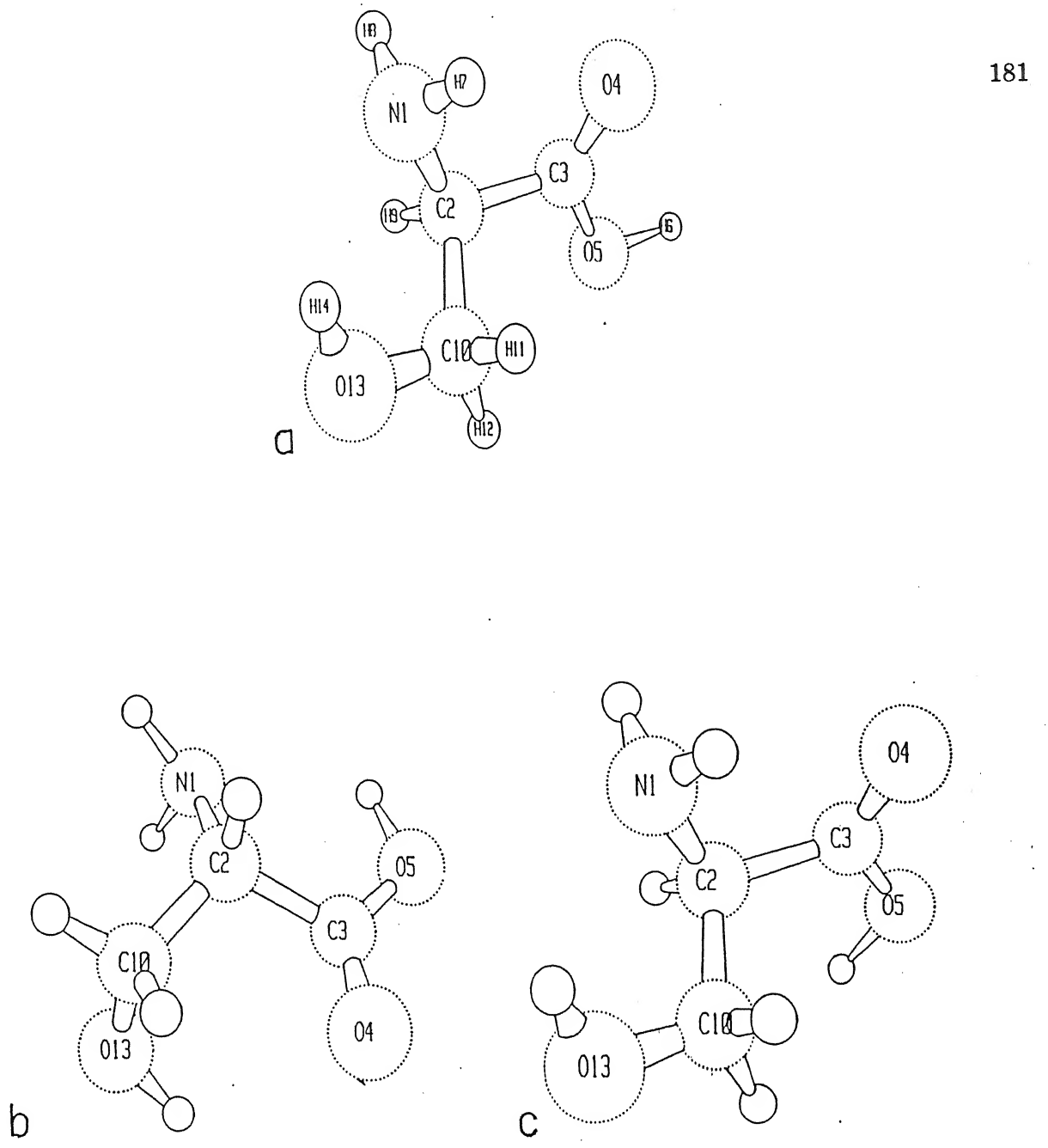

Figure 6.2: 4-31G* optimized structures of the three gas phase conformations (a) I, (b) II and (c) III of Serine.

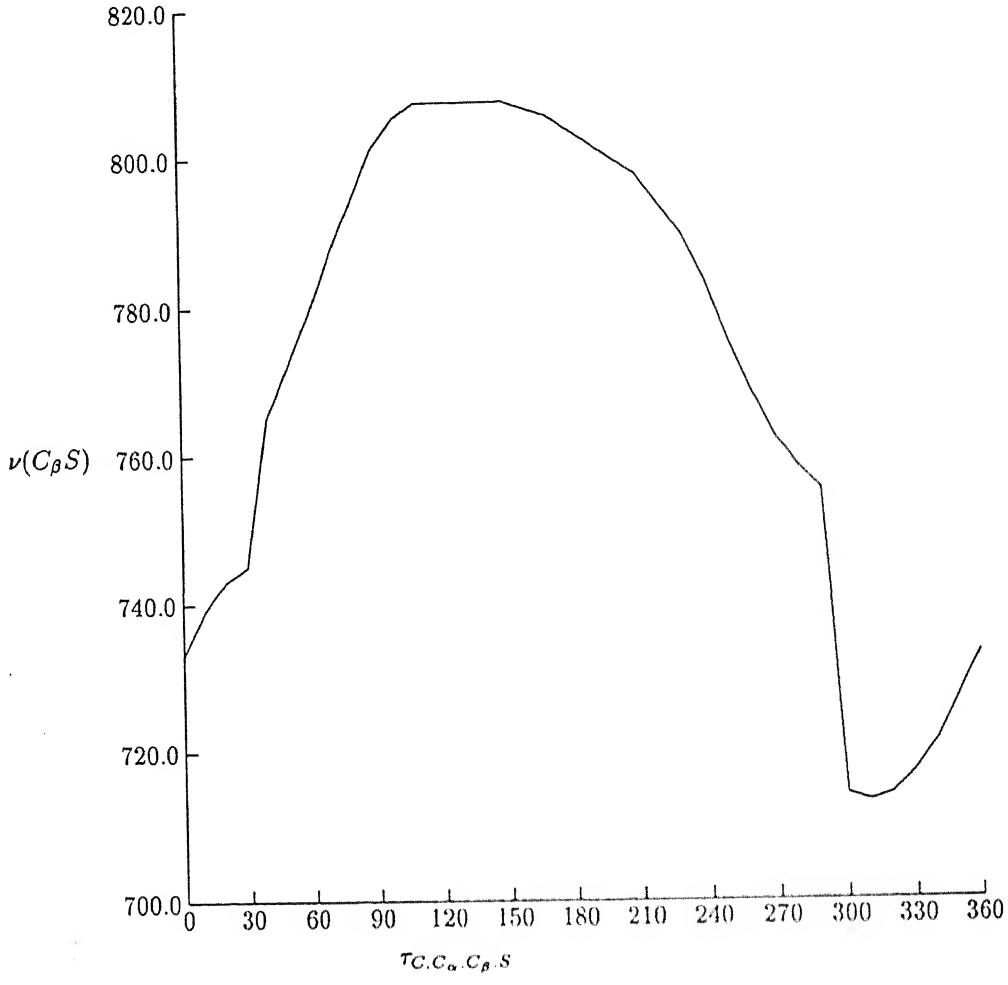

Figure 6.3: Variation of $\nu(C_\beta S)$ with the torsional angle $\chi_1[C.C_\alpha.C_\beta.S]$. Frequency is in units of Cm^{-1}

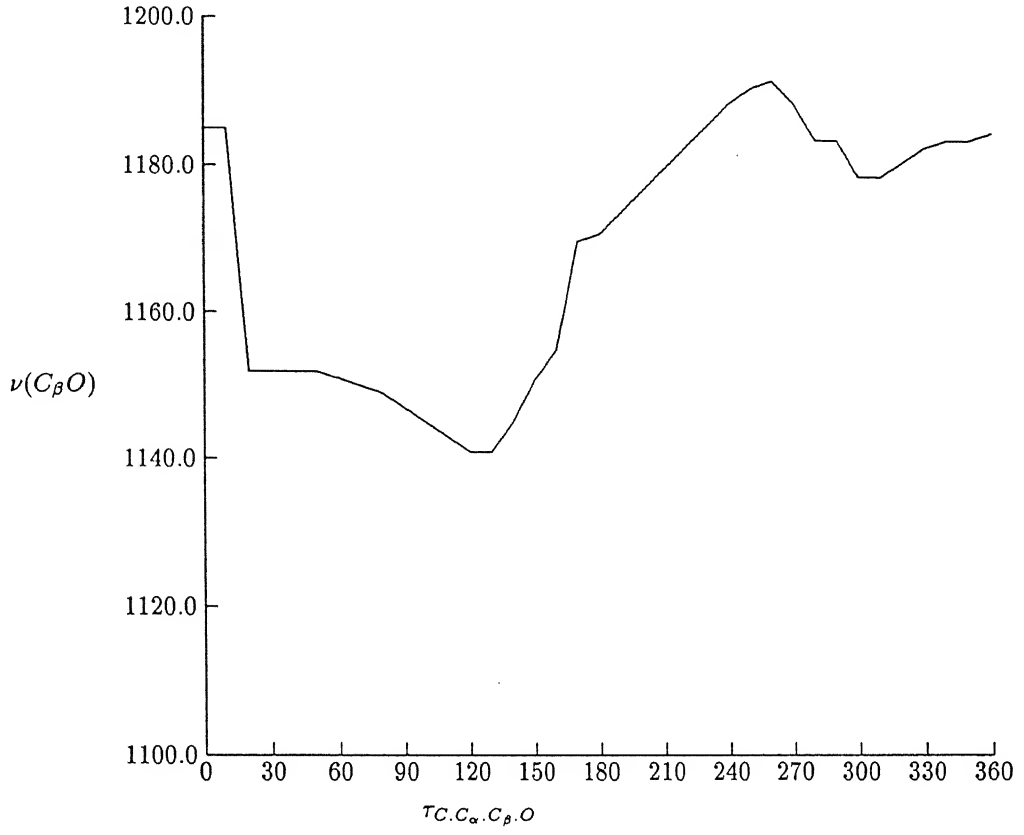

Figure 6.4: Variation of $\nu(C_\beta O)$ with the torsional angle $\chi_1[C.C_\alpha.C_\beta.O]$. Frequency is in units of Cm^{-1}.

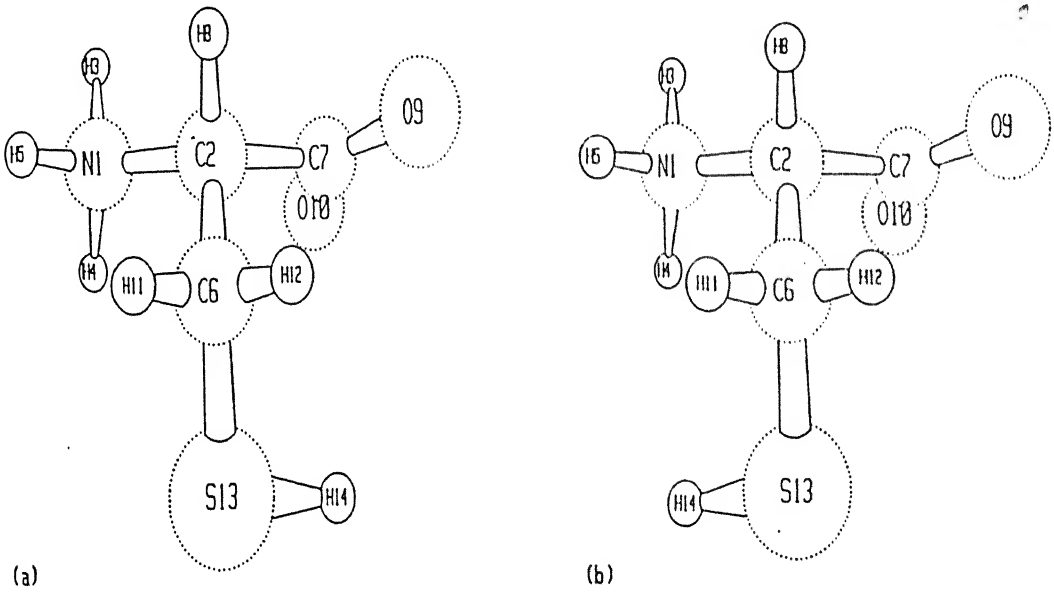

Figure 6.5: 4-31G* optimized structures of two conformations (a) I and (b) II of Cysteine zwitterion.

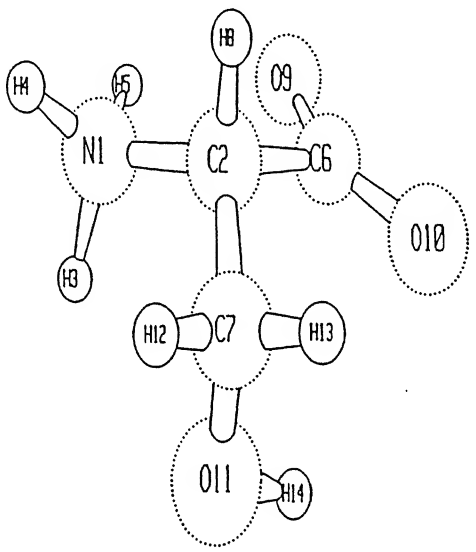

Figure 6.6: 4-31G* optimized structure of Serine zwitterion.

Table 6.1: Symmetry coordinates of cysteine

Coordinate	Description
$S_1 = R_{1.2}$	$\nu(NC_\alpha)$
$S_2 = R_{2.3}$	$\nu(C_\alpha C)$
$S_3 = \alpha_{1.2.3} + \alpha_{1.2.9} + \alpha_{3.2.9} - \alpha_{1.2.8} - \alpha_{3.2.8} - \alpha_{8.2.9}$	$\delta(NC_\alpha C)$
$S_4 = R_{1.6} + R_{1.7}$	$\nu_s(NH_2)$
$S_5 = R_{1.6} - R_{1.7}$	$\nu_a(NH_2)$
$S_6 = \alpha_{6.1.7}$	$\delta(NH_2)$
$S_7 = \alpha_{6.1.2} + \alpha_{7.1.2}$	$\omega(NH_2)$
$S_8 = \alpha_{6.1.2} - \alpha_{7.1.2}$	$\rho(NH_2)$
$S_9 = R_{2.9}$	$\nu(C_\alpha C_\beta)$
$S_{10} = R_{2.8}$	$\nu(C_\alpha H_\alpha)$
$S_{11} = \alpha_{1.2.8} - \alpha_{3.2.8}$	$\rho(C_\beta C_\alpha H_\alpha)$
$S_{12} = 2\alpha_{8.2.9} - \alpha_{1.2.8} - \alpha_{3.2.8}$	$\delta(C_\beta C_\alpha H_\alpha)$
$S_{13} = \alpha_{1.2.9} - \alpha_{3.2.9}$	$\rho(C_\beta C_\alpha C)$
$S_{14} = 2\alpha_{1.2.3} - \alpha_{1.2.9} - \alpha_{3.2.9}$	$\delta(C_\beta C_\alpha C)$
$S_{15} = R_{3.5}$	$\nu(C-O)$
$S_{16} = R_{3.4}$	$\nu(C=O)$
$S_{17} = R_{5.10}$	$\nu(OH)$
$S_{18} = 2\alpha_{2.3.5} - \alpha_{2.3.4} - \alpha_{4.3.5}$	$\delta(C-O)$
$S_{19} = \alpha_{2.3.4} - \alpha_{4.3.5}$	$\delta(C=O)$
$S_{20} = \alpha_{3.5.10}$	$\delta(COH)$
$S_{21} = R_{9.11} + R_{9.12}$	$\nu_s(C_\beta H_2)$
$S_{22} = R_{9.11} - R_{9.12}$	$\nu_a(C_\beta H_2)$
$S_{23} = R_{9.13}$	$\nu(C_\beta S)$
$S_{24} = 4\alpha_{11.9.12} - \alpha_{2.9.12} - \alpha_{2.9.11} - \alpha_{12.9.13} - \alpha_{11.9.13}$	$\delta(C_\beta H_2)$
$S_{25} = \alpha_{2.9.12} + \alpha_{2.9.11} - \alpha_{12.9.13} - \alpha_{11.9.13}$	$\omega(C_\beta H_2)$
$S_{26} = \alpha_{2.9.12} - \alpha_{2.9.11} - \alpha_{12.9.13} + \alpha_{11.9.13}$	$t(C_\beta H_2)$
$S_{27} = \alpha_{2.9.12} - \alpha_{2.9.11} + \alpha_{12.9.13} - \alpha_{11.9.13}$	$\rho(C_\beta H_2)$
$S_{28} = 5\alpha_{2.9.13} - \alpha_{11.9.12} - \alpha_{2.9.12} - \alpha_{2.9.11} - \alpha_{12.9.13} - \alpha_{11.9.13}$	$\delta(C_\alpha C_\beta S)$
$S_{29} = \tau_{11.9.13.14} + \tau_{12.9.13.14} + \tau_{2.9.13.14}$	$\tau(C_\beta S)$
$S_{30} = \alpha_{9.13.14}$	$\delta(C_\beta SH)$
$S_{31} = \tau_{6.1.2.8} + \tau_{6.1.2.3} + \tau_{6.1.2.9} + \tau_{7.1.2.8} + \tau_{7.1.2.3} + \tau_{7.1.2.9}$	$\tau(NC_\alpha)$
$S_{32} = \tau_{1.2.9.11} + \tau_{1.2.9.12} + \tau_{1.2.9.13} + \tau_{3.2.9.11} + \tau_{3.2.9.12} + \tau_{3.2.9.13} + \tau_{8.2.9.11} + \tau_{8.2.9.12} + \tau_{8.2.9.13}$	$\tau(C_\alpha C_\beta)$
$S_{33} = \tau_{1.2.3.5} + \tau_{8.2.3.5} + \tau_{9.2.3.5} + \tau_{1.2.3.4} + \tau_{8.2.3.4} + \tau_{9.2.3.4}$	$\tau(C_\alpha C)$
$S_{34} = \tau_{5.3.2.4}$	$\gamma(COO)$
$S_{35} = R_{13.14}$	$\nu(SH)$
$S_{36} = \tau_{2.3.5.10} + \tau_{4.3.5.10}$	$\tau(CO)$

Atom numbering is given in Figure 6.1a.

Table 6.2: Symmetry coordinates of serine

Coordinate	Description
$S_1 = R_{1.2}$	$\nu(NC_\alpha)$
$S_2 = R_{2.3}$	$\nu(C_\alpha C)$
$S_3 = \alpha_{1.2.3} + \alpha_{1.2.10} + \alpha_{3.2.10} - \alpha_{1.2.9} - \alpha_{3.2.9} - \alpha_{9.2.10}$	$\delta(NC_\alpha C)$
$S_4 = R_{1.7} + R_{1.8}$	$\nu_s(NH_2)$
$S_5 = R_{1.7} - R_{1.8}$	$\nu_a(NH_2)$
$S_6 = \alpha_{7.1.8}$	$\delta(NH_2)$
$S_7 = \alpha_{7.1.2} + \alpha_{8.1.2}$	$\omega(NH_2)$
$S_8 = \alpha_{7.1.2} - \alpha_{8.1.2}$	$\rho(NH_2)$
$S_9 = R_{2.10}$	$\nu(C_\alpha C_\beta)$
$S_{10} = R_{2.9}$	$\nu(C_\alpha H_\alpha)$
$S_{11} = \alpha_{1.2.9} - \alpha_{3.2.9}$	$\rho(C_\beta C_\alpha H_\alpha)$
$S_{12} = 2\alpha_{9.2.10} - \alpha_{1.2.9} - \alpha_{3.2.9}$	$\delta(C_\beta C_\alpha H_\alpha)$
$S_{13} = \alpha_{1.2.10} - \alpha_{3.2.10}$	$\rho(C_\beta C_\alpha C)$
$S_{14} = 2\alpha_{1.2.3} - \alpha_{1.2.10} - \alpha_{3.2.10}$	$\delta(C_\beta C_\alpha C)$
$S_{15} = R_{3.5}$	$\nu(C-O)$
$S_{16} = R_{3.4}$	$\nu(C=O)$
$S_{17} = R_{5.6}$	$\nu(OH)$
$S_{18} = 2\alpha_{2.3.5} - \alpha_{2.3.4} - \alpha_{4.3.5}$	$\delta(C-O)$
$S_{19} = \alpha_{2.3.4} - \alpha_{4.3.5}$	$\delta(C=O)$
$S_{20} = \alpha_{3.5.6}$	$\delta(COH)$
$S_{21} = R_{10.11} + R_{10.12}$	$\nu_s(C_\beta H_2)$
$S_{22} = R_{10.11} - R_{10.12}$	$\nu_a(C_\beta H_2)$
$S_{23} = R_{10.13}$	$\nu(C_\beta O)$
$S_{24} = 4\alpha_{11.10.12} - \alpha_{2.10.12} - \alpha_{2.10.11} - \alpha_{12.10.13} - \alpha_{11.10.13}$	$\delta(C_\beta H_2)$
$S_{25} = \alpha_{2.10.12} + \alpha_{2.10.11} - \alpha_{12.10.13} - \alpha_{11.10.13}$	$\omega(C_\beta H_2)$
$S_{26} = \alpha_{2.10.12} - \alpha_{2.10.11} - \alpha_{12.10.13} + \alpha_{11.10.13}$	$t(C_\beta H_2)$
$S_{27} = \alpha_{2.10.12} - \alpha_{2.10.11} + \alpha_{12.10.13} - \alpha_{11.10.13}$	$\rho(C_\beta H_2)$
$S_{28} = 5\alpha_{2.10.13} - \alpha_{11.10.12} - \alpha_{2.10.12} - \alpha_{2.10.11} - \alpha_{12.10.13} - \alpha_{11.10.13}$	$\delta(C_\alpha C_\beta O)$
$S_{29} = \tau_{11.10.13.14} + \tau_{12.10.13.14} + \tau_{2.10.13.14}$	$\tau(C_\beta O)$
$S_{30} = \alpha_{10.13.14}$	$\delta(C_\beta OH)$
$S_{31} = \tau_{7.1.2.9} + \tau_{7.1.2.3} + \tau_{7.1.2.10} + \tau_{8.1.2.9} + \tau_{8.1.2.3} + \tau_{8.1.2.10}$	$\tau(NC_\alpha)$
$S_{32} = \tau_{1.2.10.11} + \tau_{1.2.10.12} + \tau_{1.2.10.13} + \tau_{3.2.10.11} + \tau_{3.2.10.12} + \tau_{3.2.10.13} + \tau_{9.2.10.11} + \tau_{9.2.10.12} + \tau_{9.2.10.13}$	$\tau(C_\alpha C_\beta)$
$S_{33} = \tau_{1.2.3.5} + \tau_{9.2.3.5} + \tau_{10.2.3.5} + \tau_{1.2.3.4} + \tau_{9.2.3.4} + \tau_{10.2.3.4}$	$\tau(C_\alpha C)$
$S_{34} = \tau_{5.3.2.4}$	$\gamma(COO)$
$S_{35} = R_{13.14}$	$\nu(OH)$
$S_{36} = \tau_{2.3.5.6} + \tau_{4.3.5.6}$	$\tau(CO)$

Atom numbering is given in Figure 6.2a.

Table 6.3: 4-31G* optimized parameters of three conformations of cysteine and serine

			cysteine						serine		
			con1	con2	con3				con1	con2	con3
Rel. Energy(KJ/mol)			0	0.385	0.181	Rel. Energy(KJ/mol)			0	2.769	29.688
Bond length(A°)						Bond length(A°)					
1	2		1.443	1.439	1.442	1	2		1.447	1.455	1.445
1	6		1.001	1.001	1.001	1	7		1.003	1.001	1.003
1	7		1.003	1.003	1.002	1	8		1.001	1.004	1.001
2	3		1.523	1.523	1.523	2	3		1.517	1.530	1.524
2	8		1.082	1.087	1.086	2	9		1.083	1.087	1.086
2	9		1.534	1.531	1.530	2	10		1.534	1.524	1.536
3	4		1.185	1.184	1.184	3	4		1.186	1.186	1.180
3	5		1.327	1.331	1.328	3	5		1.327	1.315	1.331
5	10		.953	.954	.953	5	6		.953	.957	.949
9	11		1.081	1.080	1.079	10	11		1.090	1.082	1.088
9	12		1.083	1.078	1.079	10	12		1.080	1.082	1.082
9	13		1.811	1.821	1.819	10	13		1.389	1.399	1.387
13	14		1.325	1.327	1.326	13	14		.951	.950	.952
Bond angle(°)						Bond angle(°)					
6	1	2	110.774	110.296	110.135	7	1	2	109.928	111.364	109.396
7	1	2	109.859	109.793	109.575	8	1	2	111.144	109.442	111.051
6	1	7	106.363	106.509	105.666	7	1	8	106.395	107.466	106.293
1	2	3	112.505	113.158	112.771	1	2	3	113.021	108.728	113.160
1	2	8	109.155	108.279	108.233	1	2	9	108.946	107.939	108.342
1	2	9	110.446	110.772	111.109	1	2	10	108.586	114.521	108.022
3	2	8	107.507	105.240	105.929	3	2	9	107.947	105.865	108.963
3	2	9	109.120	112.497	111.945	3	2	10	110.940	110.030	110.788
8	2	9	107.965	106.427	106.443	9	2	10	107.222	109.385	107.379
2	3	4	124.891	124.963	124.791	2	3	4	124.928	122.478	123.278
2	3	5	112.295	112.509	112.394	2	3	5	112.168	114.864	115.859
4	3	5	122.809	122.493	122.788	4	3	5	122.897	122.650	120.839
3	5	10	108.532	108.259	108.334	3	5	6	108.556	108.353	112.506

Table 6.3. (Continued): 4-31G* optimized parameters of three conformations of cysteine and serine

				cysteine							serine		
				con1	con2	con3					con1	con2	con3
Torsions(°)							Torsions(°)						
6	1	2	3	-72.868	-51.611	-66.410	7	1	2	3	-41.313	-157.452	-40.467
7	1	2	3	44.350	65.460	49.415	8	1	2	3	76.211	83.873	76.547
6	1	2	8	46.382	64.644	50.441	7	1	2	9	-161.303	-43.048	-161.410
7	1	2	8	163.600	-178.285	166.266	8	1	2	9	-43.779	-161.724	-44.395
6	1	2	9	164.934	-179.009	166.970	7	1	2	10	82.230	79.033	82.565
7	1	2	9	-77.848	-61.938	-77.205	8	1	2	10	-160.246	-39.642	-160.421
1	2	3	4	-12.580	8.259	3.525	1	2	3	4	9.276	-151.950	14.317
1	2	3	5	168.212	-173.852	-178.347	1	2	3	5	-171.714	29.047	-167.454
8	2	3	4	-132.787	-109.781	-114.684	9	2	3	4	129.837	92.300	134.908
8	2	3	5	48.005	68.108	63.444	9	2	3	5	-51.153	-86.703	-46.863
9	2	3	4	110.364	134.747	129.699	10	2	3	4	-112.959	-25.791	-107.171
9	2	3	5	-68.844	-47.364	-52.173	10	2	3	5	66.051	155.206	71.058
1	2	9	11	175.724	-51.911	-58.636	1	2	10	11	-65.235	-56.369	-63.469
1	2	9	12	57.061	-170.533	-177.405	1	2	10	12	176.047	-175.241	178.127
1	2	9	13	-66.225	64.997	63.682	1	2	10	13	57.073	61.084	59.179
3	2	9	11	51.558	-179.671	174.290	3	2	10	11	59.546	-179.183	60.995
3	2	9	12	-67.105	61.707	55.521	3	2	10	12	-59.173	61.945	-57.409
3	2	9	13	169.609	-62.762	-63.392	3	2	10	13	-178.146	-61.730	-176.356
8	2	9	11	-65.001	65.576	58.986	9	2	10	11	177.193	64.921	179.880
8	2	9	12	176.337	-53.047	-59.783	9	2	10	12	58.475	-53.950	61.474
8	2	9	13	53.051	-177.516	-178.696	9	2	10	13	-60.499	-177.626	-57.473
2	9	13	14	56.196	78.872	-75.643	2	10	13	14	-46.956	79.454	-48.838
11	9	13	14	176.964	-162.909	46.416	11	10	13	14	74.068	-161.753	72.157
12	9	13	14	-67.030	-46.601	162.802	12	10	13	14	-167.646	-43.485	-170.316
2	3	5	10	178.692	-177.141	-179.655	2	3	5	6	-178.595	-8.480	4.133
4	3	5	10	-.536	.809	-1.483	4	3	5	6	.439	172.519	-177.592

Energy of the minimum energy conformation of cysteine is -718.6580943 hartrees and serine is -396.3384823 hartrees.

Table 6.4: Calculated frequencies of three geometries of cysteine

Freq.	Unscaled			Scaled			Raman Intensities			I. R. Intensities		
	Con1	Con2	Con3	Con1	Con2	Con3	Con1	Con2	Con3	Con1	Con2	Con3
1	57	58	62	51	52	55	3.3	1.7	4.7	.4	1.1	.7
2	113	97	85	101	87	76	2.0	1.0	.3	.6	.8	1.2
3	192	202	194	172	181	174	.2	.2	1.8	.4	.8	.9
4	240	254	220	215	227	197	16.0	13.2	61.1	1.6	8.2	6.5
5	266	280	280	239	251	250	6.4	22.5	7.4	3.3	1.0	1.0
6	311	315	346	278	281	310	53.8	46.2	12.7	8.5	4.4	5.0
7	341	377	381	307	339	342	14.5	30.2	25.5	3.4	1.5	2.9
8	415	497	487	374	447	438	21.9	10.7	13.2	1.7	3.7	2.9
9	547	532	536	493	480	484	16.4	12.6	12.1	.5	1.3	1.2
10	630	632	636	566	573	575	105.1	36.9	57.6	4.5	4.0	4.4
11	713	684	677	642	618	612	28.3	119.9	107.5	3.1	6.4	5.0
12	759	739	745	698	687	696	53.0	5.3	3.2	14.4	12.4	15.1
13	842	814	820	755	748	743	21.9	41.0	44.1	3.6	6.2	5.6
14	871	853	832	813	769	759	22.5	2.1	5.5	5.2	5.2	3.6
15	960	947	962	875	859	872	82.7	45.4	33.7	10.8	3.8	6.0
16	1036	1037	1030	942	940	942	28.6	94.1	61.7	4.5	4.1	4.0
17	1047	1047	1051	957	967	962	71.6	53.2	78.5	1.8	5.6	4.3
18	1128	1163	1160	1023	1050	1050	60.6	102.9	85.2	7.5	4.3	3.8
19	1247	1243	1240	1130	1125	1126	21.5	15.7	12.8	3.5	3.7	3.9
20	1268	1281	1291	1169	1172	1182	72.1	125.0	209.9	5.6	3.5	2.7
21	1310	1318	1328	1199	1203	1205	206.9	125.7	74.4	4.5	3.3	5.9
22	1391	1395	1379	1246	1265	1255	13.7	4.2	6.8	7.2	13.4	8.8
23	1441	1443	1437	1296	1300	1292	2.0	12.3	8.9	7.3	3.5	5.1
24	1470	1465	1468	1322	1313	1316	10.2	17.4	18.0	2.0	1.1	2.2
25	1515	1525	1518	1373	1377	1374	46.5	15.4	23.9	2.2	4.8	3.5
26	1575	1552	1567	1431	1414	1424	20.0	15.1	15.0	4.8	2.8	3.6
27	1625	1610	1612	1453	1443	1446	4.0	8.4	8.7	12.9	11.5	11.8
28	1850	1847	1850	1655	1652	1656	33.5	39.4	36.5	5.1	5.0	4.1
29	2040	2047	2046	1926	1933	1932	380.6	364.3	362.2	6.0	6.1	5.6
30	2873	2851	2856	2726	2704	2710	3.0	13.8	10.1	99.8	109.2	112.2
31	3239	3201	3214	3073	3037	3049	20.3	19.6	17.4	99.0	101.9	94.4
32	3268	3281	3280	3100	3112	3112	12.0	15.7	18.7	42.6	93.9	94.8
33	3307	3338	3335	3137	3167	3164	9.7	5.4	5.8	53.2	65.0	65.8
34	3726	3727	3729	3535	3536	3538	5.7	5.3	4.5	77.5	72.1	72.3
35	3807	3808	3805	3611	3613	3610	7.5	9.0	6.5	60.5	48.4	54.3
36	4034	4033	4037	3827	3826	3830	125.8	119.9	122.6	100.4	87.0	89.6

Harmonic frequencies are in units of (cm^{-1}), IR intensities are in units of (KM/Mole) and Raman activities are in units of (A^4/AMU)

Table 6.5: Calculated frequencies of three geometries of serine

Freq.	Unscaled			Scaled			Raman Intensities			I. R. Intensities		
	Con1	Con2	Con3	Con1	Con2	Con3	Con1	Con2	Con3	Con1	Con2	Con3
1	60	80	73	53	71	66	.4	.6	.8	3.9	3.8	11.7
2	142	133	139	127	119	125	.1	.1	.1	8.6	11.2	15.0
3	208	240	209	186	215	187	.5	.2	.4	3.6	4.4	16.9
4	270	322	280	242	288	251	.9	.3	1.0	13.0	18.8	12.4
5	312	370	313	279	331	280	.1	1.0	.3	4.4	27.2	13.2
6	373	406	375	337	364	338	1.6	.6	1.4	2.9	17.8	15.7
7	440	505	439	400	453	399	2.4	2.9	2.8	32.2	144.5	13.4
8	550	537	508	493	484	455	2.5	1.9	1.5	152.1	20.3	84.6
9	569	614	551	512	558	494	1.0	2.3	2.2	33.6	24.2	192.9
10	637	670	576	571	602	518	2.7	2.3	1.8	130.5	13.0	45.2
11	719	807	732	647	722	659	3.0	2.0	1.7	31.5	139.0	12.7
12	810	846	798	735	774	725	4.7	5.9	3.4	49.6	16.7	7.0
13	944	919	948	868	840	873	6.4	7.0	6.6	78.6	8.1	35.3
14	989	977	988	908	903	908	3.4	2.7	3.5	32.3	41.7	8.9
15	1073	1041	1074	967	932	968	.7	2.1	.5	139.9	102.7	170.2
16	1122	1104	1125	1024	1016	1028	2.4	3.6	2.6	27.1	110.9	46.2
17	1219	1192	1222	1132	1088	1133	4.9	1.8	4.7	146.4	43.7	146.2
18	1248	1233	1246	1159	1156	1159	4.3	5.5	2.6	57.0	73.9	8.1
19	1286	1298	1277	1171	1164	1163	2.1	2.3	4.1	20.1	5.0	1.4
20	1314	1346	1298	1206	1235	1188	2.9	2.2	3.5	234.2	2.3	30.1
21	1401	1365	1396	1256	1245	1254	6.0	5.3	4.7	5.7	15.3	120.4
22	1422	1462	1423	1280	1319	1280	3.7	5.2	3.7	14.7	83.2	23.6
23	1489	1527	1472	1344	1367	1339	4.2	10.1	2.4	52.6	32.2	326.0
24	1524	1538	1521	1373	1382	1369	9.6	3.4	10.6	11.9	199.8	29.2
25	1580	1552	1582	1423	1397	1422	3.1	1.2	5.0	30.4	111.1	20.3
26	1590	1586	1589	1440	1447	1431	2.0	1.2	1.5	77.3	231.1	82.0
27	1674	1658	1671	1497	1483	1494	10.1	9.0	9.9	.9	3.9	.1
28	1848	1837	1849	1654	1644	1654	4.8	5.8	4.6	35.7	47.2	40.4
29	2040	2049	2073	1927	1933	1957	5.8	5.7	8.9	367.9	345.8	315.8
30	3162	3215	3181	2999	3050	3018	89.7	64.3	99.9	71.4	14.8	47.4
31	3258	3244	3223	3091	3078	3058	60.5	105.7	49.7	14.4	52.5	28.6
32	3302	3286	3265	3133	3118	3097	71.7	66.5	70.5	35.3	39.8	60.7
33	3727	3719	3725	3536	3529	3535	73.4	72.7	71.4	6.8	10.9	9.3
34	3808	3810	3806	3613	3614	3611	59.1	63.6	58.1	9.4	13.1	11.6
35	4034	3944	4046	3827	3742	3839	87.8	29.7	37.5	123.4	206.3	82.0
36	4048	4074	4091	3840	3865	3881	39.2	37.3	38.3	77.9	75.7	84.5

Harmonic frequencies are in units of (cm^{-1}), IR intensities are in units of (KM/Mole) and Raman activities are in units of (A^4/AMU)

Table 6.6: Potential energy distributions of the three conformations of cysteine

	Conformation I		Conformation II		Conformation III	
	Freq.	PED	Freq.	PED	Freq.	PED
1	51	33(63.2), 3(11.5)	52	33(72.0)	55	33(66.1)
2	101	32(82.4)	87	32(65.7), 3(10.1)	76	32(55.5)
3	172	13(42.6),28(20.8),34(10.0)	181	28(49.1), 3(17.2),32(12.2)	174	28(50.1), 3(19.2)
4	215	31(70.4),29(18.1)	227	29(49.6),31(25.6)	197	31(56.6),29(35.3)
5	239	28(30.8),14(22.9),29(16.3), 18(12.9)	251	31(32.7),19(25.6),14(16.1), 13(10.7)	250	18(32.8),14(22.8),13(14.5), 19(10.9)
6	278	29(48.7),31(12.0), 3(10.2) -	281	31(32.2),29(31.5),19(13.2), 14(10.7)	310	29(45.9),31(14.3),14(10.2) -
7	307	3(21.4),18(16.7),29(14.3), 19(12.9)	339	13(37.7) -	342	13(35.9),29(17.8) -
8	374	14(29.2),13(18.8), 3(11.0) -	447	34(22.9),28(17.2),14(13.3), 3(12.6)	438	34(22.1),28(16.8),14(15.7), 18(12.1),3(10.6)
9	493	18(42.1), 3(14.1),13(12.4)	480	19(22.0),13(17.3),18(17.2)	484	18(35.6),13(16.2)
10	566	36(72.3),34(10.2) -	573	18(25.9),36(16.8),14(16.7), 19(11.3)	575	36(31.2),19(29.6),14(14.8), 14(14.8)
11	642	19(54.4)	618	36(63.9)	612	36(49.1),19(19.8)
12	698	23(33.6),34(23.5),36(13.1)	687	23(58.0)	696	23(64.1)
13	755	27(40.5),30(30.5)	748	34(23.1), 2(17.9),18(17.0)	743	27(35.7),30(25.3),34(15.9)
14	813	23(42.6), 2(16.5)	769	27(44.2),30(27.6)	759	2(22.9),27(13.2),19(11.3)
15	875	7(24.3), 2(15.2)	859	34(19.4), 3(17.8),2(16.4)	872	34(17.8), 3(17.7), 2(12.7)
16	942	7(32.7), 9(12.1)	940	7(50.2), 6(16.0)	942	7(51.7), 9(15.6), 6(14.8)
17	957	30(35.1), 9(20.0), 1(14.2), 26(11.6)	967	9(27.7),30(21.1),1(15.4) -	962	30(27.0), 1(20.2), 9(15.2), 27(10.5)
18	1023	2(12.9), 9(11.6), 8(11.4)	1050	30(19.5),27(17.2)	1050	27(16.8),30(15.6), 2(10.4)
19	1130	26(29.8), 8(22.7),12(20.3)	1125	12(38.9), 8(31.4),25(10.8)	1126	12(34.7), 8(27.0),25(11.3)
20	1169	1(41.6), 9(15.7) -	1172	26(26.4), 1(22.9) -	1182	26(19.1), 1(15.1),20(13.9), 8(12.7),15(12.6),11(12.5)
21	1199	15(28.4),20(28.0),11(13.2)	1203	20(40.2),15(32.2),26(17.8)	1205	20(33.0),26(28.0),15(27.4)
22	1246	20(24.9),25(23.9),12(20.8), 11(14.8)	1265	1(18.9),26(17.7),11(15.5), 9(13.4)	1255	1(21.4), 9(16.3),25(10.6), 26(10.5)
23	1296	26(38.9), 8(24.2), 1(14.4) -	1300	11(23.9),20(21.2),26(11.6) -	1292	20(20.8),11(19.4),12(18.9), 26(12.7)
24	1322	25(51.5),11(11.0)	1313	25(69.9),	1316	25(68.1)
25	1373	12(32.0), 8(11.0),15(10.4), 9(10.3)	1377	12(28.7), 8(27.7),11(13.8), 9(12.5)	1374	12(30.6), 8(20.2),11(11.8) -
26	1431	11(31.0),15(20.4), 2(16.4), 19(10.6)	1414	15(20.0),11(18.4),2(17.8), 24(13.6)	1424	24(24.2),11(19.5),15(16.0), 2(14.5)
27	1453	24(95.1)	1443	24(79.9)	1446	24(68.5)
28	1655	6(71.5), 7(24.5)	1652	6(71.0), 7(25.1)	1656	6(71.9), 7(24.3)
29	1926	16(83.0)	1933	16(83.0)	1932	16(82.9)
30	2726	35(100.0)	2704	35(100.0)	2710	35(100.0)
31	3073	21(83.0),22(12.8)	3037	10(98.7)	3049	10(98.4)
32	3100	10(93.5)	3112	21(97.5)	3112	21(98.5)
33	3137	22(86.9),21(10.5)	3167	22(98.2)	3164	22(99.4)
34	3535	4(99.1)	3536	4(98.8)	3538	4(99.5)
35	3611	5(99.2)	3613	5(98.9)	3610	5(99.5)
36	3827	17(99.9)	3826	17(99.9)	3830	17(99.9)

Symmetry coordinate numbers given in Table 6.1

Table 6.7: Potential energy distributions of the three conformations of serine

	Conformation I		Conformation II		Conformation III	
	Freq.	PED	Freq.	PED	Freq.	PED
1	53	33(69.3), 3(11.4)	71	33(65.0),36(12.8)	66	33(71.3)
2	127	32(71.7),29(10.9)	119	32(71.0),13(12.2)	125	32(72.3),29(11.7)
3	186	13(46.9),14(15.6),34(10.9)	215	3(34.2),28(33.4)	187	13(44.0),14(14.8),34(13.7)
4	242	31(73.8),29(14.7) -	288	18(22.0),14(21.0),13(20.4), 31(10.2)	251	31(75.6),29(13.7) -
5	279	18(28.8),14(19.9),28(12.2), 3(11.8)	331	31(54.1),36(14.5) -	280	18(27.3),14(24.1),28(14.2), 3(10.9)
6	337	3(24.5),28(20.2),34(10.3)	364	13(25.7),14(18.2),31(18.2)	338	3(23.6),28(21.0)
7	400	14(19.0), 2(16.6),28(13.2), 18(11.3)	453	29(76.8) -	399	14(19.7), 2(17.0),28(12.5), 18(11.2)
8	493	29(85.4)	484	18(21.3), 3(12.6)	455	36(90.7)
9	512	18(31.6), 3(16.9),13(12.2)	558	19(44.1), 2(16.8)	494	29(85.5)
10	571	36(72.4) -	602	28(27.8),14(24.3),34(19.6), 18(14.0)	518	18(30.6), 3(18.4),13(11.5) -
11	647	19(50.1)	722	36(93.4)	659	19(42.1),34(18.7),28(11.3)
12	735	34(43.6),36(12.8), 9(11.1)	774	34(20.6),19(20.6),2(14.3)	725	34(41.9),19(18.5), 9(13.2)
13	868	1(22.2), 7(15.1), 2(14.2) -	840	34(17.2), 2(15.6),3(15.1), 9(14.7)	873	1(21.3),27(13.9), 2(11.5) -
14	908	27(24.9), 9(21.5), 7(20.5) -	903	1(19.9),27(18.0),9(15.4), 7(15.3), 2(10.7)	908	27(23.0), 7(19.2), 9(16.0), 2(15.5)
15	967	7(24.4),27(15.7), 8(11.7)	932	7(38.7),27(35.9)	968	7(29.5),27(12.2), 8(10.5)
16	1024	9(15.3), 8(14.4), 2(12.8) 27(12.0)	1016	23(17.5),12(17.1), -	1028	9(15.7), 8(13.5),27(12.9), 2(12.2)
17	1132	23(33.8),30(24.4),26(20.0) -	1088	1(20.3), 8(15.5),30(13.6), 11(10.4),26(10.4)	1133	23(28.0),30(24.9),26(21.9) -
18	1159	1(27.8), 9(16.0),12(11.7) -	1156	23(67.4) -	1159	1(35.0),12(16.5),15(16.0), 9(11.0)
19	1171	23(36.8), 1(12.0),15(10.0) -	1164	8(25.6),11(24.0),26(19.2), 30(12.4)	1163	23(36.6),11(12.4), 8(11.0), 20(10.1)
20	1206	20(32.8),15(27.5)	1235	1(26.6), 8(14.4),26(14.2)	1188	23(22.0),20(21.6),26(12.3)
21	1256	12(34.3),11(19.9),20(19.6)	1245	20(29.5),15(29.1)	1254	12(24.9),20(23.3),11(18.8)
22	1280	8(20.2),26(18.7), 1(14.6), 30(11.3)	1319	12(36.4),20(22.7),9(13.2) -	1280	8(17.1),26(15.8), 1(14.6), 30(12.8),12(11.2),27(10.2)
23	1344	25(20.2),26(15.6),30(14.6) -	1367	30(38.3),26(15.9),11(15.9) -	1339	15(22.8),20(13.6),25(12.2), 26(11.8)
24	1373	12(19.8),26(16.1),30(14.7) -	1382	11(19.3),12(15.6),26(13.9) -	1369	30(19.4),26(17.7),12(14.9), 15(10.6)
25	1423	25(55.3),30(18.8)	1397	25(66.7), 9(11.9)	1422	25(55.4),30(17.2)
26	1440	11(28.2),15(21.0), 2(16.7), 19(10.7)	1447	15(29.5), 2(18.1),20(17.2) -	1431	11(38.2),15(12.6), 2(10.4) -
27	1497	24(94.9)	1483	24(94.3)	1494	24(95.1)
28	1654	6(71.5), 7(24.4)	1644	6(73.4), 7(22.9)	1654	6(71.8), 7(24.2)
29	1927	16(82.8)	1933	16(80.6)	1957	16(84.5)
30	2999	21(62.6),22(36.4)	3050	10(92.4)	3018	21(67.9),22(29.0)
31	3091	10(97.3)	3078	21(92.6)	3058	10(94.0)
32	3133	22(63.8),21(34.1) 3	3118	22(99.2)	3097	22(70.9),21(25.7)
33	3536	4(98.5)	3529	4(95.7)	3535	4(98.5)
34	3613	5(98.6)	3614	5(96.0)	3611	5(98.6)
35	3827	17(99.9)	3742	17(99.9)	3839	35(99.9)
36	3840	35(99.9)	3865	35(99.9)	3881	17(99.9)

Symmetry coordinate numbers given in Table 6.2

Table 6.8: Assignment of frequencies of the methyl ester, hydrochloride and zwitterion of cysteine

Mode*	Observed frequency in			Calculated
	Methyl ester	Hydrochloride	Zwitterion	frequencies
$\nu(OH)$	-	3377	-	3827,3826,3830
$\nu_a(NH_2)$	3360	-	-	3611,3613,3610
$\nu_s(NH_2)$	3295	-	-	3535,3536,3538
$\nu_a(C_\beta H_2)$	3000	-	2998	3137,3167,3164
$\nu_s(C_\beta H_2)$	2953	2943	2961	3073,3112,3112
$\nu(C_\alpha H_\alpha)$	2953	2943	2961	3100,3037,3049
$\nu(SH)$	-	2553	2551	2726,2704,2710
$\nu(C=O)$	1735	1743	-	1926,1933,1932
$\delta(NH_2)$	1593	-	-	1655,1652,1656
$\delta(C_\beta H_2)$	1437	1428	1424	1453,1443,1446
$\rho(C_\beta C_\alpha H_\alpha) + \nu(C-O) + \delta(C_\beta H_2)$	1408	1399	1397	1431,1300,1424
$\underline{\delta(C_\beta C_\alpha H_\alpha) + \rho(NH_2)}$	1377	1348	1344	1373,1125,1126
$\underline{\omega(C_\beta H_2)}$	1313	1316	1303	1322,1313,1316
$t(C_\beta H_2) + \delta(C_\beta C_\alpha H_\alpha) + \rho(NH_2)$	1243	1222	1269	1296,1377,1374
$\underline{\delta(COH) + \nu(C-O) + \omega(C_\beta H_2)}$	1205	1203	1198	1246,1203,1205
$\underline{\nu(C-O) + \delta(COH) + \rho(C_\beta C_\alpha H_\alpha)}$	1176	1141	1140	1199,1414,1292
$\underline{\nu(NC_\alpha) + \nu(C_\alpha C_\beta) + t(C_\beta H_2)}$	1176	1141	1140	1169,1265,1255
$\underline{t(C_\beta H_2) + \nu(NC_\alpha) + \rho(NH_2)}$	1118	1108	1106	1130,1172,1182
$\underline{\nu(C_\alpha C) + \rho(C_\beta H_2) + \nu(C_\alpha C_\beta) + \delta(C_\beta SH)}$	1009	1059	1004	1023,967,1050
$\delta(C_\beta SH)$	942	931	931	957,1050,962
$\underline{\omega(NH_2) + \nu(C_\alpha C_\beta) + \delta(NH_2)}$	882	-	-	942,940,942
$\underline{\gamma(COO) + \nu(C_\alpha C) + \delta(NC_\alpha C) + \delta(NH_2)}$	-	868	-	875,859,872
$\underline{\rho(C_\beta H_2) + \delta(C_\beta SH)}$	781	777	773	755,769,743
$\underline{\nu(C_\beta S) + \gamma(COO) + \nu(C_\alpha C)}$	736	738	696	813,748,759
$\nu(C_\beta S)$	637	646	642	698,687,696
$\underline{\delta(C=O) + \tau(CO)}$	618	596	-	642,480,575
$\underline{\tau(CO)}$	-	524	-	566,618,612
$\underline{\delta(C-O) + \rho(C_\beta C_\alpha C)}$	-	458	441	493,573,484
$\underline{\delta(C_\beta C_\alpha C) + \gamma(COO) + \delta(NC_\alpha C)}$	-	403	364	374,447,438
$\rho(C_\beta C_\alpha C)$	-	-	298	172,339,342
$\underline{\tau(C_\beta S) + \tau(NC_\alpha)}$	-	-	268	278,227,310
$\underline{\delta(NC_\alpha C) + \delta(C-O) + \tau(NC_\alpha) + \delta(C=O)}$	-	-	210	307,281,250
$\underline{\tau(NC_\alpha) + \tau(C_\beta S)}$	-	-	148	215,251,197
$\underline{\delta(C_\alpha C_\beta S)}$	-	-	148	239,181,174
$\tau(C_\alpha C_\beta)$	-	-	118	101,87,76
$\tau(C_\alpha C)$	-	-	-	51,52,55

(*): The underlined modes are dominant modes in all the three conformations. The modes given are contributions to that frequency from all the three conformations. Thus the contribution of a given mode in a particular conformation can be even zero.Zwitterion frequencies from reference [26]

Table 6.9: Assignment of frequencies of the methyl ester, hydrochloride and zwitterion of serine

Mode*	Observed frequency in			Calculated
	Methyl ester	Hydrochloride	Zwitterion	frequencies
$\nu(OH_{alc})$	-	-	-	3840,3865,3881
$\nu(OH_{ac})$	-	3385	-	3827,3742,3839
$\nu_a(NH_2)$	3362	-	-	3613,3614,3611
$\nu_s(NH_2)$	3280	-	-	3536,3529,3535
$\nu_a(C_\beta H_2)$	-	-	2975	3133,3118,3097
$\nu_s(C_\beta H_2)$	2956	-	2945	2999,3078,3018
$\nu(C_\alpha H_\alpha)$	2956	-	2945	3091,3050,3058
$\nu(C=O)$	1735	1734	-	1927,1933,1957
$\delta(NH_2)$	1596	-	-	1654,1644,1654
$\delta(C_\beta H_2)$	1450	-	1450	1497,1483,1494
$\underline{\rho(C_\beta C_\alpha H_\alpha)} + \nu(C-O)$	-	1408	1435	1440,1382,1431
$\underline{\omega(C_\beta H_2)}$	1378	-	1364	1423,1397,1422
$\delta(C_\beta C_\alpha H_\alpha) + \delta(C_\beta OH) + t(C_\beta H_2)$	1346	1344	1352	1373,1367,1369
$t(C_\beta H_2) + \delta(C_\beta OH) + \nu(C-O)$ + $\omega(C_\beta H_2)$	1309	-	1312	1344,1447,1339
$\underline{\rho(NH_2)} + t(C_\beta H_2) + \nu(NC_\alpha)$	1227	1242	1248	1280,1164,1280
$\underline{\delta(C_\beta C_\alpha H_\alpha)} + \rho(C_\beta C_\alpha H_\alpha) + \delta(COH)$	1227	1242	1248	1256,1319,1354
$\underline{\delta(COH)} + \nu(C_\beta O + \nu(C-O)$	1177	-	1180	1206,1245,1188
$\nu(C_\beta O)$	1177	-	1180	1171,1156,1163
$\underline{\nu(NC_\alpha)} + \nu(C_\alpha C_\beta)$	1131	1132	1162	1159, 1235,1159
$\underline{\nu(C_\beta O)} + \delta(C_\beta OH)$	1064	1077	1095	1132,1016,1133
$\underline{\nu(C_\alpha C_\beta)} + \nu(NC_\alpha) + \rho(NH_2)$	1044	1025	1030	1024,1088,1028
$\underline{\omega(NH_2)} + \rho(C_\beta H_2)$	945	970	983	967,932,968
$\underline{\rho(C_\beta H_2)} + \nu(C_\alpha C_\beta) + \nu(NC_\alpha)$ + $\gamma(COO)$	900	903	901	908,840,908
$\underline{\nu(NC_\alpha)} + \omega(NH_2) + \rho(C_\beta H_2)$	857	829	849	868,903,873
$\underline{\gamma(COO)}$	778	767	-	735,774,725
$\delta(C=O)$	635	-	-	647,558,659
$\tau(CO)$	562	538	566	571,722,455
$\underline{\delta(C-O)} + \delta(NC_\alpha C)$	514	538	525	512,484,518
$\underline{\tau(C_\beta O)}$	480	-	499	493,453,494
$\underline{\delta(C_\beta C_\alpha C)} + \nu(C_\alpha C) + \delta(C_\alpha C_\beta O)$	-	-	-	400,602,399
$\underline{\delta(NC_\alpha C)} + \delta(C_\alpha C_\beta O)$	-	-	-	337,215,338
$\underline{\rho(C_\beta C_\alpha C)} + \delta(C_\beta C_\alpha C)$	-	-	-	186,364,187
$\underline{\delta(C-O)} + \delta(C_\beta C_\alpha C)$	-	-	-	279,288,280
$\underline{\tau(NC_\alpha)} + \tau(C_\beta O) + \tau(CO)$	-	-	-	242,331,251
$\underline{\tau(C_\alpha C_\beta)} + \tau(C_\beta O)$	-	-	-	127,119,125
$\tau(C_\alpha C)$	-	-	-	53,71,66

(*): The underlined modes are dominant modes in all the three conformations. The modes given are contributions to that frequency from all the three conformations. Thus the contribution of a given mode in a particular conformation can be even zero. Zwitterion frequencies from reference [27]

Table 6.10: Symmetry coordinates of cysteine zwitterion

Coordinate	Description
$S_1 = R_{13.14}$	$\nu(SH)$
$S_2 = R_{1.4} - R_{1.5}$	$\nu_a(NH_3^+)$
$S_3 = 2R_{1.3} - R_{1.4} - R_{1.5}$	$\nu_s'(NH_3^+)$
$S_4 = R_{1.3} + R_{1.4} + R_{1.5}$	$\nu_s(NH_3^+)$
$S_5 = R_{6.11} + R_{6.12}$	$\nu_s(C_\beta H_2)$
$S_6 = R_{6.11} - R_{6.12}$	$\nu_a(C_\beta H_2)$
$S_7 = R_{2.8}$	$\nu(C_\alpha H_\alpha)$
$S_8 = R_{7.9} - R_{7.10}$	$\nu_a(COO^-)$
$S_9 = R_{7.9} + R_{7.10}$	$\nu_s(COO^-)$
$S_{10} = R_{6.13}$	$\nu(C_\beta S)$
$S_{11} = R_{1.2}$	$\nu(NC_\alpha)$
$S_{12} = R_{2.7}$	$\nu(C_\alpha C)$
$S_{13} = R_{2.6}$	$\nu(C_\alpha C_\beta)$
$S_{14} = 2\alpha_{9.7.10} - \alpha_{2.7.9} - \alpha_{2.7.10}$	$\delta(COO^-)$
$S_{15} = \alpha_{2.7.9} - \alpha_{2.7.10}$	$\rho(COO^-)$
$S_{16} = 2\alpha_{3.1.4} - \alpha_{3.1.5} - \alpha_{4.1.5}$	$\delta_s'(NH_3^+)$
$S_{17} = \alpha_{3.1.5} - \alpha_{4.1.5}$	$\delta_a(NH_3^+)$
$S_{18} = 2\alpha_{2.1.5} - \alpha_{2.1.3} - \alpha_{2.1.4}$	$\gamma_\parallel(NH_3^+)$
$S_{19} = \alpha_{2.1.3} - \alpha_{2.1.4}$	$\gamma_\perp(NH_3^+)$
$S_{20} = \alpha_{3.1.4} + \alpha_{3.1.5} + \alpha_{4.1.5} - \alpha_{2.1.3} - \alpha_{2.1.4} - \alpha_{2.1.5}$	$\delta_s(NH_3^+)$
$S_{21} = 2\alpha_{6.2.8} - \alpha_{1.2.8} - \alpha_{7.2.8}$	$\delta(C_\beta C_\alpha H_\alpha)$
$S_{22} = \alpha_{1.2.8} - \alpha_{7.2.8}$	$\rho(C_\beta C_\alpha H_\alpha)$
$S_{23} = 2\alpha_{1.2.7} - \alpha_{1.2.6} - \alpha_{6.2.7}$	$\delta(C_\beta C_\alpha C)$
$S_{24} = \alpha_{1.2.6} - \alpha_{6.2.7}$	$\rho(C_\beta C_\alpha C)$
$S_{25} = \alpha_{1.2.6} + \alpha_{1.2.7} + \alpha_{6.2.7} - \alpha_{1.2.8} - \alpha_{6.2.8} - \alpha_{7.2.8}$	$\delta(NC_\alpha C)$
$S_{26} = 4\alpha_{11.6.12} - \alpha_{2.6.11} - \alpha_{2.6.12} - \alpha_{11.6.13} - \alpha_{12.6.13}$	$\delta(C_\beta H_2)$
$S_{27} = \alpha_{2.6.11} + \alpha_{2.6.12} - \alpha_{11.6.13} - \alpha_{12.6.13}$	$\omega(C_\beta H_2)$
$S_{28} = \alpha_{2.6.11} - \alpha_{2.6.12} - \alpha_{11.6.13} + \alpha_{12.6.13}$	$t(C_\beta H_2)$
$S_{29} = \alpha_{2.6.11} - \alpha_{2.6.12} + \alpha_{11.6.13} - \alpha_{12.6.13}$	$\rho(C_\beta H_2)$
$S_{30} = 5\alpha_{2.6.13} - \alpha_{11.6.12} - \alpha_{2.6.11} - \alpha_{2.6.12} - \alpha_{11.6.13} - \alpha_{12.6.13}$	$\delta(C_\alpha C_\beta S)$
$S_{31} = \alpha_{6.13.14}$	$\delta(C_\beta SH)$
$S_{32} = \tau_{9.7.2.10}$	$\gamma(COO^-)$
$S_{33} = \tau_{2.6.13.14} + \tau_{11.6.13.14} + \tau_{12.6.13.14}$	$\tau(C_\beta S)$
$S_{34} = \tau_{3.1.2.6} + \tau_{3.1.2.7} + \tau_{3.1.2.8} + \tau_{4.1.2.6} + \tau_{4.1.2.7} + \tau_{4.1.2.8} + \tau_{5.1.2.6} + \tau_{5.1.2.7} + \tau_{5.1.2.8}$	$\tau(NC_\alpha)$
$S_{35} = \tau_{1.2.7.9} + \tau_{6.2.7.9} + \tau_{8.2.7.9} + \tau_{1.2.7.10} + \tau_{6.2.7.10} + \tau_{8.2.7.10}$	$\tau(C_\alpha C)$
$S_{36} = \tau_{1.2.6.11} + \tau_{1.2.6.12} + \tau_{1.2.6.13} + \tau_{7.2.6.11} + \tau_{7.2.6.12} + \tau_{7.2.6.13} + \tau_{8.2.6.11} + \tau_{8.2.6.12} + \tau_{8.2.6.13}$	$\tau(C_\alpha C_\beta)$

Atom numbering is given in Figure 6.5.

Table 6.11: Symmetry coordinates of serine zwitterion

Coordinate	Description
$S_1 = R_{11.14}$	$\nu(OH)$
$S_2 = R_{1.4} - R_{1.5}$	$\nu_a(NH_3^+)$
$S_3 = 2R_{1.3} - R_{1.4} - R_{1.5}$	$\nu_s'(NH_3^+)$
$S_4 = R_{1.3} + R_{1.4} + R_{1.5}$	$\nu_s(NH_3^+)$
$S_5 = R_{7.12} + R_{7.13}$	$\nu_s(C_\beta H_2)$
$S_6 = R_{7.12} - R_{7.13}$	$\nu_a(C_\beta H_2)$
$S_7 = R_{2.8}$	$\nu(C_\alpha H_\alpha)$
$S_8 = R_{6.9} - R_{6.10}$	$\nu_a(COO^-)$
$S_9 = R_{6.9} + R_{6.10}$	$\nu_s(COO^-)$
$S_{10} = R_{7.13}$	$\nu(C_\beta O)$
$S_{11} = R_{1.2}$	$\nu(NC_\alpha)$
$S_{12} = R_{2.6}$	$\nu(C_\alpha C)$
$S_{13} = R_{2.7}$	$\nu(C_\alpha C_\beta)$
$S_{14} = 2\alpha_{9.6.10} - \alpha_{2.6.9} - \alpha_{2.6.10}$	$\delta(COO^-)$
$S_{15} = \alpha_{2.6.9} - \alpha_{2.6.10}$	$\rho(COO^-)$
$S_{16} = 2\alpha_{3.1.4} - \alpha_{3.1.5} - \alpha_{4.1.5}$	$\delta_s'(NH_3^+)$
$S_{17} = \alpha_{3.1.5} - \alpha_{4.1.5}$	$\delta_a(NH_3^+)$
$S_{18} = 2\alpha_{2.1.5} - \alpha_{2.1.3} - \alpha_{2.1.4}$	$\gamma_\parallel(NH_3^+)$
$S_{19} = \alpha_{2.1.3} - \alpha_{2.1.4}$	$\gamma_\perp(NH_3^+)$
$S_{20} = \alpha_{3.1.4} + \alpha_{3.1.5} + \alpha_{4.1.5} - \alpha_{2.1.3} - \alpha_{2.1.4} - \alpha_{2.1.5}$	$\delta_s(NH_3^+)$
$S_{21} = 2\alpha_{7.2.8} - \alpha_{1.2.8} - \alpha_{6.2.8}$	$\delta(C_\beta C_\alpha H_\alpha)$
$S_{22} = \alpha_{1.2.8} - \alpha_{6.2.8}$	$\rho(C_\beta C_\alpha H_\alpha)$
$S_{23} = 2\alpha_{1.2.6} - \alpha_{1.2.7} - \alpha_{6.2.7}$	$\delta(C_\beta C_\alpha C)$
$S_{24} = \alpha_{1.2.7} - \alpha_{6.2.7}$	$\rho(C_\beta C_\alpha C)$
$S_{25} = \alpha_{1.2.6} + \alpha_{1.2.7} + \alpha_{6.2.7} - \alpha_{1.2.8} - \alpha_{6.2.8} - \alpha_{7.2.8}$	$\delta(NC_\alpha C)$
$S_{26} = 4\alpha_{12.7.13} - \alpha_{2.7.12} - \alpha_{2.7.13} - \alpha_{11.7.12} - \alpha_{11.7.13}$	$\delta(C_\beta H_2)$
$S_{27} = \alpha_{2.7.12} + \alpha_{2.7.13} - \alpha_{11.7.12} - \alpha_{11.7.13}$	$\omega(C_\beta H_2)$
$S_{28} = \alpha_{2.7.12} - \alpha_{2.7.13} - \alpha_{11.7.12} + \alpha_{11.7.13}$	$t(C_\beta H_2)$
$S_{29} = \alpha_{2.7.12} - \alpha_{2.7.13} + \alpha_{11.7.12} - \alpha_{11.7.13}$	$\rho(C_\beta H_2)$
$S_{30} = 5\alpha_{2.7.11} - \alpha_{12.7.13} - \alpha_{2.7.12} - \alpha_{2.7.13} - \alpha_{11.7.12} - \alpha_{11.7.13}$	$\delta(C_\alpha C_\beta O)$
$S_{31} = \alpha_{7.11.14}$	$\delta(C_\beta OH)$
$S_{32} = \tau_{9.7.2.10}$	$\gamma(COO^-)$
$S_{33} = \tau_{2.7.11.14} + \tau_{12.7.11.14} + \tau_{13.7.11.14}$	$\tau(C_\beta S)$
$S_{34} = \tau_{3.1.2.6} + \tau_{3.1.2.7} + \tau_{3.1.2.8} + \tau_{4.1.2.6} + \tau_{4.1.2.7} + \tau_{4.1.2.8} + \tau_{5.1.2.6} + \tau_{5.1.2.7} + \tau_{5.1.2.8}$	$\tau(NC_\alpha)$
$S_{35} = \tau_{1.2.6.9} + \tau_{7.2.6.9} + \tau_{8.2.6.9} + \tau_{1.2.6.10} + \tau_{7.2.6.10} + \tau_{8.2.6.10}$	$\tau(C_\alpha C)$
$S_{36} = \tau_{1.2.7.11} + \tau_{1.2.7.12} + \tau_{1.2.7.13} + \tau_{6.2.7.11} + \tau_{6.2.7.12} + \tau_{6.2.7.13} + \tau_{8.2.7.11} + \tau_{8.2.7.12} + \tau_{8.2.7.13}$	$\tau(C_\alpha C_\beta)$

Atom numbering is given in Figure 6.6.

Table 6.12: 4-31G* optimized parameters of cysteine and serine zwitterions

			cysteine						serine	
			X	I	II				X	I
Bond length(A°)						Bond length(A°)				
1	2		1.488	1.499	1.497	1	2		1.488	1.502
1	3		1.038	1.043	1.052	1	3		1.023	1.033
1	4		1.016	1.011	1.011	1	4		1.026	1.011
1	5		1.055	1.005	1.004	1	5		1.035	1.005
2	6		1.528	1.518	1.520	2	6		1.527	1.574
2	7		1.532	1.576	1.579	2	7		1.519	1.513
2	8		1.103	1.082	1.082	2	8		1.095	1.082
7	9		1.239	1.208	1.205	6	9		1.248	1.232
7	10		1.250	1.236	1.238	6	10		1.251	1.212
6	11		1.078	1.083	1.081	7	11		1.416	1.399
6	12		1.076	1.077	1.077	7	12		1.091	1.080
6	13		1.796	1.818	1.830	7	13		1.096	1.084
13	14		1.304	1.326	1.326	11	14		.957	.954
13	14		1.255°							
Bond angle(°)						Bond angle(°)				
3	1	2	110.600	99.808	98.703	3	1	2	109.292	101.306
4	1	2	111.939	109.722	110.158	4	1	2	113.249	108.341
5	1	2	110.662	115.685	115.769	5	1	2	108.568	115.815
3	1	4	108.683	107.953	108.075	3	1	4	110.123	108.174
4	1	5	106.789	109.853	110.114	4	1	5	109.941	109.723
3	1	5	108.008	113.242	113.354	3	1	5	105.355	112.970
1	2	6	110.926	112.881	113.890	1	2	6	110.619	103.152
1	2	7	111.106	103.984	104.128	1	2	7	111.174	110.025
1	2	8	106.856	106.907	107.171	1	2	8	106.548	107.564
7	2	6	111.111	114.452	114.566	7	2	6	111.008	112.662
7	2	8	108.996	108.145	107.286	7	2	8	108.684	112.714
6	2	8	107.674	110.019	109.323	6	2	8	108.655	110.181
2	7	9	116.982	114.814	114.795	2	6	9	118.652	112.175
2	7	10	117.328	111.831	111.593	2	6	10	116.210	114.622
9	7	10	125.688	133.355	133.587	9	6	10	125.125	133.170
2	6	11	110.318	111.989	112.059	2	7	11	111.738	109.153
2	6	12	109.387	107.295	106.150	2	7	12	108.265	108.210
2	6	13	114.726	113.567	112.859	2	7	13	110.194	111.877
11	6	12	107.824	108.593	108.876	11	7	12	108.078	111.934
11	6	13	107.295	105.862	108.366	11	7	13	110.667	107.049
12	6	13	107.028	109.446	108.396	12	7	13	107.760	108.658
6	13	14	97.265	96.487	97.429	7	11	14	108.984	106.880
6	13	14	98.321°							

Table 6.12. (Continued): 4-31G* optimized parameters of cysteine and serine zwitterions

				cysteine							serine	
				X	I	II					X	I
Torsions(°)							Torsions(°)					
3	1	2	6	178.227	-145.664	-142.276	3	1	2	6	-54.487	-27.013
4	1	2	6	-60.418	-32.443	-29.287	4	1	2	6	68.682	86.652
5	1	2	6	58.576	92.498	96.445	5	1	2	6	-168.914	-149.615
3	1	2	7	-57.652	-21.045	-16.800	3	1	2	7	-178.301	-147.429
4	1	2	7	63.702	92.175	96.189	4	1	2	7	-55.133	-33.765
5	1	2	7	-177.304	-142.883	-138.078	5	1	2	7	67.272	89.968
3	1	2	8	61.132	93.230	96.684	3	1	2	8	63.439	89.447
4	1	2	8	-177.513	-153.550	-150.328	4	1	2	8	-173.392	-156.888
5	1	2	8	-58.520	-28.608	-24.595	5	1	2	8	-50.988	-33.155
1	2	7	9	163.494	-160.288	-165.938	1	2	6	9	2.051	27.949
1	2	7	10	-16.988	19.947	15.650	1	2	6	10	-179.219	-150.239
6	2	7	9	-72.491	-36.686	-40.892	7	2	6	9	125.961	146.545
6	2	7	10	107.027	143.549	140.696	7	2	6	10	-55.309	-31.643
8	2	7	9	46.004	86.322	80.661	8	2	6	9	-114.578	-86.636
8	2	7	10	-134.478	-93.444	-97.751	8	2	6	10	64.152	95.175
1	2	6	11	-56.547	-66.234	-73.577	1	2	7	11	70.283	57.521
1	2	6	12	-174.992	174.695	167.688	1	2	7	12	-170.810	179.562
1	2	6	13	64.754	53.616	49.092	1	2	7	13	-53.187	-60.768
7	2	6	11	179.336	175.078	166.688	6	2	7	11	-53.310	-56.974
7	2	6	12	60.890	56.007	47.952	6	2	7	12	65.597	65.067
7	2	6	13	-59.364	-65.072	-70.644	6	2	7	13	-176.780	-175.262
8	2	6	11	60.047	53.088	46.256	8	2	7	11	-172.754	177.571
8	2	6	12	-58.399	-65.982	-72.479	8	2	7	12	-53.847	-60.388
8	2	6	13	-178.653	172.938	168.925	8	2	7	13	63.776	59.283
2	6	13	14	79.312	67.504	-122.536	2	7	11	14	-94.680	73.426
2	6	13	14	-77.398°			12	7	11	14	146.302	-46.342
11	6	13	14	-157.747	-169.223	2.173	13	7	11	14	28.523	-165.303
11	6	13	14	45.542°								
12	6	13	14	-42.238	-52.362	120.186						
12	6	13	14	161.052°								

Energy of the minimum energy conformation of cysteine is -718.622521 hartrees and serine is -396.304401 hartrees.

(I) Conformation I. (II) Conformation II. (X) Neutron diffraction structure parameters of cysteine and serine are from reference [24] and [25].

Table 6.13: Calculated frequencies of the two conformations of cysteine zwitterion

Freq.	Unscaled		Scaled		Expmt.			Raman Activities		I. R. Intensities	
	I	II	I	II	Ra	Ir	Ro	I	II	I	II
1	85	72	76	65	-		-	1.5	1.2	.7	5.2
2	110	80	99	72	-		-	.5	.9	21.4	5.9
3	218	184	195	165	-		-	.8	13.1	4.8	21.7
4	303	230	272	206	-	215	-	1.0	.9	17.8	7.1
5	346	297	310	266	-	-	-	.4	1.6	23.2	13.4
6	398	345	357	309	-	300	-	1.7	1.4	57.8	59.0
7	439	411	393	369	-	370	-	8.5	1.1	25.6	34.0
8	529	528	478	478	-	480	-	2.7	4.0	9.4	5.5
9	577	567	525	518	-	538	-	3.6	2.4	17.7	26.1
10	634	639	583	588	642	637	615	5.3	5.1	6.6	5.6
11	739	746	688	697	696	692	685	14.8	19.0	3.8	2.9
12	837	843	765	768	773	770	779	7.4	5.5	2.6	15.1
13	878	890	790	802	825	823	813	1.6	2.9	40.3	54.8
14	928	942	844	857	870	866	875	4.8	5.2	77.9	36.7
15	971	982	902	910	943	941	936	6.3	6.8	51.6	105.7
16	1087	1111	989	1001	1004	1003	990	5.5	8.2	33.8	20.5
17	1152	1129	1046	1034	-	-	-	5.1	5.2	15.7	21.0
18	1182	1183	1062	1061	1068	1063	1069	2.2	2.3	6.1	5.5
19	1217	1221	1095	1101	1110	1104	1118	3.3	2.7	51.7	58.8
20	1348	1333	1210	1198	1201	1195	1211	17.7	14.8	5.5	20.3
21	1433	1427	1298	1294	-	1296	1258	1.7	3.8	49.7	130.8
22	1452	1444	1314	1306	1273	1296	1278	3.3	3.7	90.3	57.5
23	1491	1477	1346	1333	1300	1320@	1312	3.5	2.5	101.1	126.7
24	1514	1512	1372	1363	1351	1348	1351	6.1	5.1	102.0	82.3
25	1560	1547	1425	1423	1400	1394	1403	2.0	2.6	445.1	447.4
26	1608	1614	1446	1447	1427	1424	1430	11.4	11.1	35.2	33.2
27	1761	1758	1577	1574	-	-	-	14.9	14.7	27.0	28.1
28	1844	1839	1650	1646	-	-	-	4.5	5.1	41.8	39.7
29	1997	2009	1886	1898	-	-	-	.5	1.0	443.4	434.8
30	2861	2851	2715	2706	2550	2555	-	89.7	142.9	1.7	15.7
31	3153	3016	2986	2853	-	-	-	24.7	24.7	378.2	474.4
32	3246	3259	3080	3092	-	-	-	80.1	56.4	27.8	19.5
33	3269	3275	3102	3108	-	-	-	113.9	117.8	19.0	20.2
34	3348	3350	3177	3179	-	-	-	54.5	47.8	.9	1.4
35	3646	3651	3460	3465	-	-	-	48.4	53.7	88.4	87.0
36	3772	3776	3580	3584	-	-	-	58.8	56.8	83.0	82.0

Harmonic frequencies are in units of (cm^{-1}), IR intensities are in units of (KM/Mole) and Raman activities are in units of (A^4/AMU). (I) Conformation I. (II) Conformation II. (Ra) Raman frequencies obtained from reference [26]. (Ir) IR frequencies obtained from reference [28]. (Ro) Frequencies obtained from the ROA spectra of L-cysteine in water(reference [31]). (@) Frequency obtained from reference [37].

Table 6.14: Calculated frequencies of serine zwitterion

Freq.	Uns.	Sca.	D,L-serine		L-serine		Ro	R Act.	I Int.
			Ra	Ir	Ra	Ir			
1	87	78	-	-	-	-	-	.9	2.5
2	144	129	-	-	-	-	-	.1	34.0
3	227	203	222(s)	228(m)	-	-	-	.3	2.4
4	335	301	288(w)	-	-	-	-	.4	11.2
5	363	325	-	324(w)	300@	300@	-	.6	21.2
6	402	361	395(m)	383(s)	369@	369(s)	-	.6	50.1
7	543	491	499(w)	499(m)	512(3)	-	-	1.2	18.2
8	614	562	528(m)	525(s)	-	525(s)	-	5.6	47.1
9	654	588	562(m)	559(m)	-	-	-	2.9	50.7
10	682	615	619(s)	617(s)	608(4)	608(s)	620	1.3	118.7
11	871	796	750(w)	729(s)	-	-	773	5.7	27.7
12	911	829	815(m)	815(w)	810(6)	800@	809	5.7	19.3
13	939	870	852(m)	848(w)	850(16)	850(m)	851	2.4	63.0
14	1036	949	900(m)	901(m)	-	915(s)	919	5.3	63.8
15	1101	1003	978(m)	982(s)	965(4)	965(m)	978	3.0	7.0
16	1176	1065	1028(s)	1029(s)	1004(9)	1012(s)	1040*	3.8	130.7
17	1194	1076	1096(m)	1093(s)	1090@	1090(w)	1083	1.3	26.5
18	1246	1154	1156(w)	1149(m)	1124(4)	1124(s)	1125	5.1	28.1
19	1321	1188	1176(s)	1182(m)	-	-	1150*	5.3	15.1
20	1443	1306	1249(m)	1247(m)	-	-	1242	1.6	50.6
21	1494	1354	1309(m)	1309(s)	1323(14)	1341(s)	1347	4.6	154.2
22	1508	1369	1309(m)	1309(s)	1323(14)	1341(s)	1347	7.2	105.6
23	1530	1383	1349(m)	1352(m)	-	-	-	2.7	49.9
24	1565	1403	1368(sh)	1377(w)	-	1390(w)	-	3.7	221.8
25	1582	1444	1436(m)	1436(s)	1410@	1410@	1412	3.1	236.3
26	1655	1481	1455(s)	1455(w)	1460(9)	1460(w)	1460	9.1	8.3
27	1767	1582	-	-	-	-	-	9.3	43.9
28	1849	1655	-	-	-	-	-	4.5	55.4
29	1985	1875	-	-	-	-	-	.3	476.1
30	3232	3067	-	-	-	-	-	89.2	47.8
31	3281	3113	-	-	-	-	-	87.9	28.1
32	3299	3127	-	-	-	-	-	34.1	264.4
33	3309	3140	-	-	-	-	-	55.4	48.4
34	3667	3480	-	-	-	-	-	39.1	91.3
35	3772	3580	-	-	-	-	-	56.9	78.5
36	4023	3818	-	-	-	-	-	31.3	108.9

Harmonic frequencies are in units of (cm^{-1}), IR intensities are in units of (KM/Mole) and Raman activities are in units of (A^4/AMU). (Ra), (Ir): Raman and IR frequencies obtained from reference [30] and reference [37]. (Ro) Frequencies obtained from the ROA spectra of L-serine in water(reference [31]). (@) Frequencies read from the spectra given in reference [37].

Table 6.15: Potential energy distributions of two conformations of cysteine zwitterion and serine zwitterion

	Cysteine I		Cysteine II		Serine	
	Freq.	PED	Freq.	PED	Freq.	PED
1	76	35(57.1),34(26.3)	65	36(42.2),35(21.2),34(14.0)	78	35(57.5),34(18.1)
2	99	36(51.2),25(11.8),35(10.7)	72	35(36.0),34(23.7),33(17.1)	129	36(60.9),24(10.7)
3	195	30(29.6),25(18.1),36(14.7)	165	33(67.5)	203	25(31.3),30(21.9),23(14.1)
4	272	24(46.5),34(12.3),15(10.5)	206	30(28.5),25(16.4),36(11.6)	301	24(33.5),34(24.9)
		-		,23(10.8)		-
5	310	34(50.9)	266	24(46.9),15(12.3)	325	34(54.2),15(10.7)
6	357	23(21.6),33(18.0),24(14.9)	309	34(37.2), 4(11.7),18(10.5)	361	23(30.6),24(21.2)
7	393	33(77.5)	369	34(27.7),23(17.7),17(14.6)	491	15(38.3)
		-		,24(10.3)		-
8	478	25(28.8),30(16.9),32(14.7)	478	25(29.0),30(18.1),32(17.1)	562	33(38.3),12(22.2),14(13.6)
		-		,10(10.3)		-
9	525	15(34.2),23(17.0),12(10.1)	518	15(41.5),12(14.6),23(12.0)	588	33(21.3),30(16.3),32(15.1)
10	583	12(28.4),23(15.1),14(14.0)	588	12(27.3),23(17.7),15(14.5)	615	33(35.1),30(16.1),23(13.2)
		,15 (12.1)		,14(11.7),13(11.2)		-
11	688	10(54.7),29(11.2),32(10.3)	697	10(61.0),32(15.3)	796	14(27.0),32(22.3),11(17.9)
12	765	29(36.9),11(16.4),31(14.6)	768	29(23.8),11(18.2),32(15.6)	829	14(20.5),32(13.8),12(13.6)
		-		,14(10.2)		,18(12.4)
13	790	14(31.5),32(23.3),31(14.0)	802	14(39.8),29(21.8),31(14.5)	870	11(29.8),29(19.9),12(19.6)
		-		-		,14(13.8)
14	844	14(24.0),12(21.1),32(11.0)	857	32(15.9),25(14.8),11(12.4)	949	19(22.8),13(20.5),29(15.5)
		,25(10.7)		,19(11.4),12(10.2)		-
15	902	11(33.1),12(17.8),31(13.4)	910	12(24.4),11(21.4),31(18.7)	1003	18(18.3),29(16.5),11(12.9)
		-		-		,21(12.3)
16	989	18(34.3),31(16.3),13(15.4)	1001	31(38.2),18(24.2),29(13.8)	1065	19(40.0),22(14.4),21(10.4)
17	1046	19(23.5),31(12.1),13(10.9)	1034	18(17.6),13(17.4),11(15.3)	1076	18(32.2),29(13.0),11(12.5)
18	1062	19(29.2),11(16.1)	1061	19(45.1),22(12.1)	1154	10(64.5),21(10.0)
19	1095	21(27.1),18(24.2),22(10.8)	1101	21(28.2),18(21.8),22(10.0)	1188	28(44.8),31(21.0)
20	1210	28(59.0),22(12.4)	1198	28(57.0),22(12.7)	1306	22(39.4),19(10.2)
21	1298	27(24.0),13(18.0),22(16.5)	1294	22(19.6),13(13.2),28(12.0)	1354	21(42.3),13(13.9)
		-		,27(11.5)		-
22	1314	27(51.6),22(10.4)	1306	27(62.1)	1369	20(25.8),31(25.2),28(12.5)
		-		-		,27(11.6)
23	1346	21(35.7),20(14.8)	1333	20(26.1),21(21.4)	1383	27(31.5), 9(23.2),20(14.4)
24	1372	20(31.8),22(13.5), 9(11.9)	1363	22(23.5),21(20.9),20(12.8)	1403	20(23.7),27(23.5),31(17.1)
25	1425	26(37.5), 9(33.9),20(12.9)	1423	9(47.8),26(16.0),20(14.5)	1444	9(45.1),20(15.6),27(14.3)
26	1446	26(51.5), 9(23.3),20(10.7)	1447	26(76.2)	1481	26(92.5)
27	1577	16(49.7),17(27.6),20(13.3)	1574	16(49.4),17(24.8),20(16.4)	1582	16(70.4),17(12.2)
28	1650	17(63.2),16(31.3)	1646	17(66.2),16(28.2)	1655	17(82.2),16(12.7)
29	1886	8(87.4)	1898	8(86.7)	1875	8(88.1)
30	2715	1(100.0)	2706	1(99.9)	3067	5(78.3), 6(18.9)
31	2986	4(56.4), 3(42.4)	2853	4(57.3), 3(41.1)	3113	7(91.6)
32	3080	5(70.4), 6(20.8)	3092	5(62.5), 7(23.2),6(13.7)	3127	4(40.6), 2(37.5), 3(14.0)
33	3102	7(90.9)	3108	7(75.8), 5(19.3)	3140	6(75.9), 5(18.1)
34	3177	6(77.6), 5(22.0)	3179	6(82.7), 5(17.0)	3480	4(45.2), 3(42.7), 2(11.9)
35	3460	3(47.1), 4(30.2), 2(22.4)	3465	3(49.9), 4(28.2),2(21.6)	3580	3(46.4), 2(46.2)
36	3580	2(83.3)	3584	2(85.0)	3818	1(99.9)

Symmetry coordinate numbers given in Tables 6.10 and 6.11

Table 6.16: Assignment of the d_4 isotope of cysteine zwitterion

Cysteine I		Cysteine II		Experimental	
Freq.	PED	Freq.	PED	Ra	Ir
74	$\tau(C_\alpha C) + \tau(NC_\alpha)$	67	$\tau(C_\alpha C) + \tau(NC_\alpha)$	-	-
95	$\tau(C_\alpha C_\beta) + \tau(C_\alpha C) + \delta(NC_\alpha C)$	64	$\tau(C_\alpha C_\beta) + \tau(C_\beta S)$	-	-
180	$\delta(C_\alpha C_\beta S) + \delta(NC_\alpha C)$	191	$\delta(C_\alpha C_\beta S) + \tau(NC_\alpha)$	-	-
225	$\tau(NC_\alpha) + \delta_a(ND_3^+)$	237	$\tau(NC_\alpha)$	-	-
267	$\rho(C_\beta C_\alpha C) + \rho(COO^-)$	261	$\rho(C_\beta C_\alpha C) + \rho(COO^-)$	-	-
290	$\tau(C_\beta S) + \rho(C_\beta C_\alpha C)$	125	$\tau(C_\beta S)$	-	-
321	$\delta(C_\beta C_\alpha C) + \rho(C_\beta C_\alpha C)$	316	$\delta(C_\beta C_\alpha C) + \rho(C_\beta C_\alpha C)$	-	-
449	$\delta(NC_\alpha C) + \delta(C_\alpha C_\beta S) + \gamma(COO^-)$	454	$\delta(NC_\alpha C) + \delta(C_\alpha C_\beta S) + \gamma(COO^-)$	424	428
513	$\rho(COO^-) + \delta(C_\beta C_\alpha C)$	505	$\rho(COO^-) + \nu(C_\alpha C)$	508	510
564	$\nu(C_\alpha C) + \delta(C_\beta SD) + \rho(COO^-)$	568	$\nu(C_\alpha C) + \delta(C_\beta SD) + \rho(COO^-)$	614	614
625	$\delta(C_\beta SD) + \rho(C_\beta H_2)$	650	$\delta(C_\beta SD) + \rho(C_\beta H_2)$	628	621
698	$\nu(C_\beta S) + \gamma(COO^-)$	705	$\nu(C_\beta S) + \gamma(COO^-) + \delta(C_\beta SD)$	687	695
738	$\gamma_\perp(ND_3^+) + \nu(C_\beta S) + \gamma(COO^-)$	733	$\gamma_\perp(ND_3^+) + \nu(C_\beta S) + \gamma(COO^-)$	-	-
775	$\delta(COO^-) + \nu(C_\alpha C)$	774	$\delta(COO^-) + \nu(C_\alpha C) + \gamma_\perp(ND_3^+)$	773	776
816	$\gamma_\parallel(ND_3^+) + \nu(C_\alpha C_\beta)$	821	$\gamma_\parallel(ND_3^+)$	808	803
848	$\delta(COO^-) + \nu(C_\alpha C) + \rho(C_\beta H_2)$	849	$\delta(COO^-) + \nu(C_\alpha C) + \rho(C_\beta H_2)$	841	850
947	$\delta(NC_\alpha C) + \gamma_\perp(ND_3^+)$	942	$\delta(NC_\alpha C) + \gamma_\perp(ND_3^+) + \gamma(COO^-)$	878	884
980	$\rho(C_\beta H_2) + \delta_s(ND_3^+) + \rho(C_\beta C_\alpha C)$	969	$\rho(C_\beta H_2) + \delta_s(ND_3^+) + \nu(C_\alpha C)$	-	966
1042	$\delta_s(ND_3^+) + \delta_s'(ND_3^+) + \delta(C_\beta C_\alpha H_\alpha)$	1031	$\delta_s(ND_3^+) + \delta_s'(ND_3^+) + \nu(NC_\alpha)$	1024	-
1082	$\delta_s'(ND_3^+) + \nu(NC_\alpha) + \delta_a(ND_3^+)$	1086	$\nu(C_\alpha C_\beta) + \delta(C_\beta C_\alpha H_\alpha) + \delta_s'(ND_3^+)$	1055	1057
1152	$\delta_s(ND_3^+) + \delta_s'(ND_3^+) + \delta_a(ND_3^+)$	1151	$\delta_s(ND_3^+) + \delta_a(ND_3^+) + \delta_s'(ND_3^+)$	1170	1168
1190	$\delta_a(ND_3^+) + \delta_s'(ND_3^+)$	1187	$\delta_a(ND_3^+) + t(C_\beta H_2) + \delta_s'(ND_3^+)$	1195	1198
1200	$t(C_\beta H_2)$	1194	$t(C_\beta H_2) + \delta_s'(ND_3^+)$	1195	1198
1286	$\rho(C_\beta C_\alpha H_\alpha) + \nu(C_\alpha C_\beta) + \omega(C_\beta H_2)$	1285	$\rho(C_\beta C_\alpha H_\alpha) + t(C_\beta H_2) + \nu(C_\alpha C_\beta)$	1285	1285
1308	$\omega(C_\beta H_2)$	1303	$\omega(C_\beta H_2) + \rho(C_\beta C_\alpha H_\alpha)$	1330	1330
1337	$\delta(C_\beta C_\alpha H_\alpha)$	1339	$\delta(C_\beta C_\alpha H_\alpha)$	1358	1350
1412	$\nu_s(COO^-)$	1404	$\nu_s(COO^-)$	1398	1393
1440	$\delta(C_\beta H_2)$	1444	$\delta(C_\beta H_2)$	1426	1430
1878	$\nu_a(COO^-)$	1886	$\nu_a(COO^-)$	1576	1590
1949	$\nu(SD)$	1944	$\nu(SD)$	1849	1857
2178	$\nu_s(ND_3^+)$	2087	$\nu_s'(ND_3^+) + \nu_s(ND_3^+)$	-	-
2518	$\nu_s'(ND_3^+)$	2518	$\nu_s(ND_3^+) + \nu_s'(ND_3^+)$	-	-
2637	$\nu_a(ND_3^+)$	2641	$\nu_a(ND_3^+)$	-	-
3080	$\nu_s(C_\beta H_2)$	3092	$\nu_s(C_\beta H_2)$	-	-
3102	$\nu(C_\alpha H_\alpha)$	3108	$\nu(C_\alpha H_\alpha)$	-	-
3177	$\nu_a(C_\beta H_2)$	3179	$\nu_a(C_\beta H_2)$	-	-

Experimental frequencies are from references [28] and reference [29].

Table 6.17: Assignment of the d_4 isotope of serine zwitterion

Serine		Experimental	
Freq.	PED	Ra	Ir
76	$\tau(C_\alpha C) + \tau(NC_\alpha)$	-	-
123	$\tau(C_\alpha C_\beta) + \rho(C_\beta C_\alpha C)$	-	-
189	$\delta(NC_\alpha C) + \delta(C_\alpha C_\beta O) + \delta(C_\beta C_\alpha C)$	214	216
234	$\tau(NC_\alpha)$	266	-
298	$\rho(C_\beta C_\alpha C) + \rho(COO^-) + \delta(C_\beta C_\alpha C)$	314	308
324	$\rho(C_\beta C_\alpha C) + \delta(C_\beta C_\alpha C)$	350	350
423	$\tau(C_\beta O)$	370	-
474	$\rho(COO^-) + \delta(C_\beta C_\alpha C)$	507	506
565	$\nu(C_\alpha C) + \gamma(COO^-) + \delta(COO^-)$	566	565
588	$\delta(C_\alpha C_\beta O) + \rho(COO^-) + \delta(C_\beta C_\alpha C) + \nu(C_\alpha C)$	608	602
717	$\gamma_\parallel(ND_3^+) + \gamma(COO^-) + \gamma_\perp(ND_3^+)$	-	723
779	$\nu(NC_\alpha) + \delta(COO^-) + \gamma_\perp(ND_3^+) + \rho(C_\beta H_2)$	771	785
800	$\gamma_\perp(ND_3^+) + \nu(C_\alpha C_\beta) + \delta(C_\beta OD)$	809	806
838	$\delta(COO^-) + \nu(C_\alpha C) + \delta(C_\beta OD) + \rho(C_\beta H_2)$	850	851
898	$\delta(C_\beta OD) + \nu(C_\alpha C)$	881	878
950	$\gamma_\parallel(ND_3^+) + \delta(NC_\alpha C) + \gamma(COO^-) + \delta(C_\beta OD)$	940	940
1004	$\delta(C_\beta C_\alpha H_\alpha) + \nu(C_\alpha C_\beta) + \delta_s(ND_3^+)$	985	984
1067	$\delta_s(ND_3^+) + \delta'_s(ND_3^+)$	1024	1022
1107	$\rho(C_\beta H_2) + \delta'_s(ND_3^+) + \nu(NC_\alpha)$	1097	1095
1148	$\nu(C_\beta O)$	1123	-
1156	$\delta'_s(ND_3^+) + \delta_s(ND_3^+)$	1163	1163
1195	$\delta_a(ND_3^+) + \delta'_s(ND_3^+)$	1190	1186
1263	$\rho(C_\beta C_\alpha H_\alpha) + t(C_\beta H_2) + \rho(C_\beta H_2)$	1277	1277
1308	$t(C_\beta H_2) + \rho(C_\beta C_\alpha H_\alpha)$	1309	1309
1344	$\delta(C_\beta C_\alpha H_\alpha) + \nu(C_\alpha C_\beta) + \rho(C_\beta C_\alpha H_\alpha)$	1340	1340
1387	$\omega(C_\beta H_2) + \nu_s(COO^-)$	1370	1384
1432	$\nu_s(COO^-) + \omega(C_\beta H_2)$	1420	1428
1481	$\delta(C_\beta H_2)$	1446	1451
1867	$\nu_a(COO^-)$	1592	1572
2274	$\nu_s(ND_3^+) + \nu_a(ND_3^+) + \nu'_s(ND_3^+)$	-	-
2535	$\nu'_s(ND_3^+) + \nu_s(ND_3^+) + \nu_a(ND_3^+)$	-	-
2639	$\nu'_s(ND_3^+) + \nu_a(ND_3^+)$	-	-
2779	$\nu(OD)$	-	-
3068	$\nu_s(C_\beta H_2) + \nu_a(C_\beta H_2)$	-	-
3114	$\nu(C_\alpha H_\alpha)$	-	-
3139	$\nu_a(C_\beta H_2) + \nu_s(C_\beta H_2)$	-	-

Experimental frequencies are from reference [32].

6.4 References

[1] H. L. Sellers and L. Scäfer, J. Am. Chem. Soc., 100 (1978) 7728.

[2] L. Schäfer, H. L. Sellers, F. J. Lovas and R. D. Suenram, J. Am. Chem. Soc., 102 (1980) 6566.

[3] F. Jensen, J. Am. Chem. Soc., 114 (1992) 9533.

[4] A. Császár, J. Am. Chem. Soc., 114 (1992) 9568.

[5] A. Vijay and D. N. Satyanarayana, J. Phys. Chem., 96 (1992) 10735.

[6] J. S. Alper, H. Dothe and D. F. Coker, Chem. Phys., 153 (1991) 51.

[7] J. S. Alper, H. Dothe and M. A. Lowe, Chem. Phys., 161 (1992) 199.

[8] H. L. Sellers and L. Schäfer, Chem. Phys. Lett., 63 (1979) 609.

[9] K. Siam, V. J. Klimkowski, J. D. Ewbank, C. Van Alsenoy, J. N. Scarsdale and L. Schäfer, J. Am. Chem. Soc., 110 (1984) 171.

[10] M. Ramek, J. Mol. Str., 208 (1990), 301.

[11] L. D. Barron, A. R. Gargaro, L. Hecht and P. L. Polavarapu, Spectrochim. Acta, 47A (1991) 1001.

[12] P. R. Lawrence and C. Thomson, Theor. Chim. Acta, 58 (1981) 121.

[13] P. G. Mezey, J. J. Ladik and S. Suhai, Theor. Chim. Acta, 51 (1979) 323.

[14] L. R. Wright and R. F. Borkman, J. Am. Chem. Soc., 102 (1980) 6207.

[15] J. Voogd, J. L. Derissen and F. B. Duijenveldt, J. Am. Chem. Soc., 103 (1981) 7701.

[16] G. E. Tranter, Mol. Phys., 4 (1985) 825.

[17] G. E. Tranter, J. Theor. Biol., 119 (1986) 467.

[18] A. E. Smolyar, A. R. Abramov, O. A. Narimanbekov and T. N. Shakhtakhtinski, Azerb. Khim. Zhu., (1984) 42.

[19] C. Van Alsenoy, J. N. Scarsdale, H. L. Sellers and L. Schäfer, Chem. Phys. Lett., 80 (1981) 124.

[20] C. V. Alsenoy, S. Kulp, K. Siam, V. J. Klimkowski, J. D. Ewbank and L. Schäfer, J. Mol. Str., 181 (1988) 169.

[21] P. R. Lawrence and C. Thomson, Theor. Chim. Acta, 58 (1981) 121.

[22] L. Schäfer, K. Siam, V. J. Klimkowski, J. D. Ewbank and C. V. Alsenoy, J. Mol. Str., 204 (1990) 361.

[23] S. J. Weiner, P. A. Kollman, D. A. Case, U. C. Singh, C. Ghio, G. Alagona, S. Profeta and P. Weiner, J. Am. Chem. Soc., 106 (1984) 765-784.

[24] K. A. Kerr, J. P. Ashmore and T. F. Koetzle, Acta Crystallogr., Sect. B. 31 (1975) 2022.

[25] M. N. Frey, M. S. Lehmann, T. F. Koetzle, Acta Crystallogr., Sect. B. 29 (1973) 876.

[26] H. Li, C. J. Wurrey and G. J. Thomas, Jr., J. Amer. Chem. Soc., 114 (1992) 7463.

[27] H. Susi, D. M. Byler and W. V. Gerasimowicz., J. Mol. Str., 102 (1983) 63.

[28] C. Madec, J. Lauransan and C. Garrigou-Lagrange, Can. J. Spectrosc., 25 (1980) 47.

[29] C. Madec, J. Lauransan and C. Garrigou-Lagrange, Can. J. Spectrosc., 23 (1978) 166.

[30] K. Machida, M. Izumi and A. Kagayama, Spectrochim. Acta, 35A (1979) 1333.

[31] A. R. Gargaro, L. D. Barron and L. Hecht, J. Raman Spectrosc. 24 (1993) 91.

[32] L. D. Barron, A. R. Gargaro, L. Hecht and P. L. Polavarapu, Spectrochim. Acta, 47A (1991) 1001.

[33] (a) Y. Grenie and C. G. Lagrange, J. Mol. Spectrosc., 41 (1972) 240. (b) Y. Grenie, J. C. Lassegues and C. G. Lagrange, J. Chem. Phys., 53 (1970) 2980.

[34] (a) N. Nogami, H. Sugeta and T. Miyazawa, Chem. Lett. (1975) 147-50. (b) N. Nogami, H. Sugeta and T. Miyazawa, Bull. Chem. Soc. Jpn. 48 (1975) 2417-20.

[35] W. O. George, J. H. S. Green and D. Pailthorpe, J. Mol. Str., 10 (1971) 297.

[36] (a) M. Kainosho and K. Ajisaka, J. Amer. Chem. Soc., 97 (1975) 5630. (b) P. E. Hansen, J. Feeney and G. C. K. Roberts, J. Magn. Reson., 17 (1975)249.

[37] B. Schrader, *Raman/ Infrared Atlas of Organic Compounds*, VCH Publishers, Weinheim, 1989.

Chapter 7

Proline and Hydroxyproline

In the previous chapter the vibrational analysis of cysteine and serine in the gas phase and zwitterionic forms using ab initio methods have been described. This chapter deals with the conformational and vibrational analysis of two imino acids, proline and hydroxyproline. Since the molecules are quite large the 4-31G* basis set could not be used, hence the 4-21G basis set is once again used in this study.

In the preceding chapter we have seen that the vibrational analysis of only a few amino acids has been done using ab initio methods. The vibrational assignment of glycine in the zwitterionic form has been studied by Apler et al. [1,2], the nonionized form has been the focus of another study [3]. Alanine in the zwitterionic and nonionized forms has also been studied [4,5]. Including our study of cysteine and serine in the gas phase and zwitterionic forms we find that the ab initio vibrational analysis of only four amino acids have been done.

The two imino acids proline and hydroxyproline in sharp contrast to the other amino acids have been difficult to study theoretically because the pucker in the five membered ring has to be taken into account. The X-Ray structure of L-proline has been determined by Vainsthein [6] and that of hydroxyproline by Donohue and Trueblood [7]. The neutron diffraction analysis of hydroxyproline has been done by Koetzle et al. [8]. Early theoretical studies include empirical calculations [9] and PCILO calculations of the prolyl and hydroxyprolyl residues [10]. More recently an ab initio calculation of proline in the non ionized form has been carried out using the STO-3G and 6-31G basis sets [11]. The deterrent for most early studies has been the description of the ring pucker in proline and hydroxyproline.

Thus in a normal coordinate study of the vibrational frequencies of a dipeptide [Gly-

Pro] the symmetry coordinates of the prolyl group were constructed using the program REDOND [12,13]. The problem however has been that there is no description of the frequencies. More recently Singh et al using the force constants transferred from imidazole and glycine have attempted a normal coordinate analysis of the Raman spectrum of proline and hydroxyproline [14].

The starting structures for both proline and hydroxyproline in the nonionized forms have been obtained from model building. The X-Ray parameters of proline [6] and hydroxyproline [7] were used in the construction of the model. The symmetry coordinates of proline and hydroxyproline are given in Tables 7.1 and 7.2. The main problem has been the description of the ring bending and ring torsion coordinates. In a recent paper on tetrahydrofuran [15] the description of these coordinates has been given. The coefficients therein had been optimized to take into account the pucker present in the five membered ring. We found that the coefficients given therein excellently described these frequencies in both proline and hydroxyproline. So no further optimization of the coefficients was carried out.

The 4-21G optimized energies, bond lengths, bond angles and dihedral angles of the two conformations of proline and hydroxyproline are given in Table 7.3 and the structures are shown in Figure 7.1. The calculated frequencies, IR intensities and Raman activities of the two conformations of proline and hydroxyproline are listed in Tables 7.4 and 7.5. The potential energy distributions obtained for the two conformations of proline and hydroxyproline are given in Tables 7.6 and 7.7. Since the vibrational frequencies of proline and hydroxyproline are not available in the gas phase, assignments have been made using the solid state IR and Raman spectra of L-Proline and L-Hydroxyproline [14,16,17]. The NH and $COOH$ frequencies of proline and hydroxyproline have been assigned based on the Raman spectra of the solution of proline at pH 1.0 and pH 11.0, and to the Raman spectra of the solutions of the hydrochloride and sodium salt of hydroxyproline [16]. The assignments have been reinforced by comparison of the calculated frequencies to the gas phase spectra of glycine [18], pyrrolidine [19], maleimide [20] and imidazole [21].

7.1 Geometries

The earlier 6-31G study of proline in the nonionized form by Sapse et al. [11] was based on the assumptions that the NC_α bond length is equal to the NC_δ bond length and the $C_\alpha C_\beta$ bond length is equal to the $C_\gamma C_\delta$ bond length. Owing to these assumptions a number of

angles become equal and most importantly the ring becomes nearly planar. The planarity in the proline ring was attributed to the deficiency of the STO-3G and 6-31G basis sets in predicting puckers. However one of the vital aspects of the five membered imino ring is the pucker. The ring pucker has been classified has either endo or exo based on the values of the torsion angles χ_1, χ_2, χ_3, χ_4 [22,23]. The PCILO study by Maigret et al. [22–23] on the role of the pucker clearly indicates that the two puckered conformations do not differ much in energies which is contrary to the case in sugar rings [24]. Moreover it is well known that the nature of the pucker does not play a vital role in the protein conformation [25]. Hence we did not take into account the other puckered conformation. A number of empirical studies have devoted their attention to the concept of pseudorotation which is an outcome of the pucker [26–30]. As for pseudorotation all the existing studies on proline were based on Kirpatrick's model of cyclopentane [27,30]. Though close approximations can be made for symmetric systems, an extension to proline which is an unsymmetric molecule is difficult. The pseudorotation profile of pyrrolidine using the 4-21G basis set has been studied [31]. Given the close correlation of the structures of pyrrolidine and proline the pseudorotation profile of proline might be similar to that of pyrrolidine. Hence our study does not include the aspect of pseudorotation.

In both the conformations that we have studied the carboxyl group is on the same side as the $N-H$ bond(cis). The two conformations differ in the orientation of the carboxyl hydrogen(cis or trans to the $C=O$ group). Our justification for the study of the trans conformation is that this structure has a direct analogy to the structure of the prolyl group in a protein. The OH group in the nonionized conformation is replaced by the amide NH in the protein.

Before discussing the major structural features of the optimized conformations we discuss the special case of the hydroxyl group in hydroxyproline. Though the hydroxyl group in hydroxyproline is attached to the C_β position in some proteins, in most proteins it is attached to the C_γ position. Thus only γ-hydroxyproline has been studied. In proteins and in the solid state of hydroxyproline the hydroxyl hydrogen is hydrogen bonded to the neighbouring groups. As a result the hydroxyl hydrogen points out of the ring, but in case of our theoretical study efforts to maintain these orientaion of the hydroxyl hydrogen proved to be futile because the resulting structure did not get optimized. In cases where such an optimization was feasible the structure gave rise to negative frequencies. Hence the hydroxyl hydrogen in our theoretical conformational study points into the ring. As a result, the hydroxyl hydrogen forms a strong hydrogen bond with the imino nitrogen. The

outcome of such an hydrogen bonding, is that some of the ring dihedral angles tend to 0^o, and more importantly the frequencies associated with the ring (bending and torsion) increase. Hence in our vibrational assignment these frequencies have not been assigned in hydroxyproline. Our calculated frequencies would however match with the gas phase frequencies of hydroxyproline because in the gas phase such an intramolecular hydrogen bonding is likely to be present.

In the absence of gas phase data, we compare the geometrical features of the 4-21G optimized conformations of both proline and hydroxyproline to the X-Ray derived parameters of zwitterionic L-proline and L-hydroxyproline. It can be seen from the geometrical data given in Table 7.3 that on optimization with the 4-21G basis set most of the *CC* bond lengths decrease except for the $C_\alpha C_\beta$ and $C_\beta C_\gamma$ bond lengths which increase. Other bond lengths involving hydrogen atoms have lower values as compared to that of the X-Ray structure. A comparsion with the electron diffraction structure of pyrrolidine [31] indicates that the 4-21G values are only slightly higher to the corresponding electron diffraction parameters. However the experimental *NH* bond length in case of pyrrolidine is $1.020A^o$as compared to the ab initio bond length of $1.004A^o$. The corresponding 4-21G *NH* bond length in case of pyrrolidine is $1.013A^o$. Ab initio studies of pyrrolidine using the 4-21G basis set with and without polarization functions [31] on the nitrogen atom had indicated the effect of the inclusion of polarization functions on the prediction of energy minimum for pyrrolidine. Though it has considerable effect on the nature of the puckered conformation there is little change in the values of the parameters. This is contrary to the observation made by Sapse et al. [11] in the ab initio study of proline in the nonionized form using the STO-3G and 6-31G basis set. They had said that the puckering of the pyrrolidine ring is poorly predicted by using split valence and minimal basis sets. In light of the observations made by Pfafferott et al. [31] after the 4-21G basis set study of the conformations of pyrrolidine and our present results it appears that the 4-21G basis set adequately describes the pucker. Discrepancies only occur in the position of the pucker.

We have calculated the barrier heights of the rotation of the carboxyl hydrogen and hydroxyl hydrogen. It can be seen from Figures 7.2, 7.3 and 7.4 that the barrier heights are around 30 kJ/mol. The barrier height in case of the hydroxyl hydrogen in hydroxyproline is slightly higher than the barrier height of the carboxyl hydrogen rotation. This indicates that the intramolecular hydrogen bonding present in hydroxyproline is quite strong.

7.2 Vibrational Frequencies

All the assignments have been done using the frequencies of the cis conformation. The corresponding frequencies of the trans conformation are correlated to those of the cis conformation. Though the experimental intensity profiles given in Tables 7.4 and 7.5 would fit the calculated intensities in most cases there would be some discrepancies. The calculated intensities are for an isolated nonionized conformation but the experimental frequencies correspond to either the solid state or the solution state vibrational frequencies. A number of correlations have been made between the experimental vibrational frequencies in various phases-gas, solid and liquid, the aid of which have been taken in this assignment. But very few correlations exist between the intensities of the peaks in various phases.

7.2.1 *NH* Frequencies

The calculated $\nu(NH)$ frequency in proline and hydroxyproline cannot be assigned to the experimental vibrational spectra of either L-proline or L-hydroxyproline due to the absence of the peaks in that region. The experimental liquid state frequencies in case of pyrrolidine for this mode occurs around $3267cm^{-1}$in the IR spectra and around $3350cm^{-1}$in the Raman spectra [19]. Gas phase frequencies for this mode are not given in the experimental spectra. In maleimide the gas phase frequency for this mode occurs at $3482cm^{-1}$[20] while in case of imidazole the gas phase frequency for this mode appear at $3518cm^{-1}$[21]. The scaled $\nu(NH)$ values of 3529 and $3536cm^{-1}$are in agreement with the corresponding experimental values. The gas phase values for the $\rho(NH)$ mode in case of pyrrolidine occurs at $1335cm^{-1}$[19], in maleimide at $1322cm^{-1}$[20] and in imidazole at $1160cm^{-1}$[21]. The corresponding liquid state data for this mode in case of pyrrolidine indicates that it occurs at $1347cm^{-1}$[19]. The calculated scaled values for this mode in proline and hydroxyproline occur at $1435cm^{-1}$and $1458cm^{-1}$. These indicate that the presence of the carboxyl group on the C_α significantly increases this frequency in proline when compared to pyrrolidine. Similarly the calculated scaled values for the $\delta(NH)$ mode in case of proline and hydroxyproline are 788 and $815cm^{-1}$. The corresponding gas phase values for this mode are 840, 620 and $513cm^{-1}$in pyrrolidine, maleimide and imidazole respectively. In this case the gas phase values for this mode are significantly higher when compared to the value in proline and hydroxyproline. In proteins the imide hydrogen is lost and hence the frequencies associated with this mode have little significance in the IR studies of proteins and peptides.

7.2.2 $COOH$ Frequencies

$\nu(OH)$ in the gas phase spectra of glycine occurs at $3561cm^{-1}$[18]. The $\nu(OH)$ frequencies of proline and hydroxyproline are substantially higher than the experimental wavenumbers. Though the comparison of the calculated frequencies of proline and hydroxyproline to the experimental frequencies of glycine is tenuous we feel that better scaling factors might give better agreement with experiment. Due to the involvement of the alcoholic hydrogen in an intramolecular hydrogen bond $\nu(OH)_{alc}$ appears at a lower frequency than $\nu(OH)_{ac}$. In case of the $\nu(C=O)$ mode the frequencies in the trans conformer appear at higher wavenumbers than the cis conformer. $\nu(CO)$ and $\delta(COH)$ modes appear as mixed modes as observed in carboxylic acids. This aspect has been extensively dealt with in chapter 4. The assignment of these modes to the experimental solid state or solution spectra is tricky because in these states due to intermolecular hydrogen bonding the frequencies associated with these modes come higher than in the gas phase. In case of the $\delta(COH)_{alc}$ and $\nu(CO)_{alc}$ modes exceptions can be made owing to the fact that a strong intramolecular hydrogen bond exists. This in a way compensates for the corresponding increase in the frequencies owing to intermolecular hydrogen bonding in the solid or liquid state. $\tau(CO)$ modes are also susceptible to the vagaries of hydrogen bonding. Thus they increase under the influence of hydrogen bonding. This mode has been assigned in some cases taking aid of the experimental and theoretical intensity profiles. The other modes associated with the $COOH$ group which are not affected by hydrogen bonding, the $\gamma(COO)$, $\delta(C-O)$, $\delta(C=O)$ have been assigned wherever possible.

7.2.3 CH_2 Frequencies

In proline there are three methylene groups in three diferent environments (groups to which these methylene groups are bonded). On the other hand, in hydroxyproline there are two different methylene groups. Based on the changes in the wave numbers of the $\nu(CH)$ frequencies the trans conformer can be easily distinguished from the cis conformer. In the trans conformer of proline $\nu_a(C_\beta H_2)$ appears at $3277cm^{-1}$and in the cis conformer at $3311cm^{-1}$. The substantial difference can be attributed to the orientation of the carboxyl hydrogen. Its proximity to the beta methylene group could be the cause of this increase. On the other hand in hydroxyproline the effect of the carboxyl hydrogen on the beta methylene group wanes. Thus in the trans conformer of hydroxyproline it appears at $3307cm^{-1}$and in the cis conformer at $3324cm^{-1}$. The fact that the trans conformer is analogous to the prolyl

groups in proteins implies that monitoring of the frequencies associated with the C_β mode might give valuable insight into the structure of the prolyl group and its neighbouring groups. The other methylene frequencies are well within the range and hence are not discussed here.

7.2.4 Ring Frequencies

The stretching frequencies associated with the ring are either associated with *CC* or *CN* bonds. All the *CC* and *CN* stretches have strong Raman bands and hence are easily assigned. Moreover frequencies associated with these modes are not affected by the phase in which the spectra have been taken. Thus they appear at nearly the same wavenumbers in the solid, liquid and gas phases. The two ring bending modes appear as dominant modes at a number of frequencies. The PED's associated with these modes are small and hence it is difficult to attribute them to a particular frequency. However based on the contribution to the PED these modes can be attributed to the frequencies at 1050, 628 and $534cm^{-1}$in the cis conformer of proline. In pyrrolidine the two ring bending modes have been attributed to the frequencies at (790,571,553) and $795cm^{-1}$in the gas phase and solid state IR spectra respectively [19]. In tetrahydrofuran the two ring bending modes appear at 657 and $591cm^{-1}$in the Raman spectra of liquid THF [15]. The calculated MP2/6-31G* frequencies for tetrahydrofuran are 674.7 and $584.9cm^{-1}$. Singh et al. [14] have attributed these modes to the frequencies at $685cm^{-1}$. In hydroxyproline due to the presence of the intramolecular hydrogen bonding, the ring bending modes appear at 686 and $761cm^{-1}$in the cis conformer. In case of hydroxyproline Singh et al. 14] attribute the frequencies at (700,619) and $(687,626)cm^{-1}$in the Raman spectra of solid state and solution of hydroxyproline respectively to these modes. It can be seen that there is a gradual increase in the ring bending frequencies as we progress from pyrrolidine to hydroxyproline. Thus substitutents in the form of either a carboxyl or hydroxyl group on the ring tend to increase the corresponding ring bending frequencies. The ring torsion modes associated with the pucker in the ring appear at very low frequencies. In general ab initio methods tend to give erroneous results for the torsional modes. Hence the frequencies associated with these modes are not discussed.

7.3 Conclusions

In this chapter the conformational and vibrational analysis of the two imino acids has been carried out using the HF/4-21G basis set. Though this study does not include the aspect of pseudorotation, pucker has been taken into account in all our calculations. The calculated frequencies have been assigned to the corresponding experimental vibrational spectra and comparisons made with the frequencies of other five membered ring compounds wherever possible. The conformational effect on some of the frequencies have also been dealt with in this study.

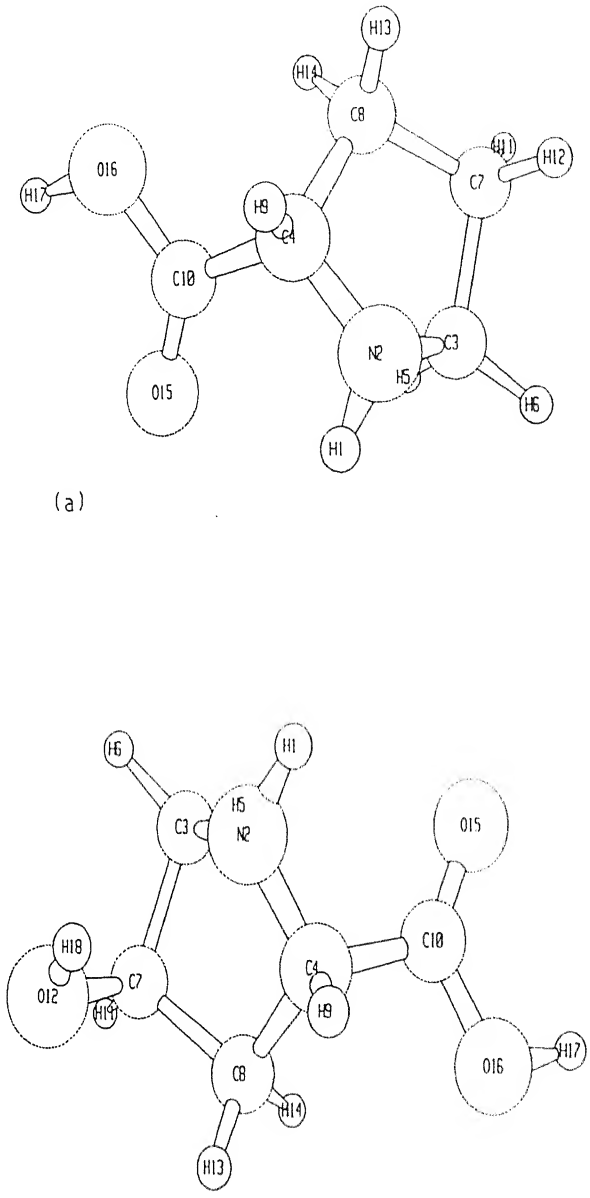

Figure 7.1: 4-21G optimized structures of the cis conformations (a) Proline and (b) Hydroxyproline.

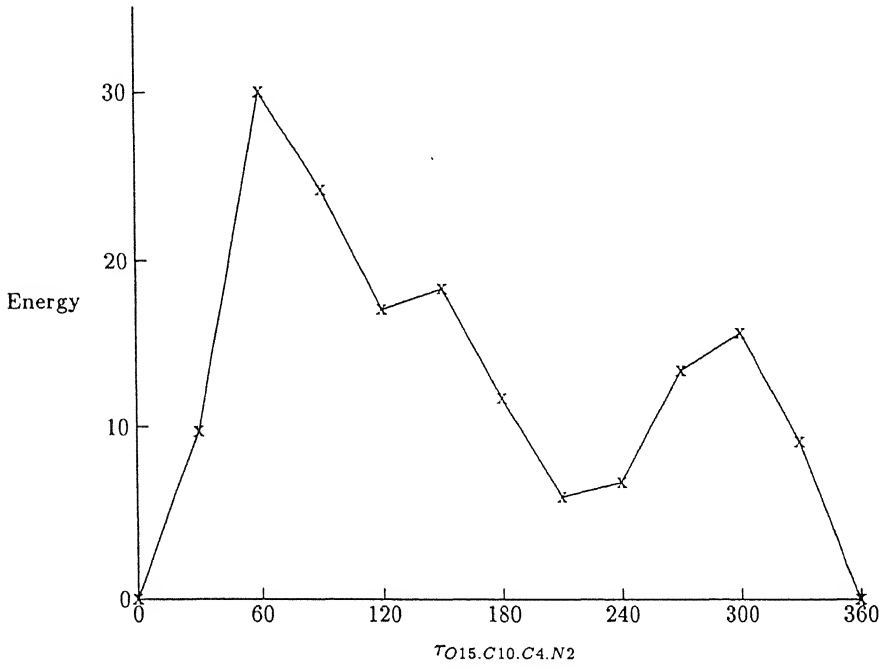

Figure 7.2: Variation of Energy with the torsional angle $\tau[O15.C10.C4.N2]$ in proline. Energy is in kJ/mol.

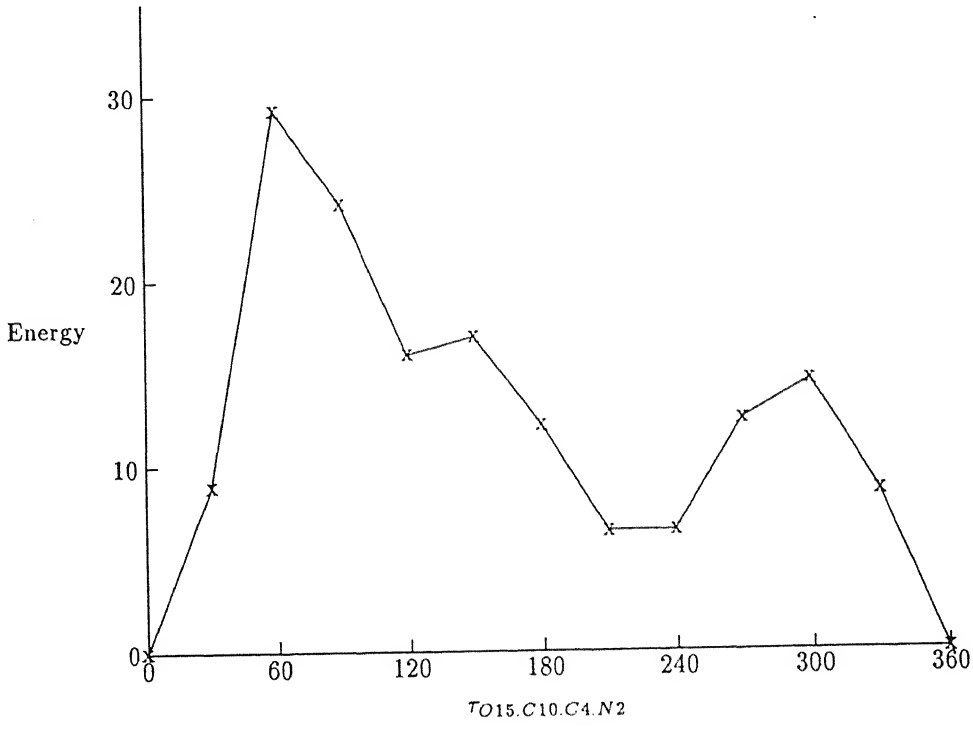

Figure 7.3: Variation of Energy with the torsional angle $\tau[O15.C10.C4.N2]$ in hydroxyproline. Energy is in kJ/mol.

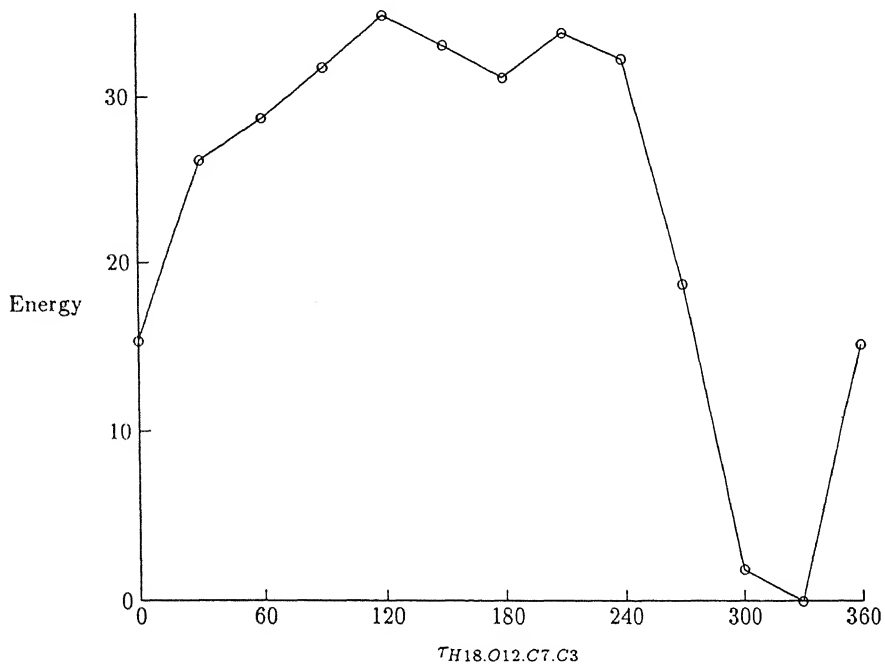

Figure 7.4: Variation of Energy with the torsional angle $\tau[H18.O12.C7.C3]$ in hydroxyproline. Energy is in kJ/mol.

Table 7.1: Symmetry Coordinates of Proline

Coordinate	Description
$S_1 = R_{1.2}$	$\nu(NH)$
$S_2 = R_{3.5} + R_{3.6}$	$\nu_s(C_\delta H_2)$
$S_3 = R_{3.5} - R_{3.6}$	$\nu_a(C_\delta H_2)$
$S_4 = R_{7.11} + R_{7.12}$	$\nu_s(C_\gamma H_2)$
$S_5 = R_{7.11} - R_{7.12}$	$\nu_a(C_\gamma H_2)$
$S_6 = R_{8.13} + R_{8.14}$	$\nu_s(C_\beta H_2)$
$S_7 = R_{8.13} - R_{8.14}$	$\nu_a(C_\beta H_2)$
$S_8 = R_{4.9}$	$\nu(C_\alpha H)$
$S_9 = R_{4.10}$	$\nu(C_\alpha C)$
$S_{10} = R_{10.15}$	$\nu(C=O)$
$S_{11} = R_{10.16}$	$\nu(C-O)$
$S_{12} = R_{16.17}$	$\nu(OH)$
$S_{13} = R_{2.4}$	$\nu(NC_\alpha)$
$S_{14} = R_{4.8}$	$\nu(C_\alpha C_\beta)$
$S_{15} = R_{7.8}$	$\nu(C_\beta C_\gamma)$
$S_{16} = R_{3.7}$	$\nu(C_\gamma C_\delta)$
$S_{17} = R_{2.3}$	$\nu(NC_\delta)$
$S_{18} = \alpha_{2.3.5} + \alpha_{5.3.7} + \alpha_{2.3.6} + \alpha_{6.3.7}$	$\delta(C_\delta H_2)$
$S_{19} = \alpha_{2.3.5} - \alpha_{5.3.7} + \alpha_{2.3.6} - \alpha_{6.3.7}$	$\omega(C_\delta H_2)$
$S_{20} = \alpha_{2.3.5} - \alpha_{5.3.7} - \alpha_{2.3.6} + \alpha_{6.3.7}$	$t(C_\delta H_2)$
$S_{21} = \alpha_{2.3.5} + \alpha_{5.3.7} - \alpha_{2.3.6} - \alpha_{6.3.7}$	$\rho(C_\delta H_2)$
$S_{22} = \alpha_{3.7.11} + \alpha_{8.7.11} + \alpha_{3.7.12} + \alpha_{8.7.12}$	$\delta(C_\gamma H_2)$
$S_{23} = \alpha_{3.7.11} - \alpha_{8.7.11} + \alpha_{3.7.12} - \alpha_{8.7.12}$	$\omega(C_\gamma H_2)$
$S_{24} = \alpha_{3.7.11} - \alpha_{8.7.11} - \alpha_{3.7.12} + \alpha_{8.7.12}$	$t(C_\gamma H_2)$
$S_{25} = \alpha_{3.7.11} + \alpha_{8.7.11} - \alpha_{3.7.12} - \alpha_{8.7.12}$	$\rho(C_\gamma H_2)$
$S_{26} = \alpha_{7.8.13} + \alpha_{4.8.13} + \alpha_{7.8.14} + \alpha_{4.8.14}$	$\delta(C_\beta H_2)$
$S_{27} = \alpha_{7.8.13} - \alpha_{4.8.13} + \alpha_{7.8.14} - \alpha_{4.8.14}$	$\omega(C_\beta H_2)$
$S_{28} = \alpha_{7.8.13} - \alpha_{4.8.13} - \alpha_{7.8.14} + \alpha_{4.8.14}$	$t(C_\beta H_2)$
$S_{29} = \alpha_{7.8.13} + \alpha_{4.8.13} - \alpha_{7.8.14} - \alpha_{4.8.14}$	$\rho(C_\beta H_2)$
$S_{30} = \alpha_{8.4.9} + \alpha_{2.4.9}$	$\delta(C_\alpha H)$
$S_{31} = \alpha_{8.4.9} - \alpha_{2.4.9}$	$\rho(C_\alpha H)$
$S_{32} = \alpha_{8.4.10} + \alpha_{2.4.10}$	$\delta(C_\alpha C)$
$S_{33} = \alpha_{8.4.10} - \alpha_{2.4.10}$	$\rho(C_\alpha C)$
$S_{34} = \alpha_{1.2.4} + \alpha_{1.2.3}$	$\delta(NH)$
$S_{35} = \alpha_{1.2.4} - \alpha_{1.2.3}$	$\rho(NH)$
$S_{36} = 2\alpha_{4.10.16} - \alpha_{15.10.16} - \alpha_{4.10.15}$	$\delta(C-O)$
$S_{37} = \alpha_{15.10.16} - \alpha_{4.10.15}$	$\delta(C=O)$
$S_{38} = \alpha_{10.16.17}$	$\delta(COH)$
$S_{39} = \tau_{4.10.16.17} + \tau_{15.10.16.17}$	$\tau(CO)$
$S_{40} = \tau_{16.10.4.15}$	$\gamma(COO)$
$S_{41} = 0.653087(\alpha_{3.2.4}) - 0.505786(\alpha_{2.4.8} + \alpha_{2.3.7}) + 0.175840(\alpha_{4.8.7} + \alpha_{3.7.8})$	ring bending I
$S_{42} = 0.615911(\tau_{4.8.7.3}) + 0.202164(\tau_{3.2.4.8} + \tau_{7.3.2.4}) - 0.519032(\tau_{2.4.8.7} + \tau_{8.7.3.2})$	ring torsion I
$S_{43} = 0.404582(\alpha_{2.3.7} - \alpha_{2.4.8}) + 0.579925(\alpha_{4.8.7} - \alpha_{3.7.8})$	ring bending II
$S_{44} = 0.610119(\tau_{7.3.2.4} - \tau_{3.2.4.8}) + 0.357428(\tau_{2.4.8.7} - \tau_{8.7.3.2})$	ring torsion II
$S_{45} = \tau_{2.4.10.15} + \tau_{2.4.10.16} + \tau_{8.4.10.15} + \tau_{8.4.10.16} + \tau_{9.4.10.15} + \tau_{9.4.10.16}$	$\tau(C_\alpha C)$

The atomic numbering is given in Figure 7.1. The coefficients for the ring bending and torsion coordinates are from reference [15].

Table 7.2: Symmetry Coordinates of Hydroxyproline

Coordinate	Description
$S_1 = R_{1.2}$	$\nu(NH)$
$S_2 = R_{3.5} + R_{3.6}$	$\nu_s(C_\delta H_2)$
$S_3 = R_{3.5} - R_{3.6}$	$\nu_a(C_\delta H_2)$
$S_4 = R_{8.13} + R_{8.14}$	$\nu_s(C_\beta H_2)$
$S_5 = R_{8.13} - R_{8.14}$	$\nu_a(C_\beta H_2)$
$S_6 = R_{7.11}$	$\nu(C_\gamma H)$
$S_7 = R_{7.12}$	$\nu(C_\gamma O)$
$S_8 = R_{4.9}$	$\nu(C_\alpha H)$
$S_9 = R_{4.10}$	$\nu(C_\alpha C)$
$S_{10} = R_{10.15}$	$\nu(C=O)$
$S_{11} = R_{10.16}$	$\nu(C-O)$
$S_{12} = R_{16.17}$	$\nu(OH)$
$S_{13} = R_{2.4}$	$\nu(NC_\alpha)$
$S_{14} = R_{4.8}$	$\nu(C_\alpha C_\beta)$
$S_{15} = R_{7.8}$	$\nu(C_\beta C_\gamma)$
$S_{16} = R_{3.7}$	$\nu(C_\gamma C_\delta)$
$S_{17} = R_{2.3}$	$\nu(NC_\delta)$
$S_{18} = \alpha_{2.3.5} + \alpha_{5.3.7} + \alpha_{2.3.6} + \alpha_{6.3.7}$	$\delta(C_\delta H_2)$
$S_{19} = \alpha_{2.3.5} - \alpha_{5.3.7} + \alpha_{2.3.6} - \alpha_{6.3.7}$	$\omega(C_\delta H_2)$
$S_{20} = \alpha_{2.3.5} - \alpha_{5.3.7} - \alpha_{2.3.6} + \alpha_{6.3.7}$	$t(C_\delta H_2)$
$S_{21} = \alpha_{2.3.5} + \alpha_{5.3.7} - \alpha_{2.3.6} - \alpha_{6.3.7}$	$\rho(C_\delta H_2)$
$S_{22} = \alpha_{7.8.13} + \alpha_{4.8.13} + \alpha_{7.8.14} + \alpha_{4.8.14}$	$\delta(C_\beta H_2)$
$S_{23} = \alpha_{7.8.13} - \alpha_{4.8.13} + \alpha_{7.8.14} - \alpha_{4.8.14}$	$\omega(C_\beta H_2)$
$S_{24} = \alpha_{7.8.13} - \alpha_{4.8.13} - \alpha_{7.8.14} + \alpha_{4.8.14}$	$t(C_\beta H_2)$
$S_{25} = \alpha_{7.8.13} + \alpha_{4.8.13} - \alpha_{7.8.14} - \alpha_{4.8.14}$	$\rho(C_\beta H_2)$
$S_{26} = \alpha_{3.7.11} + \alpha_{8.7.11}$	$\delta(C_\gamma H)$
$S_{27} = \alpha_{3.7.11} - \alpha_{8.7.11}$	$\rho(C_\gamma H)$
$S_{28} = \alpha_{3.7.12} + \alpha_{8.7.12}$	$\delta(C_\gamma O)$
$S_{29} = \alpha_{3.7.12} - \alpha_{8.7.12}$	$\rho(C_\gamma O)$
$S_{30} = \alpha_{8.4.9} + \alpha_{2.4.9}$	$\delta(C_\alpha H)$
$S_{31} = \alpha_{8.4.9} - \alpha_{2.4.9}$	$\rho(C_\alpha H)$
$S_{32} = \alpha_{8.4.10} + \alpha_{2.4.10}$	$\delta(C_\alpha C)$
$S_{33} = \alpha_{8.4.10} - \alpha_{2.4.10}$	$\rho(C_\alpha C)$
$S_{34} = \alpha_{1.2.4} + \alpha_{1.2.3}$	$\delta(NH)$
$S_{35} = \alpha_{1.2.4} - \alpha_{1.2.3}$	$\rho(NH)$
$S_{36} = 2\alpha_{4.10.16} - \alpha_{15.10.16} - \alpha_{4.10.15}$	$\delta(C-O)$
$S_{37} = \alpha_{15.10.16} - \alpha_{4.10.15}$	$\delta(C=O)$
$S_{38} = \alpha_{10.16.17}$	$\delta(COH)$
$S_{39} = \tau_{4.10.16.17} + \tau_{15.10.16.17}$	$\tau(CO)$
$S_{40} = \tau_{16.10.4.15}$	$\gamma(COO)$
$S_{41} = 0.653087(\alpha_{3.2.4}) - 0.505786(\alpha_{2.4.8} + \alpha_{2.3.7}) + 0.175840(\alpha_{4.8.7} + \alpha_{3.7.8})$	ring bending I
$S_{42} = 0.615911(\tau_{4.8.7.3}) + 0.202164(\tau_{3.2.4.8} + \tau_{7.3.2.4}) - 0.519032(\tau_{2.4.8.7} + \tau_{8.7.3.2})$	ring torsion I
$S_{43} = 0.404582(\alpha_{2.3.7} - \alpha_{2.4.8}) + 0.579925(\alpha_{4.8.7} - \alpha_{3.7.8})$	ring bending II
$S_{44} = 0.610119(\tau_{7.3.2.4} - \tau_{3.2.4.8}) + 0.357428(\tau_{2.4.8.7} - \tau_{8.7.3.2})$	ring torsion II
$S_{45} = \tau_{2.4.10.15} + \tau_{2.4.10.16} + \tau_{8.4.10.15} + \tau_{8.4.10.16} + \tau_{9.4.10.15} + \tau_{9.4.10.16}$	$\tau(C_\alpha C)$
$S_{46} = R_{12.18}$	$\nu(OH)_{alc}$
$S_{47} = \alpha_{7.12.18}$	$\delta(C_\gamma OH)$
$S_{48} = \tau_{3.7.12.18} + \tau_{8.7.12.18} + \tau_{11.7.12.18}$	$\tau(C_\gamma O)$

The atomic numbering is given in Figure 7.1. The coefficients for the ring bending and torsion coordinates are from reference [15].

Table 7.3: 4-21G optimized parameters of two conformations of proline and hydroxyproline

			Proline						*Hydroxyproline*		
			X	cis	trans				X	cis	trans
Bond length(A°)						Bond length(A°)					
1	2		-	1.004	1.005	1	2		-	1.004	1.005
2	3		1.484	1.479	1.479	2	3		1.478	1.485	1.485
2	4		1.527	1.463	1.463	2	4		1.508	1.471	1.470
3	5		1.103	1.087	1.087	3	5		1.086	1.086	1.085
3	6		1.101	1.080	1.080	3	6		1.098	1.079	1.079
3	7		1.532	1.540	1.537	3	7		1.524	1.531	1.530
4	8		1.522	1.564	1.570	4	8		1.531	1.567	1.570
4	9		1.095	1.081	1.084	4	9		1.114	1.081	1.083
4	10		1.527	1.509	1.519	4	10		1.517	1.506	1.518
7	8		1.538	1.556	1.554	7	8		1.503	1.545	1.546
7	11		1.102	1.081	1.081	7	11		1.077	1.077	1.076
7	12		1.098	1.081	1.081	7	12		1.460	1.439	1.437
8	13		1.097	1.080	1.081	8	13		1.070	1.078	1.079
8	14		1.104	1.080	1.083	8	14		1.105	1.080	1.082
10	15		1.258	1.206	1.200	10	15		1.269	1.206	1.200
10	16		1.275	1.361	1.365	10	16		1.254	1.358	1.363
16	17		-	.969	.965	16	17		-	.969	.965
						12	18		.967	.970	.970
Bond angle(°)						Bond angle(°)					
2	4	8	106.242	104.576	104.769	2	4	8	104.436	103.928	103.958
4	8	7	100.802	104.650	104.405	4	8	7	107.747	103.979	103.800
8	7	3	103.649	104.184	103.585	8	7	3	103.933	102.869	102.569
7	3	2	105.310	101.466	101.244	7	3	2	105.768	99.179	99.149
3	2	4	107.079	107.423	107.782	3	2	4	109.371	106.594	106.696
1	2	3	-	114.610	114.461	1	2	3	-	115.217	114.946
1	2	4	-	113.643	112.929	1	2	4	-	113.853	113.203
2	3	5	109.533	112.268	112.351	2	3	5	106.318	112.759	112.744
2	3	6	108.874	110.457	110.384	2	3	6	110.028	110.986	110.853
5	3	6	113.688	109.216	109.356	5	3	6	110.786	110.201	110.275
2	4	8	106.242	104.576	104.769	2	4	8	104.436	103.928	103.958
2	4	9	108.334	111.693	110.860	2	4	9	110.804	111.606	110.813
2	4	10	106.425	110.952	111.035	2	4	10	110.317	110.786	110.892
3	7	11	99.648	112.478	112.866	3	7	11	110.208	114.191	114.365
3	7	12	113.872	109.154	109.133	3	7	12	109.294	109.177	109.421
11	7	12	118.248	109.056	109.330	11	7	12	120.036	107.010	107.283
4	8	13	109.365	110.448	111.387	4	8	13	104.607	111.842	112.442
4	8	14	109.288	110.554	110.619	4	8	14	106.949	110.799	110.978
13	8	14	118.308	107.914	108.357	13	8	14	109.662	108.827	109.396
4	10	15	120.805	126.493	124.619	4	10	15	115.340	126.280	124.385
4	10	16	118.981	111.222	115.104	4	10	16	118.509	111.102	115.141
16	10	17	-	27.606	26.400	16	10	17	106.784	27.548	26.333
						7	12	18	97.444	107.098	107.219

Table 7.3. (Continued): 4-21G optimized parameters of two conformations of proline and hydroxyproline

				Proline								*Hydroxyproline*		
				X	cis	trans						X	cis	trans
Torsions(°)							Torsions(°)							
2	4	8	7	33.592	8.419	2.979	2	4	8	7	14.565	1.536	.000
4	8	7	3	-40.961	17.004	22.193	4	8	7	3	-27.180	26.746	28.199
8	7	3	2	33.634	-35.829	-38.920	8	7	3	2	29.475	-44.563	-45.431
7	3	2	4	-12.383	43.262	42.885	7	3	2	4	-21.199	47.574	47.508
3	2	4	8	-13.708	-32.518	-28.767	3	2	4	8	4.324	-30.821	-29.757
1	2	3	5	-	52.419	51.351	1	2	3	5	-	56.757	55.706
1	2	3	6	-	-69.745	-70.999	1	2	3	6	-	-67.437	-68.473
1	2	3	7	-	170.566	169.425	1	2	3	7	-	174.929	173.890
1	2	4	8	-	-160.385	-156.199	1	2	4	8	-	-158.980	-157.177
1	2	4	9	-	79.076	83.439	1	2	4	9	-	80.649	82.632
1	2	4	10	-	-41.382	-37.427	1	2	4	10	-	-40.026	-38.500
2	3	7	11	-84.276	-157.419	-160.248	2	3	7	11	142.639	-167.289	-167.827
2	3	7	12	148.838	81.399	77.979	2	3	7	12	-83.416	72.990	71.809
2	4	8	13	-81.459	-111.438	-117.465	2	4	8	13	139.813	-116.730	-118.050
2	4	8	14	147.580	129.195	121.955	2	4	8	14	-103.896	121.659	119.049
2	4	10	15	170.561	3.889	2.639	2	4	10	15	-178.390	4.433	3.214
2	4	10	16	-6.863	-176.662	-177.278	2	4	10	16	2.712	-175.878	-176.531
3	2	4	9	-130.262	-153.057	-149.128	3	2	4	9	121.382	-151.192	-149.949
3	2	4	10	105.256	86.485	90.006	3	2	4	10	-117.779	88.133	88.920
3	7	8	13	74.150	136.302	142.572	3	7	8	13	-144.625	146.493	148.386
3	7	8	14	-155.647	-102.803	-96.808	3	7	8	14	89.174	-92.777	-90.976
4	10	16	17	-	-179.436	-3.311	4	10	16	17	-	-179.429	-2.875
							3	7	12	18	-96.382	-42.454	-39.905
							8	7	12	18	152.130	70.073	72.275
							11	7	12	18	32.312	-166.517	-164.504

X : X-ray parameters of proline and hydroxyproline from references [6] and [7]. Footnote: Energies of the cis and trans conformations of proline and hydroxyproline are -397.859735, -397.847190, -472.533307, -472.520765 hartrees respectively.

Table 7.4: Calculated and Experimental frequencies of Proline

F	cis		trans		Experimental				Raman		IR	
	U	S	U	S	E1	E2	E3	E4	A1	A2	I1	I2
1	41	37	44	39	-	-	-	-	.4	.3	8.5	1.4
2	79	71	92	82	-	-	-	-	.7	.5	1.8	.7
3	198	178	342	307	-	-	-	-	.2	.8	9.6	10.9
4	263	236	211	188	292(m)	298(w)	292(w)	320(w)	.8	.1	11.8	3.0
5	341	306	259	233	369(vs)	377(w)	336(m,br)	346(w)	1.3	1.0	24.7	0.8
6	469	424	477	431	450(s)	448(m)	455(s,br)	453(s,br)	3.2	2.7	161.0	88.8
7	592	534	595	537	569(w)	-	-	582(w)	2.7	6.1	8.4	42.0
8	607	545	446	400	-	-	-	-	3.3	2.2	50.6	37.0
9	681	613	670	606	639(s)	641(m)	597	621(w)	2.0	2.4	56.2	46.4
10	696	628	690	621	661(sh)	667(w)	633(w)	646(w)	1.3	2.0	10.1	136.7
11	775	704	774	703	688(w)	698(w)	677(w)	683(w)	4.8	8.7	15.7	60.6
12	849	778	863	794	791(m)	795(m)	777(w)	785(m)	3.0	2.7	34.8	56.6
13	866	788	859	779	-	-	-	-	7.4	7.7	30.8	2.1
14	935	851	980	909	860(sh)	866(w)	868(m)	853(m)	6.3	1.7	15.6	1.2
15	949	889	940	895	900(w)	898(vs)	891(w)	875(s)	14.4	5.2	1.9	17.0
16	978	907	955	857	911(w)	919(vs)	911(vs)	915(vs)	2.0	14.7	.1	4.2
17	1011	943	1005	935	945(m)	951(m)	947(w)	953(w)	3.9	5.0	12.5	6.1
18	1060	972	1063	974	979(m)	994(w)	993(w)	986(m)	2.8	2.8	13.9	11.4
19	1137	1050	1133	1045	1051(w)	1056(m)	1046(s)	1043(m)	5.9	6.1	17.3	16.6
20	1197	1114	1259	1155	-	-	-	-	1.9	3.4	.3	77.9
21	1211	1088	1213	1090	1083(m)	1082(m)	1093(w)	1090(w)	1.4	3.1	35.5	246.9
22	1247	1149	1218	1137	1168(s)	1173(m)	1173(w)	-	6.8	1.7	6.1	3.4
23	1316	1178	1309	1173	-	1192(vw)	1191(m)	1186(m)	2.2	2.5	10.4	6.9
24	1334	1199	1326	1193	1225(sh)	1239(m)	1244(m)	1244(m)	6.5	9.1	194.7	5.9
25	1352	1211	1355	1213	1253(m)	1264(m)	-	-	7.5	16.7	263.3	3.5
26	1390	1245	1406	1260	1289(s)	-	1274(m)	1281(w)	8.6	9.0	6.7	12.0
27	1438	1294	1341	1223	-	-	-	-	15.0	9.5	7.9	3.3
28	1464	1312	1462	1311	1292(s)	1285(m)	1298(w)	1301(w)	5.7	2.1	15.2	10.5
29	1483	1328	1487	1332	1317(s)	1320(w)	1329(m)	1317(w)	4.6	2.5	4.1	21.6
30	1496	1342	1497	1343	1340(sh)	-	-	-	2.6	1.6	3.3	22.1
31	1502	1367	1478	1327	1375(s,br)	1349(w)	1357(w)	1354(m)	2.1	2.2	7.8	2.9
32	1598	1435	1603	1438	-	-	-	1396(s)	2.9	2.9	15.6	14.4
33	1645	1472	1643	1470	1447(s)	1441(w)	-	-	15.8	16.5	3.4	2.1
34	1671	1496	1667	1492	-	1451(m)	1457(s)	1456(s)	8.7	8.3	1.9	4.0
35	1689	1512	1688	1510	1472(s)	1471(w)	1481(m)	1482(m)	11.9	12.9	3.0	2.3
36	1938	1829	1976	1865	-	-	1734(s)	-	8.4	5.0	213.1	242.0
37	3177	3015	3181	3018	2875(w)	2878(w)	2893(w)	2877(w)	64.8	64.7	43.9	47.1
38	3242	3075	3247	3081	2920(sh)	2919(w)	2921(w)	2895(m)	67.5	81.6	18.7	41.8
39	3254	3087	3220	3055	2935(sh)	2952(w)	2944(m)	2921(w)	44.8	60.7	22.0	18.4
40	3266	3098	3235	3069	2955(m)	2950(s)	2962(w)	2942(m)	106.0	36.6	21.7	17.5
41	3275	3107	3278	3110	2975(m)	2976(m)	2976(w)	2966(w)	92.7	81.6	13.4	16.1
42	3286	3117	3301	3132	2982(s)	-	-	-	100.3	59.3	29.3	31.6
43	3311	3141	3277	3109	3006(m)	3007(s)	3002(s)	2983(s)	67.5	161.1	37.7	16.7
44	3720	3529	3721	3530	-	-	-	-	79.8	87.8	13.4	8.5
45	3850	3652	3894	3695	-	-	-	-	54.1	150.0	52.0	66.3

F : Frequency number, U: Unscaled frequencies, S: Scaled frequencies, E1: IR frequencies of solid L-proline from reference [17], E2: Raman frequencies of solid L-proline from reference [17], E3,E4: Raman frequencies of solution of L-proline at pH 1.0 and pH 11.0 respectively from reference [17]. (A1,A2), (I1,I2) are the calculated Raman activities and IR intensities of the cis and trans conformations respectively. Harmonic frequencies are in units of (cm^{-1}), IR intensities are in units of (KM/Mole) and Raman activities are in units of (A^4/AMU).

Table 7.5: Calculated and Experimental frequencies of Hydroxyproline

F	cis		trans		Experimental					Raman		IR	
	U	S	U	S	E1	E2	E3	E4	E5	A1	A2	I1	I2
1	67	60	67	60	-	61	-	-	-	.4	.3	17.8	4.7
2	79	71	91	81	-	76	-	-	-	.6	.4	1.4	.6
3	165	148	169	151	-	153	-	-	-	.3	.1	16.1	6.8
4	228	205	222	199	-	208	-	-	-	1.0	1.1	8.8	2.0
5	337	302	342	307	320(s)	328	326(m)	320(w)	328(w)	1.1	.8	13.6	3.5
6	410	367	412	369	-	369	-	-	-	.5	.7	17.9	.6
7	452	406	465	417	418(m)	425	418(s)	432(s)	432(m)	2.6	1.4	102.6	53.6
8	487	440	490	443	458(s)	467	460(s)	476(s)	471(m)	2.0	3.6	53.5	115.8
9	550	492	557	499	-	-	-	-	-	1.9	5.1	9.6	117.8
10	610	547	438	393	-	-	-	743(s)	-	3.4	1.2	120.9	3.4
11	646	585	654	594	-	-	-	-	-	2.4	3.5	65.1	24.2
12	697	632	685	621	-	-	-	-	-	2.2	1.9	54.0	166.8
13	752	686	762	694	-	-	-	686(m)	-	2.9	6.3	27.8	63.6
14	833	761	831	757	-	-	-	-	-	8.3	10.3	8.2	15.2
15	867	794	868	797	751(m)	780	753(m)	768(vw)	780(m)	3.3	2.1	16.5	2.5
16	884	815	888	819	-	-	-	-	-	6.0	5.5	38.2	52.9
17	915	896	916	897	877(m)	882	872(s)	884(s)	864(sh)	11.3	11.3	29.2	33.4
18	965	852	965	854	844	853	844(vs)	855(vs)	854(vs)	3.2	3.0	12.8	11.4
19	1014	950	1006	946	913(m)	923	916(m)	926	925(mw)	10.4	10.6	2.9	3.7
20	1037	962	1039	959	955(s)	959	949(s)	964(m)	969(m)	7.2	7.5	4.0	3.9
21	1078	995	1078	995	-	-	-	-	-	2.5	2.6	77.7	63.3
22	1153	1057	1155	1057	1023(m)	1036	1031(m)	1038(w)	1034(m)	5.1	4.8	21.3	49.2
23	1171	1070	1177	1071	1050(m)	1069	1059(vs)	1071(s)	1064(s)	2.5	3.7	63.1	132.3
24	1201	1111	1205	1121	1080(m)	1091	1082(m)	-	1105(w)	1.3	2.2	15.5	40.8
25	1230	1132	1256	1224	-	-	-	-	-	6.9	3.6	1.3	164.5
26	1301	1168	1299	1165	1180(wsh)	1188	1180(m)	-	1182(w)	5.4	5.5	21.6	27.3
27	1318	1180	1317	1179	-	-	-	-	-	7.2	9.5	34.1	30.2
28	1349	1213	1354	1217	1218(m)	1229	1220(m)	1226(s)	1219(m)	4.7	3.3	477.8	14.6
29	1379	1243	1386	1248	1250(m)	1261	1254(m)	-	-	4.9	8.8	7.6	15.6
30	1438	1295	1443	1300	1276(m)	1284	1274	1272(w)	-	2.7	5.5	7.1	11.3
31	1444	1303	1476	1330	-	1302	-	1302(w)	1308(ms)	9.3	2.5	10.4	2.7
32	1474	1322	1480	1327	1313(s)	1323	1316(vs)	1321(m)	-	3.5	2.0	9.5	8.3
33	1488	1335	1491	1339	1350(m)	1356	1348(m)	1341(vw)	-	3.6	1.6	.1	25.5
34	1504	1369	1336	1149	-	-	-	-	-	2.6	5.1	7.8	11.7
35	1532	1376	1532	1372	1392(vs)	1385	1385(vs)	-	1395(vs)	8.4	8.6	81.6	90.5
36	1586	1458	1589	1460	-	-	-	-	1430(m)	3.9	3.9	15.3	13.1
37	1651	1479	1648	1477	-	1445	-	-	-	10.0	10.2	4.1	5.5
38	1676	1500	1676	1500	1474(w)	1466	-	-	1459(m)	10.5	11.1	5.9	5.5
39	1939	1830	1976	1865	-	-	-	1739(vs)	-	8.6	5.2	215.5	247.9
40	3198	3034	3207	3043	2855(sh)	2866	-	-	-	55.9	61.6	31.6	37.4
41	3265	3097	3234	3068	2920(m)	2923	-	-	-	67.7	42.1	16.5	8.9
42	3269	3102	3243	3077	2948(s)	2959	2951(vs)	-	2958(sh)	74.4	89.6	12.6	13.5
43	3300	3130	3302	3132	2982(m)	2991	2982(m)	-	2976(s)	84.2	89.7	19.2	22.2
44	3313	3143	3317	3147	-	3002	-	-	-	75.6	64.9	9.9	12.0
45	3324	3153	3307	3138	3034(w)	3041	3035(m)	-	-	108.6	124.5	29.9	29.7
46	3728	3425	3726	3424	-	-	-	-	-	78.0	83.1	20.6	15.4
47	3829	3536	3827	3535	-	-	-	-	-	42.3	42.9	28.5	25.6
48	3850	3653	3893	3693	-	-	-	-	-	53.9	149.3	57.0	74.1

F : Frequency number, U: Unscaled frequencies, S: Scaled frequencies, E1, E2: IR and Raman frequencies of solid L-hydroxyproline from reference [16], E3: Raman frequencies of solid L-hydroxyproline from reference [14], E4,E5: Raman frequencies of solution of hydrochloride and sodium salt of L-hydroxyproline respectively from reference [16]. (A1,A2), (I1,I2) are the calculated Raman activities and IR intensities of the cis and trans conformations respectively. Harmonic frequencies are in units of (cm^{-1}), IR intensities are in units of (KM/Mole) and Raman activities are in units of (A^4/AMU).

Table 7.6: Potential energy distributions of two conformations of Proline

	cis		trans	
	Freq.	PED	Freq.	PED
1	41	42(51.6),44(29.2)	45	42(47.8),44(38.0)
2	79	45(69.8)	92	45(68.9)
3	198	44(21.1),42(14.7),33(14.5),32(12.2) ,36(11.9)	211	33(29.2),42(18.6),36(15.2),44(12.7) -
4	263	33(32.0),32(24.2),40(12.0),36(10.5)	259	32(28.8),33(21.7),42(13.6),40(13.1)
5	341	32(33.9),44(27.4),36(13.7)	342	32(33.4),44(23.9),36(15.3)
6	469	36(35.3),33(11.9), 9(11.1)	446	39(80.7)
7	592	41(19.8),43(12.5),34(11.6)	477	36(31.8),39(15.7),33(12.7)
8	607	39(46.9),41(18.4)	595	41(26.8),34(14.0),43(13.4)
9	681	37(32.7),43(22.6) -	670	41(20.6),13(13.3),43(13.3),40(12.6) ,34(10.6)
10	696	43(18.7),39(18.5),41(10.5),13(10.3)	690	43(28.4),37(27.5)
11	775	40(18.7),34(12.2)	775	40(19.8),37(12.9)
12	849	29(20.8), 9(17.1)	859	34(15.9),30(10.4),29(10.0)
13	866	34(17.1),14(11.1),41(10.8),30(10.4)	862	29(13.7), 9(12.7),14(12.1)
14	935	15(33.1),25(11.5)	940	15(34.6),16(11.7),25(10.1)
15	949	15(18.4),16(17.5),25(17.4) -	954	25(19.4),16(15.7),15(12.1),14(11.3) ,17(11.2)
16	978	16(26.6),15(17.6),17(14.3)	980	16(27.6),15(20.6)
17	1011	14(25.0), 9(16.9),13(10.7)	1005	14(16.8), 9(15.3),13(10.6)
18	1060	17(16.5),21(13.6),32(10.0)	1062	17(18.0),21(14.4),29(10.1)
19	1137	41(19.9),15(15.7),14(12.4),16(11.7)	1133	41(19.1),15(15.9),16(11.5),14(10.2)
20	1197	11(33.0),38(24.7)	1212	21(27.2),29(17.0),25(12.0)
21	1211	21(23.0),13(17.5),29(11.1)	1218	13(27.8),11(17.9),17(13.1),43(10.6)
22	1247	13(15.0),38(14.4),11(12.4)	1259	38(24.0),11(19.5),13(10.7)
23	1316	20(44.4),28(22.9),21(10.6)	1309	20(32.7),28(24.3),21(14.4)
24	1334	24(21.1),31(16.2),19(15.2)	1326	38(19.7),24(19.3),19(10.2)
25	1352	31(32.5),24(17.8),27(14.4),23(11.1)	1341	38(29.2),11(17.0)
26	1390	28(39.4),20(20.5),31(13.7)	1355	31(29.1),24(15.3),20(13.9),27(11.4)
27	1438	30(34.0),38(23.0)	1406	28(34.9),31(29.6),20(15.3)
28	1464	27(52.3),24(13.8)	1462	27(43.4),30(25.4),24(14.9)
29	1483	23(55.7),27(16.2)	1478	30(42.0),27(24.1)
30	1496	19(47.4),23(12.1)	1487	23(61.5)
31	1502	30(33.0), 9(12.2),19(10.9),11(10.6)	1497	19(59.2)
32	1598	35(74.1),19(11.4)	1602	35(76.6),19(10.0)
33	1645	22(87.3)	1643	22(87.7)
34	1671	26(79.0)	1667	26(79.5)
35	1689	18(84.7)	1688	18(86.5)
36	1938	10(80.1)	1976	10(81.7)
37	3177	2(68.1), 3(30.4)	3182	2(69.1), 3(29.5)
38	3242	4(87.5)	3220	8(92.9)
39	3254	8(74.8), 6(18.2)	3235	6(78.4), 4(13.4)
40	3266	6(58.2), 3(15.0), 8(13.9)	3247	4(79.1)
41	3275	3(37.4), 2(20.6), 6(15.1), 5(10.5)	3277	7(41.8), 5(23.9), 3(12.3)
42	3286	5(61.8), 7(21.7), 3(12.8)	3278	3(48.8), 7(29.1), 2(19.3)
43	3311	7(74.7), 5(22.0)	3301	5(73.4), 7(20.2)
44	3720	1(99.6)	3721	1(99.7)
45	3850	12(99.9)	3894	12(99.9)

Symmetry coordinate numbers given in Table 7.1.

Table 7.7: Potential energy distributions of two conformations of Hydroxyproline

	cis		trans	
	Freq.	PED	Freq.	PED
1	67	42(44.4),44(30.3)	67	42(45.7),44(33.2)
2	79	45(46.0),42(18.6),44(16.2)	91	45(56.9),44(14.6),42(12.0)
3	165	33(18.1),44(15.5),28(13.0),42(12.0)	169	33(21.6),44(14.9),28(12.6),42(11.7)
4	228	32(23.3),33(22.0),28(14.1)	222	32(24.2),33(20.1),28(13.8)
5	337	32(25.2),44(21.1),36(18.0)	342	32(25.7),44(20.9),36(17.7)
6	410	28(44.7),42(10.6)	412	28(41.9),42(11.4)
7	452	29(31.9),41(10.8),36(10.6)	438	39(45.7),28(12.7),29(10.3)
8	487	29(26.2),36(22.1)	465	39(36.3),29(27.2)
9	550	48(94.2)	490	36(25.7),29(20.2), 9(11.5)
10	610	39(68.7)	557	48(94.2)
11	646	37(26.7),41(21.4),34(15.6)	654	37(22.2),41(21.0),34(17.4)
12	697	41(21.5),39(14.0),34(11.6),13(10.5)	685	41(25.5),40(18.5)
13	752	40(17.5)	762	37(21.3),40(12.1)
14	833	43(36.7),16(11.7)	831	43(35.6),16(10.0)
15	867	25(22.7), 9(21.2)	868	9(20.6),25(19.6)
16	884	34(27.9),14(19.6),17(10.5)	888	34(27.3),14(17.1),17(10.7)
17	915	16(16.7),15(15.0),26(12.7)	916	16(17.8),15(16.8),26(12.9)
18	965	16(23.1),15(22.8),17(11.2)	965	15(25.0),16(23.5),17(10.1)
19	1014	14(26.7),17(23.7),13(13.8), 9(10.6)	1006	14(28.0),17(21.4), 9(12.5),13(12.4)
20	1037	7(40.8),25(11.3)	1039	7(42.5),25(12.6)
21	1078	34(15.2),17(12.6),21(10.9)	1078	34(16.8),17(15.9)
22	1153	25(15.2),14(10.5)	1155	25(16.7)
23	1171	21(23.3),13(10.8)	1177	21(30.3),47(10.5),13(10.0)
24	1201	13(18.3),21(16.8),43(12.1)	1205	13(28.7),43(15.2),17(12.0),21(11.1)
25	1230	11(29.1),38(28.6)	1256	11(29.9),38(28.4),37(10.1)
26	1301	24(38.2),26(15.0)	1299	24(37.0),26(14.0)
27	1318	20(58.3)	1317	20(52.3),26(10.4)
28	1349	31(47.5)	1336	38(40.2),11(25.2),37(11.3)
29	1379	27(27.6),23(15.7),24(12.7)	1354	31(38.9),19(12.0)
30	1438	30(15.9),23(15.9),24(11.3),38(11.2)	1386	27(25.6),23(19.8),24(12.4)
31	1444	30(18.1),38(11.5),26(11.3)	1443	23(23.6),31(16.6),24(11.4)
32	1474	23(34.6),27(20.5),26(14.2)	1476	30(47.6),26(11.9)
33	1488	19(50.9)	1480	23(25.8),27(18.4),19(11.0),30(10.6)
34	1504	30(34.6), 9(13.8),11(13.1),38(11.1)	1491	19(44.1)
35	1532	47(41.7),26(40.8)	1532	47(43.1),26(42.2)
36	1586	35(72.1),19(11.4)	1589	35(74.5),19(10.9)
37	1651	22(90.6)	1648	22(90.9)
38	1676	18(91.5)	1676	18(92.0)
39	1939	10(80.1)	1976	10(81.6)
40	3198	2(72.4), 3(26.6)	3207	2(74.8), 3(23.8)
41	3265	8(66.1), 4(32.5)	3234	8(95.4)
42	3269	4(59.4), 8(30.8)	3243	4(84.7), 5(11.1)
43	3300	3(72.6), 2(24.0)	3302	3(71.4), 2(20.7)
44	3313	6(86.8)	3307	5(79.9)
45	3324	5(88.9)	3317	6(93.9)
46	3728	1(99.6)	3726	1(99.7)
47	3829	46(99.9)	3827	46(99.9)
48	3850	12(99.9)	3893	12(99.9)

Symmetry coordinate numbers given in Table 7.2.

7.4 References

[1] J. S. Alper, H. Dothe and D. F. Coker, Chem. Phys., 153 (1991) 51.

[2] J. S. Alper, H. Dothe and M. A. Lowe, Chem. Phys., 161 (1992) 199.

[3] A. Vijay and D. N. Satyanarayana, J. Phys. Chem, 96 (1992) 10735.

[4] M. Ramek, J. Mol. Str. (Theochem), 208 (1990), 301.

[5] L. D. Barron, A. R. Gargaro, L. Hecht and P. L. Polavarapu, Spectrochim. Acta, 47A (1991) 1001.

[6] R. L. Kayushina and B. K. Vainshtein, Sov. Phys. - Crystallogr. (Engl. Transl.), 10 (1966) 698.

[7] J. Donohue and K. N. Trueblood, Acta Crystallogr., 5 (1952) 414.

[8] T. F. Koetzle, M. S. Lehmann and W. C. Hamilton, Acta Crystallogr., 29B (1973) 231.

[9] K. Wüthrich and C. Grathwohl, FEBS Letters, 43 (1974) 337.

[10] B. Pullman and A. Pullman, Adv. Protein Chem., 28 (1974) 442-459.

[11] A-M. Sapse, L. M-Levy, S. B. Daniels and B. W. Erickson, J. Am. Chem. Soc., 109 (1987) 3526.

[12] P. Lagant, M. H. L. Lefebvre, J. P. Huvenne, G. Vergoten, G. Fleury and P. Legrand, Biopolymers, 22 (1983) 1285.

[13] V. Tabacik, Program Redond, University of Montpellier, France, 1973.

[14] L. P. Singh, V. P. Gupta, R. K. Gupta, S. Rastogi and V. D. Gupta, Proc. Natl. Acad. Sci. (India), 59A (1989) 485.

[15] B. Cadioli, E. Gallinerll, C. Coulombeau, H. Jobic and G. Berthier, J. Phys. Chem., 97 (1993) 7844.

[16] M. J. Deveney, A. G. Walton and J. L. Koenig, Biopolymers, 10 (1971) 615.

[17] A. W. Herlinger and T. V. Long III, J. Am. Chem. Soc., 92 (1970) 6481.

[18] Y. Grenie and C. G. Lagrange, J. Mol. Spectrosc., 41 (1972) 240.

[19] T. S. Khoan, Y. A. Pentin and A. A. Ivlev, Opt. Spectrosc., 35 (1973) 616.

[20] P. Császár, A. Császár, L. Harsànyi and J. E. Boggs, J. Mol. Str. (Theochem), 136 (1986) 323.

[21] K. Fan, Y. Xie and J. E. Boggs, J. Mol. Str. (Theochem), 136 (1986) 339.

[22] (a) B. Maigret, D. Perahia and B. Pullman, J. Theor. Biol., 29 (1970) 275; (b) B. Maigret, D. Perahia and B. Pullman, Biopolymers, 10 (1970) 1649.

[23] (a) B. Maigret, B. Pullman and D. Perahia, J. Theor. Biol., 31 (1971) 269; (b) B. Maigret, B. Pullman and D. Perahia, Biopolymers, 10 (1971) 107

[24] C. Altona and M. Sundaralingam, J. Am. Chem. Soc., 94 (1972) 8205.

[25] M. MacArthur and J. M. Thornton, J. Mol. Biol., 218 (1991) 397.

[26] D. F. DeTar and N. P. Luthra, J. Am. Chem. Soc., 99 (1977) 1232.

[27] J. E. Kilpatrick, K. S. Pitzer and R. J. Spitzer, J. Am. Chem. Soc., 69 (1947) 2483.

[28] K. Pitzer and W. E. Donath, J. Am. Chem. Soc., 81 (1959) 3213.

[29] K. K. Chacko, S. Swaminathan and K. R. Veena, Curr. Sci., 52 (1983) 660.

[30] S. C. Shekar, M. B. Sankaran and K. R. K. Easwaran, Int. J. Pept. Protein Res., 23 (1984) 166.

[31] G. Pfafferott, H. Oberhammer, J. E. Boggs and W. Caminati, J. Am. Chem. Soc., 107 (1985) 2305.

Chapter 8

Conclusions

Our results should be seen in light of the fact that, ab initio calculations employed in this study engender molecular properties (for e. g. geometries and vibrational frequencies) which are either more complete (includes all the unobserved features), or more accurate/reliable (uncontaminated by statistical errors), or more highly resolved (showing subtle changes with minor differences), than the results of other methods, either computational or experimental. We however refer to differences between similar parameters and not to absolute values. It is the former which are frequently better determined than the latter by an order of magnitude.

8.1 Carboxylic Acids

In conclusion, our calculations indicate the diverse conformational and vibrational aspects/features displayed by carboxylic acids and carboxylate anions. The idea of a generalized force field though very much feasible with the presence of reliable gas phase data could not be achieved in this study. A beginning however has been made in this direction to achieve the same using solid state data.

In the absence of detailed theoretical studies on the conformational and vibrational analysis of large anions our studies have indicated the interesting features displayed by these systems in general. However, we feel that many more studies have to be done on similar systems before such conclusions can be generalized.

On the basis of our calculation, we can infer that the 4-21G basis set is a reliable and computationally efficient basis set for the prediction of geometries, energy barriers and vibrational frequencies of electron rich species like carboxylic acids and carboxylate

anions.

8.2 Amino Acids

The demand for force fields which describe the features of amino acids more reliably/accurately is obvious from the wide applications of them in biomolecular simulations.

The use of ab initio methods to describe the vibrational characteristics of amino acids is still in its infancy. The increase in the size of the amino acids obviously leads to more complications in the assignments of their spectra. Our studies on four amino acids cysteine, serine, proline and hydroxyproline have exhibited the nature of problems encountered in such assignments. The presence of reliable gas phase spectra could substantiate many of our results but in their absence more sophisticated theoretical models might be required to do the same.

Our studies on proline and hydroxyproline made us aware that not much literature is available on the theoretical vibrational analysis of saturated five membered rings. The few studies which exist on non-symmetric molecules have assumed that these rings are symmetrical which obviously simplifies the complications but is far from reality. It would be nice if studies which are devoid of such assumptions can be done on these systems and a general set of rules to assign them made available.